Salinity, Sanitation and Sustainability:
Biotechnology of Saline and
Sewage Wastewater Co-Treatment

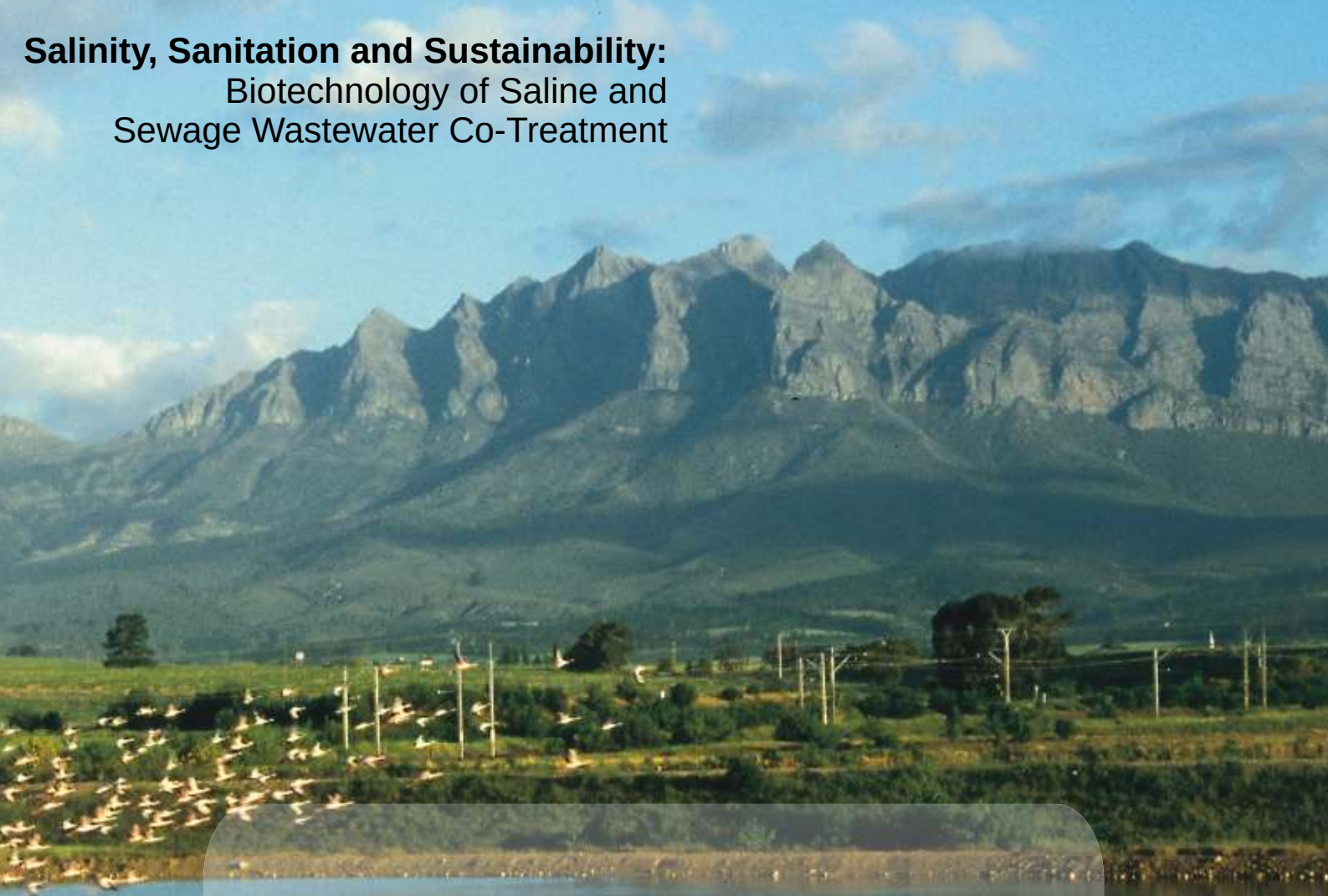

Volume 1

Integrated Physical, Chemical and Biological Process Kinetic Models for Anaerobic Digestion of Primary Sewage Sludge

NE Ristow, SW Sötemann, S Rajkumar, MC Wentzel,
CJ Brouckaert, CA Buckley, GA Ekama and PD Rose

WRC Report No TT 393/09

14

Water Research Commission

SALINITY, SANITATION and SUSTAINABILITY
A Study in Environmental Biotechnology and Integrated Wastewater Beneficiation in South Africa

Report 1: Volume 1 - Overview

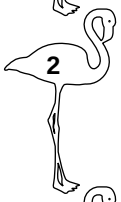

Report 2: Volume 2 - Integrated Algal Ponding Systems and the Treatment of Saline Wastewaters

Part 1: Meso-Saline Wastewaters
The *Spirulina* Model

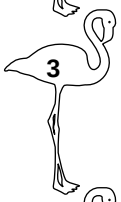

Report 3: Volume 2 - Integrated Algal Ponding Systems and the Treatment of Saline Wastewaters

Part 2: Hyper-Saline Wastewaters
The *Dunaliella* Model

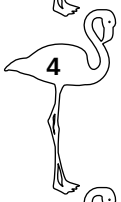

Report 4: Volume 3 - Integrated Algal Ponding Systems and the Treatment of Domestic and Industrial Wastewaters

Part 1: The AIWPS Model

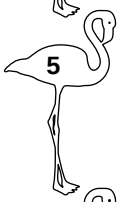

Report 5: Volume 3 - Integrated Algal Ponding Systems and the Treatment of Domestic and Industrial Wastewaters

Part 2: Abattoir Wastewaters

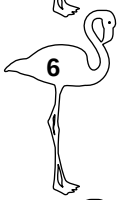

Report 6: Volume 3 - Integrated Algal Ponding Systems and the Treatment of Domestic and Industrial Wastewaters

Part 3A: Mine Drainage Wastewaters
The ASPAM Model

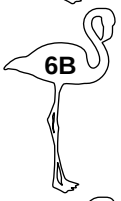

Report 6B: Volume 3 - Integrated Algal Ponding Systems and the Treatment of Domestic and Industrial Wastewaters

Part 3B: Sulphate Saline Systems:
Development of the ASPAM Process

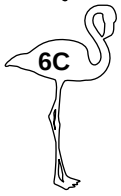

Report 6C: Volume 3 - Integrated Algal Ponding Systems and the Treatment of Domestic and Industrial Wastewaters

Part 3C: Chloride Saline Systems: The Use of Saline Waters for the Reticulation and Treatment of Domestic and Industrial Effluents

Report 7: Volume 3 - Integrated Algal Ponding Systems and the Treatment of Domestic and Industrial Wastewaters

Part 4: System Performance and Tertiary Treatment Operations

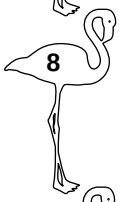

Report 8: Volume 3 - Integrated Algal Ponding Systems and the Treatment of Domestic and Industrial Wastewaters

Part 5: Winery and Distillery Wastewaters

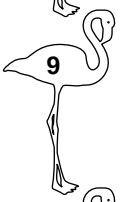

Report 9: Volume 4 - The Rhodes BioSURE Process ®

Part 1: Biodesalination of Mine Drainage Wastewaters

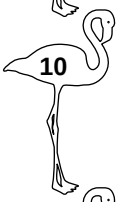

Report 10: Volume 4 - The Rhodes BioSURE Process ®

Part 2: Enhanced Hydrolysis of Organic Carbon Substrates - Development of the Recycling Sludge Bed Reactor

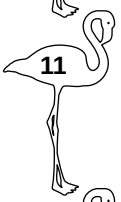

Report 11: Volume 4 - The Rhodes BioSURE Process ®

Part 3: Sulphur Production and Metal Removal Unit Operations

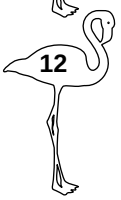

Report 12: Volume 4 - The Rhodes BioSURE Process ®

Part 4: Treatment and Disposal of Sewage Sludges

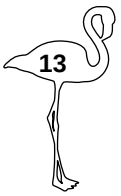

Report 13: Recovery and Re-use of Domestic Wastewaters Using Integrated Algal Ponding Systems: A Key Strategy in Sustainable Sanitation

SALINITY, SANITATION and SUSTAINABILITY
Biotechnology of Saline and Sewage Wastewater

.

Report 14: Volume 1 - Integrated Physical, Chemical and Biological Process Kinetic Models for Anaerobic Digestion of Primary Sewage Sludge

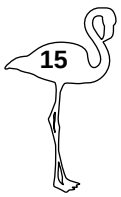

Report 15: Volume 2 - Integrated Beneficiation of Mine Wastewaters

Cover Photograph:

Flamingoes on tannery wastewater ponds at Mossop Western Leathers Co., Wellington, South Africa. The presence of Phoenicopteridae, including both the Greater and Lesser Flamingo, is an important indicator of healthy and naturally functioning saline aquatic ecosystems. This flock occupied the ponding system shortly after commissioning the novel *Spirulina*-based Integrated Algal Ponding System which had been developed for the treatment of tannery wastewaters. This apparent seal of environmental approval became an icon for the studies which followed in this series.

Photograph by Roger Rowswell, whose observation of this system, over a number of years, was instrumental in the initiation of these studies.

SALINITY, SANITATION AND SUSTAINABILITY:

BIOTECHNOLOGY OF SALINE AND SEWAGE WASTEWATER CO-TREATMENT

VOLUME 1

Integrated Physical, Chemical and Biological Process Kinetic Models for Anaerobic Digestion of Primary Sewage Sludge

NE Ristow, SW Sötemann, S Rajkumar, MC Wentzel, CJ Brouckaert, CA Buckley,
GA Ekama and PD Rose

Report to the
Water Research Commission

by

Water Research Group, Department of Civil Engineering,
University of Cape Town
Pollution Research Group, Department Chemical Engineering,
University of KwaZulu-Natal
Environmental Biotechnology Research Unit,
Rhodes University

WRC Report No. TT 393/09

April 2009

Obtainable from:

Water Research Commission
Private Bag X03
Gezina
0031

The publication of this report emanates from a project entitled: *"Biotechnological co-treatment of saline and sewage wastewaters with integrated recovery and reuse of water and organic and inorganic components for sustainable development'* (WRC Project K5/1456).

ISBN 978-1-77005-833-4
Set No. 978-1-77005-855-2

Printed in the Republic of South Africa

PREFACE

Sustainable development is, in an important sense, technologically dependent. Thus the ability to manage and treat a range of complex wastes plays a determining role in the health, and hence the long-range sustainability, of the environment in which the development takes place. Salinity is one such complex problem that has become an increasing threat to the water-scarce, inland industrial development of South Africa.

The Water Research Commission (WRC) has funded an innovative response to the problem which has focused on the synergies available in the co-treatment of saline and domestic wastewaters. The development of novel biotechnological processes in a number of WRC projects (such as the Rhodes BioSURE® Process treating acid mine drainage) has targeted the recovery from the saline sewage co-treatment operation of not only treated water, but also value-added products which may impact the financial viability of the remediation exercise. The core process technology opens up possibilities for development scenarios in which social, economic and environmental interests ("Tripple Bottom Line" economics) could be managed in an integrated manner. This would enable incorporating domestic sanitation, industrial pollution control, water resource provision to a range of users and stimulation of community economic activities and thereby also ensuring environmental protection.

The project reported here has been undertaken to advance individual key aspects of the saline sewage co-treatment research programme initiated at Rhodes University and has been managed as a collaborative research effort including the Environmental Biotechnology Research Unit and Anthropology Department (Rhodes University), Department of Civil Engineering (University of Cape Town), the Pollution Research Group (University of KwaZulu-Natal), Pulles Howard & de Lange Inc., Public Domain Management and the ERWAT Water Care Company. The research project consisted of four separate parts and the results of the studies undertaken have been published in a two-volume series as outlined below.

PART 1. An exploratory study of potential in using saline wastewaters for the reticulation and treatment of domestic and industrial wastewaters. This report includes a review of current thinking and practice in dual reticulation systems and a preliminary evaluation of the use of Integrated Algal Ponding Systems for the treatment of such wastewaters. The potential for a more detailed follow-up programme in this area has been considered. This investigation has been reported in WRC Reports TT 402/09 and 403/09.

PART 2. Further development of the Rhodes BioSURE® Process for the co-treatment of mine wastewater utilising sewage sludge as an organic carbon source. A detailed investigation of process kinetics was undertaken and the mathematical modelling of the constituent processes has been reported in Volume 1 of this series. This part of the project has combined the outputs of a number of other WRC projects relating to the modelling of Anaerobic systems and in doing this has emerged as a major study in its own right titled "Integrated Physical, Chemical and Biological Process Kinetic Models for Anaerobic Digestion of Primary Sewage Sludge". This report constitutes an important contribution to an understanding of both sulphidogenic and methanogenic systems.

Downstream treatment of sulphidic wastewaters generated in the Rhodes BioSURE® Process was also investigated. The biofilter component of this study has been reported together with WRC

Projects K5/1169 & 1291 and the sulphide oxidation study together with WRC Projects 1078, 1336 & 1545.

PART 3. Investigation of the potential for a novel development of hybrid mine wastewater treatment technology to bridge the gap between active and mine closure operations. This study has been reported but due to novelty implications will not be published until further process development has been undertaken.

PART 4. Investigation of the feasibility of the Integrated Community Benefit concept in which treated mine waters may be used in horticultural enterprise development and thus provide sustainability in the mine operation and closure environments. An industry review was undertaken including a report on the technical, business and economic, and the community components of the Minewater reuse Waste Beneficiation concept. A case study on the application of the system was investigated in the Eastern Gauteng region. This study has been reported in Volume 2 of the series.

The WRC Project 1456 has thus complemented and supported a number of investigations undertaken concurrently in closely associated WRC Research Projects related to technology development in Sewage and Saline Wastewater co-treatment. In providing incremental steps in a number of key areas, the overall objective of Waste Beneficiation has been advanced in which technology provides an enabling platform for wastes to be managed as resources with economic potential rather than as a dead cost to both the community and the environment.

Peter Rose

Project Leader

EXECUTIVE SUMMARY

1. BACKGROUND

Acid Mine Drainage (AMD) is characterized by high concentrations of heavy metals, sulphate and total dissolved solids, coupled with a low pH (Christensen *et al.*, 1996). The Rhodes BioSURE® Process has been developed as a low cost active treatment of AMD waters (Rose *et al.*, 2002). The core unit process in this system is biological sulphate reduction using primary sewage sludge (PSS) as the electron donor and organic carbon source, with the concomitant production of sulphide and carbonate alkalinity. PSS is available as a by-product at municipal wastewater treatment plants, and this co-disposal proposal provides an elegant solution to biological sulphate reduction.

To aid the design, operation and control of (and research into) the biological sulphate reduction unit process, a mathematical model would be an invaluable process evaluation tool. Mathematical models provide quantitative descriptions of the treatment system of interest that allow predictions of the system response and performance to be made. From these predictions, design and operational criteria can be identified to optimize the system performance. Also, mathematical models are very useful as research tools. By evaluating the model predictions, it is possible to test hypotheses on the behaviour of the system (e.g. biological processes, their response to system constraints, etc.) in a consistent and integrated fashion. In essence, mathematical models provide an integrated framework for the system which can give guidance to design, operation and research.

2. OBJECTIVES

Recognising the potential usefulness of a mathematical model to describe biological sulphate reduction with PSS as substrate, the Research Groups at the University of Cape Town (UCT) and the University of KwaZulu-Natal (UKZN) were subcontracted by Rhodes University to develop a kinetic model for biological sulphate reduction with PSS. This formed part of a broader research project between the Water Research Commission (WRC) and Rhodes University, K5/1456 "Biotechnological co-treatment of saline and sewage wastewaters with integrated recovery and re-use of water and organic and inorganic components for sustainable development", falling under Part 2 of the research project: "Part 2: Bio-sulphidogenic Sewage Treatment". The principle objective for the contribution by the UCT and UKZN Water Research Groups to the research contract was:

- ***The development of a kinetic based integrated biological, physical and chemical processes model for BioSURE type systems***

The aims of this kinetic model were to:

- Improve understanding of the underlying processes in these systems
- Identify the main compounds of importance
- Apply the model for system optimisation and design

The kinetic model was to be developed within both the AQUASIM and WEST simulation platforms.

The approach taken in model development was:

- To develop a more general model structure that has wider application to anaerobic digestion systems, with and without sulphate reduction and/or methanogenesis, or with both methanogenesis and sulphidogenesis

This required that the underlying chemical, physical and biological processes in all three anaerobic digestion types (methanogenic, acidogenic and sulphidogenic) with sewage sludges as substrate be identified and quantified, as well as the interactions with the environment. This in turn required both an experimental and modelling research component.

3. EXPERIMENTAL

3.1 Primary sewage sludge (PSS) hydrolysis

The objective of this section of the research was to gather experimental data to improve understanding of the basic biological, chemical and physical processes involved in methanogenic and sulphidogenic anaerobic digestion of PSS. This understanding was to be used to inform formulation of the integrated biological, physical and chemical processes kinetic models for methanogenic and/or sulphidogenic digestion of PSS (see below). The experimental data would also form the basis for calibration and validation of the kinetic models.

To generate the required experimental data, laboratory-scale stirred tank reactor (STR) anaerobic digesters have been operated. STR anaerobic digesters were selected, since in these systems:

- the bioprocesses and not the physical constraints dominate, making it easier to identify and model the bioprocesses operative in methanogenic and sulphidogenic systems;
- the PSS hydrolysis and solubilisation rates can be observed and quantified more directly and readily, as also
- the effect of sulphate and sulphate reduction on these rates.

A series of six parallel laboratory-scale STR bioreactors were commissioned. These bioreactors were operated with PSS as feed, at varying retention times and feed COD concentrations, to determine the effects of these parameters on the rates of PSS degradation. For each set of operating conditions, the bioreactors were allowed to reach a steady state, prior to data collection and were also allowed to attain their steady state operating pH, which was monitored, or had the pH controlled to a set value. The STR anaerobic digesters were operated under three “modes” – methanogenic, acidogenic and sulphidogenic, to quantify the PSS degradation under each mode of operation.

3.1.1 Methanogenic systems

Completely mixed methanogenic anaerobic digesters were operated at hydraulic retention times (= sludge retention time, SRT) from 5 to 60 d, with feed COD concentrations of 2, 9, 13, 25 and 40 g COD/P, at a controlled temperature of 35 EC, see Table 1.

For each feed COD concentration, the system hydraulic retention time was decreased step-wise until methanogenesis became unstable. At regular retention time intervals steady state periods were maintained and analysed. For these steady states:

- COD mass balances were performed to evaluate the integrity of the data. Typically, a mass balance of between 95 and 105% would be acceptable, and with only one exception, all the COD balances (most critical for these experiments) were within this range. The good COD recoveries lend credibility to the experimental data.
- Reactor (= effluent) volatile fatty acids (VFA) concentrations were below 50 mg/P (as HAc), and for most steady states considerably less than this. This provides support for stable methanogenic operation.

Table 1: Operating conditions under which **methanogenic** steady state anaerobic digestion of primary sewage sludge experimental data has been collected.

Feed COD (g/P)	**Hydraulic Retention Time (d)**							
	60	**20**	**15**	**10**	**8**	**6.6**	**5.7**	**5**
40			X	X	X	X	X	
25		X	X	X	X	X	X	X
13			X	X	X	X	X	
9	X							
2				X	X			

In analysing the data it became evident that:

- Characterisation of the primary sewage sludge (PSS) is essential in order to quantify the PSS hydrolysis rate.
- Consistent trends in the effects of SRT and PSS feed concentrations were evident, substantiating data consistency.

A simplified mass balance based steady state model was developed to evaluate and determine the hydrolysis kinetics and associated rate constants. In application of this model:

- The 60 d retention time system was used to determine the unbiodegradable particulate fraction of the PSS, and gave an unbiodegradable particulate COD fraction of 33.45%. Alternative analytical techniques (Sötemann *et al.*, 2005a, b) gave the unbiodegradable particulate fraction of the COD as 33.3% for the entire data set, and hence the value of 33.45% was accepted. This value corresponds closely with the value of 36% obtained for the data of O'Rourke (1968), and is close to the value expected from a mass balance around the primary settling tank with typical South African raw and settled wastewater characteristics.

From the experimental data, for the kinetics of PSS hydrolysis, various rate formulations were evaluated, first order, first order specific, Monod and surface reaction (Contois). From an assessment of the fit of predicted to measured values, it was concluded that:

- The first order kinetics and surface reaction kinetics most accurately predict the rate of PSS hydrolysis under methanogenic conditions for all hydraulic retention times and feed COD concentrations evaluated.
- Since first order kinetics are a simplification of the hydrolysis process (the acidogenic

biomass is not explicitly included, nor is there an upper limit to the rate), surface reaction kinetics are the most appropriate rate formulation for PSS hydrolysis, in agreement with the hydrolysis kinetics incorporated in the anaerobic digestion model (see below).

- However, due to the simplicity of first order kinetics, and since these kinetics were able to accurately predict the PSS hydrolysis rate under all operating conditions, first order kinetics were used in this study to compare the PSS hydrolysis rates under the different operation conditions.
- With the first order kinetics and a first order kinetic constant value of 0.992 d^{-1}, and an unbiodegradable particulate COD fraction of 33.45% of the total feed COD concentration, very close correlation was obtained between model predicted and calculated (from experimental data) volumetric rates of PSS hydrolysis and predicted and measured effluent COD concentrations under methanogenic conditions for all hydraulic retention times and feed COD concentrations, see Figures 1 and 2 respectively.

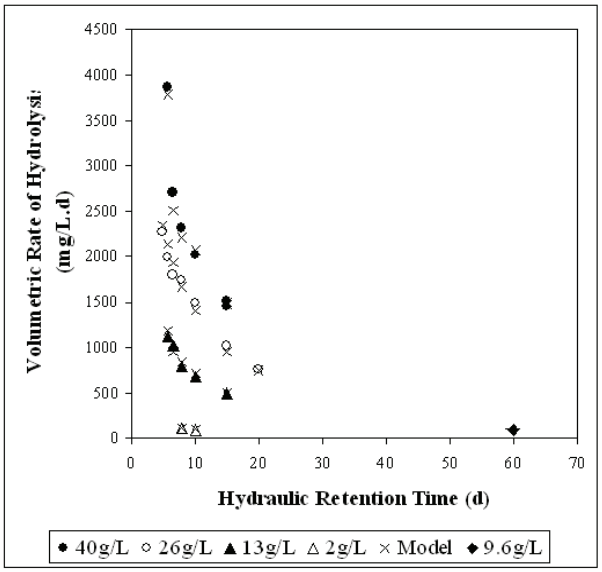

Figure 1: Calculated (from experimental data) and predicted (first order kinetics) rate of hydrolysis for each hydraulic retention time at each feed COD concentration for methanogenic systems.

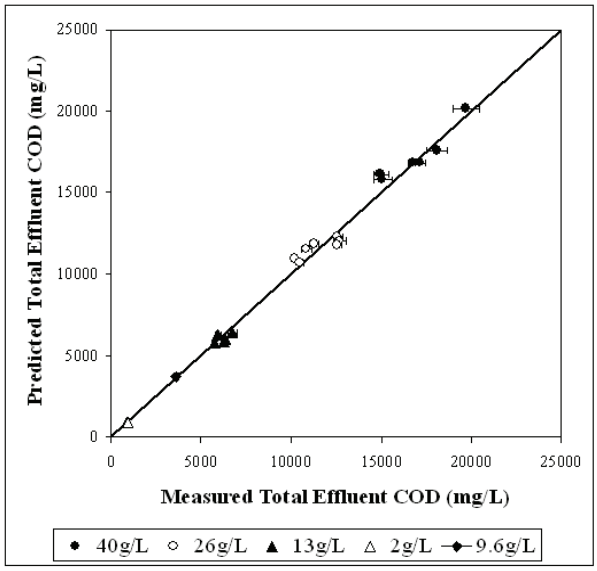

Figure 2: Predicted versus measured total effluent COD concentration for each feed COD concentration and hydraulic retention time for methanogenic systems.

The model, as calibrated above, was applied to the data collected in the independent study of O'Rourke (1968); close correlation was obtained at the longer retention times, i.e. methanogenic systems, see Figure 3:

- The good fits of the model predictions to the data collected in this and the study of O'Rourke (1968) provides powerful evidence validating the model.

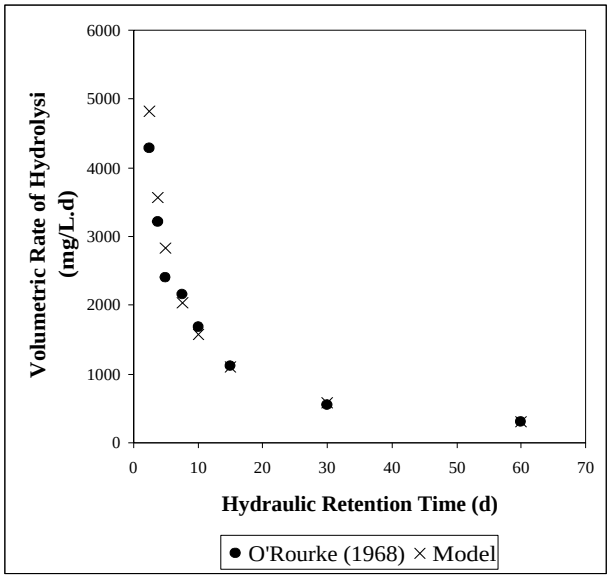

Figure 3: Calculated (from experimental data) and predicted (first order kinetics) rate of hydrolysis for each hydraulic retention time for the data of O'Rourke (1968).

From an extensive investigation into the effects of pH on methanogenic anaerobic digesters:

- The minimum operating pH for methanogenic systems was determined to be 6.38 before methanogenesis failed.
- Increasing the operating pH above 6.38 had no effect on the PSS hydrolysis rate (pH = 6.38, 6.5, 7.0, 7.5, 8.0).

The methanogenic systems formed the "base line" against which the performance of the sulphidogenic and acidogenic systems could be evaluated.

3.1.2 Acidogenic systems

Acidogenic systems were operated under varying hydraulic retention times (3.33-10 d) and feed COD concentrations (2-40 g cod/P) at a constant temperature of 35^{o}C, Table 2.

Table 2: Operating conditions under which **acidogenic** steady state anaerobic digestion of primary sewage sludge experimental data has been collected.

Feed COD Concentration (g cod/P)	**Hydraulic Retention Time (d)**		
	10	**5**	**3.33**
40		X	X
13	X	X	X
2	X	X	X

At each retention time and feed concentration, steady state periods were identified and analysed in detail:

- Very good COD mass balances were obtained (92-103%). This lends credibility to the experimental data.
- Negligible methane gas productions were recorded.

The two observations above substantiate the acidogenic condition, i.e. no methanogenesis.

For each steady state of operation, the volumetric rate of hydrolysis was calculated:

- For systems fed the same feed COD concentration and operating at the same hydraulic retention time, the volumetric rates of hydrolysis ***were significantly lower*** under acidogenic conditions compared with the corresponding methanogenic conditions.

In applying the first order PSS hydrolysis kinetics developed for the methanogenic systems to the acidogenic systems:

- The value of the first order rate constant (k_h) had to be decreased significantly, substantiating the lower hydrolysis rate.
- The first order kinetic constant for acidogenic conditions (k_h) is linearly dependent on the hydraulic retention time; the relationship was formulated to give:

- $k_h = 0.0883 - 0.0055.R_h$ (1)
- where R_h is the retention time (d)
- The formulation above indicates that increasing R_h decreases the PSS hydrolysis rate.
- With the formulation above to calculate the value of the first order kinetic constant under acidogenic conditions (Eq 1), the model was able to reasonably accurately predict the rate of PSS hydrolysis under acidogenic conditions.

To investigate the influence of pH on PSS hydrolysis under acidogenic conditions, further acidogenic steady state systems were operated at a constant hydraulic retention time (5d) and a constant feed COD concentration (2 g cod/P), but with the digester operating pH controlled, and increased from the minimum pH 5 (steady state pH), to 8 at pH intervals of 1 (5.0, 6.0, 7.0, 8.0):

- The calculated rate of PSS hydrolysis under acidogenic conditions did not change when the pH was increased from 5 to 6.
- However, when the pH was increased from 6 to 8, the observed rate of PSS hydrolysis increased linearly.
- To include the effect above in the first order kinetics, the value for k_h had to be modified:

$$k_h = (0.0883 - 0.055.R_h) + 0.06\left(\frac{pH - pH_{LL}}{pH_{UL} - pH_{LL}}\right) \quad (2)$$

where $pH_{LL} = 6.04$ and $pH_{UL} = 8.0$.

With the modification above, first order kinetics was able to accurately predict the volumetric rate of PSS hydrolysis under acidogenic conditions for all operating pH values.

3.1.3 Sulphidogenic systems

To quantify the rate of PSS hydrolysis under sulphate-reducing conditions and compare this rate with that for methanogenic systems, where possible these systems were operated in parallel digesters, Table 3.

Table 3: Sulfate-reducing steady states and corresponding methanogenic systems (Table 1) at various operating conditions (retention times, feed COD and sulfate concentrations, operating pH and sulphide concentrations)

Steady state number	Operating conditions				Comparative steady state number
	R_h (d)	Feed COD (g/P)	Feed SO_4 (g/P)	Additional factors	
6	10	26	1	Excess COD	1
15	8	13	9.6	All S_t as FeS	14
16	8	13	9.6	No Fe addition	14 and 15
20	8	2	2	pH ~ 7.5	18 and 37
22	8	2	2	pH ~ 7	19
36	8	2	2	pH ~ 6.5	27
41	16	2	2		
42	13.3	2	2		
46	10	1	1		
47	8	2	2	pH ~ 8.3	

Results from the initial experiments with limited sulphate reduction (1 g SO_4/P with PSS feed at 26 g cod/P) showed that:

- The sulphate reduction did not influence the PSS hydrolysis rate compared with a parallel purely methanogenic system.
- Methanogenesis was maintained in the digester. Therefore, a limited amount of sulphate reduction in methanogenic systems does not inhibit the hydrolysis nor methanogenesis processes, and hence limited sulphate containing wastes can be treated in existing methanogenic digesters without jeopardising the process stability.

When the feed sulphate concentration was increased (9.6 g SO_4/P with PSS feed at 13 g cod/P):

- No methanogenesis was observed.
- Sulphate-reducing biomass out competes the methanogenic biomass for organic substrate.
- Under sulphate-reducing conditions with low aqueous sulphide (precipitated with ferrous), the volumetric rate of PSS hydrolysis ***was the same*** as for the parallel methanogenic system.
- When the aqueous sulphide was not removed, sulphate reduction was inhibited, but no information regarding the PSS hydrolysis rate was collected.

From the observations above, it can be concluded that:

- High aqueous sulphide is inhibitory to sulphate reduction.

A range of systems were operated at PSS feed COD concentrations of 2 g cod/P and feed sulphate concentrations of 2 g SO_4/P, at varying retention times (8, 13.3 and 16 d):

- In all systems, sulphate was slightly in excess and effluent VFA concentrations were low (< 50 mg HAc/P), indicating absence of inhibitions. Thus, at lower aqueous sulphide concentrations, sulphate reduction is not inhibited.

For all sulphidogenic systems described above, the first order rate formulation calibrated under methanogenic conditions (k_h = 0.992d^{-1} and 33.45% unbiodegradable particulate COD fraction) was able to adequately predict the rate of PSS hydrolysis under sulphate-reducing conditions.

- The observation above led to the conclusion that the PSS hydrolysis rate is closely similar under methanogenic and sulphate-reducing conditions, ***i.e. sulphate reduction per se does not appear to influence the PSS hydrolysis rate***.

Further investigation and analysis of the data showed that:

- An operating pH between 6.5 and 7.5 did not affect the rate of PSS hydrolysis under sulphate-reducing conditions.
- The mean COD:SO_4 utilisation ratio in the sulphate-reducing systems was 0.8 g cod/g SO_4, closely similar to 0.78 g cod/g SO_4 obtained by Enongene (2003). These ratios are significantly higher than the theoretical stoichiometric ratio of 0.67 g cod/g SO_4. However, taking into account COD utilization for the production of acidogen and sulphate-reducing biomasses, the theoretical ratio should be approximately 0.85 g cod/g SO_4, which is very close to the measured values.

- The effluent suspended solids concentration was significantly higher for sulphate-reducing systems compared with methanogenic systems (Figure 4), and the operating pH did not affect this concentration.
- This has significant implications for sulphate-reducing systems in which solids and hydraulic retention times are uncoupled, as retention of sulphate-reducing biomass and PSS biodegradable particulate substrate may prove problematic.

For acidogenic systems, the suspended solids concentration increased with increasing pH, Figure 4.

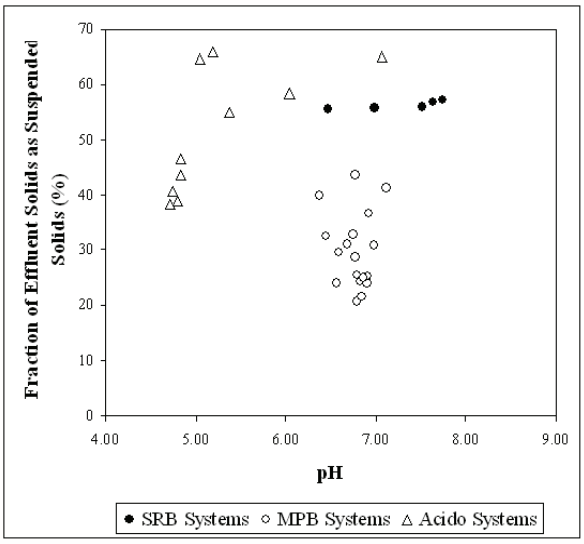

Figure 4: Ratio between the effluent suspended solids COD concentration and the effluent total particulate COD concentration (f_{SS}) for methanogenic (MPB), acidogenic (Acido) and sulphate-reducing (SRB) systems as a function of pH.

3.1.4 Comparison of PSS hydrolysis rates under methanogenic, acidogenic and sulphate reducing conditions

From a comparison of the PSS biodegradable particulate COD conversions for the systems operated in this study under methanogenic, acidogenic and sulphate reducing conditions, together with the methanogenic and acidogenic systems operated by O'Rourke (1968) (see Figure 5), it was concluded that:

- The data gathered in this study, and substantiated by the observations of O'Rourke (1968) clearly indicates that the presence of methanogenesis substantially increases the rate of PSS hydrolysis, or conversely, the absence of methanogenesis and conditions created by acidogenesis substantially reduces the rate of PSS hydrolysis.
- The effect above is not pH related; the effect of pH on PSS hydrolysis rates under acidogenic conditions is relatively small and could not account for the magnitude of the reduction in PSS hydrolysis rates.
- Under the conditions which the sulphate reducing systems were operated (sulphide not inhibitory), compared with the equivalent methanogenic systems, ***sulphate reduction per se does not influence the rate of PSS hydrolysis***. However, as for the methanogenic systems, the presence of sulphate reduction significantly increases the rate of PSS hydrolysis compared with acidogenic conditions.

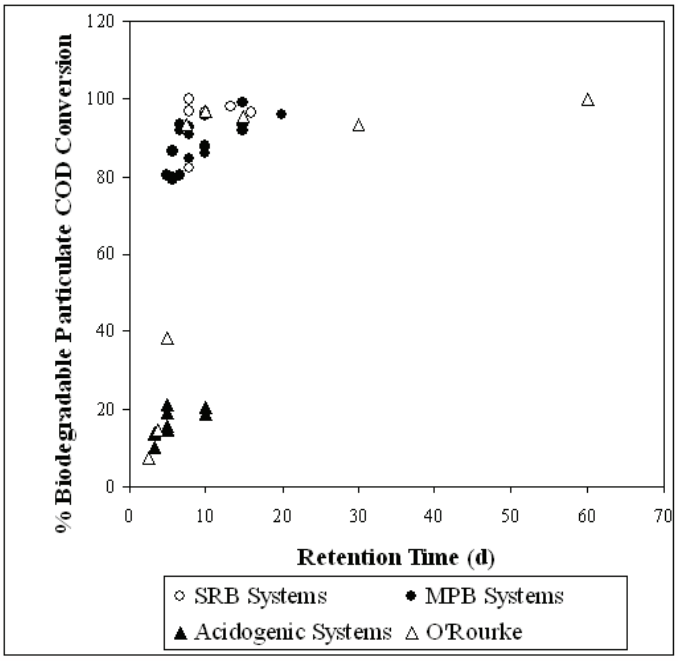

Figure 5: Biodegradable particulate COD conversions (as a % of influent PSS biodegradable particulate COD) versus retention time for the methanogenic (3.1.1), acidogenic (3.1.2) and sulphate reducing (3.1.3) systems operated in this study, and the systems operated by O'Rourke (1968).

3.1.5 Conclusions

In this part of the research, an extensive data set has been collected on anaerobic digestion of PSS under methanogenic, acidogenic and sulphate-reducing conditions, at varying retention times, feed concentrations and pH values. Through a strict attention to detail, the operating conditions for all systems were carefully controlled and completely defined.

To quantify the volumetric rate of PSS hydrolysis in such systems, a logical mathematical framework has been developed in terms of mass balance principles and characterisation of the PSS feed. This framework should provide (as shown here) a useful, common and systematic basis for comparisons of the hydrolysis rates for different systems. Further, a simple unified first order kinetics based model has been developed to describe PSS hydrolysis under methanogenic, acidogenic and sulphate-reducing conditions. This model takes into account the effects of retention time, feed COD concentration and pH, and the model has been validated both on data collected in this study and on data collected in independent studies.

Since PSS hydrolysis is the rate-limiting step in most methanogenic, acidogenic and sulphate-reducing systems, the subsequent processes are essentially stoichiometric. Hence, this simple model should be a valuable tool in the design, operation and control of steady state digestion systems. However, the model cannot take account of digester failure or behaviour under dynamic loading conditions. These require development of a more extensive dynamic simulation model. In such a model, the evaluation here would suggest that surface reaction (Contois) kinetics are the most suitable for the PSS hydrolysis process, and this kinetics has been accepted in the kinetic model being developed for methanogenic and sulphidogenic anaerobic digestion of sewage sludges (see below). In this study, extensive data on transitions between steady states has been collected, which should prove useful for the calibration and validation of such a model.

In terms of the framework developed above, comparing the rates of PSS hydrolysis under methanogenic, acidogenic and sulphate-reducing conditions, ***the rates are closely similar under methanogenic and sulphate-reducing conditions, but significantly reduced under acidogenic conditions***. This implies that the products of PSS hydrolysis (and subsequent acidogenesis) inhibit the PSS hydrolysis rate. If these products are removed, then PSS hydrolysis remains uninhibited, irrespective of whether the biological process that removes the products is methanogenesis or sulphate reduction.

3.2 UASB system for biological sulphate reduction

3.2.1 Experimental Investigation

In the experimental investigation above into completely mixed sulphidogenic systems, particularly evident was the influence of the sulphate reduction on the effluent suspended solids concentrations – the sulphate reducing systems consistently produced effluents with higher suspended solids than the corresponding methanogenic systems, i.e. higher concentrations of solids that would not settle. This has significant implications for sulphate reducing systems in which the solids and hydraulic retention times need to be uncoupled (to reduce reactor volumes), as retention of sulphate reducing biomass and PSS biodegradable particulate substrate may prove problematic. Conceptually, passing the influent through the sludge bed may considerably improve the separation. One such system in which this occurs is the Upflow Anaerobic Sludge Bed (UASB) reactor. Accordingly, a study was undertaken to evaluate the feasibility of using the UASB system for biological sulphate reduction with PSS as substrate.

This feasibility study was conducted using a laboratory-scale UASB-type reactor for biological sulphate reduction with PSS as feed. The system was fed PSS at 1.6 g cod/P and sulphate at 1.2 g SO_4/P, and operated in an upflow configuration without recycle at hydraulic retention times below 12 h, with a sludge bed retention time below 5 h (bed volume controlled). Experimental results are listed in Table 3.

Table 3: Summary of preliminary results from BSR UASB system with PSS as influent substrate.

	Sample 1		**Sample 2**	
	Influent	**Effluent**	**Influent**	**Effluent**
Total COD (mg cod/P)[1]	1611	837	1666	853
Soluble organic COD (mg cod/P)	221	56	214	89
Particulate organic COD (mg cod/P)	1390	248	1452	236
Aqueous Sulphide (mg S/P)		266		264
Sulphate (mg SO_4/P)	1200	133	1200	86
Sulphate Conversion (%)		88.9		92.8
VFA (mg HAc/P)	96	0	88	31.9
Alkalinity (mg $CaCO_3$/P)	450	1883.2	680	1810.5

[1]Total COD = organic + sulphide COD

From Table 3:

- The residual sulphate concentration was below 135 mg SO_4/P and as low as 86 mg SO_4/P, with very low soluble organic COD in the effluent (< 90 mg cod/P), indicating near complete sulphate reduction.
- Effluent particulate COD concentration was < 250 mg cod/P, indicating successful sludge retention in the system, essentially overcoming this problem identified above.

Particularly evident in the operation of the UASB system was the good solids liquid separation, giving a well defined sludge bed, see Figure 6.

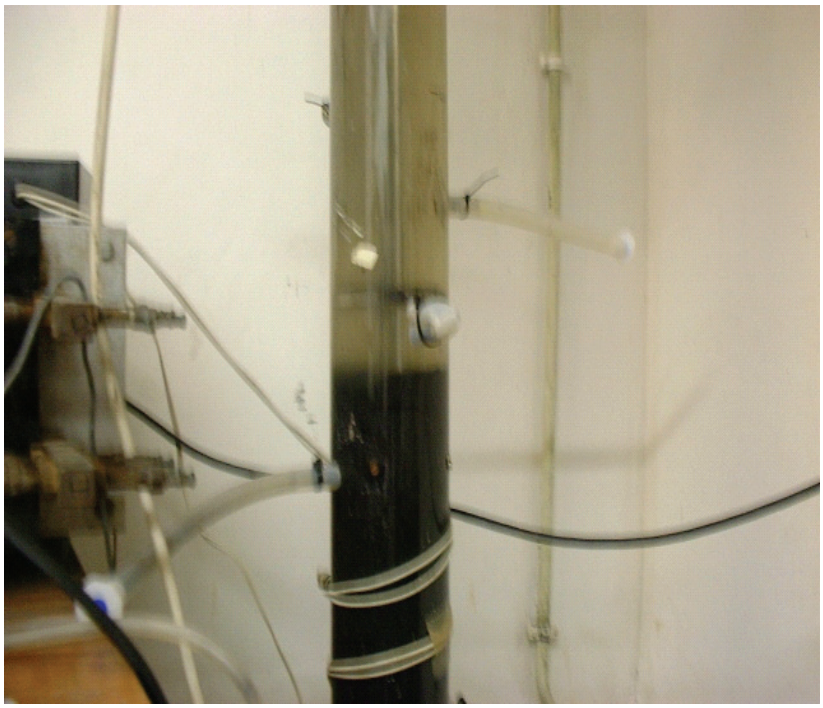

Figure 6: Sludge bed separation in the laboratory-scale USAB reactor.

These results were extremely encouraging, and it can be concluded that:

- The UASB reactor configuration is a feasible option for the treatment of large volumes of sulphate-rich water, such as acid mine drainage. Sludge bed retention times of less than 5 h seem attainable.
- A feed COD:SO_4 ratio of 1.33:1 g cod:g SO_4 is adequate for the removal of more than 90% of the feed sulphate without significant residual biodegradable organic COD concentrations.

Following the success in the feasibility study, a preliminary study on the internal dynamics in the sludge bed was undertaken, to better understand the processes operative. Concentration profiles were taken along the axis of flow through the sludge bed when the system was operating with a 6 hour bed hydraulic retention time, see Figure 7.

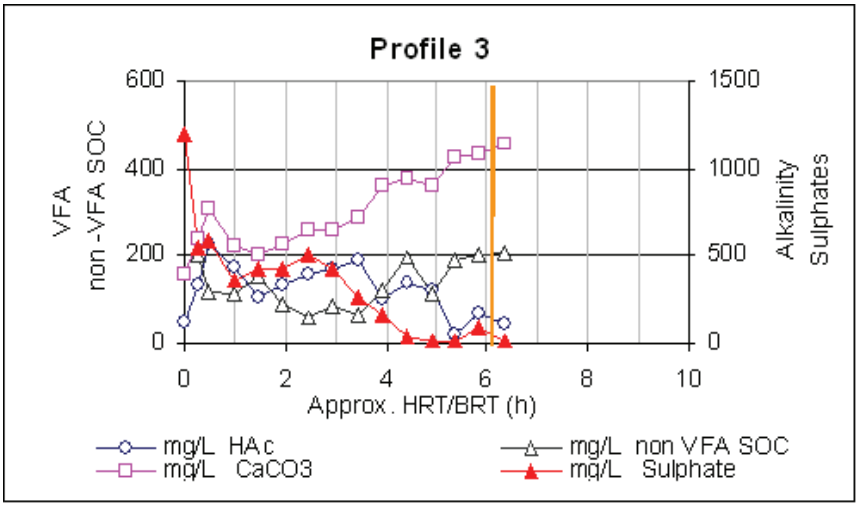

Figure 7: Profile taken along the axis of flow through the USAB reactor, receiving PSS as substrate and sulphate supplement.

From Figure 7, two regions in the sludge bed can be identified:

- In the bottom half of the bed, sulphate concentrations (and alkalinities) remain relatively constant, whereas VFA concentrations increase. This indicates that sulphate reduction is rate limiting, in this region of the bed.
- In the top half of the bed, sulphate and VFA concentrations decrease rapidly, to near zero at the exit from the sludge bed, while alkalinities increase rapidly. This indicates that hydrolysis is rate limiting, in this region of the bed.

Again, extremely encouraging results were obtained: Good bed separation and sulphate reductions were obtained. From this investigation, it can be recommended that:

- The sludge bed be recycled – this will seed sulphidogens from the top half of the bed to the bottom, initiating sulphate reduction further down the bed profile.

Clearly, this possibility warrants further research attention, and a more detailed study on sulphate reduction in UASB reactors with PSS as substrate will be undertaken at UCT, examining *inter alia* minimum bed hydraulic retention times, sludge retention times, bed dynamics, sludge recycles.

4. MODELLING

To aid the design, operation and control of (and research into) anaerobic digestion, mathematical models are invaluable system evaluation tools. Mathematical models provide quantitative descriptions of the treatment system of interest, enabling predictions of the system response and performance to be made. From the predictions, design and operational criteria can be identified for optimization of the system performance. Also, mathematical models are very useful as research tools. By evaluating the model predictions, it is possible to test hypotheses on the behaviour of the system (e.g. biological processes, their response to system constraints, etc.) in a consistent and integrated fashion. Hence, the objective of developing a mathematical model for the BioSURE®, and similar, systems. In developing such a model, the approach taken has been to:

- Develop a more general model structure that has wider application to anaerobic digestion systems, with and without sulphate reduction.

A variety of mathematical models have been developed to describe anaerobic digestion. However, these models largely have focussed on the biological processes operative in an anaerobic digester. This implicitly accepts that the biological processes take place within a regime of constant pH, and that chemical and physical processes (e.g. mineral precipitation and gas stripping) are insignificant compared with the biological processes, and accordingly can be neglected. However, in anaerobic digestion since short chain fatty acids (SCFA) are produced as the main intermediates, and in sulphate reduction the weak acid/bases sulphate and sulphide are consumed and produced respectively, the assumption of a constant pH regime may not be valid. Furthermore, pH has a significant impact on the processes: Many of the biological processes have been shown to be very sensitive to pH changes and/or to undissociated weak acid/base species, the concentrations of which are pH controlled. Hence, inclusion of pH as a parameter in some fashion in anaerobic digestion models would greatly extend, and provide greater surety in, model application. Including pH requires inclusion of compounds not directly involved in the biological processes, but in pH regulation. This would be of benefit since these compounds would enable determination of the mass parameter alkalinity, routinely used by many operators as a measure of predicting the state of health of anaerobic digesters.

Consequently, the kinetic model to be developed included two phase (aqueous and gas) processes for:

- weak acid/base chemistry
- biological processes for methanogenic anaerobic digestion of primary sludge
- biological sulphate reduction
- gas stripping

The model also needed to take account of interactions between the processes above.

The kinetic model was to be developed by the UCT Research Group in two main stages: 4.1 Methanogenic anaerobic digestion model, and 4.2 sulphidogenic anaerobic digestion model. The developed models were to be incorporated into 4.3 the WEST® platform by the UKZN Research Group.

4.1 Methanogenic anaerobic digestion model

An integrated mixed weak/acid base chemistry and biological processes methanogenic anaerobic digester model was required, formulated into AQUASIM®. This was achieved by integrating the biological kinetic processes of anaerobic digestion with 2 (aqueous/gas) of the 3 phases of the kinetic mixed weak acid/base model of Musvoto *et al.* (1997, 2000a,b,c) (solid phase excluded). The approach adopted in the model development of integrating the kinetics of weak acid/base chemistry with the biological processes has a number of advantages: It (i) greatly simplifies including pH ***directly*** (via H^+) in the anaerobic digestion model, (ii) is general and can be applied to include any additional weak acid/ base system of interest, and (iii) facilitated integrating the kinetics of biological sulphate reduction and its interactions with the weak acid/base chemistry (see Section 4.2).

In the model, the approach of characterising the sewage sludge into carbohydrates, lipids and

proteins, as is done in the IWA anaerobic digestion model no. 1 (ADM 1, Batstone *et al.*, 2002), requires measurements that are not routinely available on sewage sludges. Furthermore, this type of approach would require division of the carbohydrates, lipids and proteins into biodegradable and unbiodegradable fractions, a difficult undertaking for even ideal pure substrate mixes. Instead, the sewage sludge was characterised into the COD and its constituents (unbiodegradable particulate and soluble, biodegradable particulate, soluble fermentable and volatile fatty acids), and the carbon (C), hydrogen (H), oxygen (O) and nitrogen (N) composition of the particulates; it was envisaged that the elemental composition of the primary sludges would remain approximately constant, precluding repetitive composition analysis. The model was formulated in mole units, based on conservation of C, H, O, N and COD. The kinetics and stoichiometry for the biological processes mediated by the organism groups acidogens, acetogens, acetoclastic methanogens and hydrogenotrophic methanogens were included. Also, the kinetics and stoichiometry for the weak acid/base chemistry for the ammonia, carbonate, phosphate, acetate and water systems were included. Further, gas exchanges for carbon dioxide, ammonia, methane and hydrogen were considered, with the kinetics for carbon dioxide exchange and ammonia stripping included.

The resultant model was calibrated with kinetic and stoichiometric constants from the literature where available, appropriately modified to take account of the inclusion of specific weak acid/base species in the rate formulations. This left two parts of the methanogenic anaerobic digestion model that required calibration: (i) the kinetic constants for the hydrolysis process rate expressions, and selection of the most appropriate kinetic formulation and (ii) the sewage sludge CHON composition. Additionally, in model application the sewage sludge constituent fractions and input concentrations of the various compounds needed to be quantified. Assessment of hydrolysis kinetics and obtaining values for the various parameters were by interactive analysis of and model application to the experimental data set of Izzett *et al.* (1992). The Izzett *et al.* mesophyllic anaerobic digesters were operated from 7 to 20 days sludge age and fed a sewage primary and humus sludge mixture. These digesters yielded COD mass balances between 107-109% and N mass balances between 91-99%, and hence the experimental data could be accepted as reasonable. Assessment of different formulations for the PSS hydrolysis rates, included first order, first order specific, Monod and surface reaction (Contois) kinetics. This evaluation indicated surface reaction (Contois) kinetics as the most appropriate for the kinetic model, in agreement with the conclusion in Section 3.1 and with its widespread application in activated sludge systems acting on the same biodegradable particulate organics, but first order as simpler for data analysis. Accordingly, in the developed kinetic model the surface reaction kinetics has been implemented for PSS hydrolysis and found to exhibit the required sensitivity of unfiltered effluent COD to variation in retention time.

For the Izzett *et al.* data set, the sewage sludge was found to be 64-68% biodegradable (depending on the kinetic formulation selected for the hydrolysis process) which is similar to that expected from a mass balance around the primary settling tank, and to have a $C_{3.5}H_7O_2N_{0.196}$ composition. For the selected hydrolysis kinetics of surface mediated reaction (Contois), with a single set of kinetic and stoichiometric constants, for all retention times good correlation was obtained between predicted and measured results for (i) COD (ii) free and saline ammonia (FSA), (iii) short chain fatty acids (SCFA), (iv) $H_2CO_3^*$ alkalinity and (v) pH of the effluent stream, and (vi) CO_2 and (vii) CH_4 gases in the gas stream. The measured composition of primary sludge from two local wastewater treatment plants ranged between $C_{3.38}H_7O_{1.91}N_{0.21}$ and $C_{3.91}H_7O_{2.04}N_{0.16}$. The predicted composition is therefore within 5% of the average measured composition providing persuasive validation of the model.

The kinetic model was further validated through application to the data collected by Ristow *et al.* (2005a) on 20 steady state methanogenic anaerobic digesters fed PSS (see Section 3.1.1). Input

PSS composition was that determined by measurement and elemental analysis for each feed batch to give an average $C_{4.17}H_7O_{2.63}N_{0.22}$, which is higher than the values for the Izzett *et al.* data, but this minor difference probably arises due to the humus and PSS mixture used by Izzett *et al.* and the "pure" primary sludge used by Ristow *et al.* The unbiodegradable particulate (0.335) and soluble (0.008) COD fractions were obtained from the 60 d retention time system operated by Ristow *et al.* With a single set of kinetic and stoichiometric constants, for most retention times and influent COD concentrations, close correlation was obtained between predicted and measured (i) COD (ii) free and saline ammonia (FSA), (iii) short chain fatty acids (SCFA), (iv) $H_2CO_3^*$ alkalinity and (v) CH_4 gas production, but the model tended to under-predict the (vi) CH_4 gas composition (i.e. over-predict the CO_2 gas composition) and (vii) pH of the effluent stream. This application confirmed the suitability of the surface saturation kinetics for PSS hydrolysis.

The kinetic model validations above are for steady state only, which validates the rate limiting process, hydrolysis, and stoichiometry. However, the model was extended to include the dynamics of digester failure, by incorporating pH inhibition of the methanogens (hydrogen partial pressure effects already included). The model exhibited the expected sensitivity to a digester upset caused by a temporary inhibition of acetoclastic methanogens, and demonstrated that even a brief inhibition causes irreversible failure of the digester (pH < 6.6).

From this study, it would appear that the integration in a kinetic manner of the two phase mixed weak acid base chemistry, physical and biological processes of methanogenic anaerobic digestion has provided a sound basis for further model development. In particular, it enabled including biological sulphate reduction and associated processes (see Section 4.2), and will facilitate including the third solid phase in future kinetic models.

4.2 Development of a sulphidogenic kinetic model

Required was the development of a kinetic model for biological sulphate reduction (BSR). This necessitated development of the kinetics and stoichiometry for the biological, chemical and physical processes in BSR in two phases (aqueous/gas), and integration of these with the methanogenic anaerobic digestion model (Section 4.1 above). For the biological processes, identified from the literature for inclusion were:

1 Propionate degrading sulphate reducing bacteria (SRB)
2 Acetate degrading SRB
3 H_2 utilising SRB

Not required in the model:

4 Butyrate degrading SRB – butyrate is not present in significant concentrations in sewage sludge anaerobic digestion systems.

The stoichiometries for the respective BSR growth processes were developed by adding the catabolic (derived from the literature, Kalyuzhni *et al.*, 1998) and anabolic stoichiometric reactions, and formulating these in terms of the true organism yield. The BSR organism group endogenous decay stoichiometries were extracted from the methanogenic anaerobic digestion model. From the literature (Kalyuzhni *et al.*, 1998), Monod kinetics were accepted for the growth processes, and first order kinetics for endogenous decay. Values for the biological constants were obtained from the literature (Kalyuzhni *et al.*, 1998).

The BSR processes both consume and produce weak acid/base species, and hence these and the associated weak acid/base chemistry required inclusion with integration of BSR into the

methanogenic anaerobic digestion model. Further, the compound H_2S is produced and the compound $H_2CO_3^*$ is both produced and consumed. Both these compounds have physical gas exchange processes with the atmosphere, and hence these processes also required inclusion with the integration.

The new "weak" acid/base systems introduced with the biological processes for sulphate reduction are the sulphate and sulphide systems. Kinetic processes for these weak acid/bases were developed, on the basis that the

(i) $H_2SO_4 \Omega HSO_4^- + H^+$ ($pK_{H2SO4/HSO4}$ .0), and

(ii) $HS^- \Omega S^{2-} + H^+$ ($pK_{HS/S}$. 17.4)

acid/base equilibria are essentially strong acid/base reactions with pK values well outside the normal operating pH range for sulphate reducing systems, and hence these equilibria do not require inclusion. Accordingly, the kinetic formulations for the following equilibria were developed for inclusion, based on the kinetic approach of Musvoto *et al.* (1997):

(i) $HSO_4^- \Omega SO_4^{2-} + H^+$ ($pK_{HSO4/SO4}$. 1.99)

(ii) $H_2S \Omega HS^- + H^+$ ($pK_{H2S/HS}$ .7.1)

The gas exchange processes associated with the sulphate reduction are ammonia, carbon dioxide, and sulphide. Of these, carbon dioxide and ammonia are already included in the methanogenic anaerobic digestion model. Hence, the kinetic formulations for the sulphide gas exchange $H_2S(aq) \Omega H_2S(g)$ was developed for inclusion, based on the approach of Sötemann *et al.* (2005a) for CO_2.

With all the chemical, physical and biological two phase (aqueous-gas) processes associated with BSR defined, it remained for these various processes to be combined, to develop an integrated kinetic model for BSR systems. This integration could be in two forms: To develop a two phase (aqueous-gas) chemical, physical and biological processes kinetic model with (i) BSR as the "sole" biological processes consuming the short-chain fatty acids (SCFA) and H_2 substrates, and (ii) both BSR and methanogenesis are present in competition for the SCFA and H_2 substrates. In both types of models, the substrate source being considered is PSS, and hence biological hydrolysis and acidification of the primary sludge by the acidogens required inclusion. For both types of integrated model, the compounds and processes of relevance have been identified, so also the source for the relevant kinetic and stoichiometric formulations.

This essentially provided a complete matrix for the integrated chemical, physical and biological processes BSR kinetic model in two phases (aqueous-gas). This model requires validation through application to experimental data sets. For this purpose, the data set described in Section 1.1.3 appears suitable, and this is currently being undertaken at UCT using AQUASIM: At the Technical Meeting on 4/6/2004, it was agreed that the implementation of the BSR model in AQUASIM would not be a priority at UCT, since this could be done in WEST by University of KwaZulu-Natal (UKZN). Rather focus should be on developing the kinetics for the processes, and this was completed. Implementation in AQUASIM will be done by UCT in future research. Parallel to the implementation in AQUASIM by the UCT Group, the UKZN Research Group implemented the model described above in the WEST platform, see below.

4.3 Implementation of the anaerobic digestion kinetic models in WEST

4.3.1 Objectives

The overall objective of this section of the project was to implement the methanogenic and sulphidogenic kinetic models developed above (Sections 4.1 and 4.2 respectively) in the WEST® modelling platform, to develop a computer model of the BioSURE® process in WEST. The purpose of the model was primarily to capture the knowledge acquired in the laboratory and pilot-plant investigations carried out by the UCT and Rhodes University members of the project team, in a form which readily could be used by design engineers working on full scale implementations of the process. It was also hoped that, if the model was sufficiently developed early enough, it might contribute to the planning and interpretation of the experimental programmes.

The model was to be based on the UCT methanogenic anaerobic digestion model (Section 4.1), extended by adding sulphate reduction reactions (Section 4.2). Originally it was envisaged that the UCT Research Group would code the sulphidogenic kinetic model using the AQUASIM modelling platform for their own use in interpreting their laboratory results, and the UKZN team would translate it to the more flexible and user-friendly WEST modelling platform, which then would be adapted to represent the Erwat Ancor pilot plant, and eventually made sufficiently general to be useful for the design of new plants.

4.3.2 Overall course of the investigation

The course of the project saw several delays in and deviations from the anticipated programme, which meant that the model has not reached the anticipated level of development. The circumstances which chiefly contributed to this were:

1. The AQUASIM version of the UCT methanogenic anaerobic model (without sulphate reduction) took longer to develop than expected, due to the complexity of the model. In the interim, the UKZN student undertaking the modelling as his MSc. Eng. project withdrew, and a substitute had to be found.

2. With the agreement of the Reference Group members, to hasten implementation it was decided to incorporate the sulphate reduction processes delineated in Section 4.2 above directly into the WEST version of the methanogenic digestion model, without going through the AQUASIM version.

3. The data from the laboratory experiments investigating the sulphate reducing systems only became available at the beginning of 2005, just before the project came to an end in April 2005. This arose due to the expanded scope of the experimental investigation (Section 3.1 above).

4. In the light of the results from the laboratory investigations (Section 3.2), the conceptual design of the pilot plant was substantially changed. The new configuration pilot plant only went into operation after the official end of the project. This meant that the model of the pilot plant has had to be put together based on minimal operating data, and its accuracy is unknown.

4.3.3 Summary of results

The development of the WEST based models took place in five stages:

1. The translation of the UCT methanogenic anaerobic digestion model (without sulphate reduction) from AQUASIM into WEST.

   This was a relatively mechanical process, except for some minor details where the different approaches of the two modelling platforms needed to be taken into account. The main outcome of this was a demonstration that the AQUASIM and WEST versions of the model gave essentially identical results.

2. Application of the WEST methanogenic anaerobic digestion model to the methanogenic data sets from the UCT laboratory experiments in STRs (Section 3.1.1).

   With the hydrolysis constants determined by optimisation, the model was able to match the experimental data closely. This validated the methanogenic model as implemented in WEST.

3. The extension of the model to include the sulphate reduction reactions, and its calibration using selected data sets from the UCT laboratory experiments carried out in STRs (Section 3.1.3).

   In calibration, for the methanogenic associated processes default values were from the UCT anaerobic digestion model, and for the sulphidogenic processes, these were from the literature; the only exception were the hydrolysis rate constants which were derived by optimisation.

   The model was able to match the measurements reasonably well for the experimental datasets that were investigated. From the optimisation, consistency in hydrolysis rate constants was obtained, with no discernable difference between the values for methanogenic and sulphidogenic systems. However, it was realised that the conditions under which the laboratory experiments were carried out were very different from the operating conditions of the pilot plant and hence parameter values (including hydrolysis constants) pertaining to the laboratory conditions may have little relevance to the pilot plant.

4. The adaptation of the model to represent the pilot-plant's upflow configuration with retention and recycling of the sludge, and its calibration using extremely limited operating data. The available operating data is summarised in Figure 8.

   Because of the lack of detailed information, the simplest possible model capable of representing the essential features of the pilot plant reactor was set up; the WEST model configuration is shown in Figure 9. Solids retention in the system was based on the observed low concentration of solids in the effluent. The reaction kinetic parameters were selected based on the literature values used for the laboratory scale studies above, but adjusted according to temperature dependencies in the literature. For the limited data, reasonably close correspondence between predictions and measurements was obtained.

5. The use of the model to explore some operating scenarios for the pilot plant.

   Because, at the time of writing, the pilot plant was still in the stage of resolving equipment teething problems, not much was known about process related issues. The model was used to explore the effects of changing the ratio between PSS and mine water fed to the reactor. Figure 10 shows an example of the model results: For varying sludge feed rates it was predicted that the lower the ratio of COD to SO_4 fed, the more SO_4 is reduced by a given

amount of COD. The model predicts that this trend continues with stable operation down to much lower COD / SO_4 ratios than current operation; this may or may not be realistic. The SO_4 removal ratio increases almost linearly up to almost complete removal.

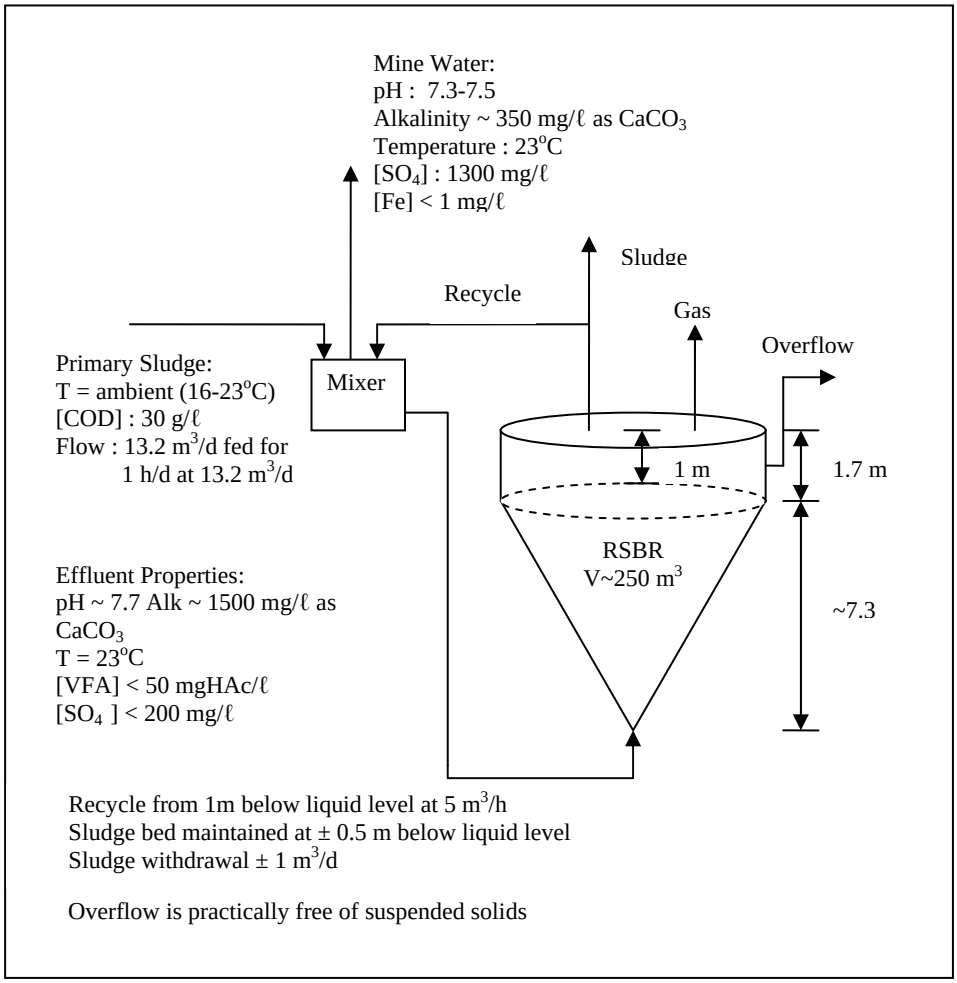

Figure 8: Configuration and operating data for the Erwat Ancor pilot plant reactor.

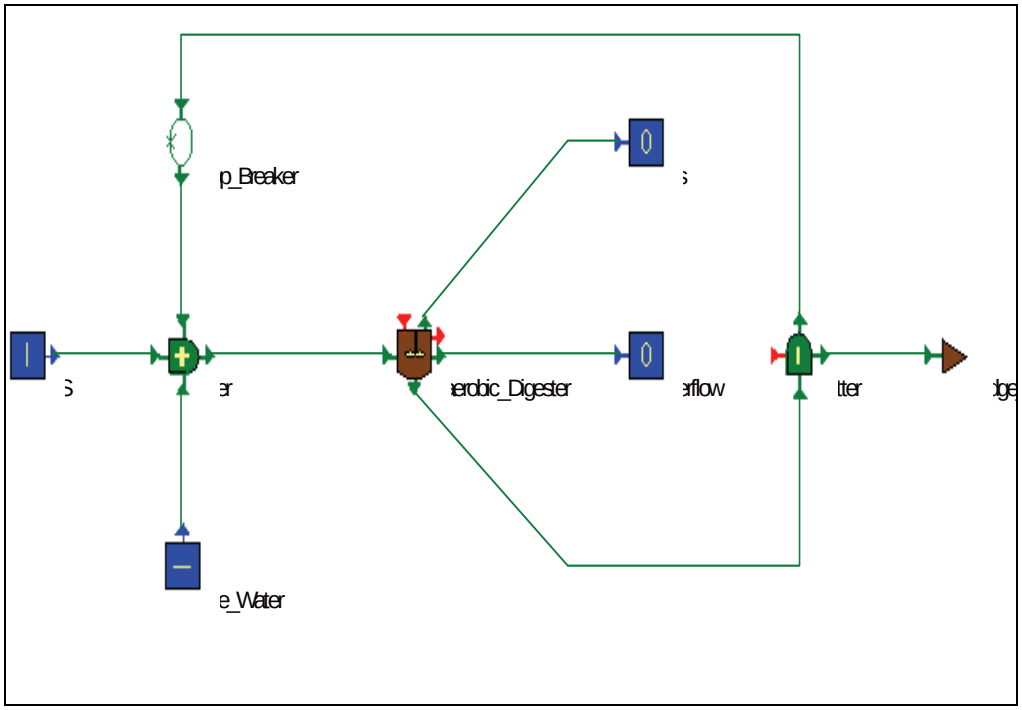

Figure 9: Configuration of the Erwat Ancor pilot plant reactor model in WEST

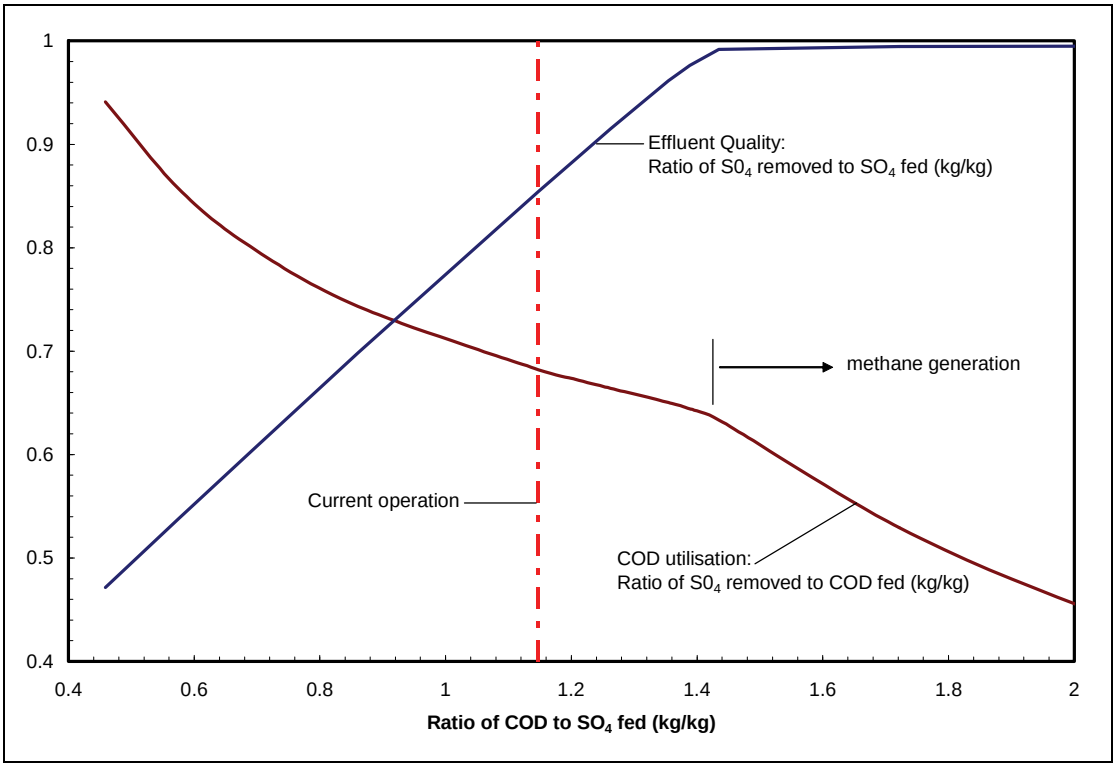

Figure 10: Simulated SO_4 removal and COD utilisation ratios for varying sludge feed rate

4.3.4 Areas for future research

The most apparent needs for further research are to reduce the uncertainties in the kinetic parameters values that are appropriate for the operating conditions of the pilot plant, and to obtain information on the hydraulic separation process that retains sludge in the reactor.

Reaction kinetics
The most important aspects of the pilot plant operating conditions seem to be:

- Operating temperatures around 20°C rather than 35°C.

  Temperature dependences are available in the literature for the methanogenic anaerobic digestion reaction rates, but not for the sulphidogenic reactions. However, the interactive nature of the model makes it probable that the entire set of reaction parameters needs to be determined together, rather than attributing an independent temperature correction to any subset.

- Feed concentrations for sludge (as COD) and mine water (as SO_4) around 1.5 g/ℓ

  The issue here appears to be the inhibitory effects of H_2S (and possibly pH). Although these effects were incorporated in the model and the appropriate terms calibrated from the literature, validation was not possible as H_2S inhibition did not appear significant in application to the laboratory scale systems. At the feed concentrations to the pilot plant, the H_2S levels are lower than those that were encountered in the laboratory studies and unlikely to be inhibitory. However, if feed SO_4 is increased in this or other applications H_2S inhibition may be significant and require evaluation.

- Separate regulation of the sludge residence time and the hydraulic residence time in the reactor.

  This would provide the clearest confirmation of the extent to which hydrolysis is the dominant limiting process in the reaction scheme.

The conventional way of addressing these needs would be to embark on a comprehensive programme of experiments similar to the ones carried out in the UCT laboratory (Section 3.1). Although the ultimately efficacy of this approach is proven, the requirements in terms of time, expense and experimental effort are known to be high.

The exercise of applying the model to the pilot plant operation has demonstrated that that it is not necessary to know all the parameters to the same degree of accuracy, and that it may well be that only a small number of them are critically important. Clearly the experience of the actual pilot plant operation is the best source of information for determining which are the critical parameters.

With the variability and contingencies of pilot plant operating conditions, it may not always be possible to determine parameters accurately, and laboratory tests might be needed to complement the pilot plant data. Here the *serum bottle tests* which have been extensively developed as part of WRC Project K5/1075 could be useful. They are relatively rapid and inexpensive, and, while not able to provide comprehensive data about a process, can be tailored to investigate specific questions by spiking the test mixture with specific components.

Hydraulic separation
The pilot plant reactor uses settling of the sludge to retain sludge in the reactor and produce a clarified effluent. Lacking any information on the settling characteristics of the sludge, this is represented in the current WEST model as a single parameter which sets the ratio between the sludge concentration in the effluent and the reactor, which was given an arbitrarily low value (0.0001) based entirely on the qualitative observation of the clarity of the effluent under current operating conditions.

In reality the retention ratio must be a function of the settling characteristics of the sludge and the flow regime in the reactor, and it sets important operating conditions and physical constraints for the reactor operation which are not currently represented in the WEST model. These relate to the biomass concentration in the reactor and the sludge retention time. In operating the pilot plant sludge the withdrawal rate is set so as to maintain the sludge level in the reactor and prevent it overflowing into the effluent. In the model simulations presented here, the sludge withdrawal flow rate was set at 1 m^3/d, the value estimated by the operators for current operation. It is quite likely that this rate would need to be adjusted to maintain the sludge separation when varying the feed rates to the reactor.

4.3.5 Conclusions and recommendations

The situation of having a model and a pilot plant investigation at a similar stage of development provides an opportunity for the modelling and experimental programmes to evolve together and mutually reinforce each other. Thus the model could be used to explore gaps in the understanding of the process and suggest experiments to be tried on the pilot plant. The data from the pilot plant can then be fed back to improve the model. This is the basic strategy of the technique referred to as *optimal experimental design*. What is novel here is the opportunity to apply the technique to such a large scale reactor, and it may represent a significant advance in the practice of piloting biological treatment processes, which frequently only confirm the operability of a process and add little to the scientific knowledge of the process.

Thus it is recommended that the continuing pilot plant investigation be supported by a simultaneous modelling investigation. To be fully effective, this should have a strong interaction with the experimental work. Theoretically this would be best achieved if the modelling and experimentation were carried out by the same team, but it could also be carried out by separate teams as long there is sufficient communication between them.

5. CLOSURE

In this research project the main objective has been to develop a kinetic model for the core unit process in BioSURE® and similar systems, of biological sulphate reduction (BSR) with primary sewage sludge (PSS) as substrate. This model was to serve as an aid to the design, operation and control of sulphidogenic anaerobic digestion systems. More fundamentally, it was to serve as a research tool to improve understanding of the underlying processes and their interactions.

Development of the BSR kinetic model required initial extensive experimental investigations, to gather data on the biological, chemical and physical processes involved in methanogenic and sulphidogenic anaerobic digestion of PSS. The experimental data also would serve as a basis for calibration and validation of the kinetic models developed. The experimental investigation quantified and compared the rate of PSS hydrolysis (the rate limiting step) under methanogenic,

acidogenic and sulphidogenic conditions. The rates under methanogenic and sulphidogenic conditions have been found to be similar, but the rate under acidogenic conditions was significantly reduced. This implies that the end products of acidogenesis inhibit the PSS hydrolysis step, but if these are removed through either methanogenesis or sulphidogenesis this inhibition is alleviated. Importantly from this comparison, since the rates under methanogenic and sulphidogenic conditions are closely similar, the model structure and kinetics developed for PSS hydrolysis can be applied under both sets of conditions, i.e. can be common.

The experimental investigation also encompassed a feasibility study to evaluate the UASB reactor configuration for BSR with PSS. By passing the entire feed through the sludge bed in the UASB system, contact between the PSS and sulphate is enhanced so that PSS hydrolysis and sulphate reduction processes occur concomitantly in the sludge bed, with no short-circuiting of the sulphate as may happen in recycling sludge bed type reactors. Furthermore, the UASB configuration should facilitate solids removal, allowing improved uncoupling of the solids and hydraulic retention times, leading to higher sulphate loading rates and reduced reactor volumes. The feasibility study demonstrated that the USAB reactor configuration is a worthwhile option for the treatment of sulphate-rich waters, but that this system requires more intensive investigation to delineate the principle design and operational parameters.

Simultaneously to the experimental investigation, model development was initiated. This development was in stages, with the underlying approach of developing a more general model structure that has wider potential application to anaerobic digestion systems. First, a two phase (aqueous/gas) integrated chemical, physical and biological processes model describing the kinetics of methanogenic anaerobic digestion of sewage sludges was developed. In this model, by incorporating the kinetics of weak acid/base chemistry, pH is included (via H^+) as a predictive parameter. This facilitated including the effect of the biological processes on the pH, and *visa versa*.

The model follows a novel approach to characterising the influent PSS, principally in terms of parameters usually or readily measured on sewage sludges (e.g. COD, TKN) and of the sewage sludge CHON composition, which can be readily determined from the measurements and model application to experimental data or elemental analysis. This approach allows COD, C and N mass balances to be set up over the digester. In the model, various formulations for the PSS hydrolysis rate were evaluated and, based on its widespread application in activated sludge systems treating the same particulate organics, surface reaction (Contois) kinetics selected for this rate limiting process. The model has been successfully calibrated principally with values for constants extracted from the literature, but also through application to experimental data sets from the literature and gathered in this research project. The methanogenic kinetic model development demonstrated that the integration in a kinetic manner of the two phase mixed weak acid/base chemistry, physical and biological processes provides a sound basis for further model development, in particular the integration of BSR and related processes.

Having completed the methanogenic anaerobic digestion model, the focus shifted to development of the BSR kinetic model by the UCT Research Group, and its implementation in the WEST platform by the UKZN Research Group. For this model, the methanogenic anaerobic digestion model served as the basis, to be extended to include BSR. This required identification of the kinetics and stoichiometry for the biological, chemical and physical processes associated with BSR in two phases (aqueous/gas). The biological processes were extracted from the literature, and the associated chemical and physical BSR biological processes delineated. Values for the required constants also were obtained from the literature.

The developed methanogenic and BSR kinetic models were implemented in WEST by the UKZN Research Group. It was envisaged that, if developed early enough, the models could be used to inform the experimental programmes at UCT and on the ERWAT Ancor pilot scale plant. However, the scope of the UCT experimental programme expanded considerably, and the methanogenic digestion model proved more complex than originally thought, and these delayed the UKZN Research Group acquiring the required information for model implementation timeously. The methanogenic anaerobic digestion model has been implemented in WEST and the implementation verified through correspondence between AQUASIM and WEST predicted results (which also provides a cross-check on the AQUASIM version). The WEST versions of the two models have been applied with success to the laboratory scale data collected at UCT on methanogenic and sulphidogenic anaerobic digestion respectively. The BSR kinetic model then was applied to the ERWAT Anchor pilot plant. Unfortunately, only limited data were available for this pilot plant, due to the change in reactor configuration to the UASB, following from the feasibility studies above. Considering the limited data available, the WEST model was able to simulate the pilot plant performance reasonably well. The model was used to evaluate operating scenarios for the pilot plant, and this demonstrates the usefulness of such a model. The model and experiments on the pilot plant can evolve mutually to provide a cross flow of information between the modelling exercise and pilot plant operation.

From the discussions above, it is evident that the principle objective of this research project, namely development of a kinetic model for BSR with PSS has been achieved. The model has been implemented in WEST (and is currently being implemented in AQUASIM), and successfully applied to the laboratory scale systems and the ERWAT Anchor pilot plant. Furthermore, the model has been applied to investigate preliminary operational scenarios for the pilot plant. However, the model has not yet reached a state of finality which would allow it to be used for design. This requires model refinement, in collaboration with the pilot plant operation.

6. FUTURE WORK

From these investigations, the following recommendations can be made:

- The experimental investigation on the feasibility of the UASB system for BSR with PSS has indicated that this system holds considerable promise. However, a more detailed investigation is required to identify the principle design and operational parameters. In this investigation, the effects of sludge bed recycling need to be examined.
- The methanogenic anaerobic digestion model developed at UCT has been applied to steady state anaerobic digesters, with good correspondence between predicted and measured data. However, application to dynamic situations was limited to hypothetical exploration of the effects of digester failure. The predicted responses appear to correspond to anecdotal information from experience, but rigorous evaluation of the model under dynamic conditions has not been undertaken. Such an evaluation will be hindered by the lack of suitable experimental information.
- The BSR kinetic model developed at UCT requires implementation in AQUASIM. This will provide a cross-check of the WEST implementation, and will be undertaken at UCT in future research. The AQUASIM implementation will be evaluated by simulation of the data collected from sulphidogenic digesters in this research project.
- In the BSR kinetic model and its integration with the methanogenic digestion model, the effect of H_2S inhibition on the biological processes was included. However, in the

application of the model implemented in WEST, the H_2S inhibition effects could not be evaluated since in the experiments simulated the H_2S concentrations were low. Limited experimental data on H_2S inhibition of the biological processes will hinder this evaluation.

- In application of the WEST model to the laboratory scale sulphidogenic systems, the methanogenic process were artificially restricted by making the initial methanogenic organism groups concentrations zero. This essentially removed competition between sulphidogens and methanogens in model application, clearly an undesirable result, since the model is structured to include such competition. This requires further investigation.
- In application to the pilot scale plant, the model in WEST and pilot plant implementation of the BioSURE system were recognised to be at similar stages of early development. It has been recommended that the model and experiments on the pilot plant evolve simultaneously to provide a mutually beneficial cross flow of information between the modelling exercise and pilot plant operation.
- The focus of this research project has been on BSR with PSS and the development of kinetic models for this system. The BSR has the main advantages of removing sulphate to low residual concentrations and generating alkalinity. However, the sulphate is reduced to sulphide which requires further treatment for sulphur recovery. One treatment train option for sulphur recovery is sulphide stripping with carrier gas, chemical oxidation of sulphide to sulphur by ferric iron, with the recovery of the ferric by biological oxidation. This sulphur recovery treatment proposal requires investigation, to evaluate its feasibility.

ACKNOWLEDGEMENTS

The writers wish to thank the Water Research Commission who funded the research, and the Research Manager who provided guidance and assistance:

Mr. G Steenveld

Also, the writers would like to acknowledge the support of the organizations that assisted the research:

University of Cape Town
University of KwaZulu-Natal
Rhodes University

Finally, acknowledgement is due to the technical staff in the Department of Civil Engineering at UCT, for their assistance with construction and maintenance of laboratory equipment:

D Botha
M Lakay
H Mafungwa
C Nicholas
E von Guerard

TABLE OF CONTENTS

LIST OF FIGURES

LIST OF TABLES

LIST OF SYMBOLS AND ABBREVIATIONS

Symbol/abbreviation	Description
Ac/HAc	Acetate/acetic acid
AD	Anaerobic digestion
ADM	Anaerobic digestion model
AMD	Acid mine drainage
ASM	Activated sludge model
BEPR	Biological excess phosphorus removal
BNR	Biological nutrient removal
BSR	Biological sulphate reduction
C	Carbon
COD	Chemical oxygen demand
DAE	Differential algebraic equations
FB	Feed batch
FSA	Free and saline ammonia
f_{PSup}	Primary sludge unbiodegradable particulate COD as a fraction of total COD
H	Hydrogen
HGE	Hierarchical graphics editor
HRT	Hydraulic retention time
IAWPRC	International Association for Water Pollution Research and Control
IAWQ	International Association on Water Quality (formerly IAWPRC)
IWA	International Water Association (formerly IAWQ, IAWPRC)
MSL	Model specification language
N	Nitrogen
N_{ai}	FSA nitrogen in the influent
O	Oxygen
orgN	Organic nitrogen
Pr/HPr	Propionate/Propionic acid
PSS	Primary sewage sludge
$rate_{acidogenesis}$, r_{AD}	Rate of acidogenesis
$rate_{hydrolysis}$, r_{HYD}	Rate of hydrolysis
$rate_{methanogenesis}$, r_{AM}	Rate of methanogenesis
RSBR	Recycling sludge bed reactor
RU	Rhodes University
R_h	Hydraulic retention time
SCFA	Short chain fatty acid
SO_4	Sulphate
SRB	Sulphate reducing bacteria
STR	Stirred tank reactor
S_{bp}	Biodegradable particulate COD in effluent
S_{bpi}	Biodegradable particulate COD in influent
S_{bs}	Biodegradable soluble COD in effluent
S_{bsi}	Biodegradable soluble COD in influent
S_{bsa}	Biodegradable soluble SCFA COD in effluent
S_{bsai}	Biodegradable soluble SCFA COD in influent
S_{bsf}	Biodegradable soluble fermentable COD in effluent

S_{bsfi}	Biodegradable soluble fermentable COD in influent
S_s	Total soluble COD in effluent
S_{si}	Total soluble COD in influent
S_t	Total effluent COD
S_{ti}	Total influent COD
S_{up}	Unbiodegradable particulate COD in effluent
S_{upi}	Unbiodegradable particulate COD in influent
S_{us}	Unbiodegradable soluble COD in effluent
S_{usi}	Unbiodegradable soluble COD in influent
S_{VFA}	Volatile fatty acids in effluent
S_{VFAi}	Volatile fatty acid in influent
TKN	Total Kjeldahl nitrogen
TSS	Total suspended solids
UASB	Upflow anaerobic sludge bed
UCT	University of Cape Town
UKZN	University of KwaZulu-Natal
VFA	Volatile Fatty Acid
VSS	Volatile suspended solids
WAS	Waste activated sludge
WRC	Water Research Commission
WWTP	Wastewater Treatment Plant
Z_{AD}	Acidogens
Z_{AM}	Acetotrophic(clastic) methanogens
Z_{AS}	Acetotrophic sulphate reducing bacteria
Z_{HM}	Hydrogenotrophic methanogens
Z_{HS}	Hydrogenotrophic sulphate reducing bacteria
Z_{PS}	Propionate degrading sulphate reducing bacteria

Note: Only symbols and abbreviations used in the text are included, those in equations are defined below the appropriate equations.

1 INTRODUCTION

1.1 BACKGROUND

Sewage treatment plants produce sludges as by-products of the treatment of the main sewage flow. Of the sewage sludges, usually primary sewage sludge (PSS) from the underflow of the primary settling tank comprises the largest fraction, at approximately two thirds of the total, with humic or waste activated sludges making up the remainder (depending on the biological treatment unit process implemented). The sewage sludges require treatment before disposal and, although the sewage sludge streams typically comprise 1% or less of the total volumetric flow treated in the plant, their treatment may represent 30-40% of the total costs (Knapp and Howell, 1978). The most common treatment method for sewage sludges is anaerobic digestion (e.g. Pipes, 1961; Gujer and Zehnder, 1983), resulting in a stabilized sludge with a low residual sludge volume.

Anaerobic digestion can occur under three operating conditions: Methanogenic systems, which produce methane gas as the final COD product; sulphate-reducing or sulphidogenic systems, which require sufficient sulphate as input and produce sulphide (aqueous, gaseous and metal sulphides precipitates); acidogenic systems, which refer to anaerobic digestion systems in which methanogenic and sulphate-reducing conditions are not present, and the end product of the digestion is in the form of soluble COD. Of these three types of systems, methanogenic systems are the most widely implemented for sludge treatment, and hence have been studied the most extensively. Conventionally, in the methanogenic treatment of PSS, acidogenic digestion and sulphate reduction are considered undesirable, as the former results in loss of methane production and the latter in odour problems (Devai and DeLaune, 1999). However, more recently for both situations PSS has been considered as a potential beneficial source of substrates. The products of the sequence of the bioprocesses of hydrolysis and acidogenesis (acidogenic digestion) are the short-chain fatty acids (SCFA, also termed volatile fatty acids, VFA) which are directly beneficial in downstream biological nutrient removal (BNR) activated sludge systems (Venter *et al.*, 1977; Barnard, 1984; Lilley *et al.*, 1991; Elefsiniotis and Oldham, 1993; Brinch *et al.*, 1994; Skalsky and Daigger, 1995; Hatziconstantinou *et al.*, 1996, Andreasen *et al.*, 1997; Banerjee *et al.*, 1998; Banister and Pretorius, 1998), or in the biological reduction of sulphate (internal or external to the digester) in the treatment of sulphate-rich acid mine drainage (AMD, Kaufman *et al.*, 1996; Whittington-Jones, 2000).

AMDs are characterized by high concentrations of heavy metals, sulphate and total dissolved solids, and a low pH (Christensen *et al.*, 1996), and pose a significant environmental threat. To ameliorate the adverse environmental impact of AMD, the BioSURE® Process has been developed by researchers at Rhodes University (South Africa) as a low cost active treatment of AMD waters (Rose *et al.*, 2002). The process flow diagram (Figure 1.1) consists of a series of interconnected biological and chemical unit operations that allow for the removal of heavy metals and salinity (particularly sulphate) from AMD, and its neutralisation. In the BioSURE® system, the core unit process is biological sulphate reduction, which is achieved using PSS as the electron donor and organic carbon source, with the concomitant production of sulphide and carbonate alkalinity. As noted above, PSS is available as a by-product at municipal sewage treatment plants, and this co-disposal proposal provides an elegant solution to biological sulphate reduction in AMD treatment. Initially it was proposed that the biological sulphate reduction reaction takes place in a recycling sludge bed reactor (RSBR)

and a second sulphate-reducing digester. The main aim of the RSBR is to solubilise the PSS to soluble organics such as SCFA (VFA), which then are used by the sulphate-reducing bacteria in the second sulphate-reducing digester. The sulphide and carbonate alkalinity thus produced are recycled and contacted with the feed AMD, neutralizing the pH and precipitating the heavy metals as metal sulphides, carbonates and hydroxides. The remaining effluent from the sulphate-reducing digester is discharged to a sulphide-oxidizing reactor, where aqueous sulphide is oxidized to elemental sulphur. A high rate algal pond polishes this effluent, which is then suitable for discharge.

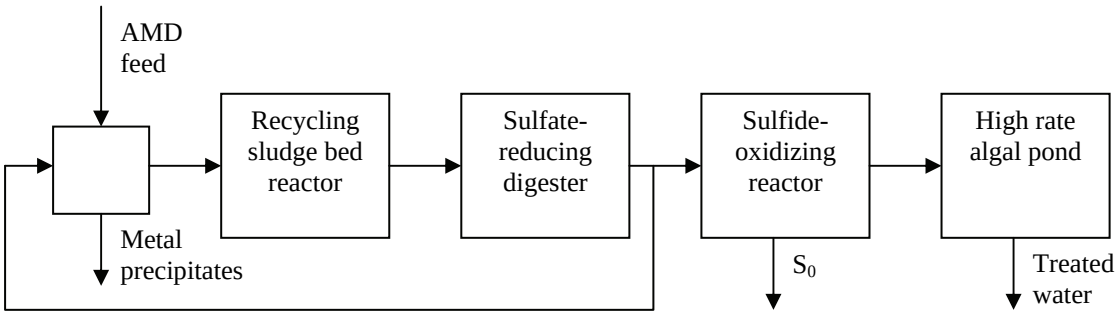

Figure 1.1: Process flow diagram of the BioSURE® system applied to the treatment of acid mine drainage (AMD) water (from Rose *et al.*, 2002).

As noted above, the core unit process in the BioSURE® system is biological sulphate reduction with PSS. To aid the design, operation and control of (and research into) this unit process, a mathematical model would be an invaluable process evaluation tool. Mathematical models provide quantitative descriptions of the treatment system of interest that allow predictions of the system response and performance to be made. From these predictions, design and operational criteria can be identified to optimize the system performance. Also, mathematical models are very useful as research tools. By evaluating the model predictions, it is possible to test hypotheses on the behaviour of the system (e.g. biological processes, their response to system constraints, etc.) in a consistent and integrated fashion. In essence, mathematical models provide an integrated framework for the system which can give guidance to design, operation and research.

1.2 OBJECTIVES

Recognising the potential usefulness of a mathematical model to describe biological sulphate reduction with PSS as substrate, the Research Groups at the University of Cape Town (UCT) and the University of KwaZulu-Natal (UKZN) were subcontracted by Rhodes University to develop a kinetic model for biological sulphate reduction with PSS. This formed part of a broader research project between the Water Research Commission (WRC) and Rhodes University, K5/1456 “Biotechnological co-treatment of saline and sewage wastewaters with integrated recovery and re-use of water and organic and inorganic components for sustainable development”, falling under Part 2 of the research project: “Part 2: Bio-sulphidogenic Sewage Treatment”. The principle objective for the contribution by the UCT and UKZN Water Research Groups to the research project was:

- ***The development of a kinetic based integrated biological, physical and chemical processes model for BIOSURE type systems***

The aims of this kinetic model were to:

- improve understanding of the underlying processes in these systems
- identify the main compounds of importance
- apply the model for system optimisation and design.

The kinetic model was to be developed within both the AQUASIM® and WEST® simulation platforms.

1.3 RESEARCH APPROACH

The approach taken in model development was:

- To develop a more general model structure that has wider application to anaerobic digestion systems, with and without sulphate reduction and/or methanogenesis, or with both methanogenesis and sulphidogenesis.

This required that the underlying chemical, physical and biological processes in all three anaerobic digestion types (methanogenic, acidogenic and sulphidogenic) with sewage sludges as substrate be identified and quantified, as well as the interactions with the environment. This in turn required both an experimental and modelling research component.

1.4 EXPERIMENTAL

1.4.1 PSS hydrolysis

Under the three operating conditions (methanogenesis, acidogenesis and sulphidogenesis), hydrolysis of the particulate PSS is the rate-limiting process, and hence the design, operation and control of these systems rely on this process being accurately quantified under different operating conditions. Several studies have investigated the digestion of PSS under each of the individual operating conditions (methanogenic, acidogenic and sulphate-reducing). However, systematic quantification of the PSS hydrolysis rate under all three conditions is limited. Further, no single study has investigated PSS hydrolysis kinetics under methanogenic, acidogenic and sulphate-reducing conditions in a manner that allows direct comparison of the PSS hydrolysis rates, and their interaction with system operational parameters, such as retention time, feed concentration and pH.

In a parallel research project, the Water Research Commission (WRC) contracted the Water Research Group at the UCT to investigate the kinetics of PSS hydrolysis under sulphate-reducing conditions, such as in the BioSURE® Process (WRC contract no. K5/1216, April 2001 to March 2003). In this project, the original specific objectives were to:

- Quantify the effects of sulphate reduction and pH on the rate of PSS hydrolysis, and to
- Establish design parameters for biological sulphate reducing systems treating AMD using PSS as the electron donor/carbon source.

To quantify the effects of sulphate reduction and pH on the rate of PSS hydrolysis, the rate of PSS hydrolysis under methanogenic and acidogenic conditions needed to be quantified as a basis for comparison. This necessitated that the original objectives in the contract be expanded to include experimental investigations into, and mathematical modelling of, the rate of PSS hydrolysis under methanogenic and acidogenic conditions. During the course of the investigation on methanogenic systems, it appeared that a number of physical constraints

imposed by the system influenced the rate of PSS hydrolysis, in particular retention time and influent PSS feed concentration. This required that these influences be quantified. Due to the considerable increase in the scope of the project, the research contract was extended for 1 year (April 2003 to March 2004) with additional funding.

Further, as described above UCT were contracted by Rhodes University as a sub-contract between the WRC and Rhodes University (K5/1456, April 2003 to March 2005); to undertake investigations into integrated biological, physical and chemical processes kinetic modelling of biological sulphate reducing systems. It was therefore envisaged that the expanded experimental investigation should cover aspects required in the modelling, primarily to generate deeper understanding of the underlying processes in these systems, in order to identify the main compounds and processes of importance, and to provide the required experimental data for model calibration and application.

Therefore, the principle aim of this part of the study was to determine the rate of hydrolysis of PSS under methanogenic, acidogenic and sulphate-reducing conditions, and the influence of the system physical constraints on the rate. This also would enable a direct comparison of the rate under each of the three conditions, to determine possible influences on the rate.

In terms of this aim, the original objectives from K5/1216 were expanded to include the information required for the kinetic model to be developed here, and encompassed the following:

1) To determine the rate of hydrolysis of PSS under methanogenic conditions.
2) To determine the effects of feed COD concentration, hydraulic retention time and pH on the rate of hydrolysis under methanogenic conditions.
3) To develop a mathematical model for the biological processes mediating PSS hydrolysis in methanogenic systems, so that the rate of hydrolysis can be predicted for various feed COD concentrations, hydraulic retention times and operating pH, based only on the feed characterization and system operation.
4) To evaluate the various rate formulations for the PSS hydrolysis at varied operating conditions, so that the most appropriate rate formulation for hydrolysis of PSS under methanogenic conditions can be identified.
5) To collect data on methanogenic systems that can be used to calibrate a more extensive dynamic mathematical model for methanogenic anaerobic digestion including physical processes such as acid/base equilibria and vapour/liquid equilibria (development of this model does not form part of this research, but is part of a parallel project).
6) To determine the rate of PSS hydrolysis under acidogenic conditions.
7) To determine the effects of feed COD concentration, hydraulic retention time and pH on the rate of hydrolysis under acidogenic conditions.
8) To appropriately modify the mathematical model selected in 4. above, to predict the rate of hydrolysis under acidogenic conditions.
9) To determine whether PSS can support internal sulphate-reduction, and to develop a greater understanding of sulphate reduction in PSS fed systems.
10) To determine the rate of PSS hydrolysis under sulphate-reducing conditions.
11) To determine the effects of sulphate-reduction on the rate of hydrolysis of PSS.

This experimental research is reported on in detail by Ristow *et al.* (2005a), and summarised in Chapter 2.

1.4.2 Upflow anaerobic sludge bed reactor (UASB)

In the BioSURE® system, the core unit process is the biological sulphate reduction with PSS as substrate (Rose *et al.*, 2002). Initially, for the biological sulphate reduction unit process, it was proposed to make use of the recycling sludge bed reactor (RSBR) which is a down-flow configuration, to enable the solids and liquid retention times to be uncoupled thereby reducing reactor volume requirements. However, in this configuration, dissolved sulphate can "short-circuit" the sludge bed to the effluent requiring downstream biological sulphate reduction, as originally proposed in the BioSURE® system. Further, in the experimental investigation into completely mixed sulphidogenic systems described above (and detailed in Chapter 2 and Ristow *et al.*, 2005), particularly evident was the influence of sulphate reduction on the effluent suspended solids concentrations – the sulphate reducing systems consistently produced effluents with higher suspended solids than the corresponding methanogenic systems, i.e. higher concentrations of solids that would not settle. This has significant implications for sulphate reducing systems in which the solids and hydraulic retention times need to be uncoupled (to reduce reactor volumes) such as in the RSBR originally proposed in the BioSURE® system, as retention of sulphate reducing biomass and PSS biodegradable particulate substrate may prove problematic.

In this research project, it was originally proposed that the UCT Research Group operate RSBR type systems to evaluate enhanced PSS hydrolysis. However, agreement was obtained from the reference group guiding the project that the UCT Research Group would not operate such RSBR type systems, because quantification of PSS hydrolysis kinetics were difficult to elucidate in such systems and the parameters identifying whether or not enhanced hydrolysis was operative were not clearly defined. As alternative, with agreement from the reference group different system configurations to improve solids liquid separation were examined. Conceptually, passing the influent through the sludge bed may considerably improve the separation and overcome sulphate "short-circuiting". One such system in which this occurs is the Upflow Anaerobic Sludge Bed (UASB) reactor. Accordingly, a study was undertaken to evaluate the feasibility of using a UASB type system for biological sulphate reduction with PSS as substrate, and is reported on in Chapter 3.

1.5 KINETIC MODEL

The principle objective of the University of Cape Town (UCT) and University of KwaZulu-Natal (UKZN) contributions to this research project was the development of a kinetic model for biological sulphate reduction using PSS as substrate. In addressing this objective, the approach taken was to develop a more general model structure, which would have wider application to anaerobic digestion systems, with and without sulphate reduction, see above. This model would require the biological processes for methanogenic anaerobic digestion and sulphate reduction, integrated with the chemical (e.g. aqueous chemistry) and physical (e.g. gas exchange) processes operative in such systems, in two phases, aqueous and gas. The Research Group at UCT was tasked to undertake model development and implementation in AQUASIM®, and the Research Group at UKZN with implementation in WEST®.

1.5.1 Model development

A variety of mathematical models have been developed to describe anaerobic digestion. However, these models largely have focused on the biological processes operative in an anaerobic digester. This implicitly accepts that the biological processes take place within a

regime of constant pH, and that chemical and physical processes (e.g. mineral precipitation and gas stripping) are insignificant compared with the biological processes, and accordingly can be neglected. However, in anaerobic digestion since short chain fatty acids (SCFA) are produced as the main intermediates, and in sulphate reduction the weak acid/bases sulphate and sulphide are consumed and produced respectively, the assumption of a constant pH regime may not be valid. Furthermore, pH has a significant impact on the processes: Many of the biological processes have been shown to be very sensitive to pH changes and/or to undissociated weak acid/base species, the concentrations of which are pH controlled. Accordingly, inclusion of pH as a parameter in some fashion in anaerobic digestion models would greatly extend, and provide greater surety in, model application, and is a requirement of the kinetic model to be developed here. Including pH requires inclusion of compounds not directly involved in the biological processes, but in pH regulation. This would be of benefit since these compounds would enable determination of the mass parameter alkalinity, routinely used by many operators as a measure of predicting the state of health of anaerobic digesters.

Consequently, the kinetic model to be developed needed to include two phase (aqueous and gas) processes for:

- weak acid/base chemistry
- biological processes for methanogenic anaerobic digestion of PSS
- biological sulphate reduction
- gas stripping/exchange.

The model would also need to take account of interactions between the processes above. The model was to be developed in stages. An integrated two phase biological, chemical and physical processes methanogenic anaerobic digestion kinetic model would be developed first, and then the biological sulphate reduction and associated chemical and physical processes merged with this kinetic model. For the methanogenic anaerobic digestion model, this was developed under parallel research projects, namely this project and the Water Research Commission (WRC) research project with UCT on mass balances modelling (K5/1338), which is reported on by Sötemann *et al.* (2005a).

In developing the methanogenic anaerobic digestion model, two phases (aqueous and gas) of the three phase (aqueous, gas and solid) kinetic model of Musvoto *et al.* (2000a,b,c) was used as a basis, since this model incorporates H^+ ($pH = -\log(H^+)$) directly in the model. The kinetics for the methanogenic anaerobic digestion bioprocesses would be integrated with the weak acid/base model, so also the physical processes for gas exchange, see Figure 1.2. In this integration, due cognizance would be taken of any interactions introduced by the integration, and of the need to incorporate any new weak acid/base species utilised/produced by the bioprocesses. The resultant methanogenic anaerobic digestion model would be validated against experimental data in the literature, and against the data generated in the experimental investigation above.

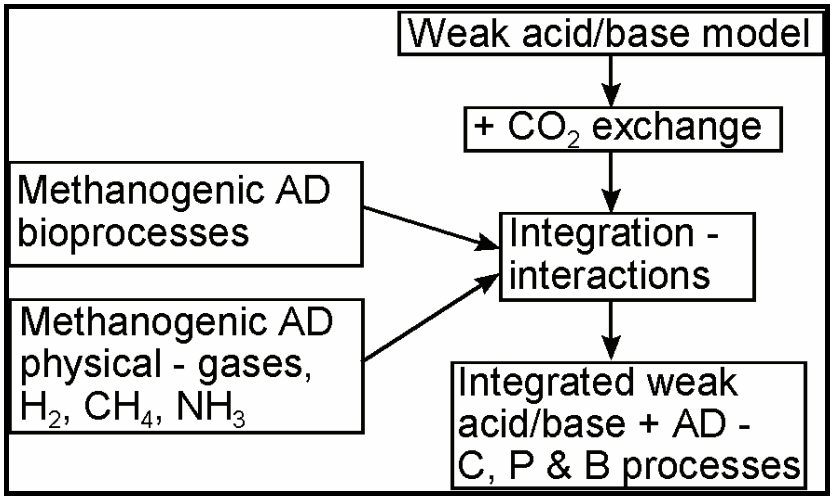

Figure 4.2: Approach followed to develop the integrated chemical (C), physical (P) and biological (B) processes two phase (aqueous-gas) methanogenic anaerobic digestion (AD) kinetic model.

The development of the methanogenic anaerobic digestion model is reported in detail by Sötemann *et al.* (2005a, b). The relevant section from the Sötemann *et al.* report has been extracted in Chapter 4, to draw together the information of importance for the research project into a single report, but also extended to include model application to the methanogenic anaerobic digesters operated in this investigation and described in Chapter 2.

Having developed the methanogenic anaerobic digestion model, this model was to be extended to include biological sulphate reduction with PSS as substrate. This would require development of the kinetics and stoichiometry for the biological, chemical and physical processes in biological sulphate reduction in two phases (aqueous/gas), and integration of these with methanogenic anaerobic digestion model, taking due cognizance of any interactions introduced with the integration, see Figure 1.3. Essentially, this would result in a two phase biological, chemical and physical processes model for the AD of PSS, with competitive methanogenesis and sulphidogenesis. The model was to be encoded in AQUASIM (Reichert, 1998) and applied to the sulphidogenic anaerobic digesters operated in this investigation and described in Chapter 2. These developments are summarised in Chapter 5 and described in detail by Van Wageningen *et al.* (2006).

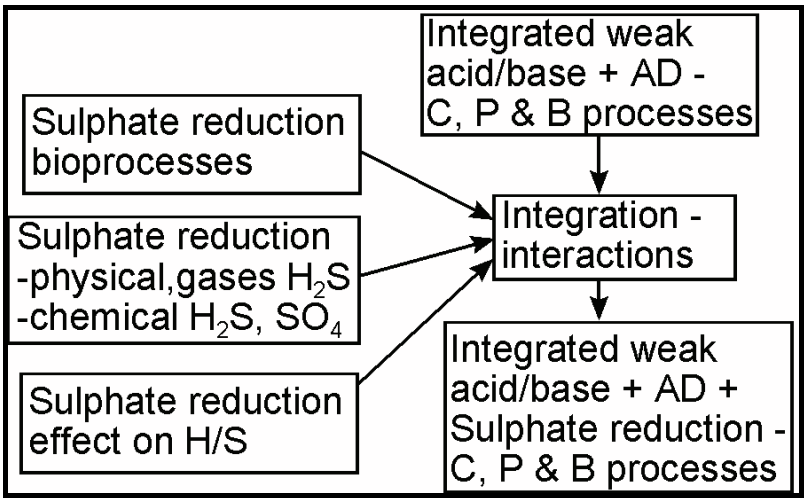

Figure 1.3: Approach followed to develop the integrated chemical (C), physical (P) and biological (B) processes two phase (aqueous-gas) methanogenic and sulphidogenic anaerobic digestion (AD) kinetic model.

1.5.2 Model implementation in WEST

The overall objective of this section of the research was for the UKZN Research Group to develop a computer model of the BioSURE® process using the WEST® modelling platform. The purpose of this implementation primarily was to capture the knowledge acquired in the laboratory- and pilot-plant investigations carried out by the UCT and Rhodes University (RU) members of the project team, in a form which could readily be used by design engineers working on full-scale implementations of the process. It was also hoped that, if the model was sufficiently developed early enough, it might contribute to the planning and interpretation of the experimental programmes.

The models implemented in WEST were to be based on the anaerobic digestion models developed at UCT, as described above. Originally it was envisaged that the UCT Research Group would code the various developed models using the AQUASIM modelling platform for their own use in interpreting their laboratory results, and the UKZN team would translate these to the more flexible and user-friendly WEST modelling platform, and adapt the biological sulphate reduction model to be able to represent the Erwat Ancor BioSURE® pilot-plant. Finally, the WEST implemented biological sulphate reduction model would be made sufficiently general to be useful for the design of new plants.

By necessity the implementation of the models in WEST by UKZN had to follow on from the developments at UCT. Thus, the approach followed was first implementation of the developed methanogenic anaerobic digestion model in AQUASIM by UCT, followed by implementation in WEST by UKZN. The UKZN Research Group then would apply the AQUASIM and WEST implementations to the same methanogenic systems. This would allow cross-checking of the models in the two platforms to eliminate coding errors and to evaluate any differences introduced by the different routines used in the two platforms to solve the resultant equations.

A similar approach was envisioned for the biological sulphate reduction model. However, the methanogenic anaerobic digestion model took longer to develop than expected due to the complexity of the model, so that this first model only became available to the UKZN Research Group relatively late in the project. This also delayed development of the biological sulphate reduction model. Recognising this, with agreement from the reference group, it was decided that the implementation of the biological sulphate reduction model in AQUASIM would not be a priority at UCT, since this could be done in WEST by UKZN. Rather the focus at UCT should be on developing the kinetics for the processes. Accordingly, UKZN would incorporate the biological sulphate reduction and associated processes delineated by UCT directly into WEST, in parallel to the implementation in AQUASIM by UCT.

Further, the experimental data on the sulphidogenic anaerobic digestion systems being collected at UCT (Chapter 2) was completed and received by UKZN relatively late in the project, delaying model application to these systems. In the light of the results from the laboratory investigations, the conceptual design of the Erwat Ancor BioSURE® pilot-plant was substantially changed to the upflow configuration (Chapter 3). The new configuration pilot-plant only went into operation after the official end of the project. This meant that the model of the pilot-plant had to be developed based on minimal operating data, and its accuracy is unknown.

The implementation by the UKZN Research Group of the various models in the WEST platform is summarised in Chapter 6, and described in detail by Rajkumar (2006).

2 EXPERIMENTAL INVESTIGATION – HYDROLYSIS OF PRIMARY SEWAGE SLUDGE UNDER METHANOGENIC, ACIDOGENIC AND SULPHIDOGENIC CONDITIONS

2.1 BACKGROUND

As set out in Chapter 1, the principle objective for this research project was the development of a kinetic model describing the core unit process in the BioSURE®, of biological sulphate reduction using primary sewage sludge (PSS) as the electron donor and organic carbon source, with the concomitant production of sulphide and carbonate alkalinity. In developing this model, the approach taken was to develop a more general model structure that has wider application to anaerobic digestion systems, with and without sulphate reduction and/or methanogenesis, or with both methanogenesis and sulphidogenesis. To develop this more general modelling framework, requires information and understanding of the underlying processes, in particular the rate limiting process of hydrolysis of the PSS to short-chain fatty acids (SCFA), which form the substrate for the subsequent methano- and/or sulphidogenesis.

This Chapter describes an experimental investigation into the hydrolysis of PSS under the three operating conditions of methanogenesis, acidogenesis and sulphidogenesis: Although several studies have investigated the digestion of PSS under each of the three operating conditions (methanogenic, acidogenic and sulphate-reducing) individually, systematic quantification of the PSS hydrolysis rate under all three conditions is limited. Further, no single study has investigated PSS hydrolysis kinetics under methanogenic, acidogenic and sulphate-reducing conditions in a manner that allows direct comparison of the PSS hydrolysis rates, and their interaction with system operational parameters, such as retention time, feed concentration and pH.

2.2 OBJECTIVES

The Water Research Commission (WRC) identified the use of PSS as electron donor for biological sulphate reduction in the remediation of AMD as of particular interest to South Africa, and accordingly contracted the Water Research Group in the Department of Civil Engineering at the University of Cape Town to investigate the kinetics of PSS hydrolysis under sulphate-reducing conditions, such as in the BioSURE® Process (WRC contract no. K5/1216, April 2001 to March 2003). The original specific objectives were to:

- Quantify the effects of sulphate reduction and pH on the rate of PSS hydrolysis, and to
- Establish design parameters for biological sulphate reducing systems treating AMD using PSS as the electron donor/carbon source.

To quantify the effects of sulphate reduction and pH on the rate of PSS hydrolysis, the rate of PSS hydrolysis under methanogenic and acidogenic conditions needed to be quantified as a basis for comparison. This necessitated that the original objectives in the contract be expanded to include experimental investigations into, and mathematical modelling of, the rate of PSS hydrolysis under methanogenic and acidogenic conditions. During the course of the investigation on methanogenic systems, it appeared that a number of physical constraints imposed by the system influenced the rate of PSS hydrolysis, in particular retention time and

influent PSS feed concentration. This required that these influences be quantified. Due to the considerable increase in the scope of the project, the research contract was extended for 1 year (April 2003 to March 2004) with additional funding.

Further, in parallel to the contract above UCT were contracted by Rhodes University as a sub-contract between the WRC and Rhodes University (K5/1456, April 2003 to March 2005), to undertake investigations into integrated biological, physical and chemical processes kinetic modelling of biological sulphate reducing systems, the research described here. It was therefore envisaged that the expanded experimental investigation should cover aspects required in the modelling, primarily to generate deeper understanding of the underlying processes in these systems, in order to identify the main compounds and processes of importance, and to provide the required experimental data for model calibration and application.

Therefore, the principle aim of the study reported in this Chapter was to determine the rate of hydrolysis of PSS under methanogenic, acidogenic and sulphate-reducing conditions, and the influence of the system physical constraints on the rate. This also would enable a direct comparison of the rate under each of the three conditions, to determine possible influences on the rate.

In terms of this aim, the original objectives were expanded to include the information required for the kinetic model to be developed here and encompassed the following:

1) To determine the rate of hydrolysis of PSS under methanogenic conditions.
2) To determine the effects of feed COD concentration, hydraulic retention time and pH on the rate of hydrolysis under methanogenic conditions.
3) To develop a mathematical model for the biological processes mediating PSS hydrolysis in methanogenic systems, so that the rate of hydrolysis can be predicted for various feed COD concentrations, hydraulic retention times and operating pH, based only on the feed characterization and system operation.
4) To evaluate the various rate formulations for the PSS hydrolysis at varied operating conditions, so that the most appropriate rate formulation for hydrolysis of PSS under methanogenic conditions can be identified.
5) To collect data on methanogenic systems that can be used to calibrate a more extensive dynamic mathematical model for methanogenic anaerobic digestion including physical processes such as acid/base equilibria and vapour/liquid equilibria (development of this model does not form part of this research, but is part of a parallel project).
6) To determine the rate of PSS hydrolysis under acidogenic conditions.
7) To determine the effects of feed COD concentration, hydraulic retention time and pH on the rate of hydrolysis under acidogenic conditions.
8) To appropriately modify the mathematical model selected in 4. Above, to predict the rate of hydrolysis under acidogenic conditions.
9) To determine whether PSS can support internal sulphate-reduction, and to develop a greater understanding of sulphate reduction in PSS fed systems.
10) To determine the rate of PSS hydrolysis under sulphate-reducing conditions.
11) To determine the effects of sulphate-reduction on the rate of hydrolysis of PSS.

This Chapter summarises this investigation; for details see Ristow *et al.* (2005a).

2.3 EXPERIMENTAL INVESTIGATION

The research approach adopted was to operate 6 parallel laboratory-scale completely-mixed anaerobic digesters with PSS as influent, and to monitor the behaviour of these systems under a range of feed COD concentrations, retention times, pH and feed sulphate concentrations under stable methanogenic, acidogenic and sulphate-reducing conditions. This experimental programme required the development and construction of novel apparatus (e.g. sealed mixed digesters, gas flow measurement devices) and analytical methods (e.g. measurement of sulphate in presence of organics); for details see Ristow *et al.* (2005a, b).

2.3.1 Reactor set-up and operation

A series of 6 completely mixed Perspex digesters with working volumes of 16 and 20 ℓ were batch fed once or twice daily (depending on the feed volume) to simulate continuous operation while avoiding problems relating to pumping of PSS under laboratory conditions. For feeding, a volume of mixed liquor was removed from the tap at the bottom of the digester, and the appropriate feed volume added, after which the digester was refilled with the mixed liquor to the operating volume. After feeding, the headspace was purged with nitrogen (99.999%) to remove oxygen and the digester resealed. The wasted mixed liquor was analysed further. The temperature was controlled to 35^{o}C by a heating coil around the walls of the digester, with a thermocouple inside the digester liquid.

2.3.2 Feed collection and characterisation

Primary sewage sludge (PSS) was collected in batches from the primary settling tanks at the Athlone Wastewater Treatment Works (Cape Town, South Africa) and stored at 4^{o}C. Each batch served as feed source for up to 7 months. The soluble fraction of the PSS changed during storage, and this (amongst others) was monitored so that the feed to the digesters at any time could be characterised (see Ristow *et al.*, 2005a for details). The PSS was screened through a 6.7 mm square mesh to remove large particles such as rags, cigarette butts, seeds and other debris, but without changing the nature of the feed by selecting an unreasonably small PSS particle size. For each feed, the PSS was diluted by weighing the required mass of PSS (measuring PSS volumes proved problematic) and adding the required mass of warm water (to around 35^{o}C).

2.3.3 Analytical methods

The reactor pH, gas volume production, effluent volatile fatty acid (VFA) and $H_2CO_3^*$ alkalinity concentrations were measured daily until steady state operation was observed. Thereafter, additionally the effluent total COD, soluble COD, TKN, free and saline ammonia (FSA), and total and soluble P and the gas composition were analysed. The pH was measured *in situ* to prevent errors due to CO_2 loss on sampling. Gas volumes were measured by an in-house developed reticulating-float gas meter with a unit volume of around 50mL/unit (calibrated to ±0.1ml/unit), and the number of units per time recorded. The VFA and $H_2CO_3^*$ alkalinity were measured using the 5-point titration method of Moosbrugger *et al.* (1992). Soluble samples were prepared by vacuum filtering (0.45 μm), and filtrates analysed for COD, TKN, FSA, total and soluble P (Standard Methods, 1985). In the sulphate reduction systems, additionally sulphate and sulphide required measurement. Sulphate was analysed

with the turbidometric method (Standard Methods, 1985), but with a novel in-house developed pre-treatment to remove organics that interfere with the method (Ristow *et al.*, 2005b). With regard to sulphide, this acts as an electron donor in the COD test and hence contributes to the measured COD. Accordingly, for the COD test on filtrate, parallel samples were tested, one with the sulphide removed by precipitation with Zn followed by filtration before the test to give organic COD, and the other with no pre-treatment, with the difference being the sulphide COD. This latter "COD" measurement could be readily converted to a sulphide concentration.

2.3.4 Experimental programme

The 6 parallel digesters were operated over a range of conditions, see below. Under each set of conditions, the systems were allowed to attain steady state (2-3 retention times) and analysed as described above. All reported steady state points were for systems with an effluent VFA concentration below 50 mg/ℓ as HAc. Hydraulic retention times were varied by keeping the reactor volume constant and increasing the feed flow rate.

2.4 DATA ANALYSIS

The aim of the study was to determine the rate of hydrolysis of PSS under varying hydraulic retention times and feed COD concentrations. Hydrolysis is defined as the extra cellular enzymatic breakdown of polymers (particulate) into monomers and dimers (soluble), which enter the subsequent acidogenesis reactions. To determine and quantify the rate of hydrolysis for a given steady state digester, a steady state model was developed.

2.4.1 Model assumptions

The model was developed from mass balances for the particulate biodegradable COD, the soluble biodegradable COD (hydrolysis products), the volatile fatty acids (acidogenesis products) and the acidogenic and methanogenic biomass concentrations (Figure 2.1). The model was based on the following assumptions:

- The PSS COD characterisation is structured around that followed for the activated sludge simulation models (Henze *et al.*, 1986, 1995) to ensure continuity in mass balances and since the PSS is common. In terms of this structure, the total PSS COD (S_{ti}) consists of an unbiodegradable particulate fraction (S_{upi}), a biodegradable particulate fraction (S_{bpi}), an unbiodegradable soluble fraction (S_{usi}), a biodegradable soluble non-VFA fraction (S_{bsfi}) and volatile fatty acids (S_{VFAi}), i.e.

$$S_{ti} = S_{upi} + S_{bpi} + S_{usi} + S_{bsfi} + S_{VFAi} \quad (2.1)$$

- Under stable operating methanogenic anaerobic conditions, three organism groups act on the PSS biodegradable COD, namely acidogens (Z_{AD}), acetoclastic methanogens (Z_{AM}) and hydrogenotrophic methanogens (Z_{HM}).

- Hydrogenotrophic methanogen biomass (Z_{HM}) is considered negligible compared with the other active organism biomasses.

- The effluent total COD (S_t) consists of the unbiodegradable particulate fraction (S_{up} =

S_{upi}), biodegradable particulate fraction (S_{bp}), unbiodegradable soluble fraction (S_{us} = S_{usi}) and the acidogenic and acetoclastic methanogenic biomasses (Z_{AD} and Z_{AM}); under stable methanogenic conditions, the effluent biodegradable soluble non-VFA fraction (S_{bsf}) and volatile fatty acids (S_{VFA}) can be accepted to be negligible, i.e.

$$S_t = S_{upi} + S_{bp} + S_{us} + Z_{AD} + Z_{AM} \quad (2.2)$$

- Active acidogenic and methanogenic biomass concentrations in the influent are negligible ($Z_{ADi} = Z_{AMi} = 0$).

- Acidogenic biomass (Z_{AD}) grows according to Monod kinetics, using hydrolysis products as organic substrate.

- Acetoclastic methanogenic biomass (Z_{AM}) grows according to Monod kinetics, using acidogenesis products (acetate) as organic substrate.

- Endogenous respiration of acidogenic (Z_{AD}) and acetoclastic methanogenic (Z_{AD}) biomass forms biodegradable particulate COD (S_{bp}); endogenous residue formation is considered negligible.

- Effluent soluble biodegradable and VFA concentrations are negligible ($S_{bsf} = S_{VFA} = 0$) under stable methanogenic conditions (confirmed experimentally).

- PSS hydrolysis is mediated by the acidogens (Z_{AD}) and rate limiting under stable digester operation.

2.4.2 Reaction stoichiometry

For the purpose of mass balances, the soluble biodegradable COD (S_{bsf}) was given the molecular formula of glucose, while the short chain fatty acids (S_{VFA}) were assumed to be acetic acid only. The molecular formulae for the particulate organics (S_{bp}) and the active biomasses (Z) were taken from Sötemann *et al.* (2005a, b) as $C_{3.5}H_7O_2N_{0.196}$ and $C_5H_7O_2N$ respectively. Therefore, for hydrolysis:

$$C_{3.5}H_7O_2N_{0.196} + 0.604H_2CO_3 \rightarrow 0.684C_6H_{12}O_6 + 0.293H_2O + 0.196NH_3 \quad (2.3)$$

For acidogenesis:

$$C_6H_{12}O_6 + Y_{AD}NH_3 \rightarrow$$
$$Y_{AD}Z_{AD} + 2\left(1-\frac{5}{6}Y_{AD}\right)CO_2 + 4\left(1-\frac{5}{6}Y_{AD}\right)H_2 + 2\left(1-\frac{5}{6}Y_{aD}\right)CH_3COOH \quad (2.4)$$

For acetoclastic methanogenesis:

$$CH_3COOH + Y_{AM}NH_3 \rightarrow Y_{AM}Z_{AM} + \left(1-\frac{5}{2}Y_{AM}\right)CH_4 + \left(1-\frac{5}{2}Y_{AM}\right)CO_2 \quad (2.5)$$

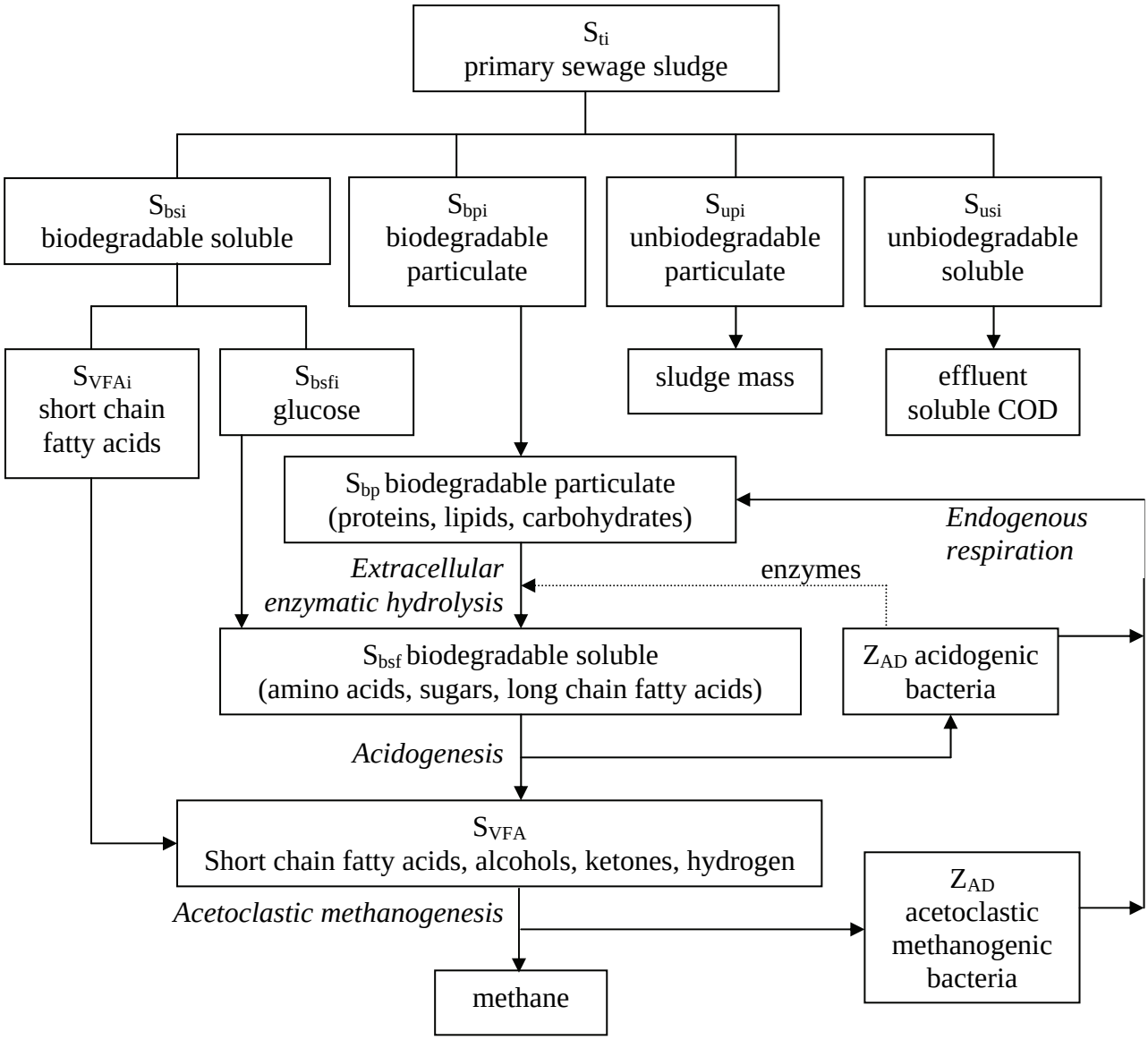

Figure 2.1: Schematic diagram (in units of COD) of the bulk processes involved in the anaerobic digestion of primary sewage sludge

2.4.3 Mass balances (as COD)

In order to determine the rates of hydrolysis, acidogenesis and methanogenesis, mass balances were developed for the major groups of substrates and products (Q = volumetric flow rate, L/day; V = reactor volume, L; R_h = retention time = V/Q, d; b = relevant organism specific endogenous respiration rate constant, 1/d; Y = relevant organism yield, mg cod/mg cod):

Biodegradable particulate COD (S_{bp}) mass balance:

$$dS_{bp}.V = Q.S_{bpi}.dt - Q.S_{bp}.dt - V.rate_{hydrolysis}.dt + V.b_{AD}.Z_{AD}.dt + V.b_{AM}.Z_{AM}.dt \quad (2.6)$$

$$\text{At steady state: } rate_{hydrolysis} = \frac{Q}{V}\left(S_{bpi} - S_{bp}\right) + b_{AD}.Z_{AD} + b_{AM}.Z_{AM} \quad (2.7)$$

Biodegradable fermentable soluble COD (S_{bsf}) mass balance:

$$dS_{bsf}.V = Q.S_{bsfi}.dt - Q.S_{bsf}.dt + V.rate_{hydrolysis}.dt - V.rate_{acidogenesis}.dt \quad (2.8)$$

At steady state, accepting $S_{bsf} = 0$: $rate_{acidogenesis} = rate_{hydrolysis} + \frac{Q}{V}(S_{bsfi})$ (2.9)

Volatile fatty acid COD (S_{VFA}) mass balance:

$$dS_{VFA}.V = Q.S_{VFAi}.dt - Q.S_{VFA}.dt + 2\left(1-\frac{5}{6}Y_{AD}\right).V.rate_{acidogenesis}.dt - V.rate_{methanogenesis}.dt \quad (2.10)$$

At steady state, accepting $S_{VFA} = 0$:

$$rate_{methanogenesis} = \frac{Q}{V}(S_{VFAi}) + 2\left(1-\frac{5}{6}Y_{AD}\right)\left(\frac{Q}{V}(S_{bpi} + S_{bsi} - S_{bp}) + b_{AD}.Z_{AD} + b_{AM}.Z_{AM}\right) \quad (2.11)$$

Acidogenic biomass COD (Z_{AD}) mass balance:

$$dZ_{AD}.V = Q.Z_{ADi}.dt - Q.Z_{AD}.dt + Y_{AD}.rate_{acidogenesis}.V.dt - b_{AD}.Z_{AD}.V.dt \quad (2.12)$$

At steady state: $Z_{AD} = \frac{Y_{AD}.rate_{acidogenesis}.R_h}{(1+b_{AD}.R_h)}$ (2.13)

Acetoclastic methanogenic biomass COD (Z_{AM}) mass balance:

$$dZ_{am}.V = Q.Z_{ami}.dt - Q.Z_{am}.dt + Y_{am}.rate_{methanogenesis}.V.dt - b_{am}.Z_{am}.V.dt \quad (2.14)$$

At steady state: $Z_{AM} = \frac{Y_{AM}.rate_{methanogenesis}.R_h}{(1+b_{AM}.R_h)}$ (2.15)

If Eqs 2.7, 2.9, 2.11, 2.13 and 2.15 can be solved simultaneously, the rates of hydrolysis, acidogenesis and methanogenesis can be calculated for experimental data measured on stable methanogenic anaerobic digesters. Accordingly, the equations were applied to experimental data gathered from the series of completely mixed anaerobic digesters operated over a range of conditions, see below.

2.5 RESULTS AND DISCUSSION

2.5.1 Methanogenic systems

Completely mixed flow-through methanogenic anaerobic digesters were operated at hydraulic retention times (= SRT) from 5 to 60d, with feed COD concentrations of 2, 13, 25 and 40 g cod/ℓ at a controlled temperature of 35°C, see Table 2.1.

Table 2.1: Methanogenic steady states measured for varying hydraulic retention times and feed COD concentrations; numbers refer to steady state period index, detailed results in Ristow *et al.* (2005a)

Feed COD Concentration (g cod/ℓ)	**Hydraulic Retention Time (d)**							
	60	**20**	**15**	**10**	**8**	**6.67**	**5.71**	**5**
40			10; 11	12	21	23	28	
25		3	4	1	2	7	8	9
13			5	13	14	24	31	
9	17							
2				25	26			

For each feed COD concentration, the system hydraulic retention time was decreased step-wise until methanogenesis became unstable. Steady states periods were operated and analysed at regular retention time intervals. For these steady states:

- The minimum hydraulic retention time at which stable operation was observed was 5 d at a feed COD concentration of 25 g cod/ℓ.
- Very good COD mass balances were obtained (mostly within 95-105%). The good COD recoveries lend credibility to the experimental data.
- Reactor volatile fatty acid (VFA) concentrations were below 50 mg HAc/ℓ and for most steady states considerably less than this.

The above latter two observations indicate that stable methanogenic conditions had been established in all systems, a requirement for further analysis of the data.

Based on an understanding of the concepts of the processes operating in the digesters:

- Characterization of the PSS is essential in order to quantify PSS hydrolysis rates correctly.
- The influent PSS was characterized according to Eq 2.1, i.e. to give:

$$S_{ti} = S_{upi} + S_{bpi} + S_{usi} + S_{bsfi} + S_{VFAi}$$

where S_{ti} is the PSS total feed COD concentration, S_{upi} is the unbiodegradable particulate concentration, S_{bpi} is the biodegradable particulate concentration, S_{usi} is the unbiodegradable soluble concentration, S_{bsfi} is the biodegradable soluble non-VFA (fermentable) concentration and S_{VFAi} is the volatile fatty acids concentration.

In terms of the characterization of the PSS above, from the application of mass balance principles (see Section 2.4.3); the volumetric rate of PSS hydrolysis ($rate_{hydrolysis}$) was quantified for each steady state of operation (Figure 2.1):

- Consistent trends in the effects of SRT and PSS feed concentration were evident, substantiating data consistency.

- For all feed COD concentrations, a decrease in the PSS feed concentration causes a corresponding decrease in $rate_{hydrolysis}$.

- From an analysis of the data for the SRT = 60 d system, the unbiodegradable particulate COD (S_{upi}) as a fraction of the total PSS COD concentration (S_{ti}) was 33.45%. Alternative analytical techniques (Sötemann *et al.*, 2005b) gave the unbiodegradable particulate fraction of the COD as 33.3% for the entire data set, and hence the value of 33.45% was accepted. This value closely corresponds with the 36% obtained for the data of O'Rourke (1968).

From the literature, various rate formulations for PSS hydrolysis were identified, and evaluated against the measured methanogenic anaerobic digester data. These included (with the appropriate calibrated kinetic constants):

- ***First order kinetics:*** $rate_{hydrolysis} = k_h.S_{bp}$ (2.16)

  where $k_h = 0.992 \pm 0.492 d^{-1}$

- ***First order specific kinetics:*** $rate_{hydrolysis} = k'_h.S_{bp}.Z_{AD}$ (2.17)

  where $k'_h = 0.00138 \pm 0.00131$ ℓ/mgZ_{AD} as COD.d

- ***Monod kinetics:*** $$rate_{hydrolysis} = \frac{\mu_{max}.S_{bp}.Z_{AD}}{Y_{AD}\left(K_S + S_{bp}\right)} \quad (2.18)$$

  where $\mu_{max} = 0.243 d^{-1}$ and $K_S = 640$ mg cod/ℓ

- ***Surface reaction kinetics:*** $$rate_{hydrolysis} = \frac{k_{max}\left(\frac{S_{bp}}{Z_{AD}}\right)}{\left(K_S + \frac{S_{bp}}{Z_{AD}}\right)} Z_{AD} \quad (2.19)$$

  where $k_{max} = 11.2$ mg cod/mgZ_{AD} as COD.d and $K_S = 13.0$ mg cod/mg Z_{AD} as COD, and where S_{bp} is the biodegradable particulate COD concentration (mg cod/ℓ) and Z_{AD} is the acidogenic biomass concentration (mg cod/ℓ).

From an assessment of the fit of predicted to calculated values, it could be concluded that:

- The first order kinetics and surface reaction kinetics most accurately predict the rate of PSS hydrolysis under methanogenic conditions for all hydraulic retention times and feed COD concentrations evaluated.

- Since first order kinetics are a simplification of the hydrolysis process (the acidogenic biomass is not explicitly included, nor is there an upper limit to the rate), surface

reaction kinetics (Eq 2.19) are the most appropriate rate formulation for PSS hydrolysis.

- However, due to the simplicity of first order kinetics, and since these kinetics were able to accurately predict the PSS hydrolysis rate under all operating conditions, first order kinetics were used in this study to compare the PSS hydrolysis rates under the different operation conditions.

- With the first order kinetics and a first order kinetic constant value of $0.992d^{-1}$, and an unbiodegradable particulate COD fraction of 33.45% of the total feed COD concentration, very close correlation was obtained between model predicted and calculated (from experimental data) volumetric rates of PSS hydrolysis and effluent COD concentrations under methanogenic conditions for all hydraulic retention times and feed COD concentrations, see Figures 2.2 and 2.3 respectively.

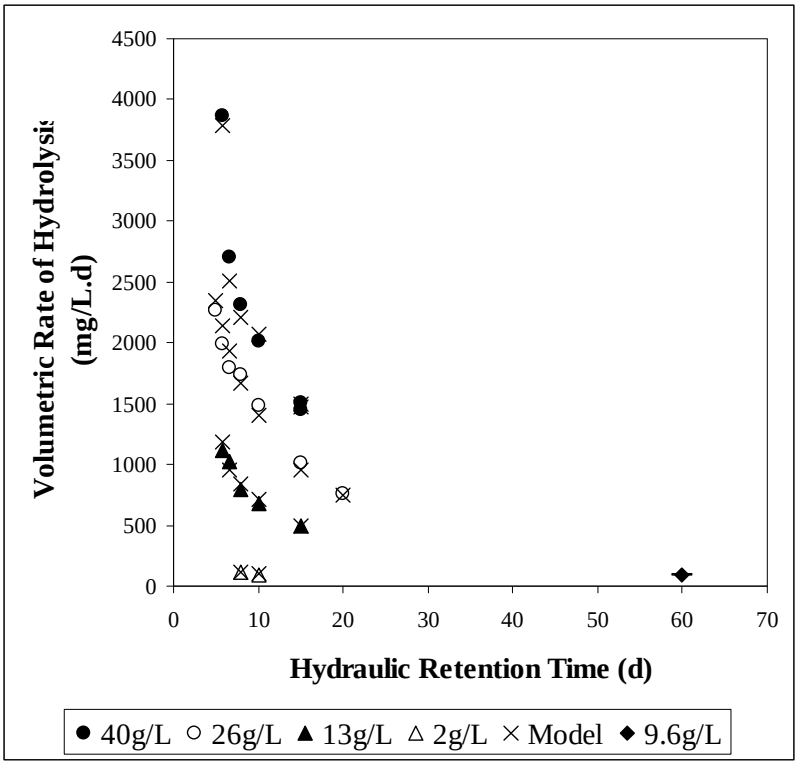

Figure 2.2: Calculated (from experimental data) and predicted (first order kinetics) rate of hydrolysis for each hydraulic retention time at each feed COD concentration for methanogenic systems.

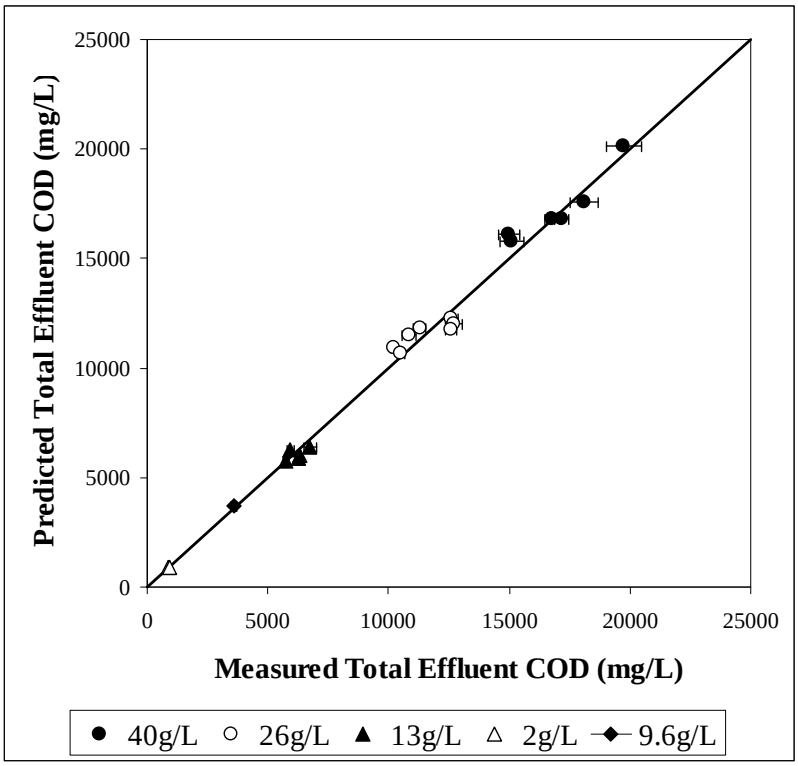

Figure 2.3: Predicted versus measured total effluent COD concentration for each feed COD concentration and hydraulic retention time for methanogenic systems.

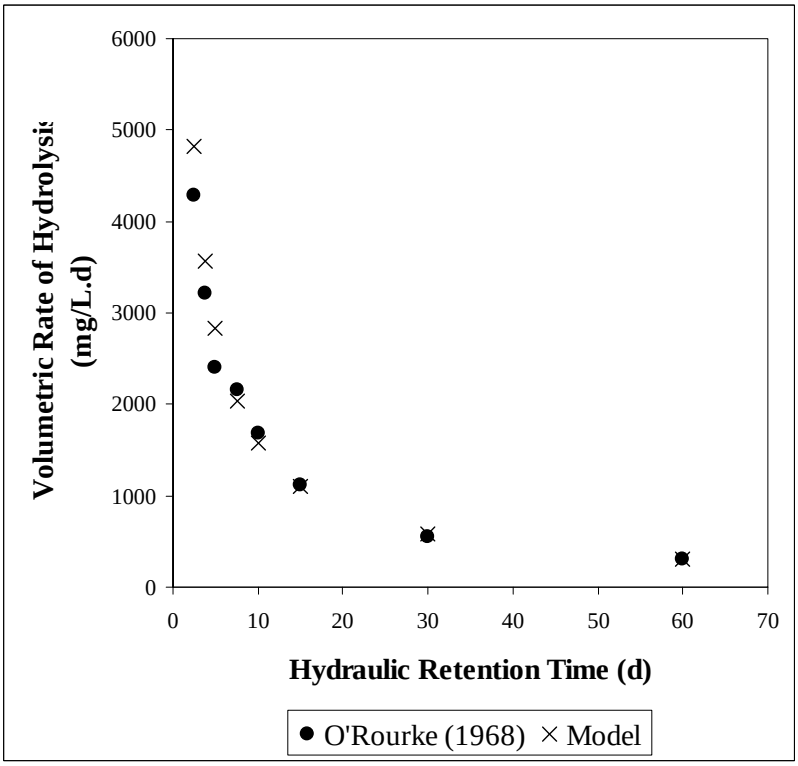

Figure 2.4: Calculated (from experimental data) and predicted (first order kinetics) rate of hydrolysis for each hydraulic retention time for the data of O'Rouke (1968).

- The model, as calibrated above, was applied to data collected in the independent study of O'Rourke (1968); close correlation was obtained for the longer retention times, i.e. the systems in which methanogenesis was complete, see Figure 2.4.

- The good fits of the model predictions to the data collected in this and the independent study of O'Rourke (1968) provides powerful evidence validating the model.

From an extensive investigation into the effect of pH on methanogenic anaerobic digesters (Figure 2.6):

- The minimum operating pH for methanogenic systems was determined at 6.38 before methanogenesis failed.

- Increase in the operating pH above 6.38 had no effect on the PSS hydrolysis rate (pH = 6.38, 6.5, 7.0, 7.5, 8.0).

2.5.2 Acidogenic systems

Acidogenic systems were operated under varying hydraulic retention times (3.33-10 d) and feed COD concentrations (2-40 g cod/ℓ) at a constant temperature of 35^{o}C, Table 2.2.

Table 2.2: Acidogenic steady states measured for varying hydraulic retention times and feed COD concentrations; numbers refer to steady state index, detailed results in Ristow *et al.* (2005a).

Feed COD Concentration (g cod/ℓ)	**Hydraulic Retention Time (d)**		
	10	**5**	**3.33**
40		30	29
13	38	33	32
2	39	35	34

At each retention time and feed concentration, steady state periods were identified and analysed in detail:

- Very good COD mass balances were obtained (92-103%). This lends credibility to the experimental data.

- Negligible methane gas productions were recorded.

- The observations above substantiate the acidogenic condition, i.e. no methanogenesis.

For each steady state of operation, the volumetric rate of hydrolysis was calculated following the procedure in Section 2.4, but recognising methanogenesis was negligible:

- For systems fed the same feed COD concentration and operating at the same hydraulic retention time, the volumetric rates of hydrolysis were significantly lower under acidogenic conditions compared with the corresponding methanogenic conditions.

In applying the first order PSS hydrolysis kinetics developed for the methanogenic systems to the acidogenic systems:

- The value of the first order rate constant (k_h) had to be decreased significantly, substantiating the lower hydrolysis rate.

- The first order kinetic constant for acidogenic conditions (k_h) is linearly dependent on the hydraulic retention time; the relationship was formulated to give:

  $$k_h = 0.0883\text{-}0.0055.R_h \qquad (2.20)$$

  where R_h is the retention time (d)

- With the formulation above to calculate the value of the first order kinetic constant under acidogenic conditions (Eq 2.20), the model was able to reasonably accurately predict the rate of PSS hydrolysis under acidogenic conditions, Figure 2.5.

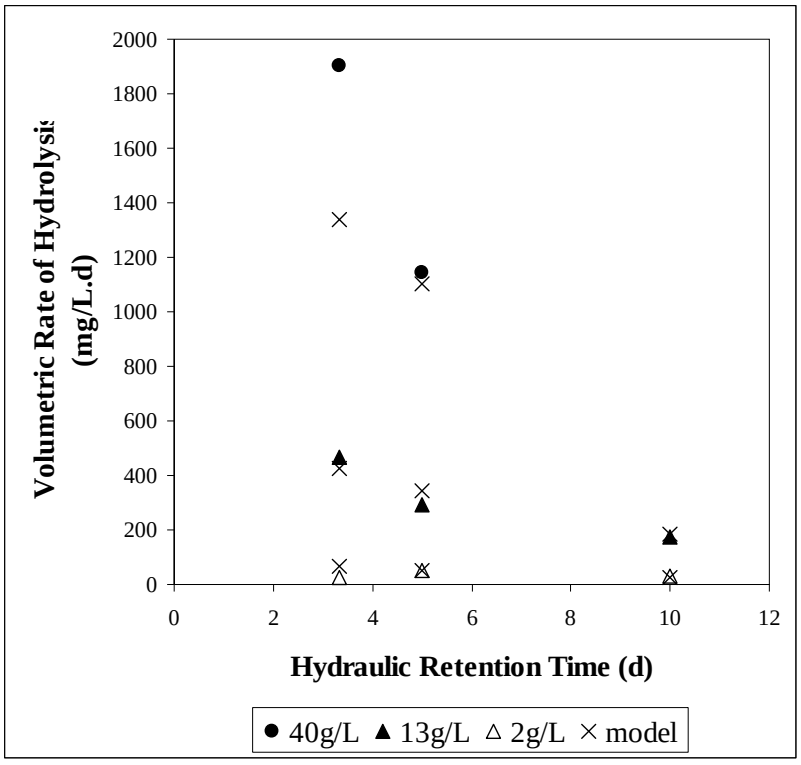

Figure 2.5: Comparison of the calculated and predicted hydrolysis rates for acidogenic systems using the first order rate formulation with the rate constant calculated from $k_h = 0.0883\text{-}0.0055.R_h$ (d^{-1}).

To investigate the influence of pH on PSS hydrolysis under acidogenic conditions, further acidogenic steady state systems were operated at a constant hydraulic retention time (5d) and feed COD concentration (2 g cod/ℓ), but with the digester operating pH controlled, and increased from the minimum pH 5 (steady state pH), to 8 at pH intervals of 1 (5.0, 6.0, 7.0, 8.0). From these investigations:

- The calculated rate of PSS hydrolysis under acidogenic conditions did not change when the pH was increased from 5 to 6.

- However, when the pH was increased from 6 to 8, the observed rate of PSS hydrolysis increased linearly.

- To include the effect above in the first order kinetics, Eq 2.20 was modified:

$$k_h = (0.0883 - 0.055.R_h) + 0.06\left(\frac{pH - pH_{LL}}{pH_{UL} - pH_{LL}}\right) \quad (2.21)$$

  where pH_{LL} = 6.04 and pH_{UL} = 8.0.

- With the modification above, first order kinetics was able to accurately predict the volumetric rate of PSS hydrolysis under acidogenic conditions for all operating pH values, see Figure 2.6.

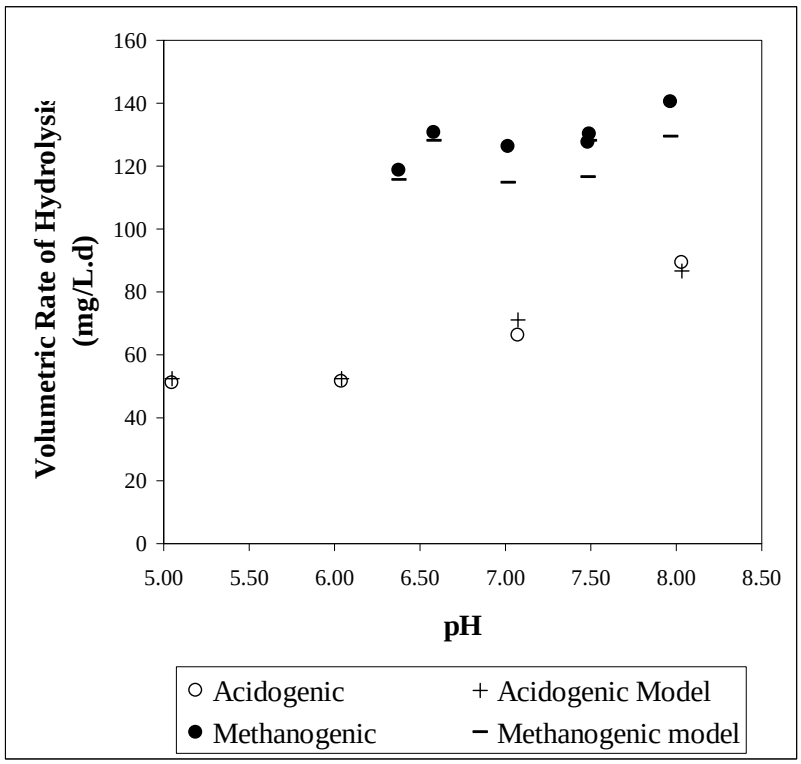

Figure 2.6: Calculated (from experimental data) and predicted (first order kinetics) rate of hydrolysis for methanogenic and acidogenic systems at varying operating pH values.

2.5.3 Sulphate reducing systems

To quantify the rate of PSS hydrolysis under sulphate-reducing conditions and compare this rate with that for methanogenic systems, where possible these systems were operated in parallel digesters, see Table 2.3.

Table 2.3: Sulfate-reducing steady states and corresponding methanogenic systems (Table 2.1) at various operating conditions (retention times, feed COD and sulfate concentrations, operating pH and sulphide concentrations)

Steady state number	Operating conditions				Comparative steady state number
	R_h (d)	Feed COD (g/ℓ)	Feed SO_4 (g/ℓ)	Additional factors	
6	10	26	1	Excess COD	1
15	8	13	9.6	All S_t as FeS	14
16	8	13	9.6	No Fe addition	14 and 15
20	8	2	2	pH ~ 7.5	18 and 37
22	8	2	2	pH ~ 7	19
36	8	2	2	pH ~ 6.5	27
41	16	2	2		
42	13.3	2	2		
46	10	1	1		
47	8	2	2	pH ~ 8.3	

Results from the initial experiments with limited sulphate reduction (1 g SO_4/ℓ with 26 g cod/ℓ; steady state 6, Table 2.3) showed that:

- The sulphate reduction did not influence the PSS hydrolysis rate compared with a parallel purely methanogenic system.
- Methanogenesis was maintained in the digester. Therefore, a limited amount of sulphate reduction in methanogenic systems does not inhibit the hydrolysis nor methanogenesis processes, and can be treated in existing methanogenic digesters without jeopardising the process stability.

When the feed sulphate concentration was increased (9.6 g SO_4/ℓ with 13 g cod/ℓ; steady states 15 and 16, Table 2.3):

- No methanogenesis was observed.
- Sulphate-reducing biomass out compete methanogenic biomass for organic substrate.
- Under sulphate-reducing conditions with low aqueous sulphide (precipitated with ferrous, steady state 15), the volumetric rate of PSS hydrolysis was the same as for the parallel methanogenic system.
- When the aqueous sulphide was not removed (steady state 16), sulphate reduction was inhibited, but no information regarding the PSS hydrolysis rate was collected.

From the observations above, it could be concluded that aqueous sulphide is inhibitory to sulphate reduction.

A range of systems were operated at feed COD concentrations of 2 g cod/ℓ and feed sulphate concentrations of 2 g SO_4/ℓ, at varying retention times (steady states 22, 36, 41, 42, 46 and 47, Table 2.3):

- In all systems, sulphate was slightly in excess and effluent VFA concentrations were low (< 50 mg HAc/ℓ), indicating absence of inhibitions. Thus, at lower aqueous sulphide concentrations, sulphate reduction is not inhibited.

The mathematical model developed for methanogenic systems in Section 2.4 was applied to the sulfate-reducing systems, except that the methanogenic biomass was replaced with acetoclastic sulfate-reducing biomass (Z_{AS}), with different growth constants (metabolic yield constant and cell decay coefficient). The rate of hydrolysis was calculated using the same algorithms as in Section 2.4, with the same feed characterization:

- The first order rate formulation calibrated under methanogenic conditions ($k_h = 0.992d^{-1}$ and 33.45% unbiodegradable particulate COD fraction) was able to adequately predict the rate of PSS hydrolysis under sulphate-reducing conditions.

- The observation above led to the conclusion that the PSS hydrolysis rate is closely similar under methanogenic and sulphate-reducing conditions, i.e. sulphate reduction *per se* does not appear to influence the PSS hydrolysis rate.

Further investigation and analysis of the data showed that:

- An operating pH between 6.5 and 7.5 did not affect the rate of PSS hydrolysis under sulphate-reducing conditions.

- The mean COD: SO4 utilisation ratio in the sulphate-reducing systems was 0.8 g cod/g SO_4, closely similar to 0.78 g cod/g SO_4 obtained by Enongene (2003). These ratios are significantly higher than the theoretical stoichiometric ratio of 0.67 g cod/g SO_4. However, taking into account COD utilization for the production of acidogen and sulphate-reducing biomasses, the theoretical ratio should be approximately 0.85 g cod/g SO_4, which is very close to the measured values.

- The suspended solids concentration was significantly higher for sulphate-reducing systems compared with methanogenic systems (Figure 2.7), and the operating pH did not affect this concentration.

- This has significant implications for sulphate-reducing systems in which solids and hydraulic retention times are uncoupled, as retention of sulphate-reducing biomass and PSS biodegradable particulate substrate may prove problematic.

In contrast to the sulphidogenic systems, for the acidogenic systems the suspended solids concentration increased with increasing pH, Figure 2.7.

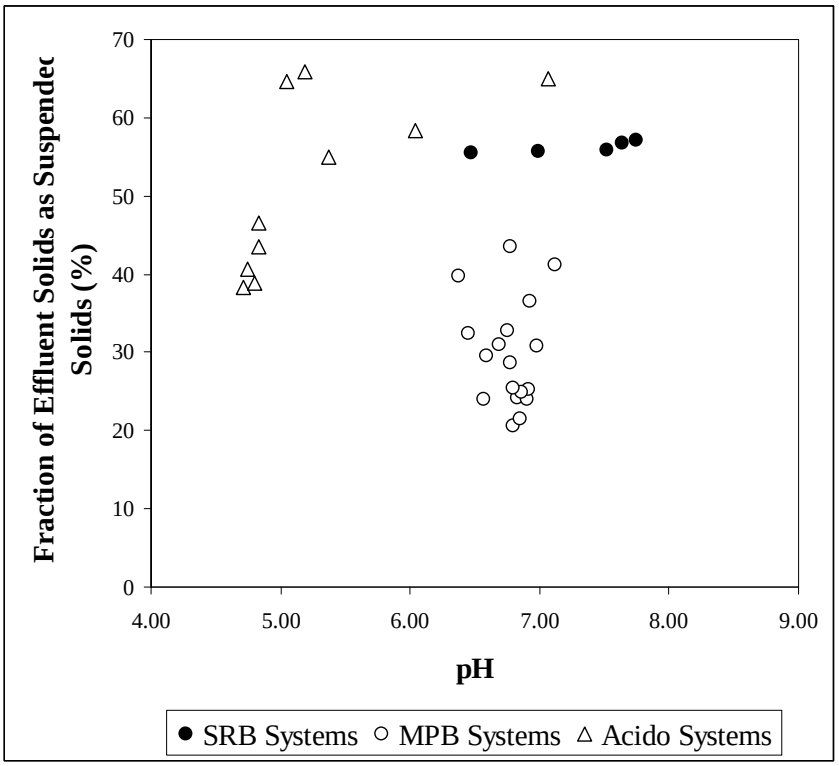

Figure 2.7: Ratio between the effluent suspended solids COD concentration and the effluent total particulate COD concentration (f_{SS}) for methanogenic (MPB), acidogenic (Acido) and sulphate-reducing (SRB) systems as a function of pH.

2.5.4 Comparison of PSS hydrolysis rates under methanogenic, acidogenic and sulphate reducing conditions

From a comparison of the PSS biodegradable particulate COD conversions for the systems operated in this study under methanogenic, acidogenic and sulphate reducing conditions, together with the methanogenic and acidogenic systems operated by O'Rouke (1968) (see Figure 2.8), it could be concluded that:

- The data gathered in this study, and substantiated by the observations of O'Rouke (1968) clearly indicates that the presence of methanogenesis substantially increases the rate of PSS hydrolysis, or conversely, the absence of methanogenesis and conditions created by acidogenesis substantially reduces the rate of PSS hydrolysis.

- The effect above is not pH related; the effect of pH on PSS hydrolysis rates under acidogenic conditions is relatively small and could not account for the magnitude of the reduction in PSS hydrolysis rates.

- Under the conditions which the sulphate reducing systems were operated (sulphide not inhibitory), compared with the equivalent methanogenic systems, sulphate reduction *per se* does not influence the rate of PSS hydrolysis.

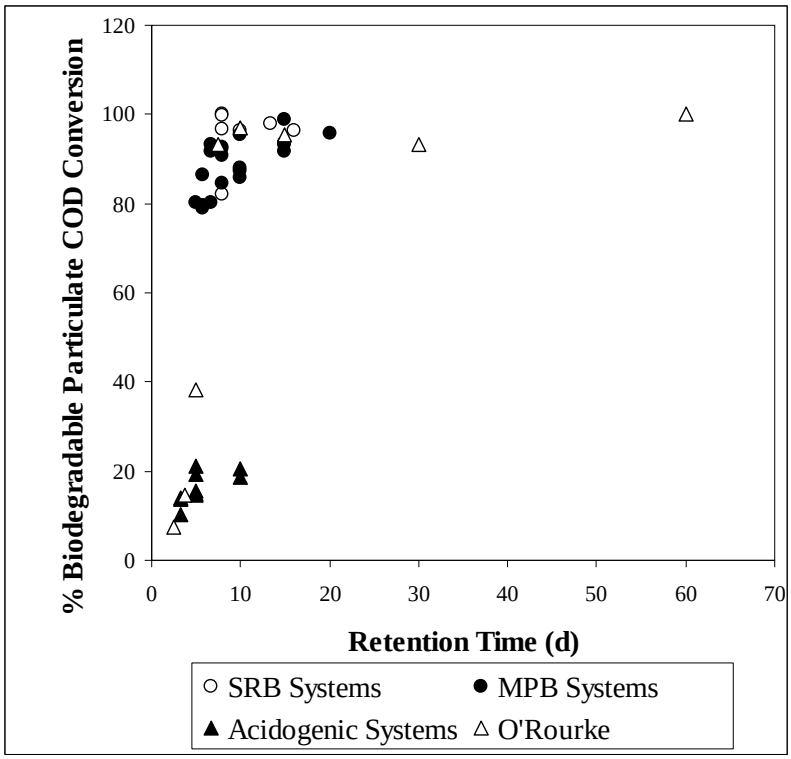

Figure 2.8: Biodegradable particulate COD conversions (as a % of influent PSS biodegradable particulate COD) versus retention time for the methanogenic, acidogenic and sulphate reducing systems operated in this study, and the systems operated by O'Rouke (1968).

2.6 CLOSURE

In this investigation, an extensive data set has been collected on anaerobic digestion of PSS under methanogenic, acidogenic and sulphate-reducing conditions, at varying retention times, feed concentrations and pH values. Through a strict attention to detail, the operating conditions for all systems were carefully controlled and completely defined.

To quantify the volumetric rate of PSS hydrolysis in such systems, a logical mathematical framework has been developed in terms of mass balance principles and characterisation of the PSS feed. This framework should provide a useful, common and systematic basis for comparisons of the hydrolysis rates for different systems. Further, a simple unified first order kinetics based model has been developed to describe PSS hydrolysis under methanogenic, acidogenic and sulphate-reducing conditions. This model takes into account the effects of retention time, feed COD concentration and pH, and the model has been validated both on data collected in this study and on data collected in independent studies.

Since PSS hydrolysis is the rate-limiting step in most methanogenic, acidogenic and sulphate-reducing systems, the subsequent processes are essentially stoichiometric. Hence, this simple model should be a valuable tool in the design, operation and control of steady state digestion systems. However, the model cannot take account of digester failure or behaviour under dynamic loading conditions. These will require development of a more extensive dynamic simulation model. In such a model, the evaluation here would suggest that surface reaction (Contois) kinetics are the most suitable for the PSS hydrolysis process, and these kinetics have been selected for the kinetic models being developed (see Chapters 4, 5 and 6). In this

study, extensive data on transitions between steady states has been collected, which should prove useful for the calibration and validation of such a model.

In terms of the framework developed above, comparing the rates of PSS hydrolysis under methanogenic, acidogenic and sulphate-reducing conditions, the rates are closely similar under methanogenic and sulphate-reducing conditions, but significantly reduced under acidogenic conditions. This implies that the products of PSS hydrolysis (and subsequent acidogenesis) inhibit the PSS hydrolysis rate. If these products are removed, then PSS hydrolysis remains uninhibited, irrespective of whether the biological process that removes the products is methanogenesis or sulphate reduction.

The information developed in this Chapter on PSS hydrolysis directly informed development of the kinetic model for anaerobic digestion of sewage sludge, see Chapters 4, 5 and 6.

3 EXPERIMENTAL INVESTIGATION – UPFLOW ANAEROBIC SLUDGE BED SYSTEM FOR BIOLOGICAL SULPHATE REDUCTION WITH PRIMARY SEWAGE SLUDGE AS SUBSTRATE

3.1 INTRODUCTION

In the BioSURE® system, the core unit process is the biological sulphate reduction with primary sewage sludge as substrate (Rose *et al.*, 2002). Initially, for the biological sulphate reduction unit process, it was proposed to make use of the recycling sludge bed reactor (RSBR) which is a down-flow configuration, to enable the solids and liquid retention times to be uncoupled thereby reducing reactor volume requirements. However, in this configuration, dissolved sulphate can "short-circuit" the sludge bed to the effluent requiring downstream biological sulphate reduction as proposed in the BioSURE® system. Further, in the experimental investigation into completely mixed sulphidogenic systems described in Chapter 2 (and detailed in Ristow *et al.*, 2005a), particularly evident was the influence of sulphate reduction on the effluent suspended solids concentrations – the sulphate reducing systems consistently produced effluents with higher suspended solids concentrations than the corresponding methanogenic systems, i.e. higher concentrations of solids that would not settle. This has significant implications for sulphate reducing systems in which the solids and hydraulic retention times need to be uncoupled (to reduce reactor volumes) such as in the RSBR proposed in the BioSURE® system, as retention of sulphate reducing biomass and PSS biodegradable particulate substrate may prove problematic. In this research project, it was originally proposed that the UCT Research Group operate recycling sludge bed reactor (RSBR) type systems to evaluate enhanced primary sewage sludge hydrolysis. However, agreement was obtained from the reference group guiding the project that the UCT Research Group would not operate such RSBR type systems, because quantification of primary sewage sludge hydrolysis kinetics were difficult to elucidate in such systems and the parameters identifying whether or not enhanced hydrolysis was operative were not clearly defined. As alternative, with agreement from the reference group different system configurations to improve solids liquid separation were examined. Conceptually, passing the influent through the sludge bed may considerably improve the separation and overcome sulphate "short-circuiting". One such system in which this occurs is the Upflow Anaerobic Sludge Bed (UASB) reactor. Accordingly, a study was undertaken to evaluate the feasibility of using the UASB-type system for biological sulphate reduction with primary sewage sludge as substrate.

3.2 BACKGROUND

Primary sewage sludge (PSS) has been identified as a low cost carbon and electron source for biological sulphate reduction in the treatment of acid mine drainage (AMD, Whittington-Jones, 1999; Corbett *et al.*, 2000, Rose *et al.*, 2002). The AMD would consist of heavy metals, sulphate (2.4 g SO_4/ℓ) and a low pH (2-3); the value for sulphate is that at the Erwat Ancor pilot-plant, but would differ for each source of AMD. A conceptual unit process train to treat AMD of this nature would consist of a number of unit operations in which the various components of AMD are treated individually. Figure 3.1 describes such a conceptual unit process train for the treatment of AMD.

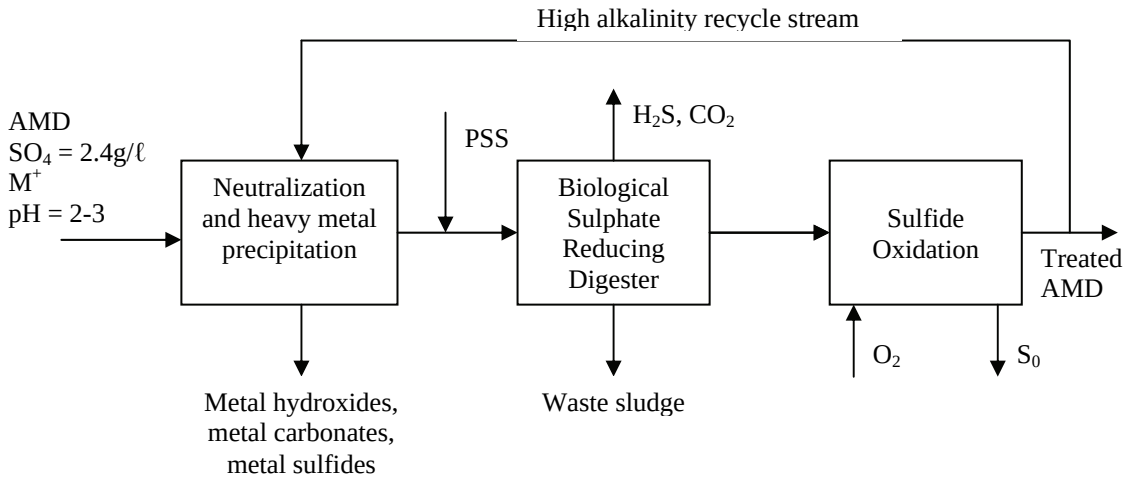

Figure 3.1: Conceptual process from the treatment of AMD using biological sulphate reduction and primary sewage sludge

The central unit operation in the above treatment is the biological sulphate reducing digester, in which the sulphate is reduced to sulphide, some of which leaves the system as hydrogen sulphide gas, but the majority leaves as aqueous sulphide. Similarly, carbon dioxide gas produced is in equilibrium with the dissolved carbonate species, and both the dissolved and gaseous forms leave the sulphate reducing digester. The next step in the process is the sulphide oxidation step, in which the aqueous sulphide produced in the sulphate-reducing digester is oxidised either chemically or biologically to elemental sulphur. The effluent from this unit operation would contain dissolved carbonate species and residual sulphide, and probably a near neutral pH. This high alkalinity effluent is split and recycled to blend with the raw AMD stream. The increase in pH of the AMD stream when blended with the recycle stream would result in precipitation of the metals as metal carbonates, hydroxides and some metal sulphides. These metal precipitates are settled out of the AMD stream, leaving a neutral pH and relatively metal-free stream. This is blended with PSS and enters the biological sulphate-reducing process. Therefore, using this type of scheme, all of the components of AMD (metals removal, pH neutralization and sulphate reduction) can be treated.

The unit operation of interest to this study is the biological sulphate-reducing digester, but clearly the feed to this unit operation is dependent on the operation and configuration of the overall treatment. For this study, the recycle stream flow rate in the conceptual process is made equal to the AMD flow rate, so that the sulphate concentration entering the sulphate-reducing digester is halved (1 200 mg SO_4/ℓ for the Erwat Ancor pilot-plant) by dilution. Also, the pH of this stream is near neutral, and probably contains some alkalinity. Based on these assumptions, the feasibility of operation of a biological sulphate-reducing system was evaluated at laboratory scale. For the biological sulphate-reducing system, an upflow configuration was selected, to combine biological reactions and phase separation in a single reactor, similar to the UASB.

3.3 LABORATORY-SCALE REACTOR OPERATION

A laboratory-scale UASB-type reactor was operated to determine the feasibility of using this type of reactor configuration as the biological sulphate-reducing digester in the treatment scheme described in Figure 3.1, see Figure 3.2. The UASB reactor had a total volume of 10.5 ℓ, and a diameter of 100 mm. The digester was heated to approximately 35^{o}C with heating wires wrapped around the column to the height of the sludge bed, with a thermocouple situated near the bottom of the column, and controlled by the same temperature controller used for the completely mixed systems (see Chapter 2; Ristow *et al.*, 2005a). The system was seeded with waste sulphate-reducing sludge from the completely mixed sulphate-reducing systems fed PSS (Chapter 2), and waste from methanogenic anaerobic digesters being fed waste activated sludge. The seed sludge thus contained acidogenic, methanogenic and sulphate-reducing biomass.

The laboratory-scale UASB reactor feed consisted of 1 200 mg SO_4/ℓ, added as dissolved Na_2SO_4, and alkalinity (500 mg $CaCO_3$/ℓ) added as $NaHCO_3$ powder. To this, 1 600 mg cod/ℓ of PSS (Athlone Treatment Plant, Cape Town) was added. The feed COD: SO4 ratio was based on the 0.8 g cod/g SO_4 utilization ratio determined in Chapter 2 (Ristow *et al.*, 2005a) (1200 mg SO_4/ℓ requires 960 mg cod/ℓ of biodegradable COD), and a total unbiodegradable COD fraction of 40% which is close enough to that determined in Chapter 2 (60% of total COD = 960 mg cod/ℓ; total COD = 1 600 mg cod/ℓ). The PSS was macerated for 1min to break up the larger particles, since the feed was to be pumped through a laboratory-scale positive displacement pump, which would be susceptible to blocking by larger particles.

The hydraulic retention time (HRT) was initially set to above 5d, to allow for the biomass to acclimatise and for the sludge bed to accumulate. The sludge bed volume was allowed to increase from the initial volume of around 2 ℓ to between 4.5 and 5 ℓ, at which time sludge was wasted from a sample port along the length of the column. The sludge was wasted from the top of the sludge bed, and although not confirmed through measurement, this sludge was thought to consist mainly of unbiodegradable particulate matter.

At regular intervals, the hydraulic retention time was reduced stepwise by increasing the dosing rate of the feed pump. At each dosing rate, the system was allowed to stabilise until the VFA concentration was negligible, and the alkalinity and pH was constant, before the next retention time decrease.

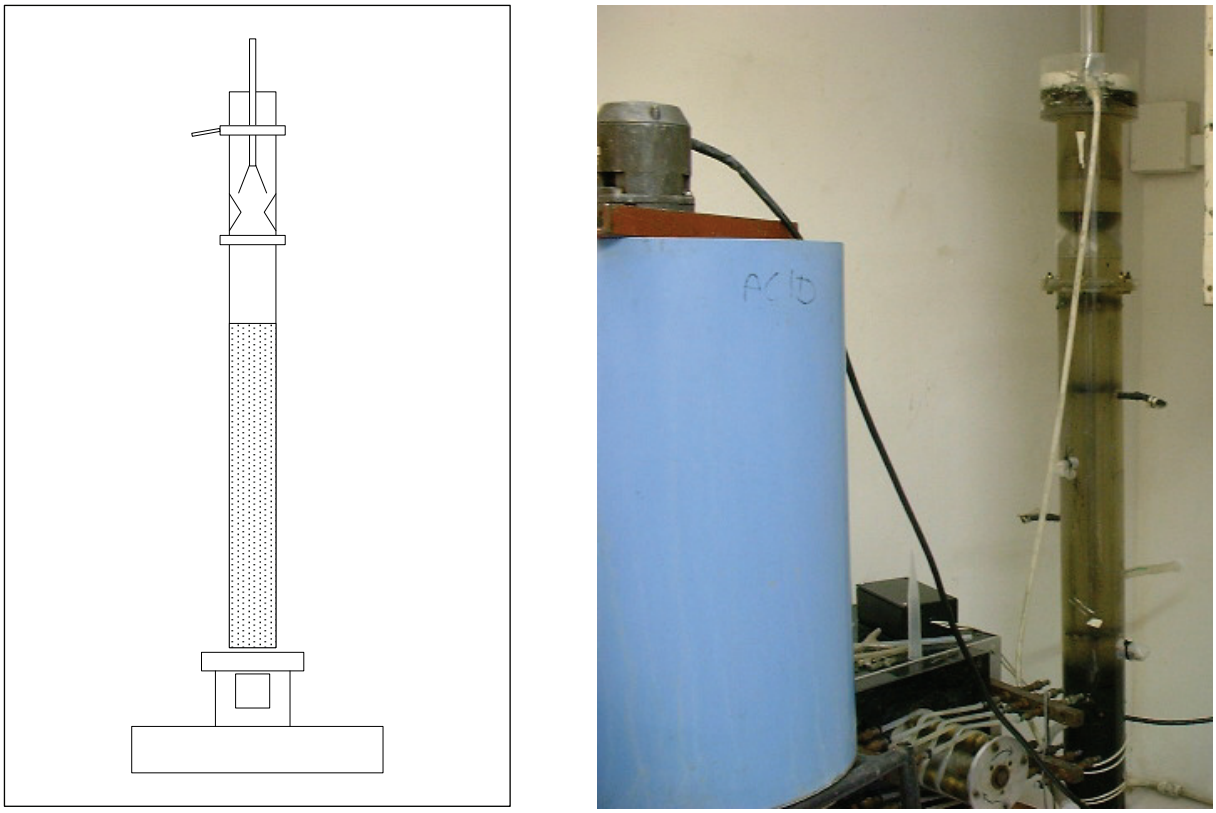

Figure 3.2: Laboratory-scale UASB system for biological sulphate reduction with primary sewage sludge as substrate.

3.4 RESULTS

Figure 3.3 plots the daily volume of feed (measured as the volume of effluent collected) fed to the UASB-type system. Based on the 10.5 ℓ reactor volume, the hydraulic retention time was calculated from the feed volume, and this is also plotted in Figure 3.3. From Figure 3.3, the system was operated with a hydraulic retention time less than 12 h without the sludge bed becoming unstable or fluidising the solids.

Initially the sludge bed was allowed to accumulate until a final volume of 4.5-5 ℓ was reached. Thereafter, sludge was wasted regularly from the top of the sludge bed (oldest sludge) to maintain a bed volume of approximately 4.5 ℓ. The hydraulic retention time in the sludge bed was calculated based on a bed volume of 4.5 ℓ , Figure 3.4. From Figure 3.4, the minimum sludge bed hydraulic retention time was 4.8h, and this was maintained for more than 1 week.

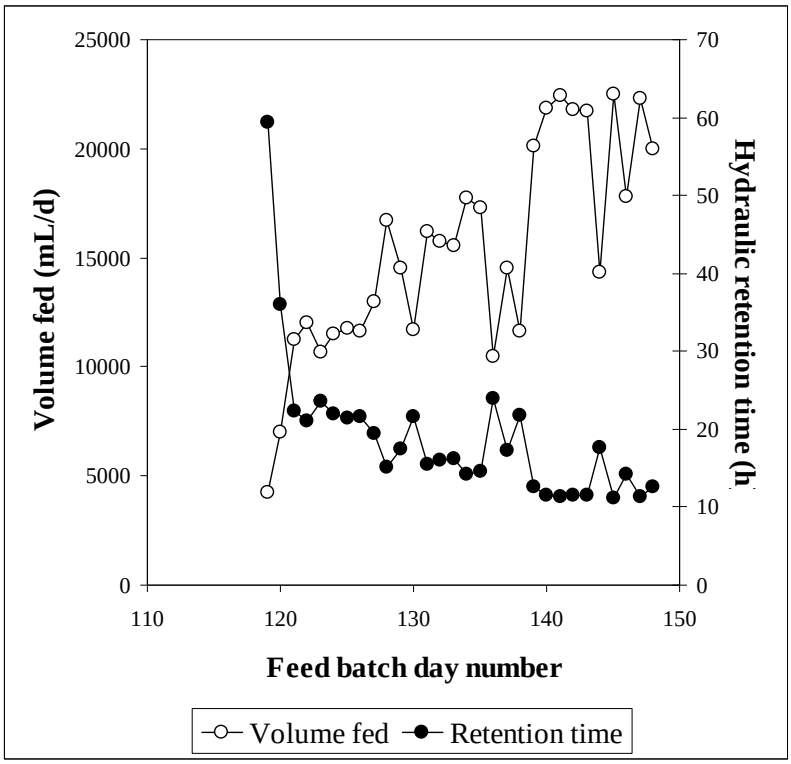

Figure 3.3: Daily feed volume and hydraulic retention time for the UASB-type digester treating the sulphate component of AMD using PSS.

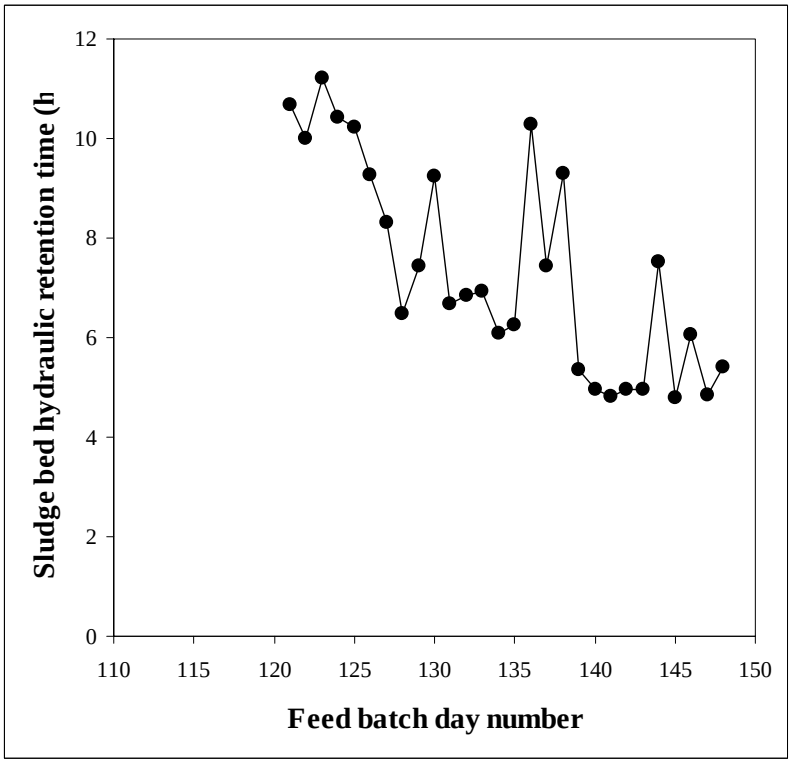

Figure 3.4: Sludge bed hydraulic retention time based on a bed volume of 4.5 ℓ (controlled).

In operation exceptional sludge separation was achieved, with a distinct sludge bed visible and a reasonably solids-free effluent even at the shortest retention times, see Figure 3.5. Considering that the biodegradable particulate organic substrate and active biomass are in significant concentrations only in the sludge bed, and that the settling zone above the bed contains negligible masses of both substrate and biomass, then the sludge bed volume is the biologically active volume of the system. If the system were designed such that the settling zone volume was small compared with the sludge bed volume, the hydraulic retention time in the system could be reduced to close to 4.8 h without negatively affecting the performance of the biological processes or the stability of the sludge bed.

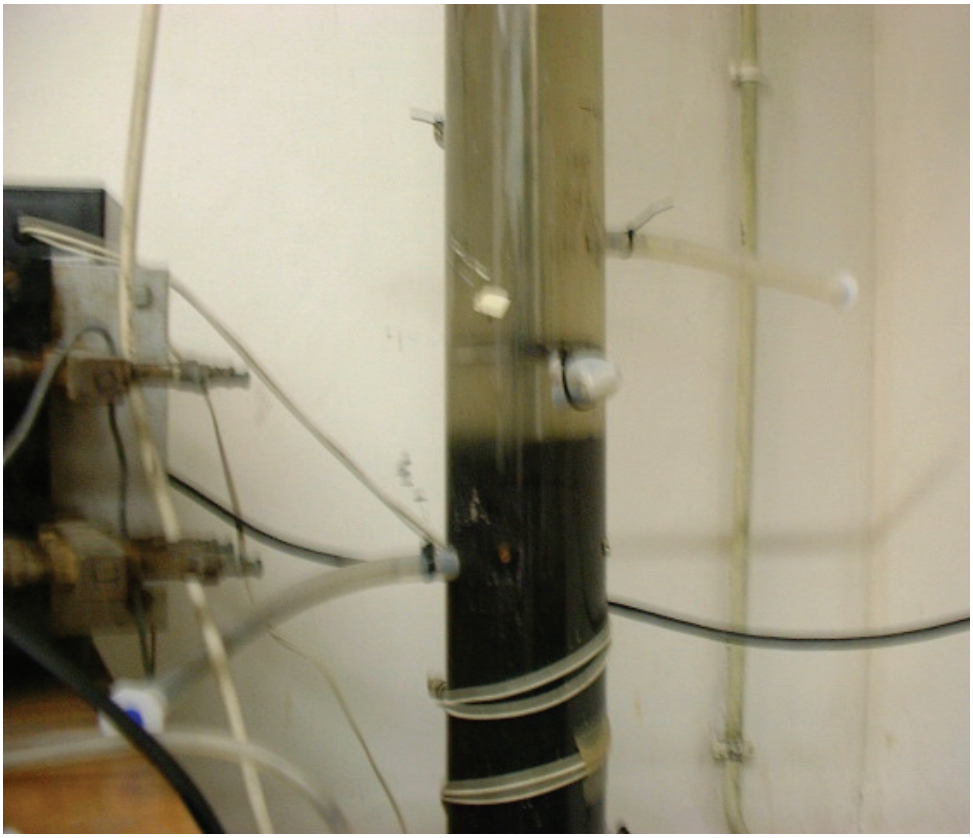

Figure 3.5: Sludge bed separation in the laboratory-scale USAB reactor.

As with the methanogenic and sulphate reducing completely mixed digesters discussed in Chapter 2 for the kinetic studies, an effluent VFA concentration below 50 mg HAc/ℓ would constitute a stable digester performance, with a balance existing between the VFA-producing hydrolysis/acidogenesis processes and the VFA-consuming sulphate-reducing processes. Figure 3.6 plots the VFA and alkalinity concentrations in the settling zone of the UASB-type system over 20 days of operation during which the hydraulic retention time was reduced to <12 h, and the sludge bed retention time was a low as 4.8h. From Figure 3.6, the VFA concentration was well below the 50 mg HAc/ℓ limit, and the alkalinity was constant at 1883 ± 108 mg $CaCO_3$/ℓ. The constant alkalinity measurement indicates that the substrates were being converted to a constant degree, since the net alkalinity production is a consequence of the overall PSS anaerobic digestion conversion, provided the VFA remain low as was the case here.

The system was analysed in more detail on two occasions. The particulate COD, soluble organic COD, aqueous sulfide and residual sulphate concentrations were analysed for both the feed and effluent where applicable.

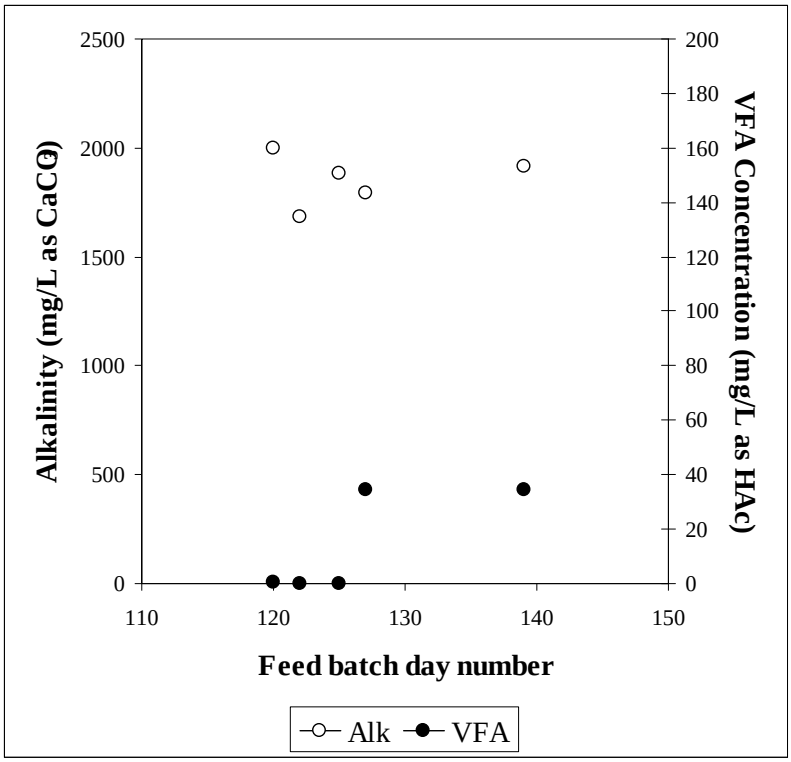

Figure 3.6: Effluent VFA and alkalinity concentrations for the UASB-type digester treating the sulfate component of AMD using PSS.

Table 3.1: Summary of preliminary results from BSR UASB system with PSS as influent substrate.

	Sample 1		**Sample 2**	
	Influent	**Effluent**	**Influent**	**Effluent**
Total COD (mg cod/ℓ)[1]	1611	837	1666	853
Soluble organic COD (mg cod/ℓ)	221	56	214	89
Particulate organic COD (mg cod/ℓ)	1390	248	1452	236
Aqueous Sulphide (mgS/ℓ)		266		264
Sulphate (mg SO_4/ℓ)	1200	133	1200	86
Sulphate Conversion (%)		88.9		92.8
VFA (mg HAc/ℓ)	96	0	88	31.9
Alkalinity (mg $CaCO_3$/ℓ)	450	1883.2	680	1810.5

[1]Total COD = organic + sulphide COD

Table 3.1 lists the results of the analysis of the feed and effluent. From Table 3.1:

- The effluent sulphate concentration was below 135 mg SO_4/ℓ and as low as 86 mg SO_4/ℓ.

- The residual soluble organic COD (<90 mg cod/ℓ) and VFAs (<32 mgHAc/ℓ) in the effluent were low, indicating that most likely the PSS hydrolysis was the rate limiting step.
- Effluent particulate COD concentration was <250 mg cod/ℓ while the feed particulate COD concentration was about 1 400 mg cod/ℓ, indicating successful sludge retention in the system.

These results were extremely encouraging, and it could be concluded that:

- This reactor configuration is a feasible option for the treatment of large volumes of sulphate-rich water, such as acid mine drainage. Sludge bed retention times of less than 5 h seem attainable.

- A feed COD: SO4 ratio of 1.33:1 g cod: g SO4 is adequate for the removal of more than 90% of the feed sulphate without significant residual biodegradable organic COD concentrations.

Particularly evident in the operation of the UASB system was the good solids liquid separation, giving a well defined sludge bed and reasonably clear effluent.

Following the success in the study above, a preliminary study on the internal dynamics in the sludge bed was undertaken, to better understand the processes operative. Concentration profiles were taken along the axis of flow through the sludge bed when the system was operating with a 6 h bed hydraulic retention time, see Figure 3.7.

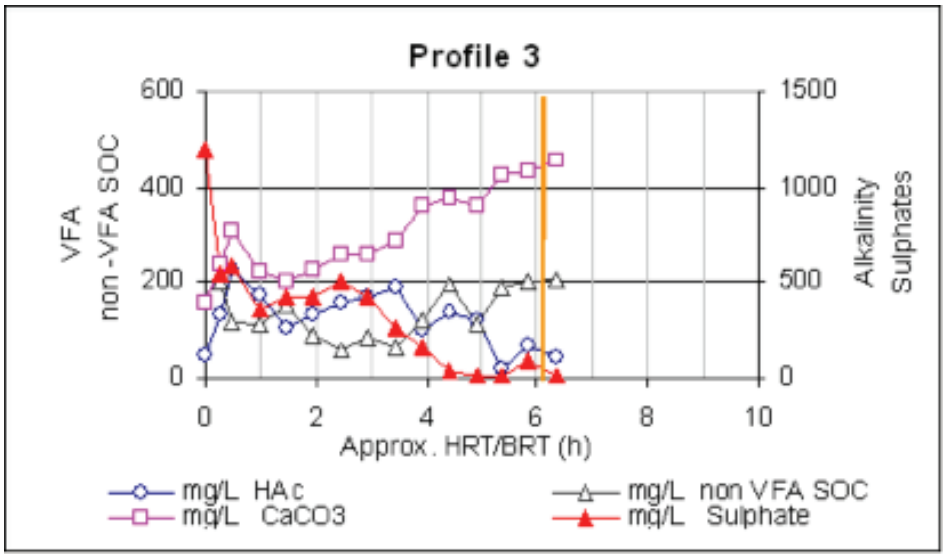

Figure 3.7: Profile taken along the axis of flow through the USAB reactor, receiving PSS as substrate and sulphate supplement, with sludge bed hydraulic (liquid) retention time of 6.2 h.

From Figure 3.7, two regions in the sludge bed can be identified:

- In the bottom half of the bed, sulphate concentrations (and alkalinities) remain relatively

constant, whereas VFA concentrations increase. This indicates that sulphate reduction is rate limiting in this region of the sludge bed.

- In the top half of the bed, sulphate and VFA concentrations decrease rapidly, to near zero at the exit from the sludge bed, while alkalinities increase rapidly. This indicates the hydrolysis is rate limiting in this region of the sludge bed.

Again, extremely encouraging results were obtained: Good bed separation and sulphate reductions were obtained. From the bed profile investigations, it can be recommended that:

- The sludge bed be recycled – this will seed sulphidogens from the top half of the bed to the bottom, initiating sulphate reduction further down the bed profile.

Clearly, this possibility warrants further research attention.

3.5 CLOSURE

This investigation was undertaken to determine the feasibility of using an up-flow type reactor configuration in the BioSURE® system for treating sulfate-containing water with PSS. The results show that stable operation and significant removal of sulfate are possible in such a configuration. Also, the effluent from such a system contains very low concentrations of soluble and particulate organic COD. The system configuration used in this feasibility study is by no means optimised, nor has the lower hydraulic retention time limit been determined. There is sufficient evidence though to suggest that this configuration has potential for the treatment of the sulfate component of AMD with PSS, and that further evaluation of the system is required. A more detailed study on sulphate reduction in UASB reactors with PSS as substrate will be undertaken at UCT, examining *inter alia* minimum bed hydraulic retention times, sludge retention times, bed dynamics, sludge recycles

4 INTEGRATED CHEMICAL, PHYSICAL AND BIOLOGICAL PROCESSES MODELING – METHANOGENIC ANAEROBIC DIGESTION OF SEWAGE SLUDGES

4.1 INTRODUCTION

The principle objective of the University of Cape Town (UCT) and University of KwaZulu-Natal (UKZN) contributions to this research project was the development of a kinetic model for biological sulphate reduction using primary sewage sludge as substrate. In addressing this objective, the approach taken was to develop a more general model structure, which would have wider application to anaerobic digestion systems, with and without sulphate reduction, see Chapter 1. This model would require the biological processes for methanogenic anaerobic digestion and sulphate reduction, integrated with the chemical (e.g. aqueous chemistry) and physical (e.g. gas exchange) processes operative in such systems, in two phases, aqueous and gas. The model was developed in stages. An integrated two phase biological, chemical and physical processes methanogenic anaerobic digestion kinetic model was developed first, and then the biological sulphate reduction and associated chemical and physical processes merged with this kinetic model. This Chapter describes the development of the methanogenic anaerobic digestion model. The model was developed under parallel research projects, namely this project and the Water Research Commission (WRC) research project with UCT on mass balances modelling (K5/1338), which is reported on by Sötemann *et al.* (2005a). The relevant section from the Sötemann *et al.* report is extracted here, to draw together the information of importance for the research project into a single report, but also extended to include modelling of the methanogenic anaerobic digesters described in Chapter 2.

4.2 BACKGROUND

Anaerobic digestion (AD) is one of the oldest biological waste treatment processes, dating back more than a century. With the development of digester heating and mixing, AD has established itself as the most common method of sludge stabilization, and has proven to be effective also in reducing the volumes of sludge with the production of energy rich bio-gas. It has been shown that AD is an effective process for the treatment of a number of types of organic sludges, ranging from municipal waste activated (WAS) and primary sludges (Kayhanian and Tchobanoglous, 1992; Cout *et al.* 1994) to industrial organic sludges and agricultural slurries (Hill and Barth, 1977). In particular, the application of AD to the stabilization of sewage sludges (primary, WAS and humus) is widespread.

Despite its widespread application, the design, operation and control of anaerobic digesters treating sewage sludges is still based largely on experience or empirical guidelines. To aid the design, operation and control of (and research into) AD, a mathematical model would be an invaluable process evaluation tool. Mathematical models provide quantitative descriptions of the treatment system of interest that allow predictions of the system response and performance to be made. From these predictions, design and operational criteria can be identified to optimize the system performance. Mathematical models provide an integrated framework for the system which can give guidance to design, operation and research.

Recognising the potential usefulness of mathematical models, various researchers have

developed such models to describe AD (e.g. McCarty, 1974, Hill and Barth, 1977; Gujer and Zehnder, 1983; Sam-Soon *et al.*, 1991; Kiely *et al.*, 1997, Batstone *et al.*, 2002). The early models focussed primarily on the biological processes operating in an anaerobic digester. Although the importance of the interaction between the biological processes and the weak acid/base chemistry environment in which they operate was recognised early on, because of the effect of pH on the biological processes, modelling this interaction proved to be a far more complex problem than delineating the biological processes themselves. Initially the impact of the biological processes on pH was assessed graphically based on equilibrium chemistry principles of the carbonate weak acid/base system (e.g. Capri and Marais, 1975). The advent of computers and development of numerical algorithms made it easier to model the interaction based on single or two phase (aqueous-gas) weak acid/base chemistry equilibrium equations to estimate the pH in anaerobic digesters. The approach of Loewenthal *et al.* (1989, 1991) made it possible to include multiple mixed weak acid/base systems, both for estimating the digester pH and in the determination and interpretation of the commonly measured digester control parameters, short chain (volatile) fatty acids (SCFA) and alkalinity (Moosbrugger *et al.*, 1992; Lahav and Loewenthal, 2000). The latest AD model (IWAADM1, Batstone *et al.*, 2002) includes algebraic algorithms, based on equilibrium weak acid/base chemistry and continuity of charge balances that seek to model the environment in which the biological processes operate, to predict the pH. These algebraic algorithms and calculation of pH operate externally to the kinetic model structure. As alternative, dynamic equilibria equations for the weak acid/base systems are described (similar to the approach of Musvoto *et al.*, 1997, 2000a). However, the weak acid/base water is not included so that pH is again algebraically calculated externally to the kinetic model, via the charge balance. Calculation of pH externally via the charge balance cannot deal simply with multiple weak acid/base systems in three phases (aqueous/gas/solid), where several minerals competing for the same species may precipitate simultaneously or sequentially (Musvoto *et al.*, 2000a,c): In some anaerobic digestion systems precipitation of minerals is significant, either within the digester itself or in pipework leading from the digester so that the relevant chemical precipitation processes would require inclusion. For such situations, the biological processes and multiple weak acid/base systems in three phases should be modelled in an integrated way within the same kinetic model structure.

In Chapter 4 of Sötemann *et al.* (2005a), an integrated chemical (C), physical (P) and biological (B) processes model for the N removal activated sludge system was developed, by integrating the biological processes of the International Water Association (IWA) Activated Sludge Model No 1 (ASM1, Henze *et al.*, 1987) into a two phase (aqueous-gas) subset of the three phase mixed weak acid/base CP model of Musvoto *et al.* (1997, 2000a,b,c), with additionally gas exchange of N_2 included. To develop the integrated two phase (aqueous-gas) chemical (C), physical (P) and biological (B) processes AD model for sewage sludges, the biological processes for AD are integrated with the same two phase subset of the three phase CP model of Musvoto *et al.* (1997, 2000a,b,c), as described below. In future research, this AD model will be extended to include the third (solid) phase of mineral precipitation. In fact, the N removal activated sludge and AD models are two parts of a single larger model being developed for simulating the entire wastewater treatment plant (WWTP) on materials mass balance and continuity principles, under the parallel WRC research contract K5/1338. In that research, it is planned to include also biological excess P removal (BEPR) and AD of P rich waste activated sludges in the WWTP model. In the research here, biological sulphate reduction is to be included, see Chapter 5.
The AD model is built up in stages. First, the biological processes are defined and then these are integrated into the mixed weak acid/base model of Musvoto *et al.* (1997, 2000a, b, c). For

ease of cross-referencing to the source papers, the same process and compound numbering system described in Chapter 4 of Sötemann *et al.* (2005a) will be followed.

4.3 BIOLOGICAL PROCESSES OF ANAEROBIC DIGESTION

4.3.1 Conceptual model

In the literature there is considerable variation in conceptual schemes for describing the biological processes of AD with sewage sludge as influent, from simple two stage reaction schemes including only hydrolysis/acidogenesis and methanogenesis (Kiely *et al.*, 1997) to the most commonly used six step reaction scheme as proposed by Gujer and Zehnder (1983).

In the reaction scheme of Gujer and Zehnder (1983) (Fig 4.1), the hydrolysis process acts separately on three main groups of complex organics, viz. (i) proteins, (ii) carbohydrates and (iii) lipids. These complex polymeric materials are hydrolysed by extracellular enzymes to soluble products that are small enough to allow their transport across the cell membrane. The products of the separate hydrolysis processes are amino acids, sugars and fatty acids respectively. These relatively simple, soluble compounds are fermented (acidogenesis) or anaerobically oxidised to short chain fatty acids (SCFAs) (acetate), alcohols, CO_2, hydrogen and ammonia. A portion of the hydrolysis products are also converted to intermediate products (propionate, butyrate, etc.), which are then converted to acetate, hydrogen gas and CO_2 through the process of acetogenesis. Lastly, methanogenesis occurs by hydrogen reduction with CO_2 (hydrogenotrophic methanogenesis) and from acetate cleavage (acetoclastic methanogenesis).

The Gujer and Zehnder (1983) reaction scheme formed the basis for the AD model developed here, but with four main modifications (Fig 4.2), viz.:

(a) Recognising that carbohydrate, protein and lipid measurements on ***sewage sludges*** are unlikely to be routinely available and indeed are difficult to do, the hydrolysis of the three separate organic materials was modified to a single hydrolysis process acting on a generic organic material representing sewage sludge ($C_XH_YO_ZN_A$, McCarty, 1974). This simplification is not unreasonable since the end products of hydrolysis and subsequent acidogenesis of the three organic groups are essentially the same, namely SCFAs. In this approach, the C, H, O and N contents of sewage sludges are needed to determine the X, Y, Z and A values in $C_XH_YO_ZN_A$; these were determined by simulation of measured data and direct measurement, see below. In follow-up work under the WRC research contract on mass balances modelling, to extend the model to AD of waste activated sludges (including biological excess P removal sludges) in 3 phases (liquid-gas-solid), i.e. including mineral precipitation, the P content of sewage sludges will be added to this formulation (i.e. $C_XH_YO_ZN_AP_B$).

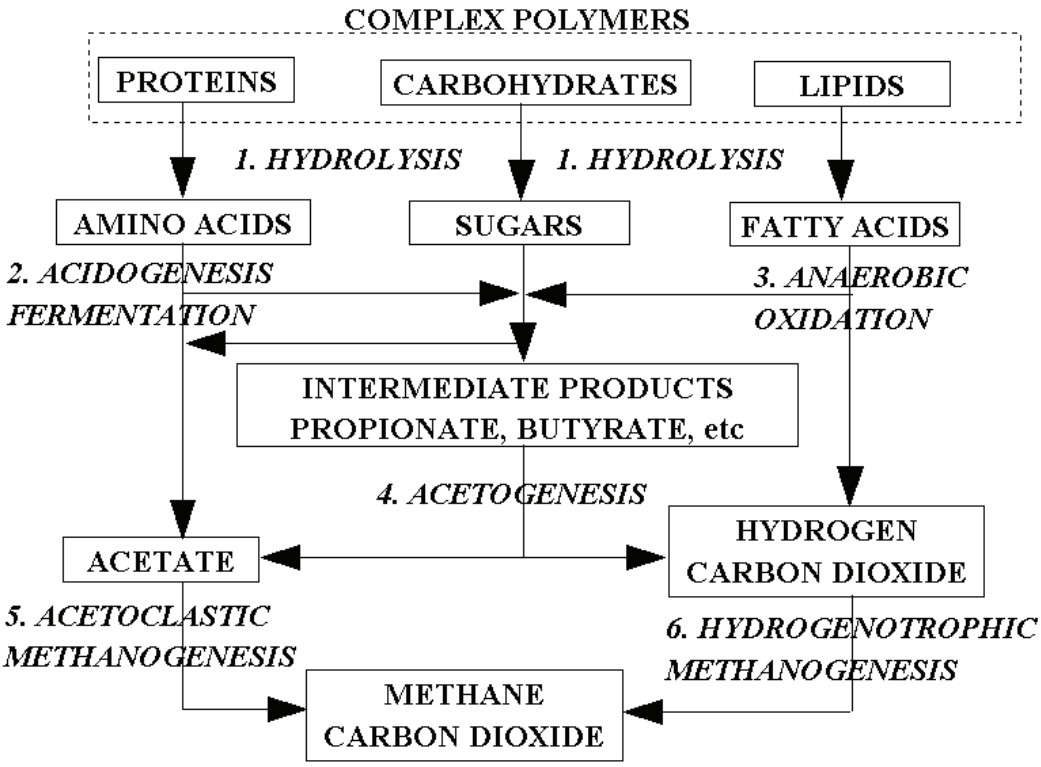

Figure 4.5: Anaerobic digestion processes scheme of Gujer and Zehnder (1983).

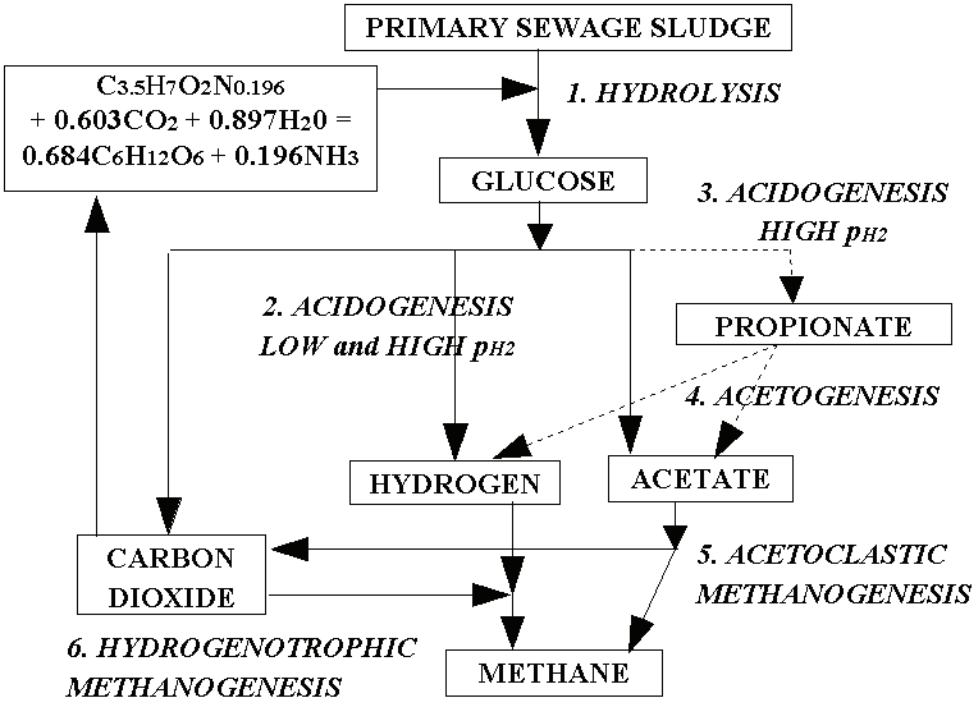

Figure 4.2: Anaerobic digestion processes scheme of University of Cape Town Anaerobic Digestion Model No 1 (UCTADM1) including (i) the effect of high hydrogen partial pressure on acidogenesis and (ii) COD, carbon and nitrogen mass balances with a generic CHON sludge composition.

(b) With the proposed single hydrolysis process, recognition of three separate hydrolysis products was no longer necessary. Accordingly, a single hydrolysis process and end product were included. This end product was chosen to be the idealised carbohydrate "glucose" for a number of reasons: The subsequent biological processes on "glucose" are reasonably well established and the acidogenic/fermentation process acting on "glucose" to convert it to SCFAs is unlikely ever to be rate limiting. Accordingly, in model application accumulation of "glucose" will not occur, even under digester failure conditions. This implies that the "glucose" acts merely as an ***intermediate*** compound, which is acidified to SCFAs as soon as it is produced. In any event, because the end products of hydrolysis and acidogenesis in the scheme of Gujer and Zehnder (1983) (Fig 4.1) are the same as in the revised scheme (Fig 4.2), the net result is the same in both schemes. In order to maintain the COD, C, H, O and N balances, water and carbon dioxide are taken up from the bulk liquid to generate the glucose from the sewage sludge (Fig 4.2), and ammonia is released.

(c) As a consequence of accepting a single hydrolysis process, separate anaerobic oxidation of fatty acids does not need to be included.

(d) In the reaction scheme of Gujer and Zehnder (1983), a fixed proportion of hydrolysis end products are converted to intermediate SCFA (propionate, butyrate, etc.) and the balance directly to acetate. As an alternative, the influence of the hydrogen partial pressure (p_{H2}) on acidogenesis of glucose to acetate and propionate as proposed by Sam-Soon *et al.* (1991) was included in the revised scheme. This provides a better description of AD behaviour under failure conditions. To include the proposals of Sam-Soon *et al.* (1991), the acidogenesis was divided into two processes – (i) under high p_{H2} conditions, acetic and Propionic acids are generated together with H_2 and CO_2 and (ii) under low p_{H2} conditions, acetic acid only is generated together with H_2 and CO_2. In this revised scheme, generation of butyrate and higher SCFAs was not considered, because with sewage sludge as influent these usually are only found in minor concentrations, even under digester failure conditions.

4.3.2 Mathematical model – UCTADM1: Biological processes

Accepting the revised reaction scheme (Fig 4.2), the biological processes mediated by the four recognized AD organism groups were included in the two phase (aqueous-gas) chemical (C), physical (P) and biological (B) anaerobic digestion model (UCTADM1, see Table 4.1). Following ASM1 for activated sludge systems (Henze *et al.*, 1987), the processes were formulated either as hydrolysis or organism group growth processes. All four organism groups were accepted to be subject to endogenous respiration and so an endogenous mass loss process was included in the model for each group. It is recognised that the organism groups are not representative of a single organism species, but rather are 'surrogates' representing all organism species performing a particular function of interest; this is similar to the approach followed for modelling of activated sludge systems (e.g. Dold *et al.*, 1980, Henze *et al.*, 1987). In formulating the model, since weak acid/base chemistry is included directly, all biological processes that act on weak acid/base species needed to be formulated in terms of the relevant dissociated or undissociated species (see below). This included both the stoichiometric consumption and production of weak acid/base species by the processes, and the formulation of the kinetic rate expressions. Whichever species is selected, in the production or consumption of weak acid/base species, because the weak acid/base chemistry is included directly, the model will automatically redistribute the weak acid/base species

including the hydrogen ion (H^+) and establish a new pH.

Table 4.1: Biological processes included in the two phase anaerobic digestion model.

PROCESS	SPECIFIC BIOLOGICAL PROCESS	ORGANISM GROUP
Hydrolysis	D1. Hydrolysis of $C_XH_YO_ZN_A$ to "glucose"	Acidogens, Z_{AD}
Growth	D2. Acidogens on 'glucose' under low p_{H2}	Acidogens, Z_{AD}
	D3. Acidogens on 'glucose' under high p_{H2}	Acidogens, Z_{AD}
	D5. Acetogens on Propionic acid	Acetogens, Z_{AC}
	D7. Acetoclastic methanogens on acetic acid	Acetoclastic methanogens, Z_{AM}
	D9. Hydrogenotrophic methanogens on H_2	Hydrogenotrophic methanogens, Z_{HM}
Death / Endogenous decay	D4. Acidogens	Acidogens, Z_{AD}
	D6. Acetogens	Acetogens, Z_{AC}
	D8. Acetoclastic methanogens	Acetoclastic methanogens, Z_{AM}
	D10. Hydrogenotrophic methanogens	Hydrogenotrophic methanogens, Z_{HM}

The 10 biological processes listed in Table 4.1 act on 14 compounds and cause changes in their concentrations. The changes in some compound concentrations may be directly measurable, but the changes in the non-measurable compound concentrations are inferred from the conceptual model of the processes (Fig 4.2) and mass balance requirements. The compounds and processes of AD based on the reaction scheme of Fig 4.2 are shown in the Petersen matrix format in Table 4.2, in which each row represents a biological process and each column a compound, and the stoichiometric relationships between the compounds and processes are listed at their intersection blocks, the process kinetic rates on the right hand side and the units of the compounds along the bottom. Note that all the compounds in Table 4.2 are specified as mol/P, including the sewage sludge. The mol/P of the sewage sludge is calculated from its measured COD concentration and its g cod/mol, which is calculated from its known composition, i.e. known X, Y, Z and A in $C_XH_YO_ZN_A$ (see below). The AD organism concentrations for all four organism groups are also specified as mol/P based on a formulation of $C_5H_7O_2N$, which has a molar mass of 113 g/mol and a COD/VSS ratio of 1.42 mg cod/mgVSS (McCarty, 1964). The g cod, gN or gH_2CO_3* Alk per mol of the compounds as appropriate are also given along the bottom of the matrix. If the g cod/mol ratios are multiplied by the corresponding stoichiometric value in the matrix and summed across a process, it will be found that these sums are zero, i.e. the COD mass balance applies across each process. The requirement to express the model compounds in mole units arises from the requirement to model CO_2 production/utilisation (zero COD), which is essential for the weak acid/base chemistry and physical processes parts of the model.

4.3.3 Stoichiometry of the biological processes

The stoichiometry in the model was deduced directly from the biochemical stoichiometric equations of the processes. The metabolic pathways used by fermentative organisms for the degradation of carbohydrates to SCFAs are reasonably well defined. As noted above, for this reason amongst others, the biodegradable particulate COD entering the system was directly hydrolysed to the intermediate "glucose", from which the remainder of the products were formed. As an example for calculating the stoichiometry, consider the process of acetogenesis.

Table 4.2: Petersen matrix representation of the biological processes and associated compounds of the University of Cape Town Anaerobic Digestion Model No 1 (UCTADM1). Influent sewage sludge concentration is in mol/P. This concentration is calculated from the measured COD concentration of the sludge and the sludge composition formula $C_XH_YO_ZN_A$ with measured values of X, Y, Z and A.

	Number	C1	C2	C3	C7	C13	C28	C29	P1†	P4	D1	D2	D3	D4	D5	D6	D7	
	Compounds	NH_4^+	NH_3	$H_2CO_3^*$	H^+	HAc	HPr	Pr^-	CO_2	CH_4	$C_XH_YO_ZN_A$	$C_6H_{12}O_6$	H_2	Z_{AD}	Z_{AC}	Z_{AM}	Z_{HM}	
No	Processes		Dslvd	Dslvd					Gas	Gas	S_{bp}	S_{bsf}	Dslvd	Acido gens	Aceto gens	AMs	HMs	Process rates
C46	Forward dissociation of HPr				1		-1	1										$K_{fPr}[HPr]$
C47	Reverse dissociation of HPr				-1		1	-1										$K_{rPr}[Pr^-][H^+]$
P6†	Dissolution of CO_2 gas			1					-1									$K_{rCO2}(pCO_2)(K_{HCO2})$
P7†	Expulsion of CO_2 gas			-1					1									$K_{rCO2}[H_2CO_3^*]$
P8†	Expulsion of NH_3 gas		-1															$K_{rNH3}[NH_3]$
D1	Hydrolysis		S1	S2							-1	S3						Eq 4.8d
D2	Acidogenesis (low pH_2)	-1		S4	1	S5						$-1/Y_{AD}$	S6	1				Eq 4.9
D3	Acidogenesis (high pH_2)	-1		S7	1	S8	S9					$-1/Y_{AD}$	S10	1				Eq 4.10
D4	Acidogen endogenous decay		S11	S12							S13			-1				$b_{AD}[Z_{AD}]$
D5	Acetogenesis	-1		S14	1	S15	$-1/Y_{AC}$						S16		1			Eq 4.11
D6	Acetogen endogenous decay		S11	S12							S13				-1			$b_{AC}[Z_{AC}]$
D7	Acetoclastic methanogenisis	-1		S17	1	$-1/Y_{AM}$				S18						1		Eq 4.12
D8	Acetoclastic methanogen endogenous decay		S11	S12							S13					-1		$b_{AM}[Z_{AM}]$
D9	Hydrogenotrophic methanogenesis	-1		S19	1					S20			$-1/Y_{HM}$				1	Eq 4.13
D10	Hydrogenotrophic methanogen endogenous decay		S11	S12							S13						-1	$b_{HM}[Z_{HM}]$
	Units	mol/P	mol/P	mol/P	mol/P	mol/P	mol/P	mol/P	mol/P	mol/P	mol/P	mol/P	mol/P	mol/P	mol/P	mol/P	mol/P	
	g COD/mol	-	-	-	-	64	112	112	0	64	131.3‡	192	16	160	160	160	160	
	g N/mol	14	14	-	-	-	-	-	-	-	2.744	-	-	-	-	-	-	
	g H_2CO_3* as $CaCO_3$ /mol	-	-	0	-50	-	-	-	-	-	-	-	-	-	-	-	-	

† These processes and compound were included in the models of Musvoto *et al.* (1997, 2000a) as follows: Processes P6 was C7, P7 was C8, and P8 was C46 and compound P1 was C6.
Because the matrix units are mol/P summing the stoichiometry across each process does not yield zero. However, if each stoichiometric value is multiplied by the compounds' g cod/mol ratio and then summed across the process, zero is obtained, i.e. COD balances across each process. Also, C, N, O and H mass balances across each process.
‡ This is the g COD/mol for the primary sludge CHON content measured and predicted in this investigation, i.e. $C_{3.5}H_7O_2N_{0.196}$

Acetogenesis (Process D5, Table 4.2) is the process whereby under low hydrogen partial pressure (p_{H2}) the acetogens convert Propionic acid (HPr) (generated by acidogenesis under high p_{H2}) to acetic acid (HAc). The stoichiometric equation for the acetogenesis reaction is:

$$CH_3CH_2COOH + 2H_2O \rightarrow CH_3COOH + CO_2 + 3H_2 \quad (4.1)$$

During acetogenesis, growth of acetogenic organisms (Z_{AC}) takes place which can be stoichiometrically represented by:

$$3CH_3CH_2COOH + CO_2 + 2NH_4^+ \rightarrow 2C_5H_7O_2N + 4H_2O + H_2 + 2H^+ \quad (4.2)$$

Note that in Eqs 4.1 and 4.2 (i) CO_2 is utilised as an additional carbon source – in all CO_2 consumption/production the undissociated carbonate species H_2CO_3* acts as source/sink respectively, (ii) ammonium is the nitrogen source for organism growth – under normal operating conditions and pH (6.5<pH<7.5) of an anaerobic digester, the ammonium species (NH_4^+) dominates over the ammonia species (NH_3) so that using ammonia as the N species for organism growth can cause numerical instability in solution procedures for the model, (iii) the undissociated propionic acid species is used as substrate source, in agreement with observations in the literature, and (iv) the chemical formulation for organisms is assumed to be $C_5H_7O_2N$, which is the formulation generally accepted to represent organism active mass in activated sludge (WRC, 1984).

Accepting that Y_{ac} mol of acetogen organisms are formed (i.e. the anabolic yield of acetogens); Eq 4.2 can be rewritten as:

$$\frac{3Y_{ac}}{2}CH_3CH_2COOH + \frac{Y_{ac}}{2}CO_2 + Y_{ac}NH_4^+ \rightarrow Y_{ac}C_5H_7O_2N + 2Y_{ac}H_2O + \frac{Y_{ac}}{2}H_2 + Y_{ac}H^+ \quad (4.3)$$

Adding Eqs 4.1 and 4.3 and dividing by Y_{ac} yields:

$$\frac{1+\frac{3Y_{ac}}{2}}{Y_{ac}}CH_3CH_2COOH + \frac{2(1-Y_{ac})}{Y_{ac}}H_2O + NH_4^+ \rightarrow \frac{1}{Y_{ac}}CH_3COOH + C_5H_7O_2N + \frac{1-\frac{Y_{ac}}{2}}{Y_{ac}}CO_2 + \frac{3+\frac{Y_{ac}}{2}}{Y_{ac}}H_2 + H^+ \quad (4.4)$$

Recognising that in Eq 4.4 the "true" acetogen yield (Y_{AC}, mole organism/mole propionate) is $Y_{ac}/(1+3/2Y_{ac})$, and substituting Y_{AC} into Eq 4.4 and solving gives:

$$\frac{1}{Y_{AC}}CH_3CH_2COOH + \frac{(2-5Y_{AC})}{Y_{AC}}H_2O + NH_4^+ \rightarrow \frac{1-\frac{3}{2}Y_{AC}}{Y_{AC}}CH_3COOH + C_5H_7O_2N + \frac{1-2Y_{AC}}{Y_{AC}}CO_2 + \frac{3-4Y_{AC}}{Y_{AC}}H_2 + H^+ \quad (4.5)$$

The stoichiometry for acetogenesis and acetogen growth was extracted from Eq 4.5 directly, and is summarised in Table 4.3. Note that compounds that are utilised (reactants, left hand side of Eq 4.5) are negative (reduction), while compounds produced (products, right hand side of Eq 4.5) are positive (production), that H_2O has been included in Eq 4.5 for an element

balance, but is not included directly in Table 4.3, and that there is a net production of CO_2 expressed as H_2CO_3* in the kinetic model ($1/Y_{AC}$ >2). Following this procedure, the stoichiometries for the remaining processes were derived and are summarised in Table 4.4.

Table 4.3: Stoichiometry for acetogenesis and acetogen growth (Process D5 in Table 4.2). The S numbers in brackets cross reference to the model Petersen matrix (Table 4.2).

C1/B10 NH_4^+	C3 (S14) H_2CO^3*	C7 H^+	C13 (S15) HAc	C28 HPr	D3 (S16) H_2	D5 Z_{AC}
moles	moles	moles	moles	moles	moles	moles
-1	$\frac{1-2Y_{AC}}{Y_{AC}}$	1	$\frac{1-\frac{3}{2}Y_{AC}}{Y_{AC}}$	$-\frac{1}{Y_{AC}}$	$\frac{3-4Y_{AC}}{Y_{AC}}$	1

Table 4.4: Stoichiometry for of the AD processes hydrolysis (D1), acidogenesis (D2, D3), acetoclastic methanogenesis (D7), hydrogenotrophic methanogenesis (D9) and endogenous respiration of the four organism species (D4, D6, D8 and D10). The S1 to S13 numbers cross-reference to the stoichiometry in the Petersen matrix (Table 4.2). Stoichiometry of process D5 is given in Table 4.3.

Hydrolysis (Process D1)			
C2 – NH_3 (S1)	C3 – $H_2CO_3^*$ (S2)	D1 – S_{bp}	D2/B2 – S_{bs} (S3)
moles	moles	moles	moles
+A	$\frac{2Z+3A-Y}{4}$	-1	$\frac{Y+4X-2Z-3A}{24}$

Acidogenesis for low pH2 (Process D2)						
C1/B10 NH_4^+	C3 (S4) $H_2CO_3^*$	C7 H^+	C13 (S5) HAc	D2/B2 S_{bsf}	D3 (S6) H_2	D4 Z_{AD}
moles	moles	moles	moles	moles	moles	moles
-1	$\frac{2(1-\frac{5}{6}Y_{AD})}{Y_{AD}}$	1	$\frac{2(1-\frac{5}{6}Y_{AD})}{Y_{AD}}$	$-\frac{1}{Y_{AD}}$	$\frac{4(1-\frac{5}{6}Y_{AD})}{Y_{AD}}$	1

Acidogenesis for high pH2 only (Process D3)							
C1/B10 NH_4^+	C3 (S7) $H_2CO_3^*$	C7 H^+	C13 (S8) HAc	C28 (S9) HPr	D2/B2 S_{bsf}	D3 (S10) H_2	D4 Z_{AD}
moles	moles	moles	moles	moles	moles	moles	moles
-1	$\frac{(1-\frac{5}{6}Y_{AD})}{Y_{AD}}$	1	$\frac{(1-\frac{5}{6}Y_{AD})}{Y_{AD}}$	$\frac{(1-\frac{5}{6}Y_{AD})}{Y_{AD}}$	$-\frac{1}{Y_{AD}}$	$\frac{(1-\frac{5}{6}Y_{AD})}{Y_{AD}}$	1

Acetoclastic methanogenesis (Process D7)					
C1/B10 NH_4^+	C3 - $H_2CO_3^*$ (S17)	C7 - H^+	C13 - HAc	P4 - CH_4 (S18)	D6 - Z_{AM}
moles	moles	moles	moles	moles	moles
-1	$\frac{(1 - \frac{5}{2} Y_{AM})}{Y_{AM}}$	1	$-\frac{1}{Y_{AM}}$	$\frac{(1 - \frac{5}{2} Y_{AM})}{Y_{AM}}$	1

Hydrogenotrophic methanogenesis (Process D9)					
C1/B10 - NH_4^+	C3 - $H_2CO_3^*$ (S19)	C7 - H^+	P4 - CH_4 (S20)	D3 - H_2	D7 - Z_{HM}
moles	moles	moles	moles	moles	moles
-1	$-\frac{(1 + 10 Y_{HM})}{4 Y_{HM}}$	1	$\frac{(1 - 10 Y_{HM})}{4 Y_{HM}}$	$-\frac{1}{Y_{HM}}$	1

Death / Endogenous respiration Processes (D4, D6, D8, D10)			
C2/B10 NH_3 (S11)	C3 $H_2CO_3^*$ (S12)	D1 S_{bp} (S13)	D4, D6, D8, D10 Z_{AC}, Z_{AD}, Z_{AM}, Z_{HM}
moles	moles	moles	moles
$\frac{Y + 4X - 2Z - 23A}{Y + 4X - 2Z - 3A}$	$\frac{5(Y - 2Z - 3A)}{Y + 4X - 2Z - 3A}$	$\frac{20}{Y + 4X - 2Z - 3A}$	-1

In the hydrolysis process (D1), the biodegradable particulate organics measured as COD (S_{bp}) in the sewage sludge are first changed to mole units “outside” of the kinetic model, i.e. matrix, by dividing by the COD/mol ratio = {(Y + 4X - 2Z - 3A)AMW$_{O2}$/4}, with MW_{O2} being the molecular weight of O_2 = 32 g/mol. Thereafter, the sewage sludge biodegradable particulate organics as moles (S_{bp}) are transformed to the intermediate organic “glucose” also as moles (S_{bs}). This process is crucial in anaerobic digestion modelling, as the amount of “glucose” formed will determine the amount of the end products (CH_4, CO_2 and biomass) in a stable digester. To develop the stoichiometry for the hydrolysis process, the stoichiometric reaction was separated into two half reactions, effectively the redox half reactions, which were added based on an electron (COD) balance. In setting up the conversion of the primary sludge COD to mole units and the two subsequent half reactions in the transformation to the intermediate “glucose”, the chemical formulation for the sewage sludge was kept as a variable, i.e. $C_XH_YO_ZN_A$, to allow the composition of the influent sewage sludge to the AD to be easily changed (McCarty, 1974). The formulation for the sewage sludge was assumed to be the same for all sewage sludge fractions (i.e. biodegradable and unbiodegradable), and to remain constant with degradation. This gives the stoichiometric reaction for sewage sludge hydrolysis as:

$$C_XH_YO_ZN_A \rightarrow$$

$$\frac{Y+4X-2Z-3A}{24}C_6H_{12}O_6 + ANH_3 + \frac{Y-4X+2Z-3A}{4}H_2O + \frac{2Z+3A-Y}{4}CO_2 \quad (4.6)$$

In the death/endogenous decay processes (D4, D6, D8, D10) for the four organism groups (Table 4.4), it was accepted that the organisms die releasing biodegradable particulate organics (S_{bp}), which are assumed to have the same formulation as the sewage sludge, i.e. $C_XH_YO_ZN_A$ with CO_2, H_2O and NH_3 released or taken up from the bulk liquid as required to maintain the C, H, O and N mass balances. Due to the low organism yields and relatively low death rates, and the relatively large fraction of unbiodegradable particulate organics in the influent, generation of endogenous residue (Dold *et al.*, 1980) was not included, but this can be done relatively simply if required. Hence, the stoichiometric reaction for organism death is (Table 4.4):

$$C_5H_7O_2N + \frac{4(2Y-2X-6A+Z)}{(Y+4X-2Z-3A)}H_2O \rightarrow \frac{20}{(Y+4Z-2Z-3A)}C_XH_YO_ZN_A + \frac{(Y+4X-2Z-23A)}{(Y+4X-2Z-3A)}NH_3 + \frac{5(Y-2Z-3A)}{(Y+4X-2Z-3A)}CO_2 \quad (4.7)$$

The position of the stoichiometric formulae of Tables 4.3 and 4.4 are shown in the Petersen matrix in Table 4.2. By tracking through with defined organism yield values (Table 4.5) the stoichiometric sequence of AD processes (ignoring high p_{H2} conditions, which has no effect under stable steady state conditions, and endogenous respiration processes, which have a very small effect, <3%), degradation of 100 g cod biodegradable particulate sewage sludge of composition $C_{3.5}H_7O_2N_{0.196}$ (see below) produces 88.3 g COD methane and 11.7 g cod biomass (Fig 4.3). Also the 100 g cod contains 2.67 mol carbon (32.0 g C). Stoichiometrically 88.3 g cod methane contains 1.38 mol C (16.5 g C) and the 11.7 g cod biomass of composition $C_5H_7O_2N$ contains 0.37 mol C (4.4 g C). The difference between the input and output mol C is the mol C CO_2 produced, viz. 2.67- (1.38 + 0.37) = 0.92 mol C (11.0 g C), which is equal to the model predicted net CO_2 production. This CO_2 production exits the digester as CO_2 gas and dissolved CO_2 in the effluent flow. The split between the gaseous and dissolved CO_2, or equivalently the partial pressure of CO_2 in the gas phase, is governed by the sludge feed COD concentration, i.e. the influent (and effluent) flow with which the 100 g cod enters the digester, and the digester pH through the mixed weak acid/base chemistry of the system. This calculation is complex because the digester pH is unknown. The pH is affected by the mol N released as ammonia in the breakdown of the sludge organics (0.15 mol N from the 100 g cod $C_{3.5}H_7O_2N_{0.196}$ sewage sludge) and the partial pressure of CO_2 in the gas phase (p_{CO2}). While estimates of the p_{CO2} and digester pH can be obtained iteratively manually (see Sötemann *et al.*, 2005a,c), the usefulness of the integrated two phase weak acid/base chemistry and biological processes kinetic model is that this calculation of the effluent gas p_{CO2} and digester pH is done seamlessly within the model structure including all the weak acid/bases in the digester influencing pH (not only the inorganic C system) and the measured (or estimated) dissolved constituents in the sludge feed as a result of prior acidogenesis. Also, while not validated for this yet, the integrated AD model can deal with cyclic flow and load conditions.

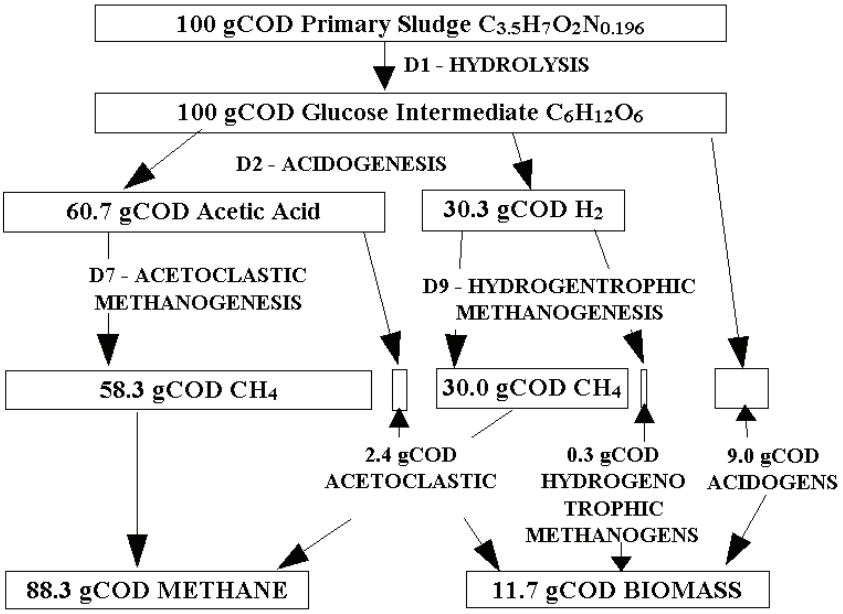

Figure 4.3: Stoichiometry of anaerobic digestion 100 g cod primary sludge ignoring high partial pressure of hydrogen and endogenous respiration

Table 4.5: Kinetic and stoichiometric constants at 37 EC for the four anaerobic digestion organism groups. The Y, $:_{max}$, K_S and b values were obtained from Sam-Soon *et al.* (1991); the $K_{max,HYD}$ and $K_{S,HYD}$ values by calibration in this application.

Organism group	Y	$:_{max}$	K_S	b
Acidogens (subscript AD)	0.1074	0.8	$7.8x10^{-4}$	0.041
Acetogens (subscript AC)	0.0278	1.15	$8.9x10^{-5}$	0.015
Acetoclastic methanogens (subscript AM)	0.0157	4.39	$1.3x10^{-5}$	0.037
Hydrogenotrophic methanogens (subscript HM)	0.004	1.2	$1.56x10^{-4}$	0.01
Hydrogen inhibition coefficient for high p_{H2}	$k_{H2} = 6.25x10^{-4}$ molH_2/P			
Acidogenic hydrolysis of biodeg particulate organics First order First order specific Monod Surface mediated reaction (Contois)	 K_h= 0.381 K_H= 40 $:_{max,HYD}$= 4.529 $k_{max,HYD}$ = 6.797		 $K_{SM,HYD}$ = 0.0486 $K_{SS,HYD}$ = 10.829	

Y= yield coefficient (mol organism/mol substrate); $:_{max}$ = maximum specific growth rate (/d);
K_S = half saturation coefficient (mol/P); b = endogenous respiration rate (/d);
K_h = first order hydrolysis rate constant (/d)
K_H = first order specific hydrolysis rate constant (P/mol Z_{AD}.d)
$:_{max,HYD}$ = Monod kinetics maximum specific hydrolysis rate (mol S_{bp}/mol Z_{AD}.d)
$K_{SM,HYD}$ = Monod kinetics hydrolysis half saturation coefficient (mol S_{bp}/P)
$k_{max,HYD}$ = surface mediated reaction kinetics maximum specific hydrolysis rate (mol S_{bp}/mol Z_{AD}.d)
$K_{SS,HYD}$ = surface mediated reaction kinetics half saturation coefficient (mol S_{bp} /mol Z_{AD})

4.3.4 Kinetic equations for the biological processes

The rate equations for the 10 biological processes (Table 4.2) were obtained from various literature sources, where possible, and modified to describe the reactions as realistically and accurately as possible. The rate equations chosen for each of the biological processes included in the two phase CPB processes AD model are briefly described below.

4.3.4.1 Hydrolysis process (D1)

A number of different kinetic formulations for the hydrolysis process were investigated:

(i) First order kinetics

The most common way of modelling the rate of hydrolysis of particulate organic material (process D1) has been to use first order kinetics. A number of researchers (e.g. Eastman and Ferguson, 1981; Gujer and Zehnder, 1983; Pavlostathis and Giraldo-Gomaz, 1991) used simple first order equations, dependent only on the biodegradable substrate (as COD) concentration:

$$r_{HYD} = K_h[S_{bp}] \tag{4.8a}$$

where:

r_{HYD} = hydrolysis rate (mol S_{bp}/P.d)
K_h = first order hydrolysis kinetic rate constant (/d)
$[S_{bp}]$ = biodegradable particulate organics concentration (mol/P).

Application of the first order kinetics has been found to result in values for the first order rate constant (K_h) that are situation specific, varying with, for example, sludge age or equivalently hydraulic retention time (e.g. Henze and Harremoës, 1983; Bryers, 1985; Pavlostathis and Giraldo-Gomez, 1991; Sötemann *et al.*, 2005c). Because the objective is to develop a kinetic model for anaerobic digestion that would be applicable over a range of sludge ages, alternative more general approaches were investigated. It is well known that the rate of hydrolysis is affected by temperature, pH, acidogen organism concentration, and type, particle size and concentration of organics. Among these, intuitively at least the acidogen organism concentration plays a major role in regulating the rate of hydrolysis and should be included in the kinetic rate expression in some way. Eliosov and Argaman (1995) included the acidogen active biomass directly into the first order kinetics:

$$r_{HYD} = K_H[S_{bp}][Z_{AD}] \tag{4.8b}$$

where:

K_H = first order specific hydrolysis kinetic rate constant (P/mol Z_{AD}.d)
$[Z_{AD}]$ = acidogen active biomass concentration (mol/P)

(ii) Monod kinetics

Monod kinetics is commonly used in modelling biological wastewater treatment processes (e.g. McCarty, 1974; Dold *et al.*, 1980, Henze *et al.*, 1987) and can be applied to hydrolysis:

$$r_{HYD} = \left[\frac{\mu_{max,HYD}[S_{bp}]}{K_{SM,HYD} + [S_{bp}]}\right][Z_{AD}] \tag{4.8c}$$

where:

$:_{max,HYD}$ = maximum specific hydrolysis rate constant (mol S_{bp}/(mol Z_{AD}.d))
$K_{SM,HYD}$ = Monod half saturation constant for hydrolysis (mol S_{bp}/P)

(iii) Surface mediated reaction (or Contois) kinetics

To model the hydrolysis of particulate slowly biodegradable COD in activated sludge systems, Dold *et al.* (1980) used Levenspiel (1972) planar surface mediated reaction kinetics (also known as Contois kinetics, Vavilin *et al.*, 1996). With a single set of constant values, these kinetics gave reasonable predictions over a wide range of activated sludge system conditions including sludge age. Since the hydrolysis processes in activated sludge and anaerobic digestion could be regarded as similar and operate on the same organics (present in raw sewage), this approach also was investigated for the AD model:

$$r_{HYD} = \left[\frac{k_{max,HYD}[S_{bp}]/[Z_{AD}]}{K_{SS,HYD} + [S_{bp}]/[Z_{AD}]}\right][Z_{AD}] \qquad (4.8d)$$

where

$k_{max,HYD}$ = maximum specific hydrolysis rate constant [mol S_{bp}/(mol Z_{AD} .d)]
$K_{SS,HYD}$ = Half saturation constant for hydrolysis (mol S_{bp}/mol Z_{AD})

Selection of the most suitable hydrolysis kinetic formulation is investigated later in this Chapter. Irrespective of the hydrolysis formulation used, no acidogen biomass growth takes place in this hydrolysis process, and 1 g cod sewage sludge forms 1 g cod "glucose" intermediate (Fig 4.3, Eq 4.6). Growth of acidogens arises from the acidogenic conversion of the glucose intermediate to SCFA and hydrogen, which, relative to the rate of hydrolysis, is immediate resulting in negligible accumulation of glucose in the AD system.

4.3.4.2 Acidogenesis process (D2 and D3)

As noted above, acidogenesis refers to the utilization of the model intermediate "glucose" (S_{bs}) by the acidogenic organisms, producing propionic acid, acetic acid, hydrogen, carbon dioxide and protons. Under conditions of low hydrogen partial pressure (p_{H2}), the acidogenic reaction (process D2) produces only acetic acid, hydrogen and CO_2. The process is formulated in terms of the growth rate of acidogens (r_{ZAD}), which is modelled with a Monod equation (Gujer and Zehnder, 1983; Pavlostathis and Giraldo-Gomez, 1991), as follows:

$$r_{Z_{AD}} = \frac{\mu_{max,AD}[S_{bsf}]}{K_{S,AD} + [S_{bsf}]}\left\{1 - \frac{[H_2]}{k_{H2} + [H_2]}\right\}[Z_{AD}] \qquad (4.9)$$

where:

$\mu_{max,AD}$ = Maximum specific growth rate constant for the acidogens (/d)
$K_{S,AD}$ = Half saturation concentration for acidogens (mol/P)
$[S_{bsf}]$ = Biodegradable soluble (glucose) substrate concentration (mol/P)
$[H_2]$ = Hydrogen concentration (mol/P)
k_{H2} = Hydrogen inhibition constant for high p_{H2} (mol/P)

The second term in { } brackets in Eq 4.9, called a non-competitive inhibition function, takes account of the reduction in rate when the p_{H2} is high. At high p_{H2}, in addition to acetic acid, hydrogen and CO_2, propionic acid also is produced (process D3). For the production of propionic acid under high p_{H2}, the growth rate of the acidogens (r_{ZAD}) is based on the same Monod kinetic equation (Eq 4.9) as for low p_{H2}, viz.:

$$r_{Z_{AD}} = \frac{\mu_{max,AD}[S_{bsf}]}{K_{S,AD}+[S_{bsf}]}\left\{\frac{[H_2]}{k_{H2}+[H_2]}\right\}[Z_{AD}] \quad (4.10)$$

To ensure that this process only operates when the p_{H2} is high, the non-competitive inhibition function in { } switches the process "on" under conditions of high p_{H2} and "off" under conditions of low p_{H2}, controlled by switching constant k_{H2}. Additionally, to ensure that the rate of glucose (S_{bsf}) utilisation is the same under both conditions and in the intermediate condition, the rate of acetate production (Eq 4.9) is reduced by subtracting the inhibition function value from 1 in Eq 4.9.

4.3.4.3 Acetogenesis process (D5)

In the process of acetogenesis, the propionic acid produced under high p_{H2} conditions is degraded under low p_{H2} by acetogenic organisms to produce acetate (Eq 4.1). This rate was modelled in terms of the acetogen growth rate (r_{ZAC}), also with a Monod equation (Pavlostathis and Geraldo-Gomez, 1991; Oude Elferink *et al.*, 1994) for the specific growth rate:

$$r_{Z_{AC}} = \frac{\mu_{max,AC}[HPr]}{K_{S,AC}+[HPr]}\left[1-\frac{H_2}{k_{H2}+H_2}\right][Z_{AC}] \quad (4.11)$$

where:

$\mu_{max,AC}$ = Maximum specific growth rate constant for the acetogens (/d)
$K_{S,AC}$ = Half saturation concentration for acetogens (mol/P)
[HPr] = Undissociated propionic acid concentration (mol/P)
$[Z_{AC}]$ = Acetogenic organism concentration (mol/P)

Since the weak acid/base chemistry is being modelled, both the undissociated and dissociated species of propionic acid are included as compounds, and the growth rate needs to be formulated in terms of the appropriate species. In Eq 4.11, the specific growth rate is a Monod function in terms of the undissociated propionic acid species, and not the more abundant dissociated species, in agreement with observations. Also, in the stoichiometry (Table 4.2) the undissociated propionic acid species (HPr) is used as substrate source. Should this approach lead to numerical instability in solution procedures (due to the low concentrations of HPr), the dissociated species (Pr^-) can be used instead without undue difficulty, but taking due cognisance of the concentration effects in the Monod expression and the requirement of the charge balance in the stoichiometric equations.

The same non-competitive inhibition function in the { } brackets of Eq 4.9 appears in Eq 4.11, because the acetogenesis process is sensitive to p_{H2}, decreasing as p_{H2} increases. This means that as p_{H2} increases, not only do acidogens begin to produce propionic acid (process D3), but also the rate of propionic acid utilization by acetogens (process D5) decreases. This causes a progressive build up of propionic acid as p_{H2} increases and contributes to the decrease in pH when the hydrogen consuming hydrogenotrophic methanogen growth rate (D9) decreases for some reason (see below).

4.3.4.4 Acetoclastic methanogenesis process (D7)

Acetoclastic methanogenesis (or acetate cleavage) is the process whereby acetic acid is

converted to methane and CO_2 (CH_3COOH Ψ CO_2 + CH_4), and growth of acetoclastic methanogens takes place. As for processes D2 and D3, the rate is modelled in terms of the rate of growth of the acetoclastic methanogens (r_{ZAM}) with a Monod equation (Pavlostathis and Geraldo-Gomez, 1991), viz.:

$$r_{Z_{AM}} = \frac{\mu_{max,AM}[HAc]}{K_{S,AM} + [HAc]}[Z_{AM}] \quad (4.12)$$

where:

$\mu_{max,AM}$	=	Acetoclastic methanogens maximum specific growth rate constant (/d)
$K_{S,AM}$	=	Half saturation concentration of acetoclastic methanogens growth on acetic acid (mol/P)
[HAc]	=	Undissociated acetic acid concentration (mol/P)
$[Z_{AM}]$	=	Acetoclastic methanogen organism concentration (mol/P)

As for the acetogens, the specific growth rate of the acetoclastic methanogens is a function of the undissociated acetic acid species (HAc). Also, in the stoichiometry acetic acid uptake is via the undissociated species, and CO_2 production via H_2CO_3*.

4.3.4.5 Hydrogenotrophic methanogenesis process (D9)

Hydrogenotrophic methanogenic organisms use H_2 and CO_2 to form methane and water (CO_2 + $4H_2$ Ψ CH_4 + $2H_2O$). This process (D9) is also modelled in terms of the rate of growth of the hydrogenotrophic methanogens (r_{ZHM}), with a Monod equation (Pavlostathis and Geraldo-Gomez, 1991; Oude Elferink *et al.*, 1994):

$$r_{Z_{HM}} = \frac{\mu_{max,HM}[H_2]}{K_{S,HM} + [H_2]}[Z_{HM}] \quad (4.13)$$

where:

$\mu_{max,HM}$	=	Maximum specific growth rate of hydrogenotrophic methanogens (/d)
$K_{S,HM}$	=	Half saturation concentration of hydrogenotrophic methanogens growth on hydrogen (mol/P)
$[H_2]$	=	Molecular hydrogen concentration (mol/P)
$[Z_{HM}]$	=	Hydrogenotrophic methanogen organism concentration (mol/P)

In agreement with the other processes, CO_2 uptake for hydrogenotrophic methanogenesis is via the H_2CO_3* species.

4.3.4.6 Death/endogenous respiration of the four organism groups (processes D4, D6, D8 and D10)

Organism death in AD consists of endogenous respiration/death only, since predation apparently does not occur under anaerobic conditions. Hence, for each organism group the organism death rate is modelled with first order kinetics, viz.:

$$r_Z = -b_Z[Z] \quad (4.14)$$

where:

b_Z = the death/endogenous mass loss rate for specific organism group (/d)

[Z] = specific organism group concentration (mol/P)

The organism mass that dies adds to the slowly biodegradable organics (S_{bp}) of the influent (Table 4.4, Eq 4.7), which passes through the same hydrolysis, acidogenesis and subsequent processes as the influent biodegradable organics. Because the organism yields and endogenous respiration rates of the AD organisms are relatively very low, it was accepted that no endogenous residue (particulate unbiodegradable organics) forms and no COD (electrons) is utilized by the AD organisms for maintenance.

The stoichiometric and kinetic constants for the four organism groups (yield coefficients, maximum specific growth rates, half saturation concentrations, endogenous mass loss rates) were obtained from the literature and are listed in Table 4.5.

4.4 AQUEOUS CHEMICAL PROCESSES

The reaction scheme for the weak acid/base part of this two phase AD model was taken unchanged from Musvoto *et al.* (1997, 2000a,b,c). The 16 chemical equilibrium dissociation (CED) processes (C1-C6 and C9- C18) of the ammonia, carbonate, phosphate, short chain (volatile) fatty acid (SCFA, acetate) and water weak acid/base systems and their 13 associated compounds (C1-C5 and C7-C14) were included in the AD model (Tables 1 of Musvoto *et al.*, 1997 and Sötemann *et al.*, 2005a). Only the five chemical (C) and one physical (P) compounds directly associated with the 10 biological (B) and 3 physical (P) processes of AD (D1-D10 and P6-P8) are shown in the Petersen matrix in Table 4.2, i.e. NH_4^+ (C1/B10), NH_3 (C2), H_2CO_3* (C3), H^+ (C7), HAc (C13) and CO_2 gas (P1/C6). Two additional CED processes had to be added, viz. the reverse and forward dissociation processes for the propionate weak acid/base system (C46 and C47), together with its two associated compounds propionic acid (HPr, C28) and propionate (Pr^-, C29). The 22 chemical ion pairing processes (CIP, C20-C41) with their 13 associated chemical compounds (C15-C27) of Musvoto *et al.* were not included in this two phase AD model, because mineral precipitation (3rd phase) is not yet included (Table 1 in Chapter 5 of Sötemann *et al.*, 2005a).

4.5 PHYSICAL PROCESSES – GAS EXCHANGE

In the three phase carbonate system weak acid/base model of Musvoto *et al.* (1997), the physical (P) processes for carbon dioxide gas exchange (PGE) with the atmosphere were included, by modelling the expulsion (reverse, K'_{rCO2}) and dissolution (forward, K'_{fCO2}) processes separately and linking the rates for these two processes through the Henry's law constant for CO_2 (K_{HCO2}), i.e. $K'_{fCO2} = K'_{rCO2}\ K'_{HCO2}XRT$. Musvoto *et al.* showed that this approach yielded identical results to the usual interphase gas mass transfer equation with an overall liquid phase mass transfer rate coefficient K_{LaCO2}, where $K_{La,CO2} = K'_{rCO2}$. In their model application, the actual CO_2 expulsion rate constant value (K'_{rCO2}) was not important because they considered initial and final steady state conditions only, not the transient dynamic conditions to the final steady state. Also, the CO_2 gas concentration ($CO_2(g)$) was kept constant at that value calculated from a selected partial pressure of CO_2 ($CO_2(g) = p_{CO2}/RT$), since gain or loss of $CO_2(g)$ did not need to be determined.

Musvoto *et al.* (2000a), Van Rensburg *et al.* (2003) and Loewenthal *et al.* (2004) extended this model to include three phase mixed weak acid/base systems to simulate multiple mineral

precipitation and active gas exchange of CO_2 and NH_3 during aeration of anaerobic digester liquor and swine wastewater. For CO_2, they followed the approach of Musvoto *et al.* (1997) above. For the NH_3, they noted that the atmospheric concentration of NH_3 is negligible (i.e. acts as an infinite sink), so that only NH_3 expulsion need be included, and dissolution could be neglected. Because they simulated transient (dynamic) conditions, the CO_2 gas exchange (as above) and NH_3 gas expulsion (stripping) (and mineral precipitation) rates were important and these were determined from the experimental results. In determining the rates for the gas exchanges, Musvoto *et al.* (2000a) noted that, if the dimensionless Henry's law constant of a gas, H_c [$=\{1/(K_H R T)\}$] is > 0.55, then O_2 can be used as a reference gas and the expulsion rate constant K'_r (= K_{La}) for the individual gases will be in the same proportion to the rate for O_2 (K'_{rO2} = K_{LaO2}) as their diffusivity is to the diffusivity of O_2. Of the two gases they considered, only NH_3 has a H_c < 0.55 (= 0.011 at 20°C), so the value for K'_{rNH3} had to be determined independently of the values for K'_{rO2}, by calibration. For CO_2, H_c = 0.95 at 20EC (Katehis *et al.*, 1998) and accordingly they defined K_{LaCO2} in terms of K_{LaO2}. However, since the compound oxygen was not included in their model, in effect only K_{LaCO2} was determined by calibration against measured data.

Sötemann *et al.* (2005a) integrated the biological processes of IWA Activated Sludge Model No 1 into the two phase (aqueous-gas) mixed weak acid/base chemistry model of Musvoto *et al.* (2000a) allowing the reactor pH to become a model predicted parameter. Four gases were considered, viz. O_2, N_2, CO_2 and NH_3. For CO_2 and NH_3, the formulations of Musvoto *et al.* and Van Rensburg *et al.* above, were accepted. However, since gas production was of interest, for CO_2 they substituted $K'_{rCO2}XK'_{HCO2}Xp_{CO2}$ for $K'_{fCO2}X[CO_2(g)]$ (Chapter 5, Table 3, Sötemann *et al.*, 2005a). This allows the $CO_2(g)$ concentration to vary without influencing the rate of CO_2 gas exchange, of importance in their implementation of the model in Aquasim (Reichert, 1998), where for simplicity the gas compounds were considered part of the bulk liquid. This approach for CO_2 was adopted for N_2 gas also. For O_2, the more conventional approach for aeration transfer to the bulk liquid was followed (Process P11 in Chapter 5, Table 3, Sötemann *et al.*, 2005a). In their application, because equilibrium between the aqueous and gas (atmosphere) phases was not reached during aeration in the aerobic reactor, the expulsion rates of the four gases were important for the simulation results and so values for K'_r (= K_{La}) for the four gases had to be determined. For the K_{La} values for the gases, they followed the approach of Musvoto *et al.* (2000a) above. The K_{La} for CO_2 and N_2 were linked to the K_{La} for O_2 through the diffusivities. The K_{LaO2} was calibrated to reflect the CO_2 supersaturation observed on samples from the aerobic reactor of full-scale plants (–20%), and cross-checked against the model determined dissolved O_2 concentration. For K'_{rNH3} (= K_{LaNH3}), this was calibrated independently. However, because negligibly little NH_3 actually strips out of the aqueous phase with aeration in the usual pH range of 6.5 to 8 for activated sludge systems, the actual NH_3 stripping rate, and hence the value for K'_{rNH3}, was of little consequence (provided it is not excessively large) and in fact the process itself could have been omitted from the integrated model without loss in accuracy.

In the application here of integrating the biological processes of AD into the two phase (aqueous-gas) mixed weak acid/base chemistry model of Musvoto *et al.* (2000a), four gases also need to be considered, i.e. CO_2, CH_4, H_2 and NH_3. Of these four, only CO_2 needs to be modelled with both expulsion and dissolution processes, because this gas is significantly soluble. Hence, both dissolved and gaseous CO_2 compounds are included (compounds C3 and P1, Table 4.2) and the process scheme of Sötemann *et al.* (2005a) above was followed. CH_4 is (i) very insoluble and (ii) not utilized in the biological or chemical processes, so it's dissolved (aqueous) phase is bypassed and only a gas phase CH_4 compound is included

(compound P4, Table 4.2). It is therefore assumed that the acetoclastic and hydrogenotrophic methanogenesis processes (D7 and D9) produce CH_4 gas directly and no CH_4 expulsion and dissolution processes need to be included in the model. Although H_2 also is very insoluble, it is utilized at an interspecies level in the hydrogenotrophic methanogenesis process (D9) and so it cannot be transferred instantaneously to the gas phase. H_2 is therefore modelled as a dissolved compound (D3, Table 4.2), but because it is utilized so rapidly and at an inter-organism species level, it's residual concentration is extremely small; from a gas production perspective, it can be ignored. Hence, expulsion and dissolution processes for H_2 are not included in the model. NH_3 is readily soluble and its production from organically bound N in the sewage sludge is one of the processes governing the pH in the digester. It can diffuse from the dissolved (aqueous) to the gas phases and so a process for expulsion of NH_3 is included in the model. However, because the rate and quantity of NH_3 expulsion into the gas phase are so slow and low respectively with respect to the total gas production of the digester, in particular in the digester pH range 6.8 to 8, the gas phase is assumed to maintain a negligible NH_3 partial pressure. An NH_3 dissolution process is therefore not included in the model, only an expulsion process (in agreement with Musvoto *et al.*, 2000a, Van Rensburg *et al.*, 2003 and Sötemann *et al.*, 2005a). The expulsion and dissolution processes for CO_2 and the expulsion process for NH_3 are shown in the Petersen matrix of the AD model (processes P6-P8, Table 4.2). Thus, only the K_r' ($=K_{La}$) values for these two gases need to be considered. However, because transient conditions are not being modelled in this particular application, but only the final steady state, the expulsion rates of the gases are not important provided the simulation run times are long enough to reach steady state. From the above it is clear that the gas phase partial pressure required in the rate formulations for CO_2 gas exchange need be calculated only from the CO_2 and CH_4 gas concentrations.

4.6 INFLUENT SEWAGE SLUDGE CHARACTERISATION

In terms of the structure of the UCTADM1 above, in addition to requiring as input the influent concentrations of the various inorganic compounds (e.g. total inorganic carbon, C_T, speciated into H_2CO_3*, HCO_3^- and CO_3^{2-} for the relevant pH), various sewage sludge organic compounds need to be specified. For UCTADM1, the sewage sludge characterisation into its constituent fractions is shown in Fig 4.4; the characterisation structure adopted is near identical to that for sewage in activated sludge modelling (ASM2, Henze *et al.*, 1995). For undigested pristine sewage sludges, the two particulate fractions (biodegradable and unbiodegradable) can be expected to dominate to the extent that the other fractions can be neglected (this is evident from a mass balance around the primary settling tank for primary sludges, and simulation of activated sludge systems for waste activated sludges). However, primary sewage sludges are seldom in the pristine state, having undergone hydrolysis and acidogenesis within the primary settling tank (e.g. Barnard, 1984 measured SCFA concentrations in primary settling tank underflows in the range 1 700 to 2 700 mg/P at various treatment plants in South Africa), and in transport and storage for laboratory investigations. The SCFA thus produced (and equal concentrations of non-SCFA soluble COD, Lilley *et al.*, 1990) have a significant influence on the predicted pH in simulating anaerobic digesters, since uptake and utilisation of dissociated SCFA generates significant alkalinity (Sötemann *et al.*, 2005c). Furthermore, the SCFAs influence the hydrolysis rate constants in model calibration (Chapter 2 and Ristow *et al.*, 2005a). Thus, quantifying and specifying the influent sludge organic fractions are essential both in model calibration and simulation. Of the sewage sludge fractions (Fig 4.4), the unbiodegradable and biodegradable particulate (S_{upi} and S_{bpi}) and the two readily biodegradable fractions (S_{bsai} and S_{bsfi}) are of importance – the unbiodegradable soluble organics (S_{usi}) usually are present in such low

concentrations that they can be neglected. For S_{bsai}, two SCFA types are recognised in the model, acetic and propionic, and hence these form two subfractions of the S_{bsai}.

The characterisation structure is based on COD units, which are widely applied to quantify wastes. Since the kinetic model is based on mole units, conversion between the COD and mole units would be needed to generate the input for the model. For the two readily biodegradable fractions, the S_{bsai} usually are measured directly, while in terms of the model presented here the S_{bsfi} is "idealised" glucose so that conversion of these to mole units is relatively simple. For the particulate fractions, the conversion to mole units requires that the stoichiometric formulation for these sewage sludge fractions be specified, i.e. X, Y, Z and A in $C_XH_YO_ZN_A$. This is discussed in more detail below.

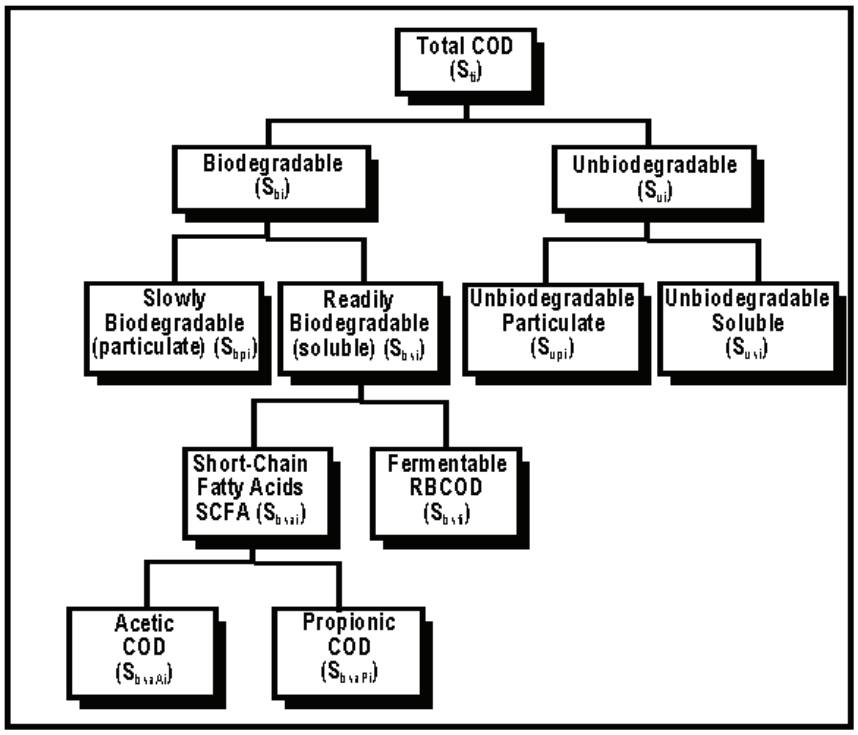

Figure 4.4: Schematic showing characterization of the influent sewage sludge organics, required as input to the model; the acetic and propionic require speciation for the influent pH.

4.7 MODEL CALIBRATION

From the above model development, the integrated two phase (aqueous-gas) chemical (C), physical (P) and biological (B) processes AD model comprises (Table 4.2): (1) the 16 forward and reverse chemical equilibrium dissociation (CED) processes (C1-C6, C9-C18) and their 13 associated compounds (C1-C2, C4-C14) – Table 1 in Musvoto *et al.* (1997); (2) the two forward and reverse CED processes for propionic acid (C47-C48) and their two associated compounds (C28-C29), (3) the three physical gas exchange processes of dissolution of CO_2 (P6) and its associated compound CO_2 gas (P1) and expulsion of CO_2 (P7) and NH_3 (P8) and, (4) the 10 biological processes for AD (D1-D10) and their 8 associated

compounds (P4 and D1-D7). The model was implemented in the computer programme AQUASIM (Reichert, 1998).

Omitted from this AD model are the five mineral precipitation processes (P1/C19 – Musvoto *et al.*, 1997 and P2/C42-P5/C45 – Musvoto *et al.*, 2000a), because mineral precipitation is not included in this two phase AD model. Also omitted are the 22 chemical iron pairing (CIP) processes (C20-C41) and their 13 associated compounds (C15-C27), because these processes are important mainly for multiple mineral precipitation modelling, which will be included in the next phase of the AD and wastewater treatment plant model development.

In implementation of the model in AQUASIM, since initial simulations were of steady state anaerobic digesters, the gas compounds were accepted to remain part of the bulk liquid and to leave the digester with the effluent flow. This is possible because at steady state the gas composition does not change. For dynamic simulations, the gas composition may change significantly and this may influence the dissolved species bulk liquid concentrations through gas exchange processes, and hence a separate gas stream may need to be included, see later.

4.7.1 Kinetic and stoichiometric constants

The kinetic constants required for the C and P processes part of the model are the equilibrium constants (pK) of the six weak acid/base systems, Henry's law constant for CO_2 ($K'_{H,CO2}$), and the apparent reverse dissociation and expulsion rate constants (K'_r) respectively for these processes. The equilibrium constants (pK) and Henry's law constant for CO_2 ($K'_{H,CO2}$), and their temperature sensitivity equations were obtained from the literature (see Table 2c of Musvoto *et al.*, 1997-1940s database). The pK value for propionic acid (pK_{Pr}) was accepted to be the same as for acetic acid, and is given by $pK_{Pr} = 1170.5/T_k - 3.165 + 0.0134T_k$, where T_k = temperature in Kelvin. The weak acid/base apparent reverse dissociation rate constants (K'_r) were set at very high values to ensure that aqueous chemical equilibrium conditions are established very rapidly at every time step (< 2 sec), e.g. ammonia $K'_{rN} = 10^{12}$ /d, see Table 2a in Musvoto *et al.* (1997). The weak acid/base apparent forward (K'_f) dissociation rate constants are linked to the apparent reverse rate constants (K'_r) and the equilibrium constants (pK) appropriately adjusted for ionic strength effects, e.g. $K'_{fC1} = K'_{rC1}\ 10^{-pKC1}/\ f_m^2$, where f_m is the mono-valent ion activity coefficient (Loewenthal *et al.*, 1989), see Table 2a, Musvoto *et al.* (1997). For the expulsion rate constants of the CO_2 and NH_3 gases modelled ($K'_r = K_{La}$), for CO_2 the K_{LaCO2} was assumed to have a high value (1000/d) since only the steady state was initially simulated, while for NH_3 the K'_{rNH3} was accepted to have a low value (1/d). As noted above, the value for K'_{rNH3} does not influence the simulations provided it is not too high, since little NH_3 is lost at the pH < 7.5.

In the B processes part of the model, required are the kinetic and stoichiometric constants (Y, $:_{max}$, K_S and b) for the four AD organism groups (Table 4.5). In the literature there is considerable variation and hence uncertainty in these values. Accepting this uncertainty, values for these constants were taken from Sam-Soon *et al.* (1991), who obtained their values from a survey of the literature. Where specific weak acid/base species are included in the rate formulation (e.g. acetoclastic methanogenesis), the rate constants (e.g. Monod half saturation coefficients) had to be appropriately adjusted to take into account weak acid/base speciation. This was done via the relevant pK values and pH. In application, the maximum specific growth rate of the acetoclastic methanogens ($:_{max,AM}$ in Eq 4.12) was increased from the range of 0.3-0.5/d used by Sam-Soon *et al.* (1991) to 4.39/d, to reproduce the observation of low HAc/Ac^- residual concentrations; due to the low HAc/Ac^- concentrations, decreasing the

intuitively more satisfying half saturation constant ($K_{S,AM}$ in Eq 4.12) as alternative caused instability in solution procedures. This aspect requires further investigation.

This left two parts of the AD model that required calibration against experimental data, viz. (i) the kinetic constants for the various hydrolysis rate expressions, e.g. maximum specific hydrolysis rate ($k_{max,HYD}$) and half saturation coefficient ($K_{S,HYD}$) in Eq 4.8d, and selection of the most appropriate kinetic formulation, and (ii) the sewage sludge CHON composition, i.e. the X, Y, Z and A values in $C_XH_YO_ZN_A$. Additionally, in model application the sewage sludge constituent fractions and the input concentrations of the various compounds would need to be quantified. Values for all these parameters were obtained interactively through analysis of and model application to the experimental data set of Izzett *et al.* (1992), as described below.

4.7.2 Experimental anaerobic digester systems

In any calibration and validation exercise, the measured parameters must conform to the same mass balance and continuity principles as in the model, and hence (i) must be sufficient to be able to calculate the material mass balances and (ii) the mass balances must be as close as possible to 100%. The data of Izzett *et al.* (1992) appeared to conform reasonably well to these criteria. They conducted a series of experiments aimed at identifying the effects of thermophyllic heat pre-treatment on the anaerobic digestibility of a mixture of primary and humus sewage sludges. In this investigation four laboratory scale anaerobic digesters were operated at a controlled temperature of 37 EC, two of which were fed heat pre-treated (70^oC for 24 h) sludge while the other two were fed untreated sludge. The digesters were run in parallel, and the retention times were progressively reduced to observe possible differences in digestibility (fraction unbiodegradable and rate of hydrolysis) between the heat pre-treated and untreated sludges. The digester fed untreated sludge was operated for a period of 211 days, during which time the retention time was reduced from 20 to 15, then 12, 10 and finally 7 days after the system had run at steady state for two to three retention times at each retention time. The data collected from this AD system (influent and effluent COD, VSS, TSS, TKN, FSA, SCFA, pH, $H_2CO_3^*$ alkalinity and gas production and CO_2 composition) at a particular retention time were averaged over the final two to three steady state retention times (Table 4.6). The averages were used to check the N and COD mass balances. The N and COD balances obtained at the 20, 15, 12, 10 and 7 day retention times were 91 to 99% and 107 to 109% respectively (Table 4.6), indicating that the measured parameters conformed closely to the mass balance requirement. The measured averages therefore could be accepted to represent the behavioural characteristics of the digester under stable operating conditions at the different retention times.

Table 4.6: Experimental results for Izzett *et al.* (1992) 14P flow though mesophilic (37°C) anaerobic digesters operated from 20 to 7 days retention time on primary sewage sludge.

Retention time (d)	20	15	12	10	7
Feed rate (P/d)	0.7	0.93	1.17	1.4	2
Feed COD (mg cod/P)	42595	42367	39222	40721	43286
Feed VFA (mg cod/P as HAc)	2249	1824	2872	1961	1871
Feed TKN (mg N/P)	1171	1075	1028	1100	1105
Feed FSA (mg N/P)	244	221	235	203	196
Feed VSS (mg VSS/P)	25690	25863	24727	25768	25971
Feed H_2CO_3* Alk (mg/P as $CaCO_3$)	56	82	90	81	80
Feed pH	5.28	5.42	5.2	5.34	5.34
Effluent COD (mg cod/P)	19005	19969	18678	20521	23637
Effluent VFA (mg cod/P as HAc)	23	27	28	28	50
Effluent TKN (mg N/P)	1157	976	992	1039	1041
Effluent FSA (mg N/P)	511	404	430	404	511
Effluent H_2CO_3* Alk (mg/P as $CaCO_3$)	2066	1994	2072	1951	1882
Effluent pH	7.15	7.14	7.2	7.11	7.12
Gas production (P/d at 20°C)	11.053	13.958	16.696	20.07	27.932
Gas composition (% methane)	63.3	63.6	63.3	62.1	63.2
COD balance (%)	107.3	106.9	109.1	108.6	108.4
N balances (%)	98.8	90.8	96.5	94.5	94.2

Model COD and N balances at all retention times 100.0053% and 99.999% respectively.

As input to the various simulations and calculations below, the influent inorganic and organic constituent fractions need to be specified. A number of these were available from direct measurements, or could be derived directly. For the inorganic concentrations, the inorganic carbon and nitrogen weak acid/base species are required. The total inorganic nitrogen (free and saline ammonia, FSA, Table 4.6) was measured directly and the total inorganic carbon (C_T) could be calculated from the measured influent H_2CO_3* alkalinity and pH (Loewenthal *et al.*, 1986). From the influent total species concentrations, pH, temperature and relevant pK values adjusted for ionic strength effects, the influent inorganic carbon and nitrogen weak acid/base species concentrations could be calculated, as required for the simulations.

For the organic concentrations (Fig 4.4), the total COD (S_{ti}) and SCFA (S_{bsai}) concentrations were available from direct measurement (Table 4.6). For the simulations, all S_{bsai} were accepted to be HAc/Ac^- and this weak acid/base was speciated from the influent total species concentration, pH, temperature and relevant pK value adjusted for ionic strength effects (Sötemann *et al.*, 2005c). Further, from the experimental work of Lilley *et al.* (1990) and Ristow *et al.* (2005a), the non-SCFA fermentable biodegradable soluble COD concentration (S_{bsfi}) was accepted to be equal to the S_{bsai} concentration. The unbiodegradable soluble COD (S_{usi}) was accepted to be so low as to be negligible. This left two COD fractions to be quantified, the unbiodegradable and biodegradable particulates (S_{upi} and S_{bpi}). In the calculations and simulation below, the S_{upi} was determined, and hence S_{bpi} was calculated by difference.

Thus, the Izzett *et al.* (1992) data set was used to calibrate three parts of the model; (i)

hydrolysis process kinetic formulation and associated rate constants, (ii) sewage sludge CHON composition, and (iii) the unbiodegradable particulate fraction of the sewage sludge. The three parts were determined interactively and iteratively through calculation and simulation of the experimental systems.

4.7.3 Sewage sludge stoichiometric formula

In the model, the biodegradable sewage sludge is hydrolysed to the intermediary compound "glucose" (Fig 4.2). Since the stoichiometry of the subsequent products for complete anaerobic oxidation of the intermediate "glucose" is reasonably well established and essentially fixed (see above), the stoichiometric transformation of the sewage sludge to the intermediate "glucose" is crucial to predict the observed digester effluent and gas compositions. This is directly influenced by the CHON stoichiometric composition for the sewage sludge, Eq 4.7. Furthermore, the carbonate weak acid/base species play an important role in fixing digester pH, $H_2CO_3^*$ alkalinity, CO_2 and CH_4 gas produced, and it is therefore necessary to establish the correct C content of the influent sewage sludge to correctly predict these parameters also.

As a starting point, the sewage sludge composition was assumed to be the same as the generally accepted stoichiometric formula for activated sludge: $C_5H_7O_2N$ (WRC, 1984). However, $C_5H_7O_2N$ could not correctly predict the digester output (pH, gas flow and composition) as measured by Izzett *et al.* (1992) and therefore needed to be changed. Accordingly an improved estimate was derived from the measurements made on the influent.

Since influent TKN and FSA measurements were available (Table 4.6), the organic nitrogen (OrgN) in the feed was calculated for the different retention times. The result was expressed as a ratio of the measured COD and remained fairly constant during the investigation, ranging between 0.0201 and 0.0220 gN/g cod for the different retention times. VSS measurements on the influent were also available (Table 4.6). Recognising that the VSS represents particulate organics, the equivalent particulate COD was determined as (total COD -2ASCFA COD, i.e. S_{ti} - $2AS_{bsai}$). The particulate COD/VSS ratio at each retention time was calculated, and ranged from 1.36 to 1.52 g cod/g VSS. Additionally the organic N/VSS ratios were calculated and ranged from 0.032 to 0.036 g N/g VSS. From these ratios and accepting the H:O ratio in $C_XH_YO_ZN_A$ as 7:2 (from $C_5H_7O_2N$ above), X and A could be calculated for each retention time, from:

$$\frac{COD}{orgN} = \frac{(Y + 4X - 2Z - 3A) \cdot MW_{O2}}{4 \cdot A \cdot MW_N} \quad (4.15)$$

$$\frac{COD}{VSS} = \frac{(Y + 4X - 2Z - 3A) \cdot MW_{O2}}{4 \cdot (MW_C \cdot X + MW_H \cdot Y + MW_O \cdot Z + MW_N \cdot A)} \quad (4.16)$$

$$\frac{orgN}{VSS} = \frac{A \cdot MW_N}{(MW_C \cdot X + MW_H \cdot Y + MW_O \cdot Z + MW_N \cdot A)} \quad (4.17)$$

where:

MW_X = molecular weight of compound X

In Eqs 4.15 to 4.17 above, accepting Y = 7 and Z = 2, from the different pairings of equations (Eqs 4.15 and 4.17, and Eqs 4.15 and 4.16) two sets of (X; A) data pairs could be calculated for each retention time. The (X; A) pairs at the different retention times were all averaged, to give X = 3.4 and A = 0.192, giving a stoichiometric formulation for the sewage sludge of $C_{3.4}H_7O_2N_{0.192}$. These calculations did not require *a priori* information on the hydrolysis

kinetics and S_{upi} and hence this formulation formed the starting point for the simulations, which were used to refine the stoichiometry (in conjunction with the hydrolysis kinetics and S_{upi}).

In the simulations the parameters that were targeted for improved estimation of the sewage sludge formulation were the gas flow and composition, which requires a carbon (C) balance over the digester. Izzett *et al.* (1992) did not measure the C content of the sewage sludge, so the influent C was calculated from an assumed 100% C balance over the digester (Fig 4.3), through combined use of measured and predicted C output values. This was reasonable because the COD balances were good (107-109%). Essentially, the C content of the influent sewage sludge appears in the outputs, as gaseous CO_2 and CH_4, dissolved inorganic carbon weak acid/base species and effluent soluble and particulate organic C, the particulate organic C being made up of biomass, S_{up} and undegraded S_{bp}.

By tracking all the measured C in CO_2 (gaseous and dissolved) and CH_4 and the simulated organic C exiting the digester at different retention times and ensuring that the predicted and measured effluent CODs corresponded, the C content of the influent could be equated to the C exiting the digester. Subtracting the influent inorganic C (calculated from the measured influent H_2CO_3* and pH) gave the influent organic C. This was expressed as an influent organic C/COD ratio for the different retention times. Like the OrgN/COD ratio, the organic C/COD ratios also varied in a narrow band for the different retention times. The average organic C/COD ratio was therefore used to calculate the C content (X) in the sewage sludge feed. Taking due consideration that the influent OrgN/COD ratio must also remain at the measured value, a sewage sludge composition formula of $C_{3.5}H_7O_2N_{0.196}$ was determined, very close to the stoichiometry calculated above from the available influent measurements. This formulation was accepted for all subsequent calculations on and simulations of the Izzett *et al.* (1992) data. In the simulations, to derive the organic C/COD ratio the hydrolysis kinetics and S_{upi} needed to be correctly specified, and hence the requirement for interactive calculations and simulations.

To check how the model sewage sludge composition compares with real sludges, primary sludge from two different full-scale wastewater treatment plants (WWTP) around Cape Town (South Africa) were analysed for VSS, TSS, COD and their organic C, H, N and phosphorus (P) contents (Sötemann *et al.*, 2005a). From the measured data, the CHON composition of the primary sludge was calculated (P was omitted because it was not measured by Izzett *et al.*, 1992). The average measured composition was $C_{3.65}H_7O_{1.97}N_{0.19}$. The model C, H, O, N content and molar mass of primary sludge are 95.9%, 100%, 98.5%, 94.5% and 98.7% of the measured values. This provides powerful validation of the UCTADM1 model.

4.7.4 Estimating the unbiodegradable fraction of sewage sludge and hydrolysis kinetics and constants

Before an even remotely reasonable correspondence could be obtained between model predicted and measured effluent parameters and gas composition and production, the fraction of unbiodegradable particulate COD of the sewage sludge ($f_{PSup} = S_{upi}/S_{ti}$) and the hydrolysis rate kinetics and constants needed to be determined. These were determined interactively between mass balance based calculations and simulations on the Izzett *et al.* data set. Initially, a value for the f_{PSup} was estimated and then the various kinetic formulations evaluated, and thereafter the estimate for f_{PSup} improved. In the mass balance based calculations below, COD units are used. The calculated values for the various parameters can

be readily converted to the mole units required in the model, see below.

For the Izzett *et al.* data set, the influent sewage sludge is characterised by (Fig 4.4):

$$S_{ti} = S_{bpi} + S_{bsfi} + S_{bsai} + S_{usi} + S_{upi} \quad \text{(mg cod/P)} \tag{4.18}$$

In Eq 4.18 as noted above, S_{ti} and S_{bsai} were directly available from measurement (Table 4.6); S_{usi} could be accepted to be negligible, and S_{bsfi} could be accepted to be equal to S_{bsai}. This left two unknowns, S_{bpi} and S_{upi}. Letting $S_{upi} = f_{PSup}AS_{ti}$, then S_{bpi} could be found by difference and hence f_{PSup} was the only unknown.

For the effluent:

$$S_{te} = S_{bpe} + S_{bsfe} + S_{bsae} + S_{use} + S_{upe} + \text{biomass} \ \text{(mg cod/P)} \tag{4.19}$$

In Eq 4.19, S_{te} and S_{bsae} were available from direct measurement and it could be accepted that $S_{bsfe} = S_{bsae}$ (the values are very low due to stable digester operation and hence do not influence the analysis significantly). Accepting negligible generation of unbiodegradable material in the anaerobic digester, then $S_{use} = S_{usi} = 0$ and $S_{upe} = S_{upi}$. With regard to the biomass, under stable digester operation three organism groups are generated, acidogens (Z_{AD}), acetoclastic methanogens (Z_{AM}) and hydrogenotrophic methanogens (Z_{HM}). Of these, the mass of Z_{HM} developed is very much smaller than that of Z_{AD} and Z_{AM}, and accordingly can be neglected in an initial steady state analysis. Thus, Eq 4.19 reduces to:

$$S_{te} = S_{bpe} + S_{bsfe} + S_{bsae} + S_{use} + S_{upe} + Z_{AD} + Z_{AM} \quad \text{(mg cod/P)} \tag{4.20}$$

Developing mass balances around the digester (Ristow *et al.*, 2004, 2005a; Chapter 2) and recognising from Table 4.2 that in the death of biomass the released organics add to the sewage sludge, for biodegradable particulate COD (S_{bp}) :

$$V \cdot S_{bp} = Q_i \cdot S_{bp} \cdot dt - Q_e \cdot S_{bpe} \cdot dt - r^*_{HYD} \cdot V \cdot dt + (b_{AD} \cdot Z_{AD} + b_{AM} \cdot Z_{AM}) \cdot V \cdot dt$$

(mg cod/P) (4.21)

where:

r^*_{HYD}	=	volumetric hydrolysis rate, COD units (mg cod/P.d)
V_d	=	digester volume (P)
$Q_i = Q_e$	=	influent and effluent flow rate respectively (P/d)

At steady state, solving for r_{HYD} :

$$r^*_{HYD} = \frac{1}{R_h}(S_{bpi} - S_{bpe}) + b_{AD} \cdot Z_{AD} + b_{AM} \cdot Z_{AM} \quad \text{(mg cod/P.d)} \tag{4.22}$$

where:

R_h $= V_d/Q_i$ = hydraulic retention time (d)

Similarly for S_{bsf} and S_{bsa} with r^*_{AD} and r^*_{AM} as the volumetric rates in COD units of acidogenesis and acetoclastic methanogenesis respectively:

$$r^*_{AD} = \frac{1}{R_h}(S_{bsfi} - S_{bsfe}) + r^*_{HYD} \quad \text{(mg cod/P.d)} \tag{4.23}$$

$$r^*_{AM} = \frac{1}{R_h}(S_{bsai} - S_{bsae}) + f_{Sbsa/Sbsf} \cdot r^*_{AD} \quad \text{(mg cod/P.d)} \tag{4.24}$$

where:

$f_{Sbsa/Sbsf}$= fraction of S_{bsf} appearing as S_{bsa} in the acidogenesis reaction (Table 4.4)

= 0.607 (mg cod/mg cod)

Developing similar mass balances for the biomass concentrations:

$$Z_{AD} = \frac{r^*_{AD} \cdot Y^*_{AD} \cdot R_h}{(1 + b_{AD} \cdot R_h)} \quad \text{(mg cod/P)} \tag{4.25}$$

$$Z_{AM} = \frac{r^*_{AM} \cdot Y^*_{AM} \cdot R_h}{(1 + b_{AM} \cdot R_h)} \quad \text{(mg cod/P)} \tag{4.26}$$

where:

Y^*_{AD} = acidogen yield in COD units (mg COD/mg COD)

Y^*_{AM} = acetoclastic methanogen yield in COD units (mg COD/mg COD)

Recognising that from Eq 4.20:

$$S_{bpe} = S_{te} - S_{bsfe} - S_{bsae} - f_{PSup} \cdot S_{ti} - Z_{AD} - Z_{AM} \quad \text{(mg COD/P)} \tag{4.27}$$

In the set of equations above, f_{PSup}, S_{bpe}, Z_{AD} and Z_{AM} are the principal unknowns. If an estimate for f_{PSup} is available, then S_{bpe}, Z_{AD} and Z_{AM} can be calculated through iteration. However, f_{PSup} is not known for the Izzett *et al.* data set, and would need to be determined via some other technique, see later.

4.7.5 Determining hydrolysis rate constants

In the section above, for any selected f_{PSup}, the volumetric rate of hydrolysis (r^*_{HYD}) can be calculated, as well as Z_{AD}, Z_{AM} and S_{bpe}, all in COD units. Converting these values to mole units:

$$r_{HYD} = r^*_{HYD} / \left(\frac{COD}{mol}\right)_{S_{bp}} \quad \text{(mol } S_{bp}\text{/P.d)} \tag{4.28}$$

$$[S_{bpe}] = S_{bpe} / \left(\frac{COD}{mol}\right)_{S_{bp}} \quad \text{(mol } S_{bp}\text{/P)} \tag{4.29}$$

$$[Z] = Z / \left(\frac{COD}{mol}\right)_{Z} \quad \text{(mol Z/P)} \tag{4.30}$$

where:

$\left(\frac{COD}{mol}\right)_{S_{bp}}$ = COD/mol ratio for S_{bp}

= 131.3 g cod/mol for $C_{3.5}H_7O_2N_{0.196}$

$\left(\frac{COD}{mol}\right)_{Z}$ = COD/mol ratio for biomass

= 160 g cod/mol for $C_5H_7O_2N$

[ ] = mole concentration

Equating this r_{HYD} with the first order and first order specific kinetic expressions for the hydrolysis (Eqs 4.8a and 4.8b respectively), and solving for K_H and K_{Hspec} yields:

$$K_h = r_{HYD}/[S_{bpe}] \quad \text{(/d)} \tag{4.31}$$

$K_H = r_{HYD}/([S_{bpe}][Z_{AD}])$ (P/mol Z_{AD}.d) (4.32)

where as indicated by [ ], S_{bpe} and Z_{AD} are expressed in mole units.

Thus, from Eqs 4.31 and 4.32 above, values for K_h and K_H could be determined, provided f_{PSup} was known.

Similarly, for the Monod (Eq 4.8c) and surface mediated reaction (saturation, Contois, Eq 4.8d) kinetics:

$$r_{HYD} = \left[\frac{\mu_{max,HYD}[S_{bp}]}{K_{SM,HYD} + [S_{bp}]}\right][Z_{AD}] \quad (4.33)$$

$$r_{HYD} = \left[\frac{k_{max,HYD}\,[S_{bp}]/[Z_{AD}]}{K_{SS,HYD} + [S_{bp}]/[Z_{AD}]}\right][Z_{AD}] \quad (4.34)$$

In each of Eqs 4.33 and 4.34 above, the values for the two constants needed to be determined, namely :$_{max,HYD}$ and $K_{SM,HYD}$ and $k_{max,HYD}$ and $K_{SS,HYD}$ respectively. To determine these constants, the equations were linearised by three different methods, i.e. (i) Lineweaver-Burke, (ii) inversion and (iii) Eadie-Hofstee (Lehninger, 1977). For the Monod kinetics for example, these yielded respectively:

(i) $$\frac{[Z_{AD}]}{r_{HYD}} = \frac{K_{SM,HYD}}{\mu_{max,HYD}} \cdot \frac{1}{[S_{bpe}]} + \frac{1}{\mu_{max,HYD}} \quad (4.35a)$$

(ii) $$\frac{[S_{bpe}]}{r_{HYD}} = \frac{K_{SM,HYD}}{\mu_{max,HYD}} + [S_{bpe}] \cdot \frac{1}{\mu_{max,HYD}} \quad (4.35b)$$

(iii) $$\frac{r_{HYD}}{[Z_{AD}]} = -K_{SM,HYD} \cdot \frac{r_{HYD}}{[S_{bpe}] \cdot [Z_{AD}]} + \mu_{max,HYD} \quad (4.35c)$$

Linear regression was fitted to the Izzett *et al.* experimental data plotted according to the three linearization methods, for example see Figs 4.5a, b and c respectively for Monod kinetics. From the slopes and y-intercepts of the fitted lines, the appropriate pair of kinetic constants was determined. Again these calculations required that the value for f_{PSup} was known.

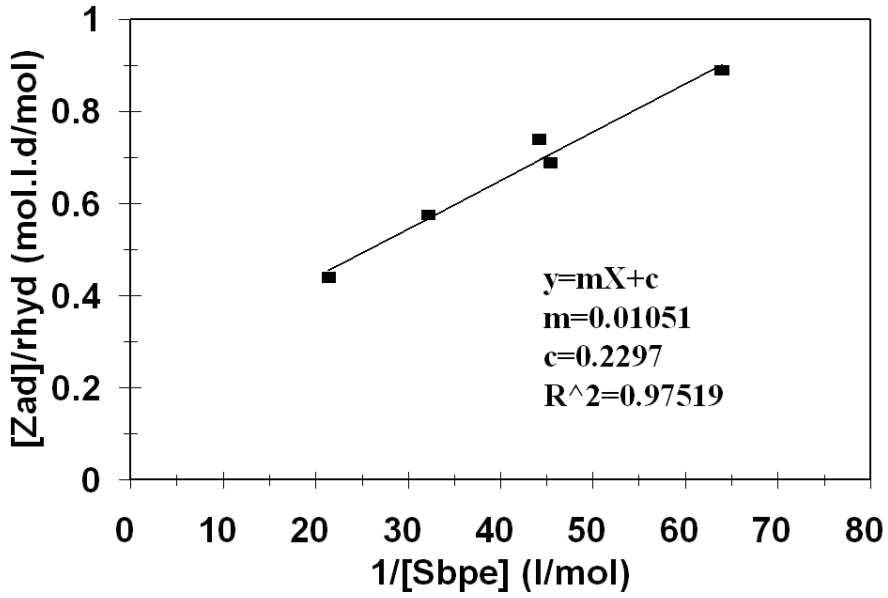

Figure 4.5a: Linearisation by Lineweaver-Burke of Monod kinetics for hydrolysis of sewage sludge for the data of Izzet *et al.* (1992) at retention times of 7, 10, 12, 15 and 20d, with linear regression fit of straight line to data.

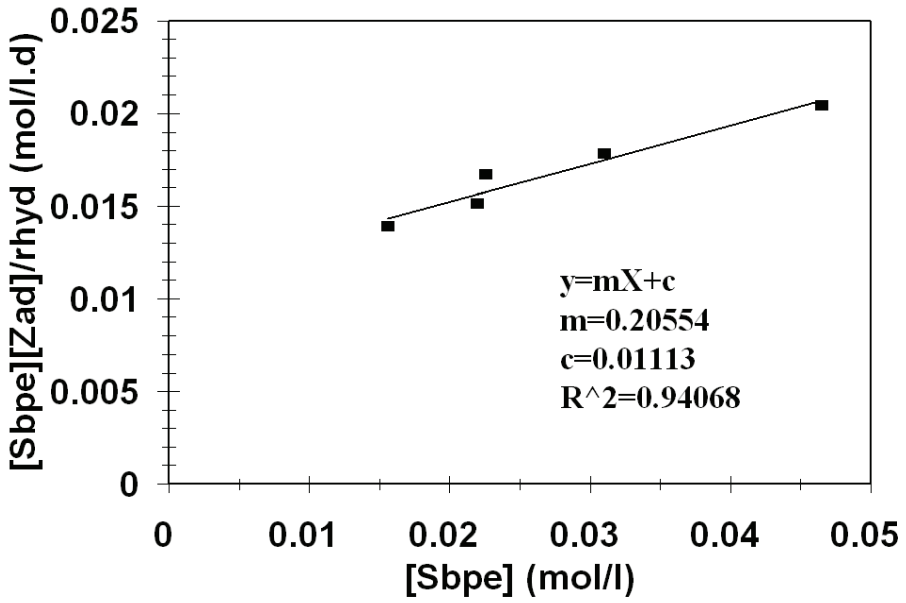

Figure 4.5b: Linearisation by inversion of Monod kinetics for hydrolysis of sewage sludge for the data of Izzet *et al.* (1992) at retention times of 7, 10, 12, 15 and 20d, with linear regression fit of straight line to data.

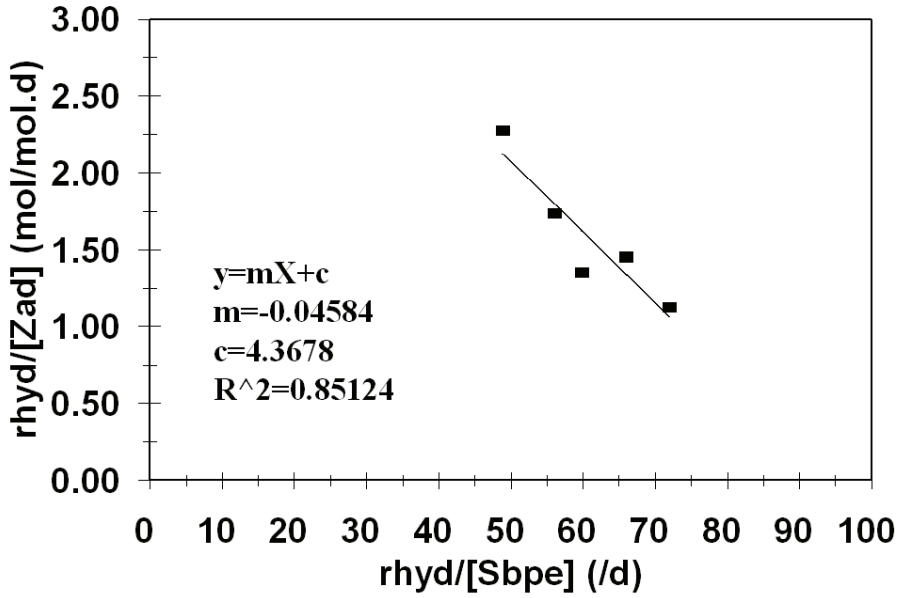

Figure 4.5c: Linearisation by Eadie-Hofstee of Monod kinetics for hydrolysis of sewage sludge for the data of Izzet *et al.* (1992) at retention times of 7, 10, 12, 15 and 20d, with linear regression fit of straight line to data.

4.7.6 Determining the sewage sludge unbiodegradable particulate fraction (f_{PSup})

In all the calculations above, a value for f_{PSup} needed to be known. However, this value was not directly available from the Izzett *et al.* data set. In the calculations, for each value of f_{PSup} selected, a different set of kinetic constants was obtained for the different kinetic formulations.

Working on the principle that the most appropriate set of kinetic constants would be the one that provides the greatest consistency between predicted and measured values for all retention times of the Izzett *et al.* data set, techniques were devised to identify these constants and the corresponding f_{PSup} value. For the first order and first order specific kinetic formulations, the value for f_{PSup} was varied and the coefficient of variation (standard deviation/average) calculated for the relevant K values for the four retention times, for each f_{Psup} value. The coefficients of variations were then plotted against f_{PSup}, see Fig 4.6. From Fig 4.6, the coefficients of variations for first order and first order specific kinetics both exhibit minima; for the first order kinetics this is at $f_{PSup} = 0.34$, and for the first order specific kinetics at $f_{PSup} = 0.32$. In effect these values of f_{PSup} are the ones that give the least variation in the relevant kinetic rate constants across the four retention times. Since the Izzett *et al.* systems were operated on the same source sewage sludge, these values would provide the most suitable estimate for f_{PSup} and the kinetic constants. Furthermore, these values for f_{PSup} are very similar to that determined by O'Rourke (1968) of 0.36, and that expected (0.32 or 0.36) from a mass balance around the primary settling tank with typical South African raw and settled wastewater characteristics, i.e. raw ($f_{S,upR}$) and settled ($f_{S,upS}$) wastewater unbiodegradable particulate COD fractions of 0.15 and 0.04 and a COD removal (f_{PSR}) of 40% or 35% respectively in primary sedimentation (WRC, 1984), where (Sötemann *et al.*, 2005a,c):

$$f_{PSup} = f_{S,upS} + (f_{S,upR} - f_{S,upS}) / f_{PSR} \quad (4.36)$$

Thus, accepting that for the first order kinetics f_{PSup} = 0.34, then K_h = 0.381 /d ∀ 0.0066, and for first order specific kinetics that f_{PSup} = 0.32, then K_H = 40 P/mol Z_{AD}/d ∀ 2.0.

For the Monod and surface mediated reaction kinetics, in the three linearization techniques, linear regression was used to fit a straight line to the data, and the correlation coefficients (R^2) of these lines calculated, for example see Figs 4.5a, b and c for linearization of the Monod kinetics. Thus, for each selected value of f_{PSup} three correlation coefficients were obtained for each of Monod and surface mediated reaction kinetics. These correlation coefficients were plotted against f_{PSup}, see Figs 4.7 and 4.8 for Monod and surface mediated reaction kinetics respectively. Both sets of R^2 values exhibit maximum values at f_{PSup} = 0.36, and hence this value was selected for these kinetics. Averaging the values for the three linearisations gives :$_{max,HYD}$ = 4.529 mol S_{bp}/(mol Z_{AD}.d) and $K_{SM,HYD}$ = 0.0486 mol S_{bp}/P for Monod kinetics and $k_{max,HYD}$ = 6.797 mol S_{bp}/(mol Z_{AD}.d) and $K_{SS,HYD}$ = 10.829 mol S_{bp}/mol Z_{AD} for surface mediated reaction kinetics. To confirm the values determined with this method, the experimental data and predicted lines were plotted on the Monod type plot for both Monod kinetics (Fig 4.9) and surface saturation kinetics (Fig 4.10); in both cases a close fit to the data is obtained.

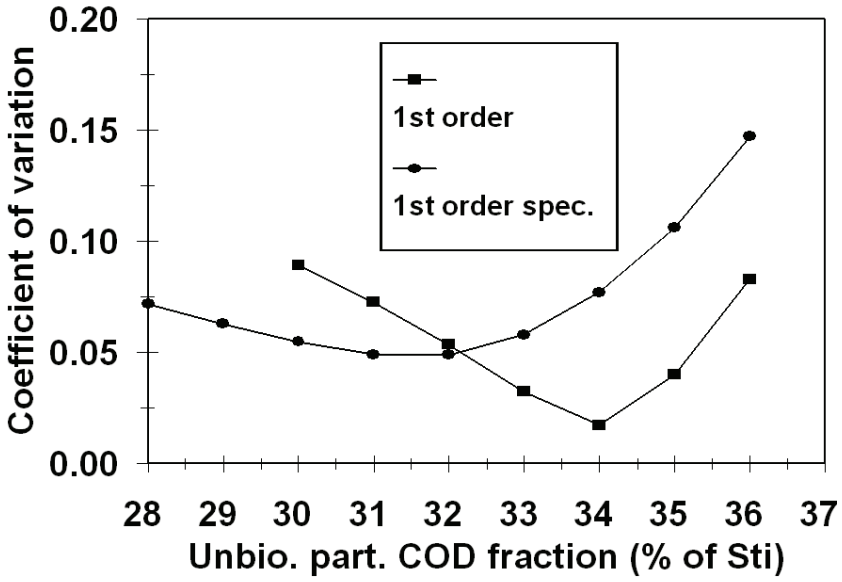

Figure 4.6: Coefficient of variation in the kinetic constants for 1st order and 1st order specific kinetics for sewage sludge hydrolysis, for the data of Izzet *et al.* (1992) at retention times of 7, 10, 12, 15 and 20d.

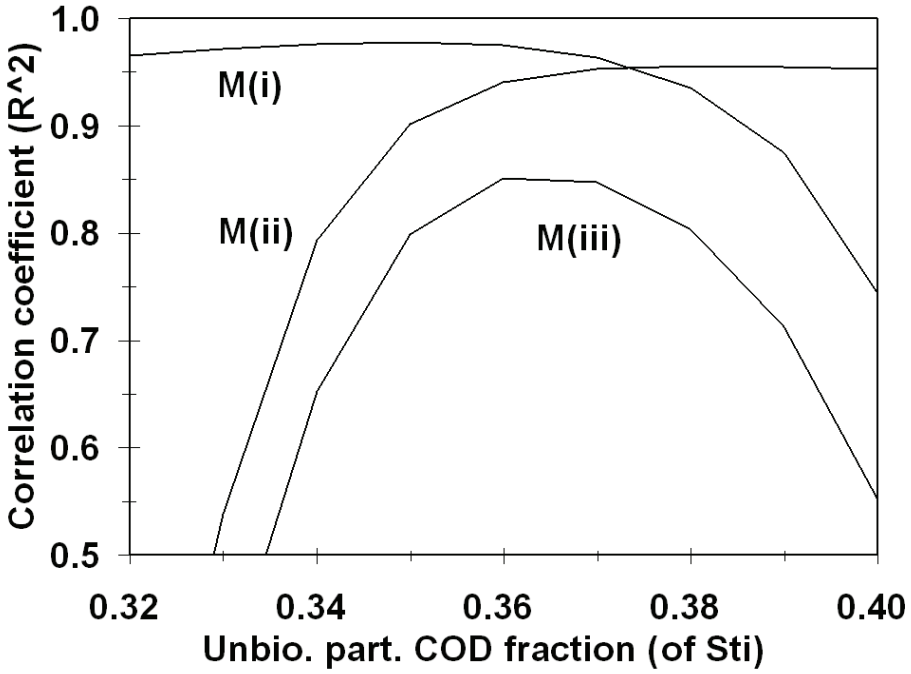

Figure 4.7: Correlation coefficients versus unbiodegradable particulate COD fraction for linear fits to Monod hydrolysis kinetics, for the data of Izzet *et al.* (1992) at retention times of 7, 10, 12, 15 and 20d: M(i) Lineweaver-Burke, M(ii) inversion, M(iii) Eadie-Hofstee linearisations (see Figs 4.5a to c).

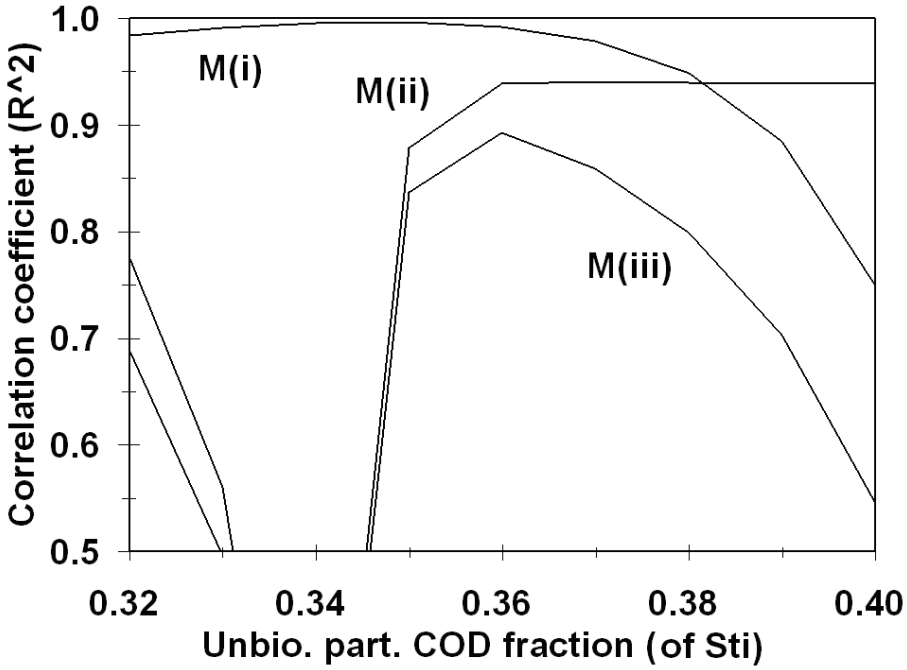

Figure 4.8: Correlation coefficients versus unbiodegradable particulate COD fraction for linear fits to surface mediated reaction hydrolysis kinetics, for the data of Izzet *et al.* (1992) at retention times of 7, 10, 12, 15 and 20d: M(i) Lineweaver-Burke, M(ii) inversion, M(iii) Eadie-Hofstee linearisations.

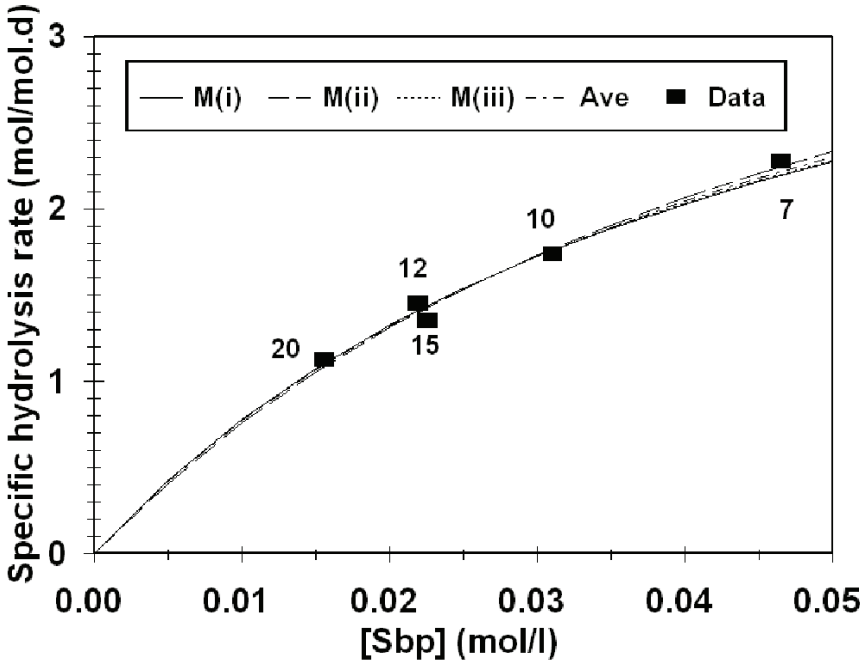

Figure 4.9: Monod specific hydrolysis rate versus biodegradable particulate organics (S_{bp}, mole/ℓ) for the Izzet *et al.* (1992) data at 7, 10, 12, 15 and 20 d retention time: M(i) Lineweaver-Burke, M(ii) inversion, M(iii) Eadie-Hofstee linearisations, see Fig 4.5.

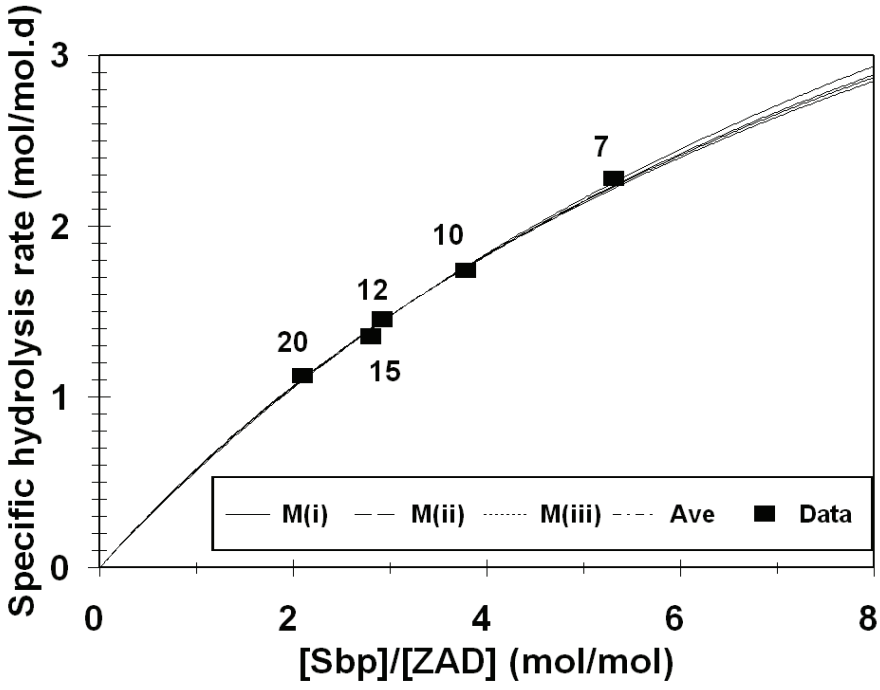

Figure 4.10: Surface mediated reaction specific hydrolysis rate versus biodegradable particulate organics (Sbp, mole/ℓ) to acidogen biomass (ZAD, mole/ℓ) ratio for the Izzet *et al.* (1992) data at 7, 10, 12, 15 and 20 d retention time: M(i) Lineweaver-Burke, M(ii) inversion, M(iii) Eadie-Hofstee linearisations, see Fig 4.5.

4.7.7 Selection of hydrolysis kinetics

In the section above, the data set of Izzett *et al.* was used to calibrate the constants for the four variations in hydrolysis kinetics, first order (Eq 4.8a), first order specific (Eq 4.8b), Monod (Eq 4.8c) and surface mediated reaction or Contois (Eq 4.8d). In this exercise, measures of variability were derived for the various kinetic expressions, namely coefficient of variation for the first two formulations and correlation coefficients (R^2) for the second two. Comparing the coefficients of variation (Fig 4.6), the minimum value for the first order kinetics is smaller than that for the first order specific, which would suggest that the former describes this data set marginally better. Comparing the R^2 values (Figs 4.7 and 4.8), the values for surface mediated reaction kinetics are higher than those for Monod kinetics, also suggesting that the former kinetics describes the data set marginally better. With regard to first order versus surface mediated reaction kinetics, the data set cannot provide guidance as to which is superior, i.e. both kinetic formulations with the appropriate constants provide equally acceptable descriptions of the hydrolysis process for the Izzett *et al.* data set. However, since this process is mediated by the acidogens, the surface mediated reaction kinetics which includes this organism group intuitively would appear more reasonable. Furthermore, this kinetic formulation has been applied with considerable success in activated sludge system models (e.g. ASM1, Henze *et al.*, 1987), in which the organisms act on the same biodegradable particulate substrate. Accordingly, the surface mediated reaction kinetics was accepted for incorporation in UCTADM1, in agreement with the conclusions in Chapter 2.

4.7.8 Refinement of values for sewage sludge composition, and model validation

Accepting the surface mediated reaction kinetics for hydrolysis and the estimates for the various constants (f_{PSup}, $k_{max,HYD}$ and $K_{SS,HYD}$) as determined above, the averages of the Izzett *et al.* measured influent parameters were set as input to AD model, with the influent weak acid/bases (NH_3/NH_4^+; HAc/Ac^-; $H_2CO_3^*/HCO_3^-/CO_3^{2-}$; phosphorus not included as measurements not available). The model predictions for the effluent parameters and gas streams compositions and flows were compared with the corresponding measured averages at the different retention times. Only one part of the model required refinement, the sewage sludge CHON composition, and this was then adjusted iteratively until the best correspondence between predicted and measured results at all retention times was obtained, to give $C_{3.5}H_7O_2N_{0.196}$; because the model is internally consistent and fixed by the kinetic and stoichiometric equations and determined constants, the only way a different effluent pH or gas composition can be predicted by the model is by changing the influent composition of the feed sludge. As noted above, independent validation was obtained by comparing the determined primary sludge composition with measured values. The model predicted parameters are compared with the corresponding measured values for all retention times in Fig 4.11 a to f. The predicted COD removal (Fig 4.11a) and gas composition (Fig 4.11c) correspond very well to those measured. The gas production (Fig 4.11b) is under predicted, because the model is based on 100% COD balance and the experimental data COD balances range from 107 to 109% (Table 4.6) – model calibration was on COD removal and hence the COD over recovery manifests in the gas production. The predicted effluent free and saline ammonia (FSA) concentration is generally higher than that measured, because the model is based on 100% N mass balance and the experimental mass balances were 91 to 99% (Table 4.6). By decreasing the N content of the influent organics (A in $C_XH_YO_ZN_A$) by a small amount (5% to 0.186), the predicted effluent FSA could be made to closely match the measured values, but this would cause the influent organic N concentration to be in error. The

effluent H_2CO_3* alkalinity is over predicted, and this prediction can be improved by decreasing the N content of the organics or including some of the influent SCFA as propionic. However, both these would cause the predicted pH to decrease causing it to deviate from the measured value. Since insufficient experimental data are available to resolve this, these changes were not implemented. The experimentally measured pH, H_2CO_3* alkalinity and p_{CO2} show inconsistency in that these are not in equilibrium. Accepting the gas composition and H_2CO_3* alkalinity as the most reliable measurements (CO_2 loss on sampling would influence pH but not H_2CO_3* alkalinity, Loewenthal *et al.*, 1991), the equilibrium "corrected" pH was calculated. Both experimentally measured and "corrected pH is shown in Fig 4.11f together with the predicted pH values; the predicted and "corrected" pH values correspond closely. Overall, accepting the margin for error in the experimental measurements, good correlation between measured and predicted parameters was obtained. More extensive simulations with the model of a wider range of experimental systems are required for further model validation.

4.8 FURTHER MODEL VALIDATION

Chapter 2 (and reported in detail by Ristow *et al.*, 2005a) studied the rate of hydrolysis of primary sewage sludge under methanogenic, acidogenic and sulfate reducing conditions, and the influence of system physical constraints on the hydrolysis rate. The research approach adopted in Chapter 2 was to operate parallel laboratory-scale, completely mixed anaerobic digesters with primary sewage sludge as influent, and to monitor the behaviour of these systems under a range of feed COD concentrations, retention times, pH and feed sulfate concentrations under stable methanogenic, acidogenic and sulfate reducing conditions. To further validate the methanogenic anaerobic digestion model developed in this Chapter, the methanogenic experimental laboratory-scale completely mixed anaerobic digesters operated in Chapter 2 were simulated with the anaerobic model developed here.

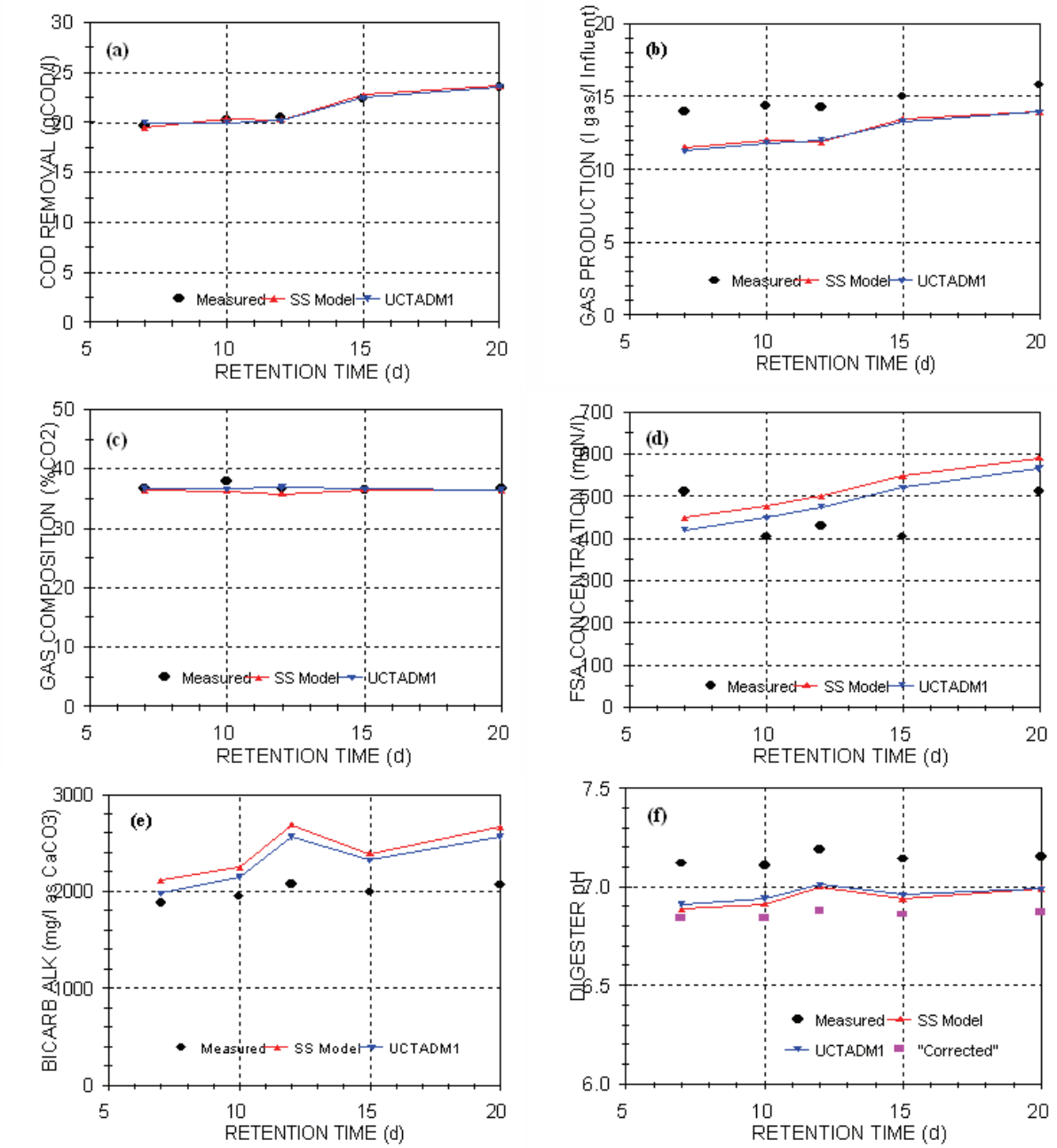

Figure 4.11: Comparison between kinetic simulation model (UCTADM1) predicted (lines) and measured (points) (a) OD removal, (b) gas production, (c) gas composition, (d) free and saline ammonia, (e) H_2CO_3* alkalinity and (f) digester pH versus retention time for the Izzet *et al.* (1992) data set; also shown are the predictions of the steady state AD model presented by Sötemann *et al.* (2005c).

4.8.1 The laboratory-scale completely mixed methanogenic anaerobic digesters operated in Chapter 2

During the research reported in Chapter 2, 21 methanogenic laboratory scale completely mixed anaerobic digesters were operated at a controlled temperature of 35^{o}C at various hydraulic retention times between 5 and 60 days. Primary sewage sludge was fed at varying concentrations, from 1.950 g cod/ℓ up to 41.441 g cod/ℓ. The feed primary sewage sludge originated from the primary settling tanks at the Athlone Wastewater Treatment Works (City of Cape Town, South Africa), which treats municipal wastewater of mainly domestic origin, but with a significant mixed industrial component. The primary sludge was collected in batches using a number of 25 ℓ plastic drums, and each batch of feed was given a feed batch number (for details see Ristow *et al.*, 2005a). Table 4.7 gives a summary of the 21 digesters operated, where FB is the feed batch number for the digester, with the corresponding steady state systems listed in Table 2.1.

Table 4.7: Steady states measured for varying hydraulic retention times and feed COD concentrations (numbers indicate feed batch, FB, number); see Chapter 2, Table 2.1 for steady state periods.

Feed COD Concentration	**Hydraulic Retention Time (d)**							
(g cod/ℓ)	**60**	**20**	**15**	**10**	**8**	**6.67**	**5.71**	**5**
40			FB13	FB13	FB14	FB14	FB15	
25		FB12	FB12	FB12	FB12	FB13	FB13	FB13
13			FB12	FB13	FB13	FB14	FB15	
9	FB12							
1.95				FB14	FB14			

4.8.2 Feed characterization and effluent experimental data

In Chapter 2 (see Ristow *et al.*, 2005a for details), the unbiodegradable particulate and unbiodegradable soluble fractions for all the feed batches were determined as 0.3345 and 0.008 respectively. The unbiodegradable particulate fraction was derived from the 60 day experimental unit. It was argued that 60 days are sufficient time for all the biodegradable organic material to be utilized, and therefore the effluent particulate COD (that is not organism mass) can be accepted to be unbiodegradable particulate organic material only. The unbiodegradable soluble fraction was calculated from the measured dissolved effluent COD of all the systems, as the average of the measured filtered (0.45µm) effluent COD minus twice the effluent measured VFA (Section 4.6.4).

Alkalinity and pH were measured on the undiluted feed for feed batches 9, 10, 12 and 13 (Table 4.7), but not for feed batches 14 and 15. By omission, the influent alkalinity and pH were not measured on the diluted feed. The alkalinity and pH data collected on the undiluted influent primary sludge are given in Table 4.8. Included in Table 4.8 are the data for feed batches 9 and 10, which were not used for the methanogenic systems in the research in Chapter 2, but are used here, together with the measured data from feed batches 12 and 13 to estimate values for the influent alkalinity and pH for feed batches 13 and 14. The primary sludge stoichiometric formulations are also given in Table 4.8; these were calculated in the same way as those for the data set of Izzett *et al.* (1992) described above.

Table 4.8: Sludge stoichiometric formula, alkalinity and pH data for feed batches 9, 10, 12, 13, 14 and 15 from Chapter 2 (Ristow *et al.*, 2005a).

Feed Batch No.	Sludge Stoichiometric Formula	Alkalinity mg/l as $CaCO_3$	pH
9	-	86.7	5.35
10	-	75.52	5.54
12	$C_{4.15}H_7O_{2.42}N_{0.22}$	47.3	4.91
13	$C_{4.17}H_7O_{2.63}N_{0.22}$	151.6	5.73
14	$C_{4.31}H_7O_{3.03}N_{0.24}$	90.28 *	5.38 *
15	$C_{4.06}H_7O_{2.43}N_{0.19}$	90.28 *	5.38 *

* Calculated averages from feed batches 9,10,12 and 13.

In calculating the pH and alkalinity values for the diluted feed, it was recognised that when tap water is added to the raw primary sludge to dilute it to the required feed concentration, the alkalinity and pH values are not merely diluted by volume, but change in a complex manner, dependent on the aqueous chemistry of the primary sludge/tap water blend. Therefore, the alkalinity and pH measurements on the diluted feeds could not be calculated by simply multiplying the measured undiluted feed values with the corresponding dilution factor. To obtain a more accurate estimate of the alkalinity and pH values of the diluted feeds, the primary sludge fraction and the corresponding fraction of tap water (alkalinity and pH accepted to be 35.0 mg/ℓ as $CaCO_3$ and 7.0 respectively from previous experience) were entered into the computer program STASOFT version 2.4 (Loewenthal *et al.*, 1988) to obtain the estimated primary sludge/tap water blend alkalinity and pH. These alkalinity and pH values were used as input to the anaerobic model developed in this Chapter.

All influent data for the feed to each experimental methanogenic system are listed in Table 4.9. The total COD (S_{ti}), soluble COD (S_{bsi}), VFA (S_{bsai}) and FSA (N_{ai}) were measured on the undiluted primary sludge. These values were multiplied by their corresponding dilution factors to calculate the corresponding diluted values. All data listed in Table 4.9 refer to the diluted influent that was fed to the anaerobic digesters.

After start-up of each digester, it was operated for three full sludge ages to allow it to reach steady state, see Chapter 2. Once steady state was reached, daily data collection commenced for at least 20 days. The average effluent data measured for each steady state are given in Table 4.10.

Table 4.9: Feed data for the methanogenic laboratory scale, completely mixed anaerobic digesters operated in Chapter 2 (Table 2.1).

Ret. Time days	Feed Rate ℓ/d	React. Vol. ℓ	Feed Batch No.	S_{ti} mgCOD/ℓ	S_{bsi} mgCOD/ℓ	S_{bsai} mgCOD/ℓ as HAc	S_{usi} mgCOD/ℓ	N_{ai} mgN/ℓ	Alkalinity mg/ℓ as $CaCO_3$	pH
60	0.33	20	12	9810	1204	528	78	15	37.3	5.55
20	1	20	12	25953	2327	994	208	39	41.1	5.16
15	1.33	20	13	39790	3550	1516	318	180	139.9	5.74
15	1.33	20	12	25953	2647	1145	208	39	41.1	5.16
15	1.33	20	12	13618	1432	621	109	20	38.2	5.42
10	2	20	13	39810	4446	1937	318	214	139.9	5.74
10	1.6	16	12	25953	2331	996	208	39	41.1	5.16
10	2	20	13	13270	1164	496	106	59	70	5.93
10	2	20	14	1950	254	112	16	5	38.1	6.24
8	2.5	20	14	34818	3828	1665	279	44	90.28	5.38
8	2	16	12	25953	2675	1158	208	39	41.1	5.16
8	2.5	20	13	13270	1525	666	106	73	70	5.93
8	2.5	20	14	1950	284	126	16	7	38.1	6.24
6.67	3	20	14	34818	4354	1912	279	70	90.28	5.38
6.67	2.4	16	13	24818	2038	863	199	106	100.6	5.81
6.67	3	20	14	13579	1845	815	109	37	56.6	5.6
5.71	3.5	20	15	41441	2583	1056	332	40	69.7	5.48
5.71	2.8	16	13	24960	2516	1087	200	124	100.6	5.81
5.71	3.5	20	15	13186	957	400	105	18	46.1	5.81
5	3.2	16	13	24881	2703	1175	199	131	100.6	5.81

Table 4.10: Effluent data for the methanogenic laboratory scale completely mixed anaerobic digesters operated in Chapter 2 (Table 2.1).

Ret. Time days	Effluent total COD mgCOD/ℓ	Effluent total soluble COD mgCOD/ℓ	Effluent VFA mgCOD/ℓ as HAc	Effluent FSA mgN/ℓ	Effluent Alk mg/ℓ as $CaCO_3$	pH	Methane Volume l/d	Gas Comp. % Methane	COD Bal. %	N Bal %
60	3590	88	5	101	775	6.74	0.78	66.51	100.0	103.0
20	10525	179	11	231	1577	6.89	5.41	63.11	96.0	107.5
15	16972	250	28	347	2446	6.98	12.12	61.40	103.4	86.9
15	10212	157	17	212	1539	6.85	7.71	63.08	98.6	108.3
15	5751	97	6	114	845	6.80	3.95	63.26	100.1	116.4
10	18085	256	27	260	2362	6.92	17.33	62.73	103.4	78.3
10	10849	178	24	208	2424	7.00	10.69	63.24	110.3	107.5
10	6249	108	8	127	854	6.69	5.00	60.98	97.2	92.2
10	905	32	0	19	170	6.59	0.62	53.20	88.4	92.8
8	15094	205	22	258	1868	6.90	19.39	58.85	102.7	84.5
8	11299	168	21	186	1394	6.80	10.94	63.24	99.6	113.3
8	6299	104	7	112	863	6.78	6.40	63.06	98.8	43.7
8	892	51	10	15	144	6.38	0.84	59.30	91.9	83.5
6.67	14984	207	12	255	1821	6.83	22.71	59.32	100.9	75.1
6.67	12595	200	19	196	1504	6.86	11.66	60.98	102.6	94.6
6.67	5944	96	5	104	789	6.57	8.74	60.95	100.9	81.9
5.71	19737	295	26	183	1612	6.75	30.32	63.76	103.3	81.8
5.71	12729	205	32	200	1463	6.93	13.24	61.67	101.4	93.2
5.71	6757	120	19	63	564	6.45	9.23	65.70	104.5	81.7
5	12610	301	87	193	1359	6.78	13.57	65.70	96.0	74.1

4.8.3 Modelling the methanogenic laboratory scale completely mixed anaerobic digesters

The data listed in Table 4.9, together with the unbiodegradable particulate and soluble fractions, the operating temperature of the digesters and the hydrolysis rate constants are required as input to the anaerobic model. In Chapter 2, it was concluded that the first order kinetics and surface mediated reaction kinetics most accurately predict the rate of primary sewage sludge hydrolysis under methanogenic conditions for all hydraulic retention times and feed COD concentrations. Since first order kinetics are (i) a simplification of the hydrolysis process (ii) do not explicitly include the acidogenic biomass and (iii) does not set an upper limit to the rate, surface mediated reaction kinetics were selected as the most appropriate rate formulation to model primary sewage sludge hydrolysis. Following similar procedures to those described above, Ristow *et al.* (2005a) determined the $k_{max,HYD}$ and $K_{SS,HYD}$ rate constants for the surface mediated reaction kinetics for their methanogenic systems to be 11.2 g cod S_{bp}/(g cod Z_{AD}.d) and 13.0 g cod S_{bp}/g cod Z_{AD} for the systems reported in Chapter 2; converting these to the mole units required in the model gave 12.32 mol S_{bp}/(mol Z_{AD}.d) and 14.30 mol S_{bp}/mol Z_{AD} respectively. These values are higher than the values calculated for the data of Izzett *et al.* (1992) above ($k_{max,HYD}$ = 6.797 mol S_{bp}/(mol Z_{AD}.d) and $K_{SS,HYD}$ = 10.829 mol S_{bp}/mol Z_{AD}), which is reasonable, because the influent sludge used by Izzett *et al.* (1992) was a mixture of primary sewage and humus sludges, while the systems in Chapter 2 used pure primary sewage sludge as feed. It was therefore decided to use the hydrolysis rate constants for the surface mediated reaction kinetics calculated by Ristow *et al.* (2205a) to model the methanogenic anaerobic digesters reported in Chapter 2. Figures 4.13 (for feed concentrations 9 to 13 g cod/ℓ), 4.14 (for feed concentrations 24 to 26 g cod/ℓ) and 4.15 (for feed concentrations 34 to 42 g cod/ℓ) show the results simulated by the anaerobic model, together with the experimental results measured for the systems in Chapter 2.

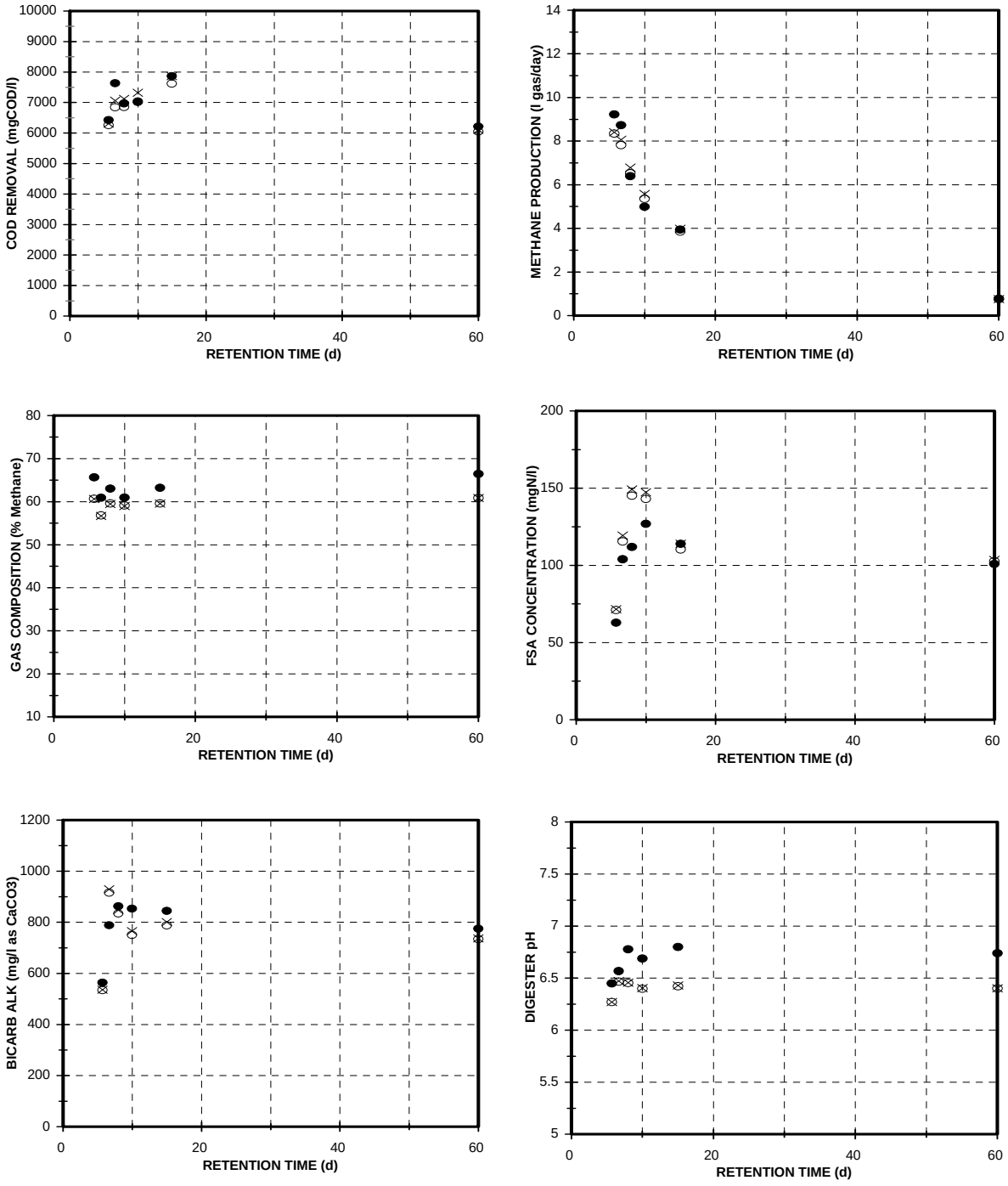

Fig 4.12: Comparison between kinetic simulation model (UCTADM1) predicted and measured (a) COD removal, (b) gas production, (c) gas composition, (d) free and saline ammonia, (e) $H_2CO_3^*$ alkalinity and (f) digester pH versus retention time for the Chapter 2 (Ristow *et al.*, 2005a) data set for feed COD concentrations between 9 and 13 g cod/ℓ.

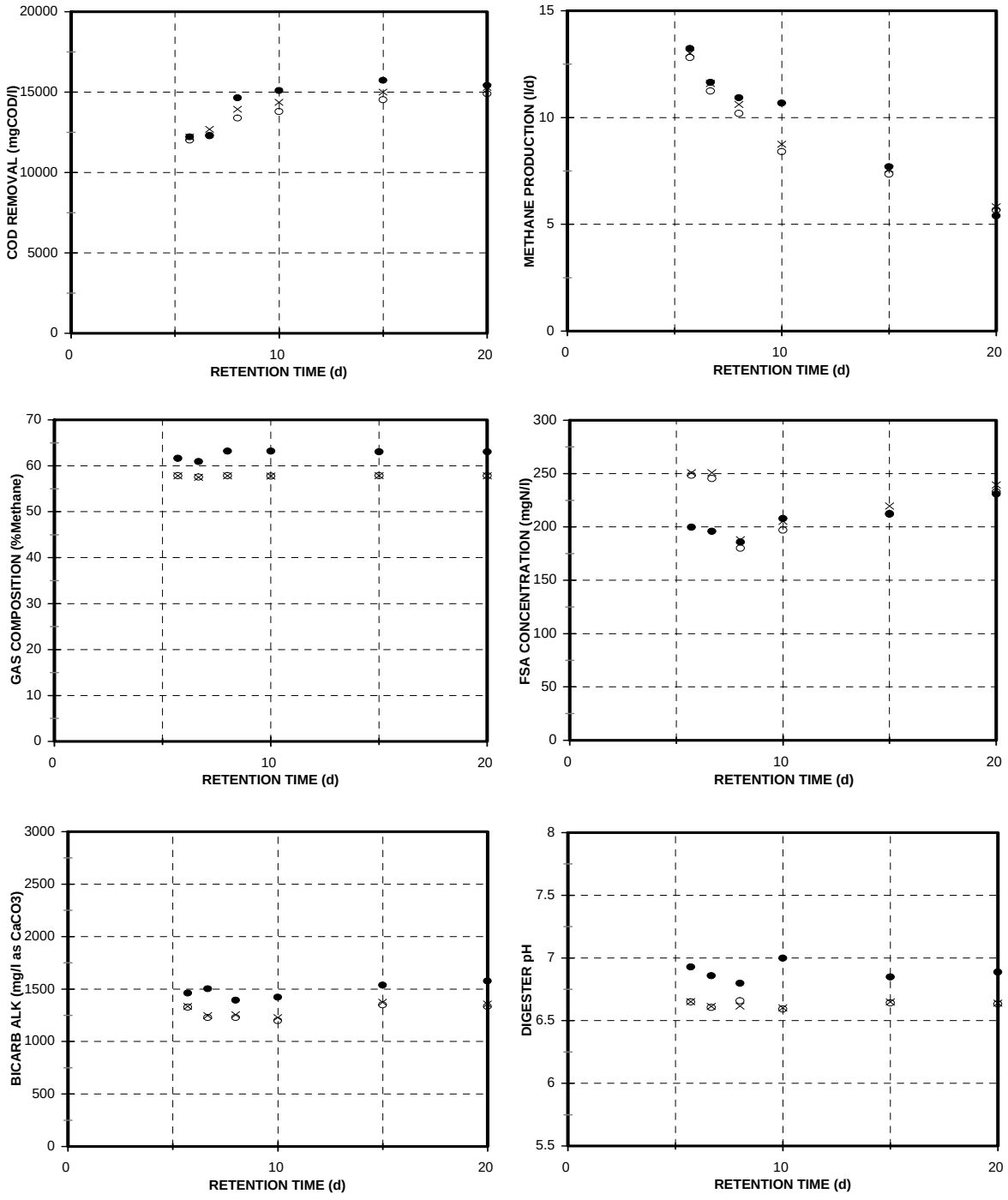

Fig 4.13: Comparison between kinetic simulation model (UCTADM1) predicted and measured (a) COD removal, (b) gas production, (c) gas composition, (d) free and saline ammonia, (e) $H_2CO_3^*$ alkalinity and (f) digester pH versus retention time for the Chapter 2 (Ristow *et al.*, 2005a) data set for feed COD concentrations between 24 and 26 g cod/ℓ.

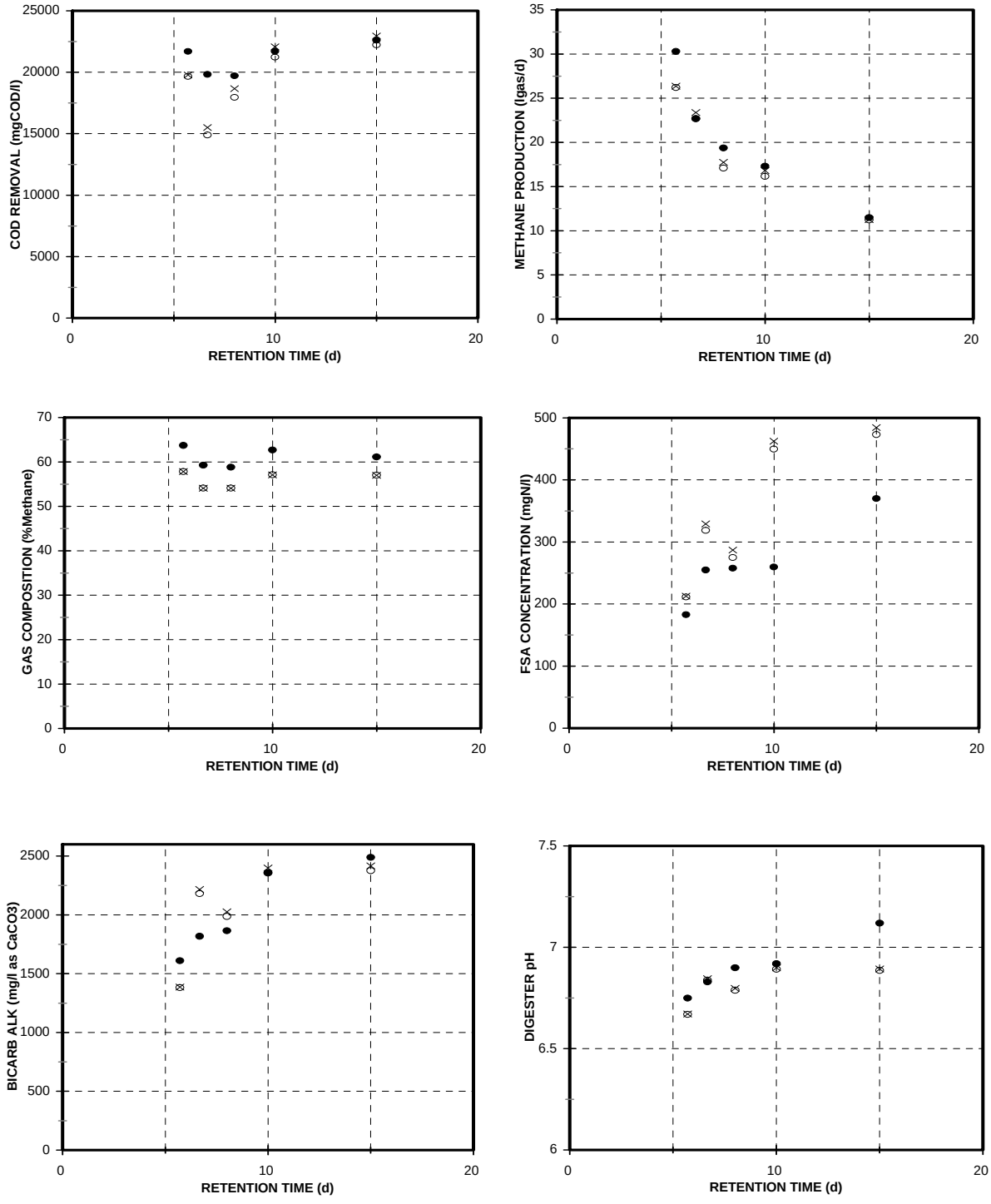

Fig 4.14: Comparison between kinetic simulation model (UCTADM1) predicted and measured (a) COD removal, (b) gas production, (c) gas composition, (d) free and saline ammonia, (e) $H_2CO_3^*$ alkalinity and (f) digester pH versus retention time for the Chapter 2 (Ristow *et al.*, 2005a) data set for feed COD concentrations between 34 and 42 g cod/ℓ.

In Figures 4.13, 4.14 and 4.15 the solid circles represent the experimental data measured in Chapter 2 (Ristow *et al.*, 2005a) and the open circles show the anaerobic model predictions using the hydrolysis rate constants calculated by Ristow *et al.* (2005a). The crosses show the anaerobic model predictions using recalculated hydrolysis rate constants (see below); these will be discussed further below in Section 4.7.4.

Comparing the COD removals measured in Chapter 2 with the predictions by UCTADM1 using the hydrolysis rate constants calculated by Ristow *et al.* (Figs. 4.13a, 4.14a and 4.15a), it can be seen that for all the systems receiving low feed COD concentrations (9 to 13 g COD/ℓ), intermediate COD concentrations (24 and 26 COD/ℓ) and high feed COD concentrations (34 to 42 g cod/ℓ), the simulated COD removals compare reasonably well with the measurements, which is expected due to the low residual biodegradable COD concentrations which causes the COD removal to be relatively insensitive to the exact values for hydrolysis constants selected. For the COD removal, there appears to be no discernable trend linked to influent COD concentration or retention time, but the shorter retention times at the higher influent COD concentrations show the greatest deviation between simulated and measured results. These deviations are thought to be a result of a combination of (i) the hydrolysis rate constants chosen by Ristow *et al.* and (ii) the experimental outliers mentioned by Ristow *et al.* The hydrolysis rate constants are considered further in Section 4.7.4 below.

The simulated and measured methane productions (Figs. 4.13b, 4.14b and 4.15b) correspond closely for most systems and mirror the COD removal, which is expected, because the methane production is directly proportional to the COD removal. For specific systems, differences between COD removal and methane production correspondences of simulated and measured results arise due to the measured COD mass balances not being 100%, whereas the simulations are based on a 100% mass balance. This is particularly evident for the influent COD concentrations between 24 and 26 g cod/ℓ where the simulated methane productions correspond closely to the measured values for all retention times, except for the 10 day system; this 10 day system has the poorest COD balance (110%, see Table 4.10), which explains why it is an outlier here. The simulated and measured gas compositions (Figs. 4.13c, 4.14c and 4.15c) correspond equally well for all feed COD concentrations and retention times, but the simulated gas compositions are consistently lower than those measured. This results from a combination of factors, namely (i) the lower COD removals predicted by UCTADM1, (ii) and the resulting lower methane production, (iii) the measured and calculated influent sludge stoichiometric formulae and (iv) the estimated influent pH and alkalinity parameters (that were not measured directly). It may, however, also indicate that in simulations with UCTADM1 too much CO_2 is expelled (or produced), which would show in higher simulated bulk liquid pH values, which was not the case. In the comparison of the experimental and simulated Izzett *et al.* (1992) data, the simulated and measured gas compositions corresponded more closely, but that may merely indicate that the Izzett *et al.* (1992) data is of better quality.

The measured and simulated effluent FSA concentrations (Figs. 4.13d, 4.14d and 4.15d) are not consistent with the COD removals, with systems exhibiting good correspondence between predicted and measured COD removals having poor correspondence between predicted and measured effluent FSA, and *visa versa*. It is expected that lower predicted COD removals would result in less biodegradable particulate organics hydrolysed and therefore less organic N released as FSA to the effluent. These variations probably arise from the N mass balance, where measured N mass balances do not conform to 100% whereas simulations are based on 100% mass balance. For example, in some cases the predicted

effluent FSA are substantially higher than the measured values (e.g. 5.71 and 6.67 day systems for 24 to 26 g cod/ℓ feed COD concentrations and 10 and 15 day systems for 34 to 42 g cod/ℓ feed COD concentrations); these over predictions all correspond to the systems with the lowest N balances (81.7, 81.9 and 78.3 and 85.5% respectively, see Table 4.10) which explains why for these cases the predicted effluent FSA is so much higher than the measured values.

The measured and predicted alkalinities (Figs. 4.13e, 4.14e and 4.15e) correspond better than the corresponding comparison of the experimental and simulated Izzett *et al.* (1992) data. However, the simulated alkalinities do tend to be lower than the measured values, particularly for the influent feed concentration of 24 to 26 g cod/ℓ. Possibly these deviations arise because the influent alkalinity and pH values were estimated, since direct measurements were not available. Had more accurate influent and alkalinity data been available, the simulated effluent alkalinity results most likely would have corresponded even better to the measured values. The simulated and measured pH values (Figs. 4.13f, 4.14f and 4.15f) correspond similarly to those from the comparison of the simulated and measured data of Izzett *et al.* (1992) above: The simulated pH's are virtually all lower than the measured values. For the data from Chapter 2 (Ristow *et al.*, 2005a), the influent pH values were estimated, which will have had an effect on the simulated values. Further, the simulated alkalinities tend to be lower and more CO_2 was expelled in the simulations, which also had an effect on the pH values. However, the trend of lower simulated pH values observed with the data of Izzett *et al.* (1992) clearly also applies here, and required further investigation.

Considering (i) that the influent alkalinity and pH values were estimated, (ii) the low N mass balances of the Chapter 2 (Ristow *et al.*, 2005a) data and (iii) experimental outliers, on the whole the simulated data compares reasonably well with the experimental results reported in Chapter 2 (detailed in Ristow *et al.*, 2005a) and provides further validation of the UCTADM1 anaerobic model developed in this Chapter.

4.8.4 The hydrolysis rate constants

The above comparison indicates that the hydrolysis rate constants calculated by Ristow *et al.* (2005a and reported in Chapter 2) ($k_{max,HYD}$ and $K_{SS,HYD}$ rate constants for the surface mediated reaction kinetics for the methanogenic experimental systems of 12.58 mol S_{bp}/(mol Z_{AD}.d) and 14.61 mol S_{bp}/mol Z_{AD}) may require re-calibration to improve the simulations.

Figure 4.16 shows the hydrolysis rate vs. the biodegradable COD/acidogen ratio for the methanogenic systems of Chapter 2 for the surface mediated reaction kinetics. The data (each laboratory scale system) is represented by a solid dot ( ) or a cross (X). The crosses show the five systems used by Ristow *et al.* to calculate their hydrolysis rate constants ('Ristow' on the graph, see Ristow *et al.*, 2005a for details). The lines represent the hydrolysis rate constants calculated by the Lineweaver-Burke (L-B), Double-reciprocal (DR) and Eadie-Hofstee (E-H) and the average of all three methods (Avg) with all the data points (excluding the 60 day system) as was done above for the Izzett *et al.* (1992) data set. All concentrations are in COD units.

From Fig. 4.16 it can be seen that there is appreciable scatter in the experimental data, with two discernable bands of data, one higher band lying above the other. This shows that obtaining good estimates for the hydrolysis rate constants from this experimental data set is difficult. In Ristow *et al.*, the five experimental systems chosen (crosses on Fig. 4.16) for

estimation of the hydrolysis rate constants, were selected because these represent the five systems with the shortest retention times. In selecting these five systems, Ristow *et al.* reasoned that the short retention times dictate the hydrolysis rate constants, and therefore the systems with retention times less than 8 d, without outliers, were selected to calculate the hydrolysis rate constants (steady states 7, 8, 9, 14 and 31 in Table 2.1). However, from the comparison of measured and simulated results above, the short retention time systems may not provide the best estimate for the hydrolysis rate constants and the approach excludes a number of the systems operated.

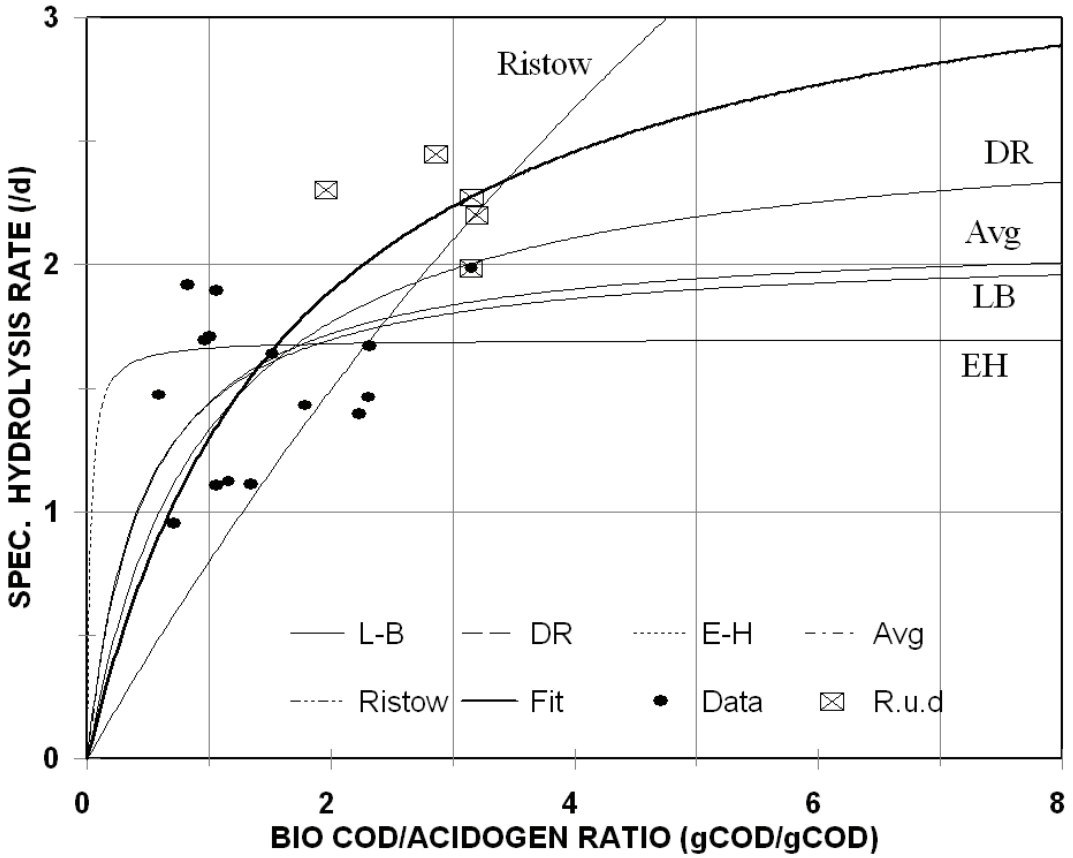

Figure 4.15: Specific hydrolysis rate vs. biodegradable COD/acidogen ratio for the methanogenic laboratory scale completely mixed anaerobic digesters from Chapter 2 (Ristow *et al.*, 2005a).

The lines represent the hydrolysis rate constants calculated by the Lineweaver-Burke (L-B), Double-reciprocal (DR) and Eadie-Hofstee (E-H) and the average of all three methods (Avg) with all the data points (excluding the 60 day system); R.u.d. are the data points selected by Ristow *et al.* (2005a) to determine the hydrolysis constants.

The hydrolysis rate constants calculated from the Lineweaver-Burke, Double-reciprocal and Eadie-Hofstee methods ($k_{max,HYD}$ and $K_{SS,HYD}$ of 2.07 $S_{bp}/(Z_{AD}.d)$ and 0.436 S_{bp}/Z_{AD}, 2.62

$S_{bp}/(Z_{AD}.d)$ and 0.961 S_{bp}/Z_{AD}, 1.70 $S_{bp}/(Z_{AD}.d)$ and 0.022 S_{bp}/Z_{AD} respectively, all in COD units) seem very low, and therefore it seems that for this data set, there is too much scatter to obtain a reasonable estimate of the hydrolysis rate constants by linearization methods. A further set of hydrolysis rate constants were obtained by fitting a line through the data by eye ('Fit' on Fig. 4.16). This resulted in the following hydrolysis rate constants: $k_{max,HYD}$ = 3.5 $S_{bp}/(Z_{AD}.d)$ and $K_{SS,HYD}$ = 1.7 S_{bp}/Z_{AD} in COD units; converted to mole units = 3.93 and 1.91 respectively.

The Chapter 2 (Ristow *et al.*, 2005a) methanogenic systems were re-simulated, with the hydrolysis rate constants obtained by the "eye" fit, converted to mole units. The results are shown on Figs. 4.13, 4.14 and 4.15 as crosses. From Figs. 4.13, 4.14 and 4.15 it can be seen that this change improved the simulated results marginally for some of the parameters, but exacerbated the bad correlations for others, showing that the hydrolysis rate values chosen by Ristow *et al.* for the shorter retention time systems give a reasonable fit.

From Fig. 4.16 it can be seen that because of the amount of scatter in the experimental data, many different lines could be fitted and as a result many different combinations of hydrolysis rate constants could be determined. To obtain a few other hydrolysis rate constant combinations, the experimental data were grouped by (i) influent COD concentration and (ii) retention time, and the hydrolysis rate constants recalculated for each group. Simulations with these recalculated hydrolysis rate constants were performed, but no discernible improvement was achieved: The results for the shorter retention time systems would either marginally improve or deteriorate, with an opposite but equally small deterioration or improvement for the simulated results of the longer retention time systems. It therefore seems reasonable to assume that given the scatter in the experimental data (see Fig. 4.16) and the relative insensitivity of COD removal to the exact values for the hydrolysis rate constants, the hydrolysis rate constants calculated by Ristow *et al.* are as good as any other combination that can be obtained from their methanogenic data set. In implementation of the methanogenic anaerobic digestion model in WEST (Chapter 6), parameter estimation was used to determine the hydrolysis rate constants for this data set with considerable success.

4.9 MODELLING DIGESTER FAILURE

The model applications above are all to stable anaerobic digesters operating at steady state. Under such conditions the rate limiting process is the hydrolysis, so that the other processes are essentially stoichiometric. This precluded assessment of the ability of the model to predict dynamic variations (except for hydrolysis). Very little quantitative information is available in the literature on the dynamics of anaerobic digestion. Accordingly, a theoretical simulation exercise was undertaken to evaluate dynamics, namely anaerobic digester failure. Acetoclastic methanogens are probably the most sensitive organisms in anaerobic digesters (Gujer and Zehnder, 1983) and so are strongly influenced by their surrounding environment. It is commonly accepted that failure of anaerobic digesters usually starts with the inhibition of acetoclastic methanogens. This can happen by an inhibitor or toxins in the influent, a shock load on the digester and/or a sudden drop in temperature because the acetoclastic methanogens (e.g. *Methanothrix soehngenii)* have been reported to show extreme temperature sensitivity (Zehnder *et al.*, 1980). Any of these factors will slow down or inhibit the growth rate of the acetoclastic methanogens, resulting in an increase in acetic acid concentration in the digester. This increase causes a decrease in pH. Both acetoclastic methanogens and hydrogenotrophic methanogens (e.g. *Methanobrevibacter arboriphilus*) are pH sensitive, the latter also showing some sensitivity to temperature changes. Thus, the drop

in pH will slow down their rates of growth, resulting in a further increase in acetic acid and an increase in hydrogen partial pressure p_{H2}. The increase in p_{H2} affects the acidogenesis process as described above (Eqs 4.9 and 4.10) and instead of producing only acetic acid, propionic acid also is produced. The increase in p_{H2} also slows the acetogenesis process (Eq 4.11) so that the propionic acid concentration increases, causing a further decrease in pH. Clearly, anaerobic digestion is a poised system and even a small disturbance in one of the methanogenic processes causes irreversible system collapse. Such a collapse, called digester souring, is characterized by increases in acetic and propionic acid concentrations and hydrogen partial pressure and decreases in pH and gas production. The digester pH should not drop below 6.6 to maintain methanogenesis processes uninhibited by pH (Moosbrugger *et al.*, 1993). The AD kinetic model was extended to include the above failure condition.

4.9.1 Inhibition of acetoclastic methanogens (process D7)

These organisms are inhibited by the hydrogen ion concentration (pH). To include this, the inhibition term commonly used with Monod kinetics of $(1+ I/K_I)$, where I is the aqueous inhibitor compound concentration and K_I the concentration at which the growth rate is half the normal rate (Batstone *et al.*, 2002), was introduced into the growth rate equation (Eq 4.12) i.e.:

$$r_{Z_{AM}} = \frac{\mu_{max,AM}[HAc]}{(K_{S,AM}+[HAc])\left(1+\frac{[H^+]}{K_{I,AM}}\right)}[Z_{AM}] \qquad (4.37)$$

where:

$K_{I,AM}$ = Inhibition constant i.e. the hydrogen ion concentration at which the growth of acetoclastic methanogens is half the normal rate (mol/P)

$[H^+]$ = Hydrogen ion concentration (mol/P) from which pH = -log (H^+)

4.9.2 Inhibition of hydrogenotrophic methanogens (process D9)

Hydrogenotrophic methanogens function to keep the hydrogen partial pressure p_{H2} low, and like the acetoclastic methanogens, they are also neutrophiles and are inhibited at pH values below 6.6 (Gujer and Zehnder, 1983, Zehnder and Wuhrmann, 1977). Hence, an inhibition term was also introduced into the growth rate equation for this organism group (Eq 4.13) i.e.:

$$r_{Z_{HM}} = \frac{\mu_{max,HM}[H_2]}{(K_{S,HM}+[H_2])\left(1+\frac{[H^+]}{K_{I,HM}}\right)}[Z_{HM}] \qquad (4.38)$$

4.9.3 Inhibition of acetogens (process D5)

Due to the thermodynamics of the acetogenic process, the growth of acetogens decreases when the hydrogen partial pressure p_{H2} increases. This reduces the rate of propionic acid conversion to acetic acid and hydrogen. This reduction in growth rate at elevated p_{H2} already has been included in the acetogen growth process (Eq 4.11).

The inhibition constants for the above are listed in Table 4.11.

Organism group	Process	Compound	Symbol	Value	Units
Acetoclastic methanogens	D7	Hydrogen ion	$K_{I,AM}$	$1.15x10^{-6}$	mol/P
Hydrogenotrophic methanogens	D9	Hydrogen ion	$K_{I,HM}$	$530x10^{-6}$	mol/P
Acetogens	D5	Hydrogen gas	$K_{I,AC}$	$0.45x10^{-6}$	mol/P

Table 4.11 Inhibition constants for the different organism groups in anaerobic digestion

4.9.4 Gas expulsion from aqueous to head space gas phases

In the implementation above of the kinetic model in Aquasim, the exchange of gases between the aqueous and gas (head-space) phases was not specifically modelled; the dissolved and non-dissolved gases were accepted to be part of the bulk liquid and hence flow out of the digester with the effluent, which is equivalent to a zero volume head-space. For steady state conditions this is acceptable, because the molar gas composition remains constant with time. Under digester failure conditions, the molar composition of the gas phase may not remain constant with time and hence have an influence on the dissolved gas concentrations. To ensure a more realistic AD system under failure conditions, a head-space compartment was added to the model in Aquasim, with a diffusive link to the reactor aqueous phase. The dissolved gaseous compounds CO_2 (as H_2CO_3*), CH_4 and H_2 diffuse from the aqueous phase to the gas phase in the head-space, in accordance with the usual diffusion gas exchange equations (Batstone *et al.*, 2002), i.e. the gas exchange equations are applied across the diffusive link. In such an implementation, due cognizance must be taken of the different forms of the Henry's law constant and its dimensions. In Aquasim, the diffusive link is modelled as:

$$r_{gas} = K_{Lagas}(K_{cgas} \cdot C_{hsgas} - C_{disgas}) \quad \text{(mol gas/d)} \tag{4.39}$$

where:

r_{gas} = Rate of gas diffusion across head-space – bioreactor link
$K_{La\ gas}$ = Specific gas mass transfer rate (/d)
K_{cgas} = Constant for the phase change from liquid to gas
= K_{Hgas} or $1/K_{Hgas}$ depending on the form of the Henry's law constant
K_{Hgas} = ***Dimensionless*** Henry's law constant for the gas
C_{disgas} = Dissolved (aqueous) gas concentration in reactor liquid (mol/P)
C_{hsgas} = Concentration of gas in the headspace (mol/P)
p_{gas} = Partial pressure of the gas
= C_{hsgas} x RT_k
R = Universal gas constant = $8.206x10^{-2}$ (P.atm)/ (mol.K)
T_k = Temperature in Kelvin = (T in ^oC +273).

In modelling this gas exchange ammonia was omitted, because with its high pK value (9.1), negligibly little diffuses into the gas phase for pH < 8. The partial pressure of the three gases were calculated from the head-space gas concentrations (C_{hsgas}) using Dalton's law of partial pressures (p_{gas} = [C_{hsgas}] RT) and the total gas pressure in head-space (P_{tot}) is sum of the partial pressures. The vent gas flow rate from the head-space (q_{gas}) was calculated from a proportional control loop (Batstone *et al.*, 2002) with respect to atmospheric pressure (P_{atm}), which was accepted to be 101.3 kPa, viz.

$$q_{gas} = K_p \frac{(P_{tot} - P_{atm})}{P_{atm}} V_h \quad (P/d) \qquad (4.40)$$

where:

K_p = Gas vent rate constant (/d)

V_h = Volume of head space (1P for Izzett *et al.* digesters)

One constant in Eq 4.39 has an important influence on the dynamics of the head-space gas concentrations, i.e. the specific gas mass transfer rate (K_{Lagas}). If this rate is very rapid, then the head-space concentrations respond very quickly to the dissolved gas concentrations. The actual rate would be situation specific, depending on the mixing regime in the anaerobic digester, and would be faster with gas recirculation mixing than with mechanical mixing. Since no guidance in the literature could be found for this value, a fast rate of 1000 /d was selected for all K_{Lagas} so that the head-space gas concentrations rapidly respond to the dissolved gas concentrations. To provide a sense of the magnitude of this value, Musvoto *et al.* (2000a) observed K_{La} values between 200 and 600 /d for CO_2 stripping in their anaerobic digester liquor aeration batch tests. The value for this constant requires further investigation.

4.9.5 Simulating digester failure

With the model set up as described, digester failure was simulated by halving the maximum specific growth rate of the acetoclastic methanogens ($:_{max,AM}$) for three days (72 h) in the middle of a 60 day simulation. The anaerobic digester at 15 d retention time in Table 4.6 was simulated for sufficient time to ensure steady state – very low effluent SCFA concentrations and hydrogen partial pressure were obtained and the pH was about 6.9. Failure was then artificially induced by temporarily halving the $:_{max,AM}$ value for the period of 3 days, and thereafter restoring it to its original value.

Immediately after halving $:_{max,AM}$, the acetic acid concentration increased sharply to reach a maximum of 0.14 mol/P (8 400 mg HAc/P) after 15h. This increase caused the pH to decrease from 6.9 to 4.5 in 4h. The reduction in pH caused (i) the acetoclastic methanogen growth rate to reduce further, contributing to the sharp increase in acetic acid concentration and (ii) the hydrogenotrophic methanogen growth rate to reduce causing the hydrogen concentration to increase to a maximum of 0.00012 mol/P (0.24 mgH_2/P) after 22 h. The increased H_2 concentration raised the p_{H2} which caused the acidogens to produce also propionic acid, which increased from a very low concentration at around 5 h to a maximum concentration of 0.15 mol/P (11 100 mg HPr/P) at 55h. Immediately after halving $:_{max,AM}$ of the acetoclastic methanogens, their concentration decreased sharply to reach 10% of its initial value after 15h. The hydrogenotrophic methanogen organism concentration also decreased rapidly after about 4 h to less than 10% of its initial value after 40 h. Concomitantly with the decrease in methanogen biomass concentrations, the CO_2 and CH_4 gas production rates decreased rapidly, reaching 10% of their original rates at 20 and 28 h respectively. Restoring the $:_{max,AM}$ of the acetoclastic methanogens to its original rate after 72 h had no affect on the results indicating that the failure was irreversible. Also, simulating this digester failure situation with and without the head-space gas dynamics made negligibly little difference to the results.

This simulation of AD failure by halving temporarily the acetoclastic methanogen growth rate indicates that (i) the AD model correctly reflects the qualitatively observed digester failure behaviour and (ii) even a short (3 days) inhibition of these species causes irreversible

failure (pH<5.5) within 4 h. The % decrease in acetoclastic methanogen growth rate from which the digester can recover without intervention was not determined. Because the conceptual AD model (Fig 4.2) is similar to that developed for upflow anaerobic sludge bed (UASB) digesters (Sam-Soon *et al.*, 1991), the simulation model shows the same progression to failure as the lower bed volume of an UASB digester, except that in the UASB system, collapse of the methanogens does not take place because the pH is maintained above 6.6 in the high SCFA concentration region (Moosbrugger *et al.*, 1993). From the UASB digester behaviour and practical experience, anaerobic digestion failure due to a reduction in methanogen activity can be averted if the pH can be maintained above 6.6. This may require dosing lime which needs to be carefully controlled to avoid calcium carbonate precipitation (Capri and Marais, 1974). Digester failure and recovery is a dynamic modelling problem and will be examined in further research.

4.10 CONCLUSIONS

An integrated two phase (aqueous-gas) mixed weak acid/base chemistry, physical and biological processes anaerobic digester kinetic model for sewage sludge is presented. The salient features of this model are:

1. As an alternative to characterizing the sewage sludge feed into carbohydrates, proteins and lipids, as is done in IWA ADM1 (Batstone *et al.*, 2002), it is characterized in terms of total COD, its unbiodegradable particulate COD fraction (f_{PSup}), the short chain fatty acid (SCFA) COD and the CHON content of the particulate organics, i.e. X, Y, Z and A in $C_XH_YO_ZN_A$. This approach characterizes the sludge in terms of measurable parameters and allows COD, C and N mass balances to be set up over the anaerobic digestion system. With this approach, the interactions between the biological processes and weak acid/base chemistry could be correctly predicted for stable steady state operation of anaerobic digesters. While not validated for dynamic flow and load conditions, the model has the capability of being applied to such conditions.

2. The COD, C and N mass balances and continuity basis of the model fixes quantitatively, via the interrelated chemical, physical and biological processes, the relationship between all the compounds of the system so that for a given biodegradation the digester outputs (i.e. effluent COD, TKN, FSA, SCFA, H_2CO_3* Alk, pH, gaseous CO_2 and CH_4 production and partial pressures) are governed completely by the input sludge (and aqueous) characteristics. All the kinetic and stoichiometric constants in the model, except those for hydrolysis, were obtained from the literature so that model calibration reduced to determining (i) the unbiodegradable particulate COD fraction of the sewage sludge (f_{PSup}), (ii) the hydrolysis kinetics formulation and associated constants and (iii) the sewage sludge CHON composition, i.e. the X, Y, Z and A values in $C_XH_YO_ZN_A$.

3. Interactively with determining the hydrolysis kinetics ((4) below), the unbiodegradable particulate fraction of the sewage sludge was estimated at 0.32-0.36 for the sewage sludge fed to the mesophilic anaerobic digesters of Izzett *et al.* (1992) ranging over 7-20 days retention time, depending on the type of hydrolysis kinetics selected. These values are very close to the value of 0.36 determined by O'Rourke (1968) and the values estimated from a COD mass balance around the primary settling tank from typical raw and settled wastewater characteristics (0.32-0.36 for COD

removals of 40-35%).

4. Various formulations for the hydrolysis rate of sewage sludge particulate biodegradable organics were evaluated, see below. Surface mediated reaction (Contois) kinetics similar to that used by Dold *et al.* (1980) and IWA Activated Sludge Model 1 (Henze *et al.*, 1987) for slowly biodegradable organics in activated sludge systems, were selected. Once calibrated against the Izzett *et al.* (1992) data, this formulation showed the required sensitivity of gas production and unfiltered effluent COD concentration to variation in retention time, without changing the constants in the hydrolysis rate equation. In the experimental study in Chapter 2, it was also concluded that the surface reaction kinetics most accurately predict the rate of primary sewage sludge under methanogenic conditions for all hydraulic retention times and feed COD concentrations of their experimental methanogenic anaerobic digesters, further justifying the selection of surface mediated reaction (Contois) kinetics to describe the hydrolysis rate of sewage sludge particulate biodegradable organics for the UCTADM1 model.

5. From the influent COD, organic N and VSS measurements of Izzett *et al.*, the stoichiometric formulation of the influent sewage sludge was estimated to be $C_{3.4}H_7O_2N_{0.192}$. With the sludge biodegradability and hydrolysis process rate defined, to match the anaerobic digester performance data of Izzett *et al.* (1992) ranging over 7-20 days retention time, (i.e. effluent COD, TKN, FSA, SCFA, H_2CO_3* Alk, pH, gaseous CO_2 and CH_4 production and partial pressures), the sewage sludge composition was refined to $C_{3.5}H_7O_2N_{0.196}$ to conform to the COD, C and N mass balances of the model. This formulation was confirmed with primary sludge CHON composition tests, the average of which was $C_{3.65}H_7O_{1.97}N_{0.19}$. The model predicted CHON content and molar mass of the PS was therefore 95.9%, 100%, 98.5%, 94.5% and 98.7% of the measured values. This provides persuasive validation of the UCTADM1 model. For the data from Chapter 2, the sewage sludge formulation was not estimated because the CHON composition experimental results were used directly to further validate the model. The average sewage sludge formulation for the Chapter 2 ‘pure’ primary sludge feed was $C_{4.17}H_7O_{2.63}N_{0.22}$. The C, O and N content of this ‘pure’ primary sludge is higher than that of the Izzett *et al.* (1992) feed. However, Izzett *et al.* used a mixture of primary and humus sludge and hence a minor difference in composition is not unexpected.

6. Validation of the AD model under steady state conditions validates only its stoichiometry and the system rate limiting process, which is hydrolysis. However, the model, which includes the influence of high hydrogen partial pressure on the acidogenesis and acetogenesis processes, showed the expected sensitivity to a digester upset initiated by temporary inhibition of the acetoclastic methanogens, which is the usual cause in practise. The model demonstrated that even a brief inhibition of this organism group causes an irreversible failure of the digester (pH < 6.6).

The proposed surface mediated reaction (or Contois kinetic) hydrolysis rate equation reproduced the observed change in biodegradable particulate COD acidified versus retention time with the same kinetic constants. Based on the Izzett *et al.* anaerobic digester data, a Monod type hydrolysis rate equation also showed consistency of constants over 7 to 20 d retention time, but simple first order and first order specific hydrolysis rate equations yielded different rate constants at different retention times. However, by changing the

unbiodegradable particulate COD fraction of the sewage sludge (f_{PSup}) the fit of both the first order and first order specific hydrolysis rate equations to the experimental data of Izzett *et al.* (1992) could be significantly improved (with concomitant deterioration in the fit with Contois and Monod kinetics). In the study in Chapter 2 it was concluded that the first order kinetics and surface reaction kinetics most accurately predict the rate of PSS hydrolysis under methanogenic conditions for all hydraulic retention times and feed COD concentrations of the experimental methanogenic anaerobic digesters. Modelling the Chapter 2 experimental data with the unbiodegradable particulate COD fraction and hydrolysis rate constants determined in that study, and a surface mediated reaction (or Contois kinetic) hydrolysis rate equation resulted in a reasonable correlation between the experimental and simulated data. However, because of scatter in the Chapter 2 experimental data, it proved difficult to derive hydrolysis rate constants that would result in a better fit between the experimental and simulated data. Hence, the Izzet *et al.* anaerobic digester data set is too limited and the Chapter 2 data too variable to make a definitive conclusion as to which is the best equation to model the hydrolysis process, and what the best value for f_{PSup} is. Intuitively and based on its widespread application in activated sludge systems acting on the same biodegradable particulates, the surface mediated reaction (Contois) kinetics has been selected for hydrolysis.

The characterisation of sewage sludge in terms of its CHON(P) contents appears a sound approach. While testing primary sludges for the UCTADM1 model validation, a range of other sewage sludges were also tested, such as waste activated, anaerobic digested and mixtures of primary and waste activated. From the tests done to date, it seems that the CHON contents of sludges are consistent and grouped approximately in conformity with type. It appears likely, therefore, that typical CHON(P) contents of the different sludges may be selected, and that the standard characterisation tests such as COD, TKN and VSS, are sufficiently discerning and accurate for modelling AD of sewage sludges. Measurement of sewage sludge composition is continuing and its effect on digester pH and gas composition will be evaluated when more information has been collected.

The successful integration in a kinetic way of the two phase mixed weak acid/base chemistry, physical and biological processes of AD has provided a sound basis for further model development. Still to be included in the AD model in this project is biological sulphate reduction, and associated chemical and physical processes – this is addressed in Chapters 5 and 6.

The integrated physical, chemical and biological processes kinetic modelling approach, applied in this research to methanogenic anaerobic digesters, has opened the way to develop a kinetic simulation model for the entire wastewater treatment plant on a materials mass balance and continuity basis, which is the area of research under the WRC contract with UCT on the mass balances modelling (Sötemann *et al.*, 2005a – WRC Report 1338/1/05).

5 INTEGRATED CHEMICAL, PHYSICAL AND BIOLOGICAL PROCESSES MODELING – DEVELOPMENT OF A KINETIC MODEL FOR BIOLOGICAL SULPHATE REDUCTION WITH PRIMARY SEWAGE SLUDGE AS SUBSTRATE

5.1 INTRODUCTION

In Chapter 4, the development of an integrated two phase (aqueous-gas) biological, chemical and physical processes kinetic model for the methanogenic anaerobic digestion of sewage sludges (UCTADM1) has been described. To extend application of this model to biological sulphate reduction systems, the biological processes for sulphate reduction need to be integrated into UCTADM1 together with the associated chemical and physical processes in the two phases. This Chapter describes the development of the kinetic model for the biological processes for biological sulphate reduction, and associated chemical and physical processes, and integration of these with the methanogenic anaerobic digestion model developed in Chapter 4. Chapter 6 describes implementation of the model developed here in the WEST simulation platform.

5.2 EXISTING KINETIC MODELS

The approach taken to develop the kinetic model for biological sulphate reduction (BSR) systems with primary sewage sludge (PSS) was to evaluate existing kinetic models in the literature, select the most suitable and to extend/ modify/ integrate these as required. Ristow and Hansford (2001) and Hansford (2004) developed a kinetic model for BSR with PSS as substrate. In this model, the focus was on the biological processes, and the chemical and physical processes considered to be important in BSR were not explicitly included. In development of their model, Ristow and Hansford recognised that under steady state the hydrolysis of PSS was the rate limiting step. However, they noted that for this process a variety of kinetic rate formulations and data incompatibilities were evident in the literature. From the available information they were not able to determine the most appropriate kinetic rate formulation for this crucial process. Due to these deficiencies and limitations, in Chapter 2 (detailed by Ristow *et al.*, 2005a) an extensive investigation was undertaken to describe and model the PSS hydrolysis step, under methanogenic, sulphidogenic and acidogenic conditions. It was concluded *inter alia* that BSR does not appear to influence the rate of PSS hydrolysis (implying that methanogenic rate formulations and rate constants can be applied under BSR conditions also) and that for simple steady state models first order kinetics (which analytically are simpler to apply) for PSS hydrolysis are adequate, but for more extensive kinetic models surface saturation (Contois) kinetics would be more suitable (and are followed in Chapter 4 and Sötemann *et al.*, 2005a, see below). In Chapter 2, pH was included only empirically in the developed first order kinetic formulation, by adjusting the value for the rate constant according to pH and the kinetics for the reactions subsequent to the hydrolysis process were not considered.

The IWA task group for mathematical modelling of anaerobic digestion processes developed Anaerobic Digestion Model No. 1 (ADM1, Batstone *et al.*, 2002). In this model the substrate, in this case PSS is characterised into carbohydrates, lipids and proteins. For PSS, such

measurements are not routinely available. In contrast, in the model developed by Van Rensburg *et al.* (2001), and extended and modified in Chapter 4 for methanogenic anaerobic digestion of sewage sludges, the sludge is characterised with the usual COD, TKN and VSS measurements and the carbon, hydrogen, oxygen and nitrogen (CHON) composition which can be readily derived from the listed measurements and model application, or by direct elemental analysis. In Chapter 4 the biological kinetic processes for methanogenic anaerobic digestion (AD) were integrated into a two phase (aqueous/gas) subset of the three phase mixed weak acid / base chemistry kinetic model of Musvoto *et al.* (1997). The model was calibrated and validated with data from the laboratory mesophilic anaerobic digesters of Izzett *et al.* (1992). The sewage sludge COD was found to be 32-36% unbiodegradable (depending on the kinetic formulation selected for the hydrolysis process) and to have a $C_{3.5}H_7O_2N_{0.196}$ composition. For the selected hydrolysis kinetics (surface mediated reaction (Contois)), with a single set of kinetic and stoichiometric constants, reasonable correlation was obtained between predicted and measured results for all retention times for (i) COD (ii) free and saline ammonia (FSA), (iii) short chain fatty acids (SCFA), (iv) $H_2CO_3^*$ alkalinity and (v) pH of the effluent stream, and (vi) CO_2 and (vii) CH_4 gases in the gas stream. The measured composition of PSS from two Cape Town wastewater treatment plants ranged between $C_{3.38}H_7O_{1.91}N_{0.21}$ and $C_{3.91}H_7O_{2.04}N_{0.16}$. The predicted composition based on mass balances in model application was within 5% of the average measured composition, providing persuasive validation of the model. The model also was applied also to the data collected in Chapter 2, and again reasonable correlation was obtained between predicted and measured data, further validating the model.

The kinetic model described in Chapter 4 was to be extended to include BSR with PSS as substrate. This required development of the kinetics and stoichiometry for the biological, chemical and physical processes in BSR in two phases (aqueous/gas), and integration of these with UCTADM1, taking due cognizance of any interactions introduced with the integration. Essentially, this would result in a two phase biological, chemical and physical processes model for the AD of PSS, with competitive methanogenesis and sulphidogenesis. This development is described below.

5.3 DEVELOPMENT OF A KINETIC MODEL FOR BSR WITH PSS AS SUBSTRATE

The kinetic model for BSR with PSS was developed and integrated into the UCTADM1 model in three parts. Part 1 developed the biological processes: For the biologically mediated processes, the PSS first requires hydrolysis / solubilisation (usually the rate limiting step) and acidification, mediated by the acidogenic group of organisms, in common with sewage sludge methanogenic AD systems described in Chapter 4. The products of these processes, the short chain fatty acids (SCFA), can then enter into the methanogenic or sulphate reduction processes, which operate in competition. One end product of BSR is sulphide, which is inhibitory to the methanogens, requiring that this inhibition be included.

Part 2 considered the aqueous chemistry and physical processes. The background acid / base chemistry was included because the biological processes consume and produce significant acid/base species, e.g. SCFA, sulphide and sulphate. Consumption and production of acid/base species will influence the pH established in the reactor, which in turn can influence the biologically mediated processes. Hence, pH needed to be incorporated directly into the model, as a model predictive parameter, and its interaction with the biological processes modelled. Some of the end products have gaseous equilibria (sulphide, carbon dioxide,

ammonia and methane); so that these physical processes also required inclusion (the third solid phase was not included at this stage).

Finally, Part 3 considered the integration of the BSR aqueous chemistry and physical processes with the biological processes, and these processes with UCTADM1.

5.3.1 Biomass Population Biology

The approach of Kalyuzhnyi *et al.* (1998) formed the basis for the kinetic model for the biology of sulphate reducing bacteria (SRB). Kalyuzhnyi *et al.* (1998) described an anaerobic reaction sequence by which substrates are transformed by 9 trophic groups of bacteria:

(i)	Fermentative bacteria	(Sugars → Acetate)
(ii)	Butyrate degrading acetogenic bacteria	(Butyrate → Acetate)
(iii)	Butyrate degrading SRB	(Buryrate → Acetate & H_2S)
(iv)	Propionate degrading acetogenic bacteria	(Propionate → Acetate)
(v)	Propionate degrading SRB	(Propionate → Acetate & H_2S)
(vi)	Acetotrophic methanogenic bacteria	(Acetate → Methane & CO_2)
(vii)	Acetotrophic SRB	(Acetate → H_2S & CO_2)
(viii)	Hydrogenotrophic methanogenic bacteria	(H_2 & CO_2 → Methane)
(ix)	Hydrogenotrophic SRB	(H_2 → H_2S)

Of the 9 bacterial groups, of interest here are the four sulphate reducing bacteria (SRB) groups only (i.e. iii, v, vii and ix), since BSR was to be integrated with the existing methanogenic and acetogenic UCTADM1 model described in Chapter 4, which already explicitly includes (i), (iv) and (viii). Butyrate degrading acetogenic (ii) and SRB (iii) groups were not incorporated into the model, as butyrate is not commonly encountered in significant concentrations in sewage sludge digestion systems. Accordingly, the process stoichiometry and kinetics for the four SRB groups were considered, for both growth and decay.

5.3.1.1 Growth Stoichiometry

For each SRB group, by following the procedure described in Chapter 4 and taking the catabolic and anabolic stoichiometric reactions and adding these, the stoichiometry for the growth bioprocesses could be determined (Table 5.1). For example, for the propionate degrading SRBs (Z_{PS}), the catabolic substrate utilisation is (Kalyuzhnyi *et al.*, 1998):

$$C_2H_5COOH + \frac{3}{4}SO_4^{2-} + \frac{3}{2}H^+ \rightarrow CH_3COOH + \frac{3}{4}H_2S + CO_2 + H_2O \qquad (5.1)$$

For the anabolic organism growth of Z_{PS}, accepting the stoichiometric composition for biomass as $C_5H_7O_2N$ (Chapter 4):

$$3C_2H_5COOH + CO_2 + 2NH_4^+ \rightarrow 2C_5H_7O_2N + 4H_2O + H_2 + 2H^+ \qquad (5.2)$$

Adding Eqs 5.1 and 5.2 and solving in terms of the true yield Y_{PS} (Chapter 4), gives the growth stoichiometry listed in Table 5.1, Process S1 (H_2O excluded from Table 5.1, but implicit from the stoichiometry). Similarly, the growth stoichiometries were derived for the other two SRB groups, Acetotrophic SRB (Z_{AS}, Process S3) and Hydrogenotrophic SRB (Z_{HS}, Process S5).

Table 5.1: Petersen matrix of the biological kinetic model for sulphate reducing bacteria (SRB's).

No	Process↓ Compound→	NH_4^+	NH3 dis.	$H_2CO_3^*$	H^+	HAc	HPr	H_2 dslvd	SO_4^{2-}	H_2S	S_{bp}	Z_{PS}	Z_{AS}	Z_{HS}	
S1	Growth of propionate degrading SRB	-1		$\left(\frac{1}{Y_{PS}}-2\right)$	$\left(\frac{13}{4}-\frac{3}{2Y_{PS}}\right)$	$\left(\frac{1}{Y_{PS}}-\frac{3}{2}\right)$	$-\left(\frac{1}{Y_{PS}}\right)$	$\frac{1}{2}$	$-\left(\frac{3}{4Y_{PS}}-\frac{9}{8}\right)$	$\left(\frac{3}{4Y_{PS}}-\frac{9}{8}\right)$		1			$\frac{\mu_{max}[HPr]}{K_S+[HPr]}\left[1-\frac{[H_2S]}{K_I}\right]\left[\frac{[SO_4^{2-}]}{K_N+[SO_4^{2-}]}\right]Z$
S2	Endogenous decay of propionate degrading SRB		0.761[2]	0.7335[2]							160[2]	-1			$b_{PS}[Z_{PS}]$
S3	Growth of Acetotrophic SRB	-1		$\left(\frac{2}{Y_{AS}}-5\right)$	$\left(6-\frac{2}{Y_{AS}}\right)$	$-\left(\frac{1}{Y_{AS}}\right)$			$-\left(\frac{1}{Y_{AS}}-\frac{5}{2}\right)$	$\left(\frac{1}{Y_{AS}}-\frac{5}{2}\right)$			1		$\frac{\mu_{max}[HAc]}{K_S+[HAc]}\left[1-\frac{[H_2S]}{K_I}\right]\left[\frac{[SO_4^{2-}]}{K_N+[SO_4^{2-}]}\right]Z_S$
S4	Endogenous decay of Acetotrophic SRB		0.761[2]	0.7335[2]							160[2]		-1		$b_{AS}[Z_{AS}]$
S5	Growth of hydrogenotrophic SRB	-1		-5	$\left(6-\frac{1}{2Y_{HS}}\right)$			$-\left(\frac{1}{Y_{HS}}\right)$	$-\left(\frac{1}{4Y_{HS}}-\frac{5}{2}\right)$	$\left(\frac{1}{4Y_{HS}}-\frac{5}{2}\right)$				1	$\frac{\mu_{max}[H_2]}{K_S+[H_2]}\left[1-\frac{[H_2S]}{K_I}\right]\left[\frac{[SO_4^{2-}]}{K_N+[SO_4^{2-}]}\right]Z_{HS}$
S6	Endogenous decay of hydrogenotrophic SRB		0.761[2]	0.7335[2]							160[2]			-1	$b_{HS}[Z_{HS}]$
		mol/ℓ	**mol/ℓ**	**mol/ℓ**	**mol/ℓ**	**mol/ℓ**	**mol/ℓ**	**mol/ℓ**	**mol/ℓ**	**mol/ℓ**	**g cod/ℓ[1]**	**mol/ℓ**			

[1]See Table 5.3 for units in mol/ℓ

[2]This is for the formulation for biodegradable particulate substrate $S_{bp} = C_{3.5}H_7O_2N_{0.196}$; see Table 5.3 for the generalised formulation for $S_{bp} = C_XH_YO_ZN_A$

Zj = SRB j concentration; Y = true organism yield; b = specific decay rate; rate symbols defined in Eq 5.5. Subscripts PS, AS and HS = propionate degrading, acetotrophic and hydrogenotrophic SRB respectively. Compound and process numbering system follows Chapter 4 and Sötemann *et al.* (2005a).

5.3.1.2 Endogenous Decay Stoichiometry

It was assumed that organism death/decay for the SRB groups is the same as for the bacterial groups in the UCTADM1 model (Chapter 4), and therefore the same approach was followed here. In UCTADM1 and in this SRB model, it was assumed that the organism mass is represented by the $C_5H_7O_2N$ formulation. In endogenous decay, this organism mass transforms to biodegradable particulate COD (S_{bp}); due to the low anaerobic organism yield and endogenous decay rates, it was accepted that generation of endogenous residue was small and could be neglected. Initially it was accepted that the S_{bp} formulation is $C_{3.5}H_7O_2N_{0.196}$, as determined by Sötemann *et al.* (2005a), and described in Chapter 4. The COD/VSS ratio for $C_5H_7O_2N$ = 1.413 mg cod/mg VSS and 1 mol $C_5H_7O_2N$ ~ 160 mg cod. Therefore, 160 g organism COD is 102.17 gVSS organisms which equates to 1.219 mol $C_{3.5}H_7O_2N_{0.196}$ (COD/VSS ratio of $C_{3.5}H_7O_2N_{0.196}$ = 1.566 mg cod/mgVSS). Accordingly, endogenous decay of the organisms was represented by the following equation:

$$C_5H_7O_2N + 1.905H_2O \rightarrow 1.219C_{3.5}H_7O_2N_{0.196} + 0.7335CO_2 + 0.761NH_3 \quad (5.3)$$

The stoichiometry for endogenous decay was taken directly from Eq 5.3, see Tables 5.1 and 5.2.

Table 5.2: Stoichiometry for the endogenous respiration of all organism groups (Z_j), with biodegradable particulate COD (S_{bp}) formulation as $C_{3.5}H_7O_2N_{0.196}$.

Z_j mol	H_2CO_3* mol	NH_3 mol	S_{bp}	
			g COD	Mol
-1	0.7335	0.761	160	1.219

If the generalised formulation for S_{bp} of $C_XH_YO_ZN_A$ is accepted, then the stoichiometry for endogenous decay can be extracted directly from Chapter 4 (Sötemann *et al.*, 2005a), see Table 5.3.

Table 5.3: Stoichiometry for the endogenous respiration of all organism groups (Zj), with biodegradable particulate COD (Sbp) formulation as CXHYOZNA

NH_3 mol	$H_2CO_3^*$ mol	S_{bp} mol	Z_j mol
$\frac{Y+4X-2Z-23A}{Y+4X-2Z-3A}$	$\frac{5(Y-2Z-3A)}{Y+4X-2Z-3A}$	$\frac{20}{Y+4X-2Z-3A}$	-1

5.3.1.3 Growth Kinetic Rates

For the growth of SRB the principles of the kinetic rate descriptions were taken from Kalyuzhnyi *et al.* (1998), who modelled the bacterial growth of each SRB group using Monod kinetics, with simultaneous inhibition by pH and undissociated H_2S. The undissociated H_2S inhibition was formulated as first order for all bacterial groups. Thus, the

specific growth rate (μ_j) equation for the SRB groups was expressed by Kalyuzhnyi *et al.* (1998) as:

$$\mu_j = \mu_{max,j} \frac{[S_i]F(pH)}{K_{Sj} + [S_i]} \left[1 - \left(\frac{[H_2S]_f}{K_{I,j}} \right) \right] \left(\frac{[SO_4^{2-}]}{K_n + [SO_4^{2-}]} \right) \quad (5.4)$$

Where:

F (pH) = pH inhibition function
$\mu_{max,j}$ = Maximum specific growth rate for SRB group j
$[S_i]$ = Organic substrate i concentration
K_{Sj} = Monod saturation constant for organic substrate
$K_{I,j}$ = Inhibition constant for undissociated hydrogen sulphide $[H_2S]$
K_n = Monod saturation constant for sulphate $[SO_4^{2-}]$

In the H_2S inhibition term in Eq 5.4, $[H_2S]$ must be less than $K_{I,j}$ otherwise the inhibition term becomes negative; if this is encountered in model application the alternative non-competitive inhibition kinetics (Chapter 4; Sötemann *et al.*, 2005a) will be considered. No reference is made in Kalyuzhnyi *et al.* (1998) to the exact pH inhibition formulation for F(pH) that was used in their model. Therefore, pH inhibition was excluded here initially. If required, when the SRB is integrated in the UCTADM1 model the pH inhibition function in the UCTADM1 model (non-competitive inhibition) could be used for the SRB's also. Hence, the SRB growth rate used was as given by Eq 5.4, but with F(pH) excluded (Table 5.1). The approach to formulating the kinetic rates of Kalyuzhnyi *et al.* (1998) is the same as that used in the UCTADM1 model (Chapter 4). Hence, only the H_2S inhibition term had to be added to the existing kinetic rate equations for the acidogenic, acetogenic and methanogenic bacterial groups in the UCTADM1 model when BSR was integrated with the UCT AD model.

5.3.1.4 Endogenous Decay Kinetic Rates

Bacterial decay both in Kalyuzhnyi *et al.* (1998) and Chapter 4 (Sötemann *et al.*, 2005) is described by first order kinetics, and hence this approach was also followed here. The specific rate for bacterial decay is thus = $b_j[X_j]$ where b_j is the specific decay constant for the bacterial population concerned, X_j, Table 5.1.

5.3.1.5 Values for Constants

Values for the stoichiometric and kinetic constants for the SRBs were taken from Kalyuzhnyi *et al.* (1998), and are listed in Table 5.4.

Table 5.4: Values for SRB stoichiometric and kinetic constants used in the BSR kinetic model (from Kalyuzhnyi *et al.*, 1998).

	μ_{max}	**K_S[1]**	**K_N[1]**	**K_I[1]**	**Y[1]**	**b**
	/d	g cod/ℓ	G SO_4^{2-}	G S/ℓ	G VSS/g cod	/d
Propionate degrading SRB	0.583	0.295	0.0074	0.185	0.027	0.0185
Acetotrophic SRB	0.612	0.024	0.1920	0.164	0.033	0.0275
Hydrogenotrophic SRB	2.8	7E-05	0.1920	0.550	0.050	0.0600

[1]Constants to be converted to mole units on integration with UCTADM1, to ensure consistency in units.

5.3.2 Aqueous chemistry and physical processes

The BSR processes described above both produce and consume weak acid / base species, and hence these and the associated weak acid / base chemistry required inclusion in developing a kinetic model for BSR. Further, the compound H_2S is produced and the compound H_2CO_3* is produced as well as consumed. Both these compounds have physical gas exchange processes with the atmosphere, and therefore these processes were also included in the model.

5.3.2.1 Aqueous Chemistry

The following acid / base systems were identified as having direct relevance to BSR:

1.	Water	:	H^+ / OH^-
2.	Ammonia	:	NH_3 / NH_4^+
3.	Carbonate	:	$H_2CO_3^*$ / HCO_3^- / CO_3^{2-}
4.	Acetate	:	HAc / Ac^-
5.	Propionate	:	HPr / Pr^-
6.	Sulphate	:	H_2SO_4 / HSO_4^- / SO_4^{2-}
7.	Sulphide	:	H_2S / HS^- / S^{2-}

Of these acid / base systems, 1 to 5 already have been included in the methanogenic UCTADM1 model, whereas 6 and 7 have not (Chapter 4; Sötemann *et al.*, 2005). Accordingly, for 1 to 4 the compounds and processes were taken unmodified from Table 1 in Mosvuto *et al.* (1997) and for 5 (propionate) this was taken unmodified from Table 4.2 in Chapter 4. For 6 (sulphate) the dissociation reactions are as follows:

$$1) \quad H_2SO_4 \Leftrightarrow HSO_4^- + H^+ \ (pK_{H2SO4\,/\,HSO4} \approx 0) \tag{5.5}$$

$$2) \quad HSO_4^- \Leftrightarrow SO_4^{2-} + H^+ \ (pK_{HSO4\,/\,SO4} \approx 1.99) \tag{5.6}$$

Sulphuric acid acts as a strong acid, and since the pK values for both the equilibria are so low ($\approx$0 and 1.99) and the pH range of the systems to be modelled is unlikely to be $< \approx$ 4, it could be accepted in the kinetic modelling that the only sulphate system species of any consequence is SO_4^{2-}. However, in the AMD to be treated, the pH values may be very low (pH $\approx$ 2-5). This will influence the species distribution of the equilibrium Eq 5.6 in the influent, and hence this equilibrium needed to be included in the model. Thus, the sulphate acid/base was treated as a monoprotic acid/base, with the single equilibrium reaction Eq 5.6. To model this chemical dissociation equilibrium reaction, the approach developed by Musvoto *et al.* (1997) was followed, viz. the kinetics of the forward and reverse dissociation reactions were modelled. This required the inclusion of 2 new processes (C48 for forward dissociation, C49 for reverse dissociation), and two new compounds, HSO_4^- (C30) and SO_4^{2-} (C31), see Table 5.5.

Table 5.5: Petersen Matrix representation of the HSO_4^- acid / base dissociation processes.

↓No	↓Process — Number→ / Compound→	C7 H^+	C30 HSO_4^-	C31 SO_4^{2-}	↓Process rates
C48	Forward dissociation HSO_4^-	+1	-1	+1	$K'_{fHSO4}[HSO_4^-]$
C49	Reverse dissociation HSO_4^-	-1	+1	-1	$K'_{rHSO4}[SO_4^{2-}][H^+]$
		mol/ℓ	mol/ℓ	mol/ℓ	

For 7 (sulphide) the dissociation reactions are:

$$1) \qquad H_2S \Leftrightarrow HS^- + H^+ \ (pK_{H2S\,/\,HS} \approx 7.1) \tag{5.7}$$

$$2) \qquad HS^- \Leftrightarrow S^{2-} + H^+ \ (pK_{HS\,/\,S} \approx 17.4) \tag{5.8}$$

Since the $pK_{H2S\,/\,HS}$ is high (i.e. S^{2-} acts as a strong base) and the pH range of the systems to be modelled is unlikely to be $> \approx 10$, the sulphide acid/base system could be accepted to act as a monoprotic acid/base in the kinetic model with Eq 5.7 only. Again, the approach developed by Musvoto *et al.* (1997) for acid/base modelling was accepted. This required the inclusion of 2 new processes (C50 for the forward dissociation, C51 for the reverse dissociation), and two new compounds, H_2S (C32) and HS^- (C33), see Table 5.6.

Table 5.6: Petersen Matrix representation of the H_2S acid / base dissociation processes.

↓No	↓Process Number→ Compound→	C7 H^+	C32 H_2S	C33 HS^-	↓Process rates
C50	Forward dissociation H_2S	+1	-1	+1	$K'_{fH2S}[H_2S]$
C51	Reverse dissociation H_2S	-1	+1	-1	$K'_{rH2S}[HS^-][H^+]$
		mol/ℓ	mol/ℓ	mol/ℓ	

In Tables 5.5 and 5.6, from Musvoto *et al.* (1997) K'_r was given a very high value (of the order 10^7 to 10^{15} with time units dependent on the integration period), the exact value depending on the stability of the solution procedure. The value for K'_f was then determined from the relationship with the appropriate equilibrium constant pK. This ensured that the dissociation reactions were effectively instantaneous, and that the concentrations of the species established were the equilibrium concentrations.

The phosphate weak acid/base system was not included in the stoichiometry for the SRB growth and decay processes (Tables 5.1, 5.2 and 5.3), but is included in the weak acid/base chemistry model of Musvoto *et al.* (1997). This weak acid/base system also required inclusion in the BSR model, since this system may impact on the pH through buffering type effects depending on its' total species concentration. The kinetics and stoichiometry for this system were taken directly from Musvoto *et al.* Including the phosphate weak acid/base system chemistry may require that the biological processes kinetic model (Table 5.1) be revised to include uptake of P for growth of SRB and release of P in death of these organisms. This will be evaluated in model application and validation.

In the kinetic model developed for BSR, mineral precipitation reactions (i.e. the third solid phase) have not been included at this stage. Hence, ion paring reactions which directly impact the precipitation (Musvoto *et al.*, 1997) also have not included.

5.3.2.2 Physical Processes

In BSR the compound H_2S is produced and the compound $H_2CO_3^*$ is produced and consumed. The weak acid/base species NH_3 is present and involved in the biological processes. All these compounds have physical gas exchange processes with the atmosphere in the reactor, and therefore these processes were included:

1. $H_2CO_3^*$ $\Leftrightarrow$ $CO_2(g)$ exchange, where $H_2CO_3^* = CO_2(aq) + H_2CO_3$ (5.9)
2. $NH_3(aq)$ $\Leftrightarrow$ $NH_3(g)$ exchange (5.10)
3. $H_2S(aq)$ $\Leftrightarrow$ $H_2S(g)$ exchange (5.11)

For gas exchange 1. (CO_2), this had been included in the UCTADM1 model (Chapter 4, Table 4.2) and could be taken unmodified from this model, i.e. physical processes for dissolution (P6) and expulsion (P7), and associated compounds $CO_2(g)$ (P1) and $H_2CO_3^*$ (C3). For gas exchange 2. (NH_3), in the UCTADM1 model it was accepted that the atmosphere acts as an infinite sink for NH_3, and hence only gas expulsion required inclusion. This was accepted for the BSR model also, and hence the single expulsion process (P8) was included, with associated compound $NH_3(aq)$ (C2 from weak acid / base chemistry), and could be taken unmodified from Chapter 4, Table 4.2.

For gas exchange 3. (H_2S), this is not included in any of the models developed to date and hence required inclusion. Either of the approaches for CO_2 or NH_3 could have been followed. However, it was considered prudent to follow the approach for CO_2 and include both expulsion and dissolution reactions, as the atmosphere in the sulphate reducing bioreactor may develop significant sulphide gas concentrations, i.e. the atmosphere cannot be considered as an infinite sink. This required the inclusion of 2 new processes (P12 for H_2S dissolution and P13 for H_2S expulsion), and two new compounds, $H_2S(aq)$(C32) and $H_2S(g)$(P5), see Table 5.7.

In Table 5.7, K'_{rH2Sg} equals the K'_{La_H2S} for H_2S, which possibly could be linked to the K_{La_O2} for oxygen, through the proportionality of the diffusivities for O_2 and H_2S (Chapter 4, Sötemann *et al.*, 2005a, Musvoto *et al.*, 1997). Even though BSR systems are not aerated and significant O_2 is not present or input (and hence the actual K_{La_O2} is zero), linking the K_{La_H2S} to K_{La_O2} would be advantageous because this indirectly links the K_{La} values for CO_2 and H_2S. The requirement to link the K_{La} of a gas to that of O_2 as a reference gas is that the dimensionless Henry's law constant of the gas > 0.55; for H_2S, the Henry's law constant is 40.9 to 0.41. Thus, a strong possibility exists that the K_{LA} for H_2S can be linked in a fixed relationship to the K_{La} for O_2. In model application to BSR systems, the K_{La_O2} is calibrated which sets the values for K_{La_CO2} and K_{La_H2S}, but the system is not aerated with air (aeration process excluded, or switched off). This option will be explored in model application and validation.

Table 5.7: Petersen Matrix representation of the H_2S exchange physical processes.

↓No	↓Process Number→ Compound→	C32 H_2S dslvd	P5 $H_2S(g)$ Gas	↓Process rates
P12	Dissolution of H_2S gas	+1	-1	$K'_{rH2Sg}(\rho_{H2S})(K_{H2S})$
P13	Expulsion of H_2S gas	-1	+1	$K'_{rH2Sg}[H_2S]$
		mol/ℓ	mol/ℓ	

Following the approach in UCTADM1, since H_2 exchange occurs at an inter-species level, it was considered as a dissolved compound (Chapter 4).

5.3.3 Integrating aqueous chemistry and physical processes with biological processes

In the descriptions above, (i) a mathematical model has been developed describing the stoichiometry and kinetics of the biological processes directly involved with BSR (Table 5.1); (ii) the compounds associated with the aqueous chemical and the physical processes have been identified; and (iii) the kinetics and stoichiometry for the new aqueous chemistry and physical processes introduced by BSR have been developed (Tables 5.5, 5.6 and 5.7). It remains for these various processes to be combined and integrated with the UCTADM1 model, to give an integrated kinetic model for BSR systems. This integration was done to give two model types:

1. BSR as the "sole" biological processes consuming the short-chain fatty acids (SCFA) and H_2 substrates (i.e. methanogenesis excluded), and
2. both BSR and methanogenesis are present in competition for the SCFA and H_2 substrates.

In both model types the substrate source is PSS, and hence biological hydrolysis and acidification of the PSS by the acidogens will require inclusion. This Section considers aspects of the integration to develop both model types.

5.3.3.1 Aqueous chemistry

In both model types the chemical and physical processes are common. For the aqueous acid/base chemistry, the relevant processes were extracted from the various sources as described above (ammonia, carbonate, phosphate, acetate, water from Table 1 in Musvoto *et al.*, 1997; propionate from Table 4.2 in Chapter 4; sulphate and sulphide from Tables 5.5 and 5.6 respectively here), and are summarised in Table 5.8.

Table 5.8: Processes and compounds for acid/base chemistry for inclusion in kinetic models for biological sulphate reduction.

Acid/base	Compounds	Processes		Source
Ammonia	C1: NH_4^+ C2: NH_3	C1	FD of NH_4^+	Musvoto *et al.* (1997), Table 1
		C2	RD of NH_4^+	
Carbonate:	C3: $H_2CO_3^*$ C4: HCO_3^- C5: CO_3^{2-}	C3	FD of $H_2CO_3^*$	Musvoto *et al.* (1997), Table 1
		C4	RD of $H_2CO_3^*$	
		C5	FD of HCO_3^-	
		C6	RD of HCO_3^-	
Phosphate	C9: $H_3PO_4^-$ C10: $H_2PO_4^-$ C11: HPO_4^2 C12: PO_4^{3-}	C9	FD of H_3PO_4	Musvoto *et al.* (1997), Table 1
		C10	RD of H_3PO_4	
		C11	FD of $H_2PO_4^-$	
		C12	RD of $H_2PO_4^-$	
		C13	FD of HPO_4^{2-}	
		C14	RD of HPO_4^{2-}	
Acetate	C13: HAc C14: Ac^-	C15	FD of HAc	Musvoto *et al.* (1997), Table 1
		C16	RD of HAc	
Water	C7: H^+ C8: OH^-	C17	FD of water	Musvoto *et al.* (1997), Table 1
		C18	RD of water	
Propionate	C28: HPr C29: Pr^-	C46	FD of HPr	Sötemann *et al.* (2005a), Table
		C47	RD of HPr	
Sulphate	C30: HSO_4^- C31: SO_4^{2-}	C48	FD of HSO_4^-	Table 5.5
		C49	RD of HSO_4^-	
Sulphide	C32: H_2S C33: HS^-	C50	FD of H_2S	Table 5.6
		C51	RD of H_2S	

FD = forward dissociation RD = reverse dissociation

In the kinetic model to be developed for BSR, mineral precipitation reactions were not being considered at this stage. Hence, ion pairing reactions were not included. If required these can be incorporated readily, by following the approach of Musvoto *et al.* (2000).

5.3.3.2 Physical processes

For the physical gas exchange processes, for both model types these were extracted from the various sources described above (carbon dioxide and ammonia from Table 4.2 in Chapter 4; sulphide from Table 5.7 here), and are summarised in Table 5.9. In both types of kinetic models, H_2 is both produced and consumed. Thus, gas exchange for this compound requires consideration. Sötemann *et al.* (2005a) note that although H_2 is very insoluble, it is utilised at an inter-species level, and so cannot be transferred to the gas phase. Hence, in the methanogenic anaerobic digestion model (Chapter 4), H_2 was modelled as a dissolved species, but because it is utilised so rapidly and at an inter-species level, its' residual concentration is small. Accordingly, Sötemann *et al.* noted that from a gas production perspective it can be ignored and hence can be treated as a dissolved species. This approach will be followed here also.

When methanogenesis was included (model Type 2), then the approach described in Chapter 4 (Sötemann *et al.*, 2005a) to modelling methane was followed, in which methane was considered as very insoluble and, since it is not utilised in any of the processes, needed only to be included as a gas phase compound (i.e. methane is generated directly as a gas).

Table 5.9: Processes and compounds for physical gas exchange processes for inclusion in kinetic models for biological sulphate reduction.

Gaseous system	Compounds	Processes		Source
Carbon dioxide	C3: $H_2CO_3^*$ P1: $CO_2(g)$	P6	Dissolution of CO_2 gas	Sötemann *et al.* (2000a), Table 2 Table 4.2
		P7	Expulsion of CO_2 gas	
Ammonia	C2: NH_3	P8	Expulsion of NH_3 gas	Sötemann *et al.* (2000a), Table 2 Table 4.2
Sulphide	C32: H_2S C33: $H_2S(g)$	P12	Dissolution of H_2S gas	Table 5.7
		P13	Expulsion of H_2S gas	

Although Musvoto *et al.* (2000) developed the kinetics for precipitation of minerals, in the BSR kinetic models being developed these processes were not being considered at this stage. If required, mineral precipitation can be included relatively simply by following the approach developed by Musvoto *et al.* Should mineral precipitation be included, the sulphide minerals will require attention. Also, ion pairing effects (5.3.3.1 above) will require inclusion, with attention paid to sulphide ion pairs.

5.3.3.3 Biological processes

The kinetics and stoichiometry for BSR with PSS substrate have been developed. These need to be integrated with the aqueous and physical processes above, to give an integrated kinetic model for BSR. As described above, this integration can be in two forms: To develop a two phase (aqueous-gas) chemical, physical and biological processes kinetic model with (1) biological sulphate reduction as the "sole" biological processes consuming the short-chain fatty acids (SCFA) and H_2 substrates, and (2) both biological sulphate reduction and methanogenesis are present in competition for the SCFA and H_2 substrates. In both types of models, the substrate source being considered is PSS, and hence biological hydrolysis and acidification of the PSS by the acidogens will require inclusion in both model types.

For the Type 1 model, since the substrate being considered is PSS, the bioprocesses generating the substrates for BSR need to be included. These were taken from UCTADM1 (acidogens – Processes D1 to D4; acetogens – processes D5 and D6; Tables 4.2, 4.3 and 4.4 and Eqs 4.8 to 4.11 and 4.14 in Chapter 4). These were combined with the SRB bioprocesses developed above and listed in Table 5.1 (propionate consuming SRB, processes S1 and S2; acetotrophic SRB, processes S3 and S4 and hydrogenotrophic SRB, processes S5 and S6). These processes are summarised in Table 5.10. Integrating these bioprocesses with the chemical and physical processes gave a "stand alone" integrated two phase chemical, physical and biological processes model for BSR with PSS as substrate.

For the Type 2 model, additionally to the above the acetotrophic(clastic) and hydrogenotrophic methanogen associated processes required inclusion. These were extracted from UCTADM1 (acetotrophic(clastic) methanogens – Processes D7 to D8; hydrogenotrophic methanogen – processes D9 and D10; Tables 4.2, 4.3 and 4.4 and Eqs 4.12 to 4.13 in Chapter 4), as summarised in Table 5.11. Integrating these bioprocesses with the Type 1 model above gave a complete two phase chemical, physical and biological processes kinetic model for competitive methanogenic and sulphidogenic anaerobic digestion with PSS

as substrate.

Table 5.10: Processes and compounds for biologically mediated processes for inclusion in kinetic models for biological sulphate reduction.

Organism Group	**Compounds**	**Processes**		**Source**
Acidogens	D1: $C_XH_YO_ZN_A$ (S_{bp}) D2: $C_6H_{12}O_6$ (S_{bsf})	D1	Hydrolysis	Sötemann *et al.* (2005a), Table 2 Tables 4.2, 4.3 & 4.4
	C1: NH_4^+ C3: $H_2CO_3^*$ C7: H^+ C13: HAc D2: $C_6H_{12}O_6$ (S_{bsf}) D3: H_2 D4: Z_{AD}	D2	Acidogenesis (low pH_2)	
	C1: NH_4^+ C3: $H_2CO_3^*$ C7: H^+ C13: HAc C28: HPr D2: $C_6H_{12}O_6$ (S_{bsf}) D3: H_2 D4: Z_{AD}	D3	Acidogenesis (high pH_2)	
	C2: NH_3 C3: $H_2CO_3^*$ D1: $C_XH_YO_ZN_A$ (S_{bp}) D4: Z_{AD}	D4	Acidogen endogenous decay	
Acetogens	C1: NH_4^+ C3: $H_2CO_3^*$ C7: H^+ C13: HAc C28: HPr D3: H_2 D5: Z_{AC}	D5	Acetogenesis	Sötemann *et al.* (2005a), Table 2 Tables 4.2, 4.3 & 4.4
	C2: NH_3 C3: $H_2CO_3^*$ D1: $C_XH_YO_ZN_A$ (S_{bp}) D4: Z_{AC}	D6	Acetogen endogenous decay	
Propionate SRB	C1: NH_4^+ C3: $H_2CO_3^*$ C7: H^+ C13: HAc C28: HPr D3: H_2 C31: SO_4^{2-} C32: H_2S S1: Z_{PS}	S1	Growth of propionate SRB	Table 5.1
	C2: NH_3 C3: $H_2CO_3^*$ D1: $C_XH_YO_ZN_A$ (S_{bp}) S1: Z_{PS}	S2	Propionate SRB endogenous decay	

Acetotrophic SRB	C1: NH_4^+ C3: $H_2CO_3^*$ C7: H^+ C13: HAc C31: SO_4^{2-} C32: H_2S S1: Z_{AS}	S3	Growth of acetotrophic SRB	Table 5.1
	C2: NH_3 C3: $H_2CO_3^*$ D1: $C_XH_YO_ZN_A$ (S_{bp}) S1: Z_{AS}	S4	Acetotrophic SRB endogenous decay	
Hydrogeno-trophic SRB	C1: NH_4^+ C3: $H_2CO_3^*$ C7: H^+ D3: H_2 C31: SO_4^{2-} C32: H_2S S1: Z_{HS}	S5	Growth of hydrogenotrophic SRB	Table 5.1
	C2: NH_3 C3: $H_2CO_3^*$ D1: $C_XH_YO_ZN_A$ (S_{bp}) S1: Z_{HS}	S6	Hydrogenotrophic SRB endogenous decay	

SRB = sulphate reducing bacteria

Table 5.11: Processes and compounds for biologically mediated processes for inclusion in kinetic models for combined biological sulphate reduction and methanogenesis (in addition to those listed in Table 5.10 above).

Organism Group	**Compounds**	**Processes**		**Source**
Acetoclastic methanogens	C1: NH_4^+ C3: $H_2CO_3^*$ C7: H^+ C13: HAc P4: CH_4 D6: Z_{AM}	D7	Acetoclastic methanogenesis	Sötemann *et al.* (2005a), Table 2 Tables 4.2, 4.3 & 4.4
	C2: NH_3 C3: $H_2CO_3^*$ D1: $C_XH_YO_ZN_A$ (S_{bp}) D4: Z_{AM}	D8	Acetoclastic methanogen endogenous decay	
Hydrogenotrophic methanogens	C1: NH_4^+ C3: $H_2CO_3^*$ C7: H^+ P4: CH_4 D3: H_2 D6: Z_{HM}	D9	Hydrogenotrophic methanogenesis	Sötemann *et al.* (2005a), Table 2 Tables 4.2, 4.3 & 4.4
	C2: NH_3 C3: $H_2CO_3^*$ D1: $C_XH_YO_ZN_A$ (S_{bp}) D4: Z_{HM}	D8	Hydrogenotrophic methanogen endogenous decay	

5.4 MODEL CALIBRATION, VERIFICATION AND VALIDATION

The kinetic models developed above were implemented in the computer program AQUASIM (Reichert, 1998). Currently, the models are undergoing calibration, verification and validation. This involves confirming mass balances and that the predicted behaviour

conforms to that expected, determining kinetic and stoichiometric constant values from the literature and through model application, and simulation and comparison of predicted and measured results for experimental systems in the literature. For these purposes, the data set described in Chapter 2 (detailed by Ristow *et al.*, 2005a) appears suitable; a series of experimental lab-scale systems were operated which were fed a mixture of PSS and sulphate, operated over a range of retention times and pH values, and i) COD, ii) free and saline ammonia (FSA), iii) short chain fatty acids (SCFA), iv) $H_2CO_3^*$ alkalinity, v) pH of the effluent stream and vi) effluent sulphate concentration vii) CO_2 and viii) CH_4 gasses in the gas stream determined.

5.5 CONCLUSIONS

An integrated two phase (aqueous, gas) chemical, physical and biological processes kinetic model for competitive methanogenic and sulphidogenic anaerobic digestion with PSS as substrate has been developed. This model requires validation through application to experimental data sets. For this purpose, the data set described in Chapter 2 (detailed by Ristow *et al.*, 2005a) appears suitable, and this validation exercise is currently being undertaken using the Aquasim modelling platform. Parallel to the implementation in Aquasim by the UCT Research Group, the University of KwaZulu-Natal (UKZN) Research Group implemented the model described in this Chapter in the WEST platform. This implementation is described in Chapter 6.

6 IMPLEMENTATION OF THE ANAEROBIC DIGESTION MODELS IN WEST

6.1 INTRODUCTION

The overall objective of this section of the research was to implement the methanogenic and sulphidogenic anaerobic digestion models developed in Chapters 4 and 5 respectively in the WEST® modelling platform. The purpose of the model primarily was to capture the knowledge acquired in the laboratory and pilot-plant investigations carried out by the UCT and Rhodes University (RU) members of the project team, in a form which could readily be used by design engineers working on full scale implementations of the process. To achieve this objective a number of tasks were identified:

i. Translation and coding of the basic UCTADM1 (without sulphate reduction, Chapter 4) from AQUASIM to WEST.
ii. Extension of the model to include reactions for sulphate reducing processes (Chapter 5).
iii. Calibration of the model using data sets from the UCT laboratory experiments carried out in completely mixed reactors (Chapter 2).
iv. Adaptation of the model to represent the Rhodes BioSURE® Erwat Ancor pilot plant configuration and its calibration using available operating data.
v. Highlight areas for further information and research.

This Chapter summarises progress in completing these tasks; for details see Rajkumar (2006).

6.2 THE WEST MODELLING AND SIMULATION SOFTWARE

6.2.1 Introduction to WEST

The ability to utilise empirical or mechanistic mathematical models is dependent on an efficient software tool to implement and solve these models, thereby to simulate treatment plants of interest. The modelling and simulation package WEST (**W**astewater Treatment Plant **E**ngine for **S**imulation and **T**raining) provides the modeller with a user-friendly platform to utilise existing models or to implement and test new models. WEST is a modelling and simulation environment that can be applied to any type of process and can be described as a structured collection of Differential Algebraic Equations (DAEs). WEST was developed at BIOMATH, the Department of Applied Mathematics, Biometrics and Process Control of Ghent University (Belgium) in conjunction with HEMMIS, a Belgium based Software Company. In the WEST modelling and simulation environment a strict distinction is made between a modelling environment, which aims to enable the reuse of model knowledge, and the experimentation environment, which aims to maximise accuracy and performance (Vanhooren *et al.*, 2003).

6.2.2 WEST Software Architecture

The functional architecture of WEST and the different steps that need to be followed to build a model and perform experiments with it, as explained by Vanhooren and co-workers (2003), is graphically represented in Figure 6.1.

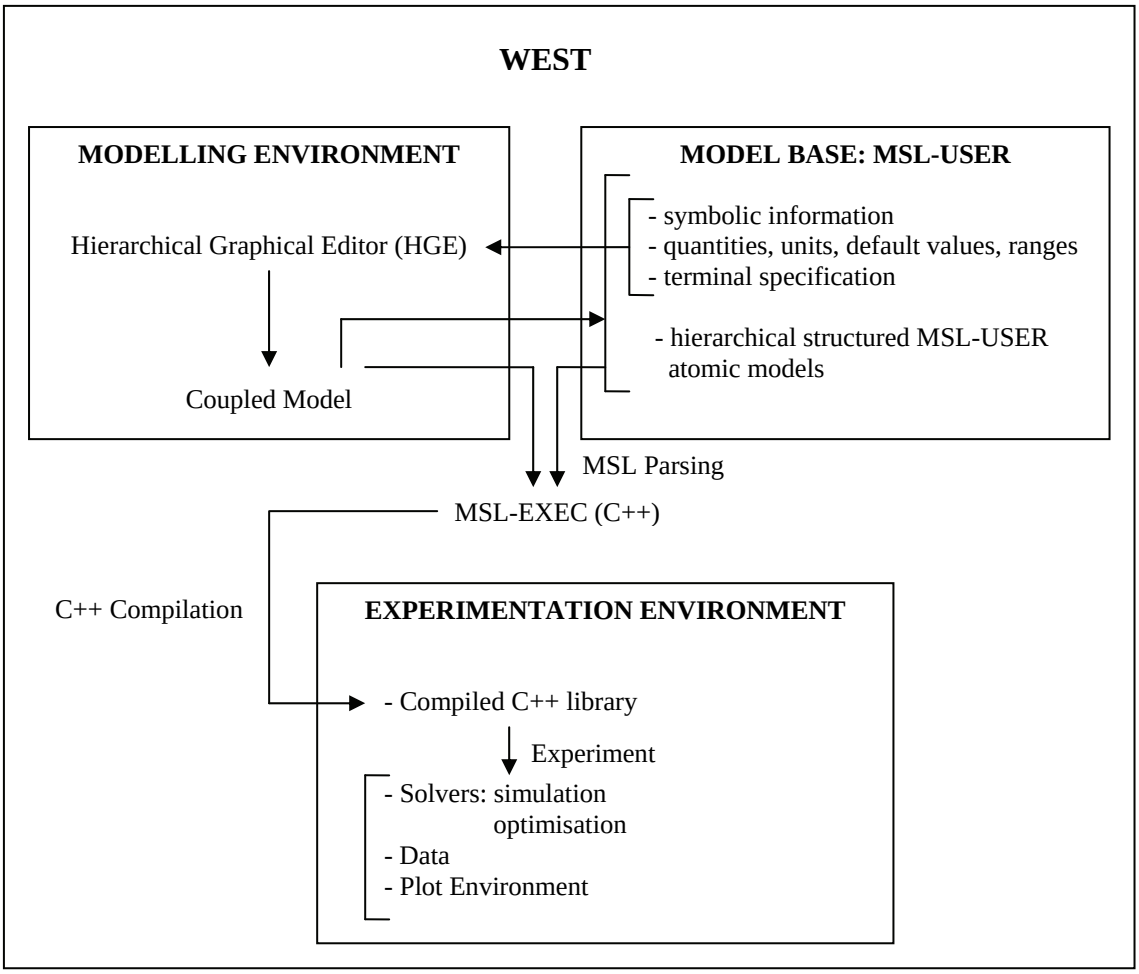

Figure 6.1: Functional architecture of WEST (from Vanhooren *et al.*, 2003)

The model base (Figure 6.1) is the core of WEST whereby models are described in MSL-USER (MSL stands for model specification language), a high level object-oriented declarative language specifically developed to incorporate models. Figure 6.2 represents a model base in the WEST MSL Editor. The purpose of the model base is to maximise the reuse of existing knowledge such as mass balances, physical units, default parameter values and applicable ranges, and is therefore structured hierarchically. This reusable knowledge is defined centrally and can be used by an expert to build new models. WEST therefore has an open structure which allows the user to make changes to existing models and define new ones as required.

Once the modelling environment is started, the model base is loaded and all relevant information extracted from it. By using the symbolic information from the model base, such as model structure and listings of parameters and variables, the 'atomic' models (Figure 6.2) available in the model base are linked to a graphical representation. A hierarchical graphical editor (HGE, Figure 6.1) allows for an interactive composition of complex treatment plant

configurations from these graphical building blocks. An example of a wastewater treatment plant configuration in the HGE of the WEST configuration builder is shown in Figure 6.3. Input and output terminals of the models are also extracted from the model base to decide whether or not two models can be linked together in the HGE.

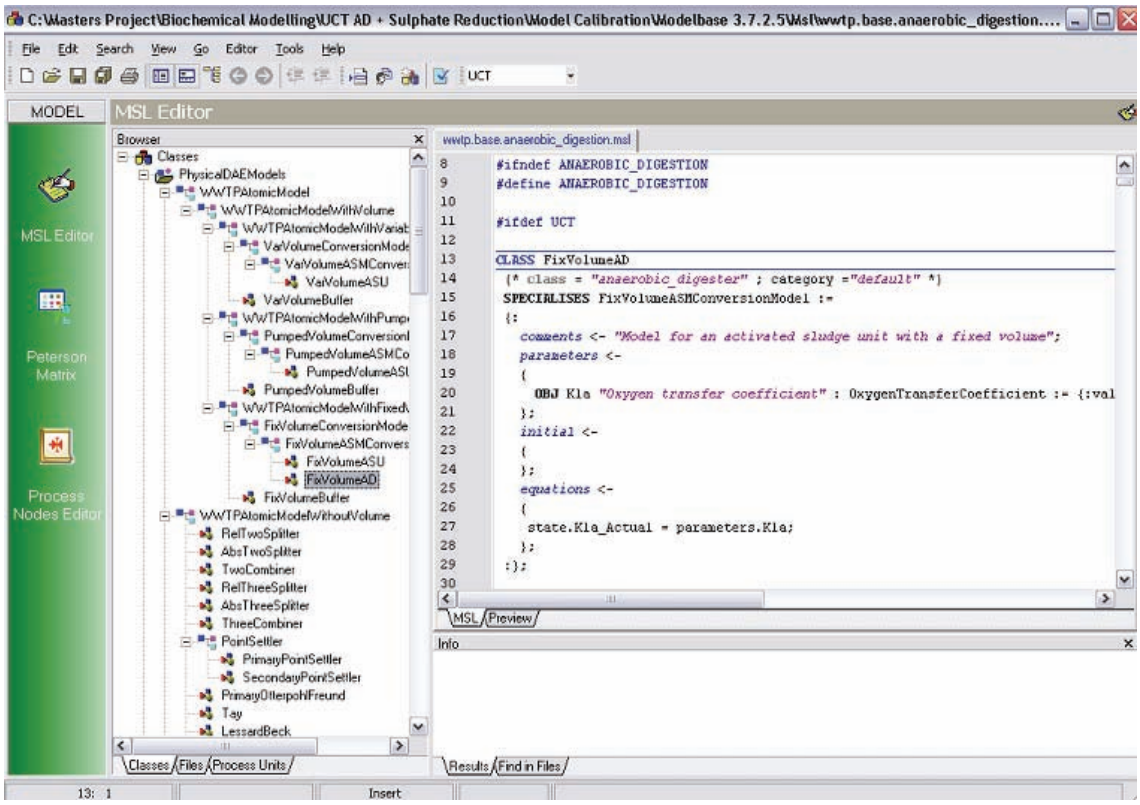

Figure 6.2: Representation of a model base in the WEST MSL Editor

Once a configuration is built, using the information extracted from the model base the HGE creates and outputs a coupled model in MSL-USER (Figure 6.1), which is automatically added to the model base for further use in new modelling exercises. In the following step the model parser is utilised to generate low-level MSL-EXEC (C++) code (Figure 6.1), from the MSL-USER model and the atomic model representations in the model base. After the C++ compilation step, a model library is formed which can be utilised for execution within the experimentation environment (Figures 6.1 and 6.4). In the experimentation environment the compiled model is loaded and symbolic information (model structures, listings of parameters and variables) retrieved from the library. These listings contain the units, descriptions, default values, initial values, lower and upper bounds for parameters and variables. Once the model library is loaded, several virtual experiments can be performed. Experiment types include simulation, sensitivity analysis, scenario analysis, Monte-Carlo experiments, optimal experimental design and process optimisation (parameter estimation). Solvers within the experimentation environment are able to generate data that is utilised for plotting (as shown in Figure 6.4) and outputs to file.

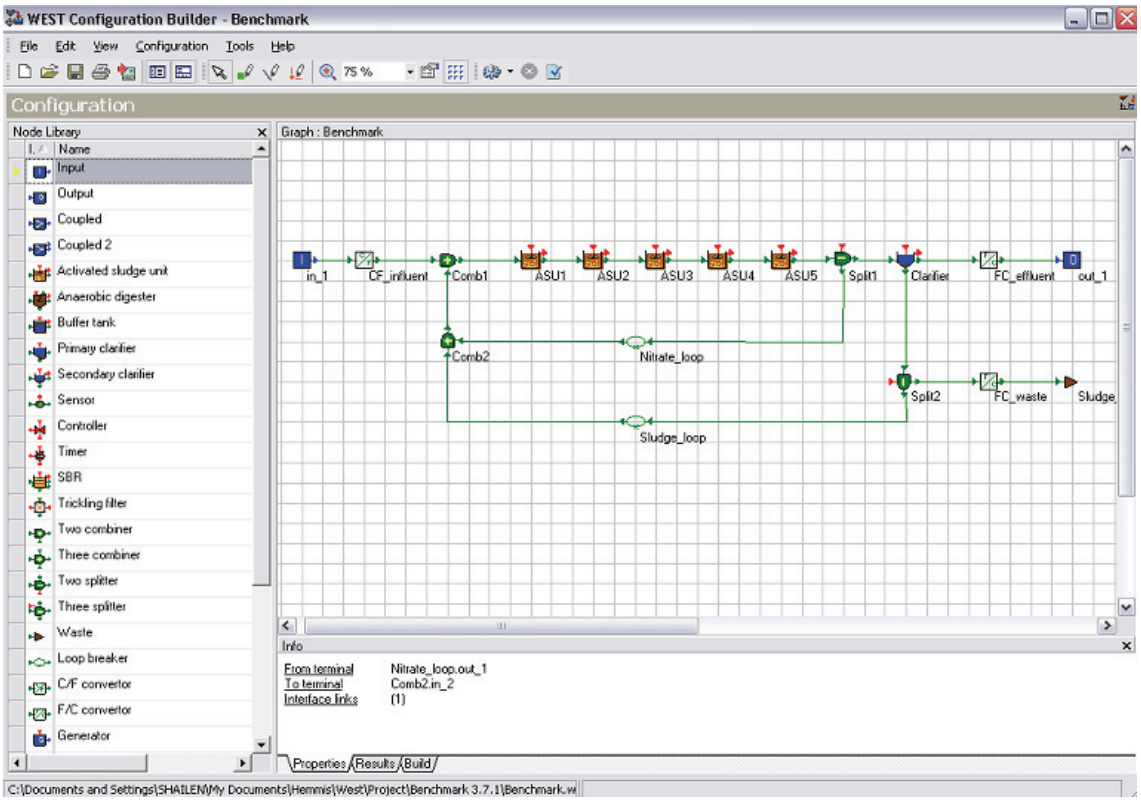

Figure 6.3: Depiction of a wastewater treatment plant model in the Hierarchical Graphical Editor (HGE) of the configuration builder

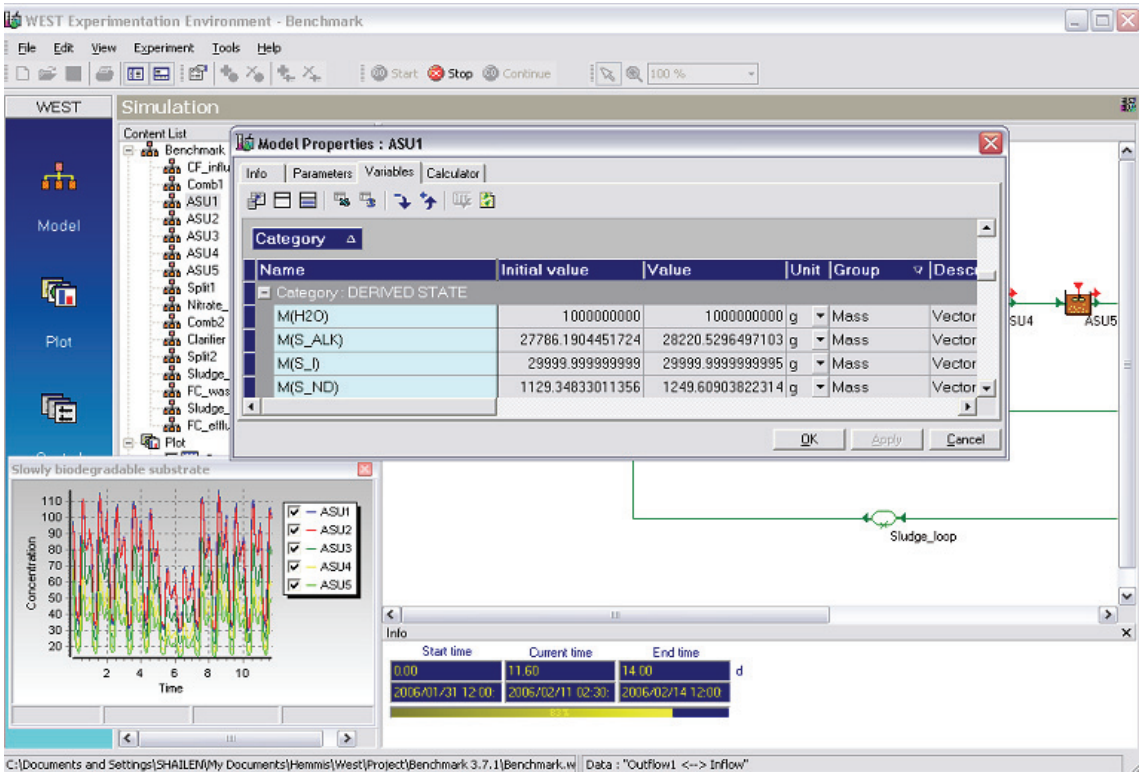

Figure 6.4: The WEST experimentation environment, showing a plot and a variable listing

6.3 IMPLEMENTATION OF THE METHANOGENIC ANAEROBIC DIGESTION MODEL (UCTADM1) IN WEST

6.3.1 Preliminary validation of model implementation

This preliminary step involved the translation of the methanogenic anaerobic digestion model (without sulphate reduction) developed in Chapter 4 from AQUASIM into WEST. This was a relatively straightforward process, except for some minor details where the different approaches of the two modelling platforms needed to be taken into account. These were:

1. Representation of water as a specific component in the model. In the AQUASIM version of the model as developed by UCT, water is not explicitly included, but is represented by the flows into and out of the reactors. This is because only the processes within the reactor are considered; in WEST the reactor is a module that can be linked to other modules to create an integrated model of a larger system, so all components (including water) need to be explicitly accounted for in the feed and effluent streams and mass balances.
2. The feed stream to the reactor is specified separately from the reactor module. In the AQUASIM implementation the feed is represented by a set of model parameters which are not separated from the rest of the parameters, whereas in the WEST implementation it is set up as an external file, which simplifies input of time varying flow and composition.

The main outcome of this initial step was a demonstration that the two versions of the model gave essentially identical results. Table 6.1 shows the steady state values for all the state variables produced by the two versions of the model for the same feed specification and system operation.

Small differences in the values can be attributed to differences between the two simulation platforms in the handling of numerical integration, particularly with the very small values. The relatively large discrepancies for the propionate components (HPr and Pr) were found to be due to an error in the propionate equilibrium calculation in the AQUASIM version of the model, which was subsequently corrected in both the AQUASIM and WEST versions. This demonstrates one of the advantages of the comparison between the models implemented in the two simulation platforms.

At this stage the WEST version of the model simply duplicated the functionality of the AQUASIM version, except that it had the standard WEST feature of connectivity to other compatible unit process models. In implementation in WEST, an issue that was identified was the way that the biodegradable particulates in the reactor feed are described in UCTADM1 (Chapter 4), which is not well suited to the WEST modular modelling approach. The problem is that the feed particulate organic component is characterised in terms of the stoichiometric coefficients of its composition, which also are parameters in the reaction scheme, which is part of the reactor model; this was done so that the feed particulate organic composition could remain an input variable. This means that the representation of the feed stream and the reactor are inextricably inter-related, which negates the modular interconnectivity of units which WEST should provide. A preliminary theoretical analysis of how to re-formulate the model to separate the feed composition representation from the reaction scheme is presented in Appendix A. However, since this re-formulation has not yet

been implemented in WEST, the model retains the UCTADM1 structure, as described in Chapter 4.

Table 6.1: Comparison of model component concentrations between the AQUASIM and WEST implementations of the UCT anaerobic digestion model.

Component	WEST	AQUASIM	% Difference
AD1_CODbp	5.745501379	6.1433866	-6.5
AD2_B2_CODbs	0.000233051	0.000233051	0.0
AD3_H2	4.30287E-07	4.30E-07	0.0
AD4_HPr	5.05898E-07	4.23E-07	19.7
AD5_Pr	7.94034E-05	7.08E-05	12.1
AD6_CH4	0.368315663	0.32966099	11.7
AD7_Xa_ad	0.010640276	0.009486141	12.2
AD8_Xa_ac	1.01192E-25	1.84E-20	-100.0
AD9_Xa_am	0.003290791	0.00295067	11.5
AD10_Xa_hm	0.00043904	0.000391418	12.2
B1_CODus	0	0	-
B3_CODup	15.4460665	15.446066	0.0
C1_B10_NH4	0.031770838	0.032692043	-2.8
C2_NH3	0.000269221	0.00029589	-9.0
C3_H2CO3	0.009450594	0.00904162	4.5
C4_HCO3	0.042920944	0.043843574	-2.1
C5_CO3	3.2489E-05	3.54E-05	-8.2
C6_CO2 gas	0.226843725	0.18953393	19.7
C7_H	1.5431E-07	1.44E-07	6.9
C8_OH	9.14167E-08	9.76E-08	-6.3
C9_H3PO4	0	0	-
C10_H2PO4	0	0	-
C11_HPO4	0	0	-
C12_PO4	0	0	-
C13_HAc	4.26854E-08	4.27E-08	0.0
C14_Ac	7.0743E-06	7.56E-06	-6.5

6.3.2 Application to the UCT laboratory experiments

6.3.2.1 Systems simulated

The experimental data used to calibrate the model were obtained from Ristow *et al.* (2005a), who investigated the hydrolysis of PSS under methanogenic, acidogenic and sulphidogenic conditions, carried out in completely mixed reactors at 35 ^{o}C, see Chapter 2. Acidogenic or acid forming systems were not considered in model calibration as the mechanisms for the observed decrease in the rate of PSS hydrolysis under acidogenic conditions (Chapter 2) had not been elucidated, and hence not incorporated in UCTADM1. Variables were added to the model to allow a direct comparison of the WEST output data with the effluent experimental data for the purpose of calibration, such as total weak acid/base species concentrations, alkalinity, and conversion to COD concentration units. The experimental setup described in

Chapter 2 was modelled in WEST using UCTADM1 which is symbolically represented by an anaerobic digester icon together with an input and output node representing the interface of the model and which contain the characteristics of the feed and of the treated water respectively (refer Figure 6.5).

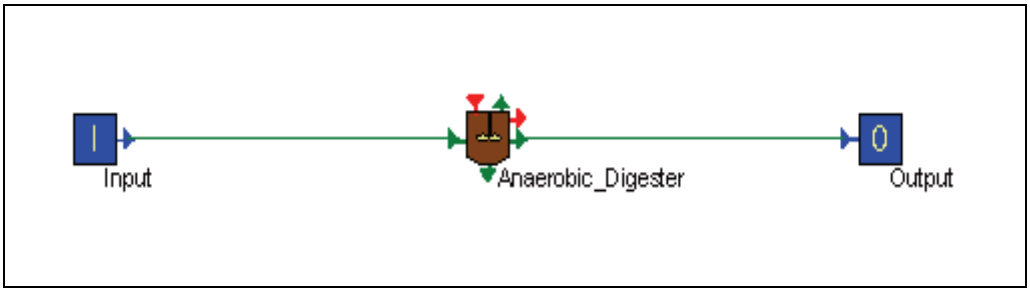

Figure 6.5: Configuration of the UCT experimental system in WEST

6.3.2.2 Kinetic parameters

The kinetic parameters used in the application of the model were not obtained by fitting simulated data to the experimental data, but were those obtained from Sötemann *et al.* (2005a,b; Chapter 4) and Kalyuzhnyi *et al.* (1998; Chapter 5). In selecting a set of kinetic constants it is imperative that these accurately predict the behaviour of the experimental systems. Initially the single, complete set of kinetic parameters (for both methano- and sulphidogenic digestion) from Kalyuzhnyi *et al.* (1998) was selected for the simulation of experimental data sets; since Kalyuzhnyi *et al.* do not consider solid organics as feed, the hydrolysis kinetic parameters initially were obtained from Sötemann *et al.* (2005a,b). However, upon preliminary simulations, it was observed that the experimental systems showed little response to these kinetic parameters, i.e. death of organisms and non-utilisation of influent COD, except if the hydrolysis kinetic constants were adjusted (see Section 6.5). Therefore, to maintain consistency in the two modelling exercises, it was decided to use a combination of kinetic parameters from Sötemann *et al.* (2005a,b; Chapter 4) and Kalyuzhnyi *et al.* (1998; Chapter 5). Thus, in addition to the hydrolysis kinetic parameters, kinetic and stoichiometric constants for the four methanogenic anaerobic digestion organism groups of acidogens, acetogens, acetoclastic methanogens and hydrogenotrophic methanogens were obtained from Sötemann *et al.* (2005a,b), as was done in Chapter 4. The remaining kinetic and stoichiometric parameters for acetogenic, acetoclastic and hydrogenotrophic sulphate reducing bacteria (SRB) were acquired from Kalyuzhnyi *et al.* (1998), as was done in Chapter 5. Merging these two sets of kinetic parameters proved successful and considering that parameter adjustments were made to the kinetic constants for only one process (that of hydrolysis, see Section 6.5), the simulation results corresponded remarkably well to the experimental data, see below. The set of kinetic parameters utilised in application of the model to the methanogenic experimental systems in Chapter 2 (at 35 ^{o}C) is shown in Table 6.2, except for those for hydrolysis, see below.

Table 6.2: Kinetic parameters used in model calibration with experimental data at 35°C

Organism Group	**μ_{max} (d^{-1})**	**K_s (mol/ℓ)**	**K_n (mol/ℓ)**	**K_i (mol/ℓ)**	**Y (mol org/ mol substrate)**	**b (d^{-1})**
Acidogens, Z_{AD}	0.8	7.8E-04	-	0.55	0.1074	0.041
Acetogens, Z_{AC}	1.15	8.9E-05	-	0.19	0.0278	0.015
Propionate SRB, Z_{PS}	0.814	2.63E-03	7.71E-05	5.78E-03	0.0268	0.026
Acetoclastic methanogens, Z_{AM}	4.39	1.3E-05	-	0.185	0.0157	0.037
Acetate SRB, Z_{AS}	0.854	3.75E-04	2.00E-04	5.13E-03	0.0187	0.038
Hydrogenotrophic methanogens, Z_{HM}	1.2	1.56E-04	-	0.165	0.004	0.01
Hydrogen SRB, Z_{HS}	3.908	4.38E-06	2.00E-04	1.72E-02	0.0071	0.084

In application of the model, from a sensitivity analysis it was determined that the two hydrolysis rate constants ($K_{max,HYD}$ and $K_{SS,HYD}$) most significantly influenced the simulation results (Section 6.5). This is not unexpected, since hydrolysis is the rate limiting process. Accordingly, for each system simulated these two constants were calibrated using the optimiser function in WEST (see Section 6.5).

6.3.2.3 Influent characterisation

The influent characterisation for all steady state experiments is a crucial step in the model application. Available data from Ristow *et al.* (2005a) as reported in Chapter 2 was used to characterise the influent for simulation in WEST according to the procedure outlined briefly in Chapter 2 and in detail by Rajkumar (2006). The characterisation procedure was performed externally to the simulation software.

COD Fractionation

Measured and calculated values of the various components of the feed (in mg cod/ℓ) were obtained from Chapter 2 and Ristow *et al.* (2005a), and as described below.

From Chapters 2 and 4, the total COD balance on the influent is given by:

$$S_{ti} = S_{upi} + S_{bpi} + S_{usi} + S_{bsfi} + S_{VFAi} \quad (6.1)$$

Where:

S_{ti} = Total COD
S_{si} = Total soluble COD
= $S_{usi} + S_{bsfi} + S_{VFAi}$
S_{upi} = Unbiodegradable particulate COD
S_{bpi} = Biodegradable particulate COD
S_{usi} = Unbiodegradable soluble COD
S_{bsfi} = Biodegradable soluble/fermentable COD (glucose)
S_{VFAi} = Volatile fatty acid (short chain fatty acids) COD

Available from measurement were influent and effluent total and soluble COD concentrations, as well as the effluent VFA concentrations. From Chapter 2, it was accepted that the influent unbiodegradable particulate COD $S_{upi} = 0.334\ S_{ti}$. This accepts the value for the S_{upi} fraction as that determined in Chapter 2 from the 60 d retention time methanogenic system (steady state number 17, Table 2.1), and is the same as accepted in Chapter 4 for application of the AQUASIM version to the same experimental systems. The influent unbiodegradable soluble COD (S_{usi}) fraction of 0.008 determined in Chapter 2 from the effluent COD was accepted, again as in the AQUASIM version applied to the same systems.

Direct independent measurements of the influent soluble biodegradable fermentable (S_{bsfi}) and VFA (S_{VFAi}) COD concentrations were not available. In Chapter 2 and Ristow *et al.* (2005a), from experimental observations and the conclusions of Lilley *et al.* (1990) it was accepted that $S_{bsfi} = S_{VFAi}$. With the derived value for S_{usi}, this enabled S_{bsfi} and S_{VFAi} to be calculated from the measured soluble COD concentration (S_{si}) for the steady state systems. However, since equality of S_{bsfi} and S_{VFAi} was not directly measured for all the feed batches, this assumption was evaluated. The steady state model of Sötemann *et al.* (2005a,c) was used to regress data from each steady state experiment described in Chapter 2 (detailed by Ristow *et al.*, 2005a), thereby predicting the S_{VFAi} fraction of the feed. This was achieved by specifying a feed input of S_{ti}, S_{VFAi}, pH, alkalinity, FSA, S_{upi} fraction (from measurements), relative proportions of carbon, hydrogen, oxygen and nitrogen in PSS (from Chapter 4), and, together with flow variables and effluent data of S_t, FSA, alkalinity and pH (from measurement), the steady state model was used to minimise the sum of squared errors of effluent alkalinity, FSA and CO_2 partial pressure, to predict a value of S_{VFAi}. Some of the values of S_{VFAi} obtained were significantly higher than those determined by Ristow *et al.* (2005a), particularly for steady state experiments supplied with influent from feed batch number F12 (Table 4.7), steady state numbers 1-6 (Table 2.1). However, with this exception and a few steady state experiments fed with influent from feed batch number F13 (Table 4.7) (steady state numbers 7, 8, 9, 10 and 11, Table 2.1), the remaining steady state S_{VFAi} experimental values remained unchanged at the values determined by Ristow *et al.* All S_{VFAi} was accepted as being acetate, as in Chapter 4.

The remaining COD fraction (S_{bpi}) was determined by difference, i.e. $S_{bpi} = S_{ti} - S_{upi} - S_{si}$, to completely characterise the influent COD fractions. The characterised influent utilised as input for simulation in WEST for each steady state experiment is summarised in Appendix B and shown in detail by Rajkumar (2006).

By utilising the influent flow rate to the reactor, all COD fractions were converted from concentration units of mg cod/ℓ to flux units of g cod/d.

Primary sewage sludge stoichiometric formulation

The stoichiometric formulation for the PSS was accepted to be $C_{3.5}H_7O_2N_{0.196}$, from the simulations of the Izzett *et al.* (1992) systems with the AQUASIM version of the model, see Chapter 4. In later applications of the AQUASIM model to the Ristow *et al.* (2005a) data set and from measurement, the PSS formulation was refined, but this was not available in time for the WEST simulations and the refinements were relatively minor (Section 4.7).

Influent weak acid/base speciation

In UCTADM1, the weak acid/base chemistry is integrated with the biological and physical processes, and the individual weak acid/base species specified as compounds in the model (see Chapter 4). This requires that the influent weak acid/bases are speciated according to the influent pH and total species concentrations, as described below.

H^+ and OH^-

The influent pHs for the various feed batches were determined as described in Chapter 4, Section 4.7. The calculation of the hydrogen and hydroxyl ion influx was based on the influent pH:

$$[H^+](mol/L) = 10^{-(in\_pH)} \quad (6.2)$$

$$[OH^-](mol/L) = 10^{-(14-in\_pH)} \quad (6.3)$$

These molar concentrations were converted to flux units (g/d) by multiplying with the reactor flow rate and their respective molecular weights.

Volatile Fatty Acids (VFA)

The species which form the VFA component are HPr (propionic acid), Pr^- (propionate), HAc (acetic acid) and Ac^- (acetate). These species were fractioned from the VFA component of COD (determined above) as follows:

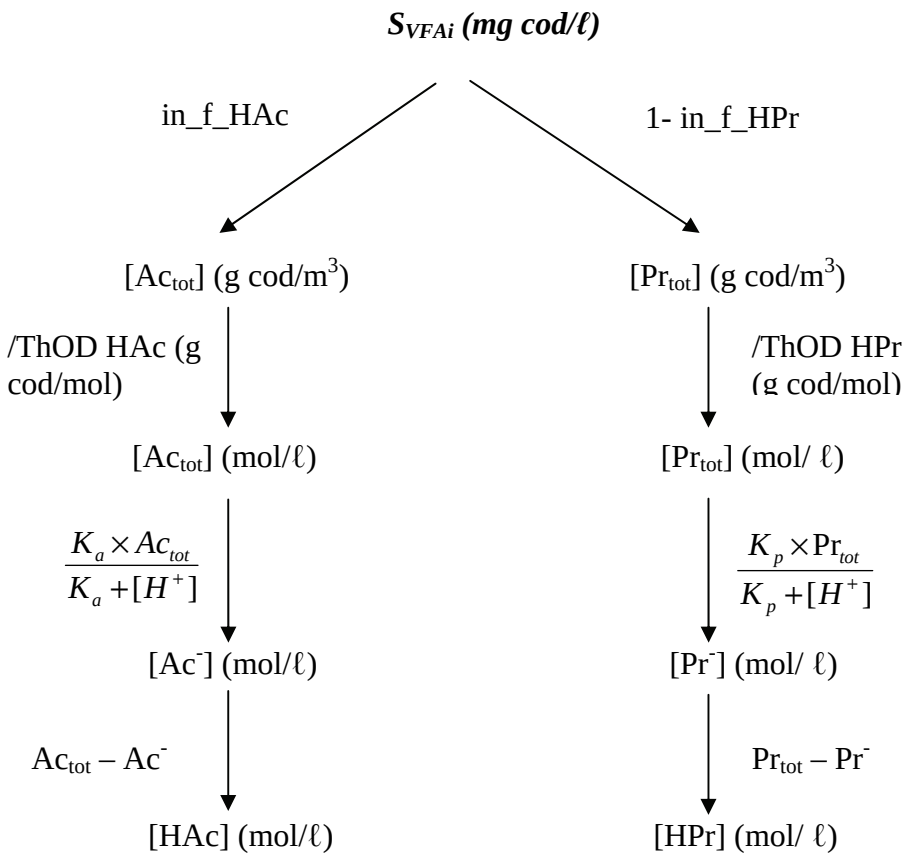

where:

S_{VFAi}	= Volatile fatty acid (short chain fatty acids) COD
in_f_HAc	= fraction total VFA that is acetate
Ac_{tot}	= Acetate system (HAc and Ac^-) total concentration
Pr_{tot}	= Propionate system (HPr and Pr^-) total concentration
ThOD HAc	= Theoretical oxygen demand for acetic acid
ThOD HPr	= Theoretical oxygen demand for propionic acid
K_a	= Equilibrium constant for acetic acid at 35 ^oC
K_p	= Equilibrium constant for propionic acid at 35 ^oC
$[H^+]$	= Influent hydrogen ion molar concentration (from above)

The molar concentrations of the species that make up the VFA component were converted to flux units (g/d) by multiplying with the reactor flowrate and their respective molecular weights.

Free and Saline Ammonia (FSA)

The PSS influent FSA values for the various feed batches were available from measurement. The calculation of ammonia and the ammonium ion influx was based on the influent FSA (mg N/ℓ) together with the ammonium ion equilibrium constant.

$$[NH_3](mol/L) = \frac{K_n \times \left(\frac{in\_FSA}{AW\_N \times 1000} \right)}{K_n + [H^+]} \qquad (6.4)$$

$$\left[NH_4^+\right](mol/L) = \frac{[NH_3]\times[H^+]}{K_n} \tag{6.5}$$

where:

K_n = Equilibrium constant for the ammonium ion at 35°C
in_FSA = Influent FSA concentration expressed as nitrogen (mg N/ℓ)
AW_N = Atomic weight of nitrogen (g/mol)
$[H^+]$ = Influent hydrogen ion molar concentration (mol/ℓ) (from above)

The molar concentrations of NH_3 and NH_4^+ were converted to flux units (g/d) by multiplying with the reactor flowrate and their respective molecular weights.

Alkalinity

The influent alkalinities for the various PSS feed batches were determined as described in Chapter 4, Section 4.7. The carbonate system CO_3^{2-}, HCO_3^- and H_2CO_3 influxes were determined from the influent alkalinity (mg/ℓ as $CaCO_3$) together with the equilibrium constants for the carbonate system.

$$\left[CO_3^{2-}\right](mol/L) = \frac{\left(\frac{in\_Alk}{MW\_CaCO_3\times 1000}\times 2\right)+[H^+]-[OH^-]}{2+\left(\frac{[H^+]}{K_{c2}}\right)} \tag{6.6}$$

$$\left[HCO_3^-\right](mol/L) = \frac{\left[CO_3^{2-}\right]\times[H^+]}{K_{c2}} \tag{6.7}$$

$$[H_2CO_3](mol/L) = \frac{\left[HCO_3^-\right]\times[H^+]}{K_{c1}} \tag{6.8}$$

where:

in_Alk = Influent alkalinity expressed in mg/ℓ as $CaCO_3$
MW_ $CaCO_3$ = Molecular weight of calcium carbonate (g/mol)
$[H^+]$ = Influent hydrogen ion molar concentration (mol/ℓ) (from above)
$[OH^-]$ = Influent hydroxyl ion molar concentration (mol/ℓ) (from above)
K_{c2} = Equilibrium constant for bicarbonate at 35°C $\left(HCO_3^- \leftrightarrow CO_3^{2-} + H^+\right)$
K_{c1} = Equilibrium constant for carbonic acid at 35°C $\left(H_2CO_3 \leftrightarrow HCO_3^- + H^+\right)$

The molar concentrations of CO_3^{2-}, HCO_3^- and H_2CO_3 were converted to flux units (g/d) by multiplying with the influent flowrate and their respective molecular weights.

The characterised influent utilised as input for simulation of each steady state experiment with WEST is summarised in Appendix B, and shown in detail by Rajkumar (2006).

6.3.2.4 Comparison with Methanogenic Systems

The steady states measured for varying hydraulic retention times and feed COD concentrations under stable methanogenic operation listed in Table 2.1, Chapter 2, were modelled and simulated in WEST. All steady states had acidogenic, acetogenic and methanogenic biological groups present. From the steady state simulation of methanogenic systems, it was possible to predict critical variables required for the calibration of the model. The experimental measurements include effluent total and soluble COD concentrations, pH, VFA, alkalinity, FSA and TKN, and methane production and methane composition. A summary of results for the steady state simulation of methanogenic systems is presented in Table 6.3; for details see Rajkumar (2006). Influent total and soluble COD concentrations for steady states 1- 8, 10 and 11 have been adjusted to include the additional predicted fraction of S_{VFAi}, as described above.

The following sections compare calibration variables from the predicted model outputs of steady state periods, via simulation in WEST, to the measured data obtained from steady state experiments for methanogenic and sulphidogenic systems. Detailed data for each steady state are listed in Rajkumar (2006).

Table 6.3: Summary of results from the simulation of each steady state methanogenic system; steady state number refers to Table 2.1

		INFLUENT			EFFLUENT								
Steady State Number	**Reactor Volume (ℓ)**	**Retention Time (d)**	**Total COD (S_{ti}) (mg COD/ℓ)**	**Soluble COD (S_{si}) (mg COD/ℓ)**	**Total COD (S_t) (mg COD/ℓ)**	**Soluble COD (S_s) (mg COD/ℓ)**	**pH**	**VFA (mg HAc/ℓ)**	**Alkalinity (mg/ℓ as $CaCO_3$)**	**Methane Production (ℓ/d)**	**Methane Composition (% vol)**	**FSA (mg N/ℓ)**	**TKN (mg N/ℓ)**
1	16	10	28876	5254	11035.99	211.46	6.83	0.88	2490.12	12.26	59.83	209.15	491.85
2	16	8	26439	3161	11189.24	209.69	6.57	1.38	1420.30	13.22	58.58	199.60	483.77
3	20	20	26654	3027	10343.74	198.92	6.62	0.53	1595.71	7.08	58.69	245.26	521.06
4	20	15	26608	3302	10316.18	186.10	6.62	0.86	1577.96	9.41	58.69	222.75	498.37
5	20	15	14011	1825	5685.70	126.42	6.34	1.19	863.10	4.85	57.00	113.80	261.38
7	16	6.67	25228	2374	12559.41	249.86	6.63	1.61	1525.98	13.18	61.46	241.95	532.14
8	16	5.71	25061	2604	12723.14	264.04	6.62	1.99	1477.48	15.00	61.29	248.23	540.45
9	16	5	24880	2693	12855.40	369.98	6.60	2.43	1418.19	16.70	61.25	249.20	541.15
10	20	15	39984	3715	16974.78	274.31	6.84	0.59	2466.35	13.33	61.09	465.90	900.03
11	20	15	39965	4165	17160.89	323.29	6.85	0.58	2559.09	13.20	61.11	473.17	908.66
12	20	10	39810	4436	18621.17	289.62	6.83	0.87	2442.76	18.38	61.13	442.56	893.17
13	20	10	13270	1174	6144.73	142.49	6.36	1.41	826.71	6.20	60.53	143.26	292.55
14	20	8	13269	1524	6380.69	146.29	6.40	1.71	908.29	7.47	60.71	144.40	295.88
17	20	60	9810	1204	3636.08	100.26	6.18	0.41	625.95	0.90	55.40	106.24	207.60
18	16	8	1949	283	856.37	91.78	7.48	0.87	1537.02	0.95	94.44	18.89	39.63
19	16	8	1949	283	856.60	92.01	7.02	1.00	1329.37	0.95	86.16	19.90	40.64
21	20	8	34819	3829	15457.81	246.37	6.73	1.19	1967.41	21.01	60.40	249.75	635.74
23	20	6.67	34819	4399	15372.41	256.54	6.76	1.44	2095.23	25.28	60.50	261.15	646.21
24	20	6.67	13580	1846	6077.66	146.94	6.38	2.20	898.73	9.75	59.42	109.01	259.53
25	20	10	1950	254	928.24	79.08	5.65	8.23	195.43	0.89	52.21	16.56	38.15
26	20	8	1949	283	912.18	109.30	5.65	10.45	196.54	1.12	52.33	18.42	39.54
27	16	8	2017	224	912.89	57.70	6.58	1.37	950.19	0.96	72.70	20.52	42.62
28	20	5.71	41442	2583	20399.00	353.86	6.67	1.89	1683.48	32.11	60.55	283.86	762.69
31	20	5.71	13186	956	7017.47	182.45	6.20	3.85	599.08	9.40	59.08	87.40	244.29

6.3.2.5 Total and Soluble COD

For each steady state, when compared to the experimental data the model was able to accurately predict the effluent total COD concentration, see Figure 6.6. This is not unexpected since the model predicted total COD concentration is the result of optimised hydrolysis kinetic parameters (see Section 6.5).

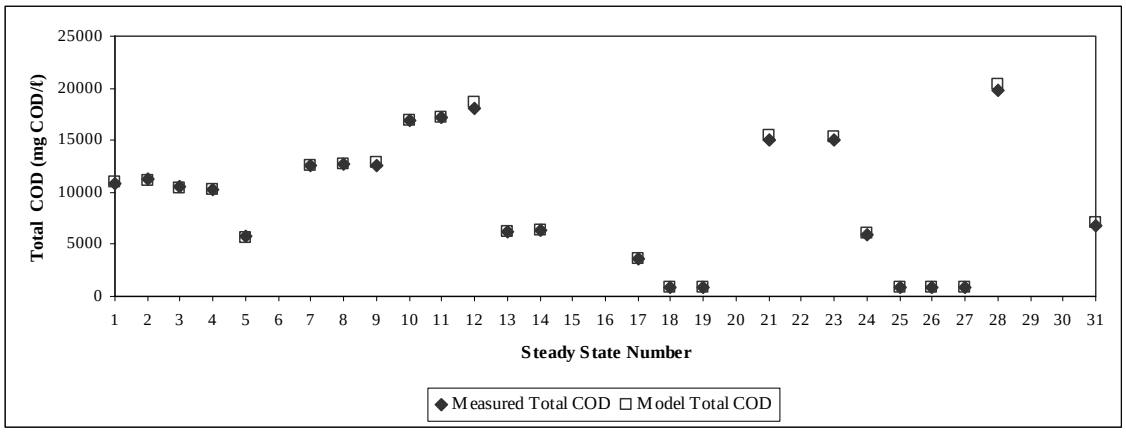

Figure 6.6: Measured and predicted effluent total COD concentrations for respective steady state methanogenic systems

As shown in Figure 6.7, for all steady state methanogenic systems the predicted effluent soluble COD concentrations were higher than those observed. This difference across all steady states is due to the insufficient utilisation of the biodegradable soluble COD fraction in the form of the intermediate "glucose" (see Chapter 4), possibly due to the equilibrium established in the completely mixed reactor between the hydrolysis process producing this compound and the acidogenic processes consuming it; this requires further investigation.

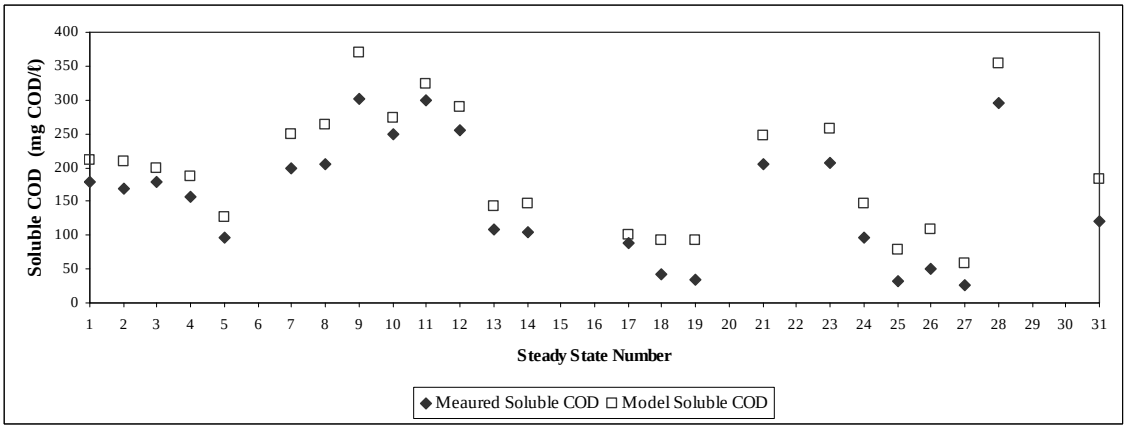

Figure 6.7: Measured and predicted effluent soluble COD concentrations for respective steady state methanogenic systems

6.3.2.6 pH and Alkalinity

The model predicted steady state operating pH and effluent alkalinity values for each methanogenic system are compared to the measured values in Figure 6.8. In the experiments,

the pHs for steady states 18, 19 and 27 were controlled to 7.5, 7, and 6.5 respectively. In the simulations, this was achieved by manually adding either hydrogen or hydroxyl ion to the influent to maintain a given pH. The model predicted pH and alkalinities compare remarkably well to the experimental data for most steady states. Increased influent S_{VFAi} fraction for steady states 1-8, 10 and 11 resulted in increased effluent model pH and alkalinity values (see above).

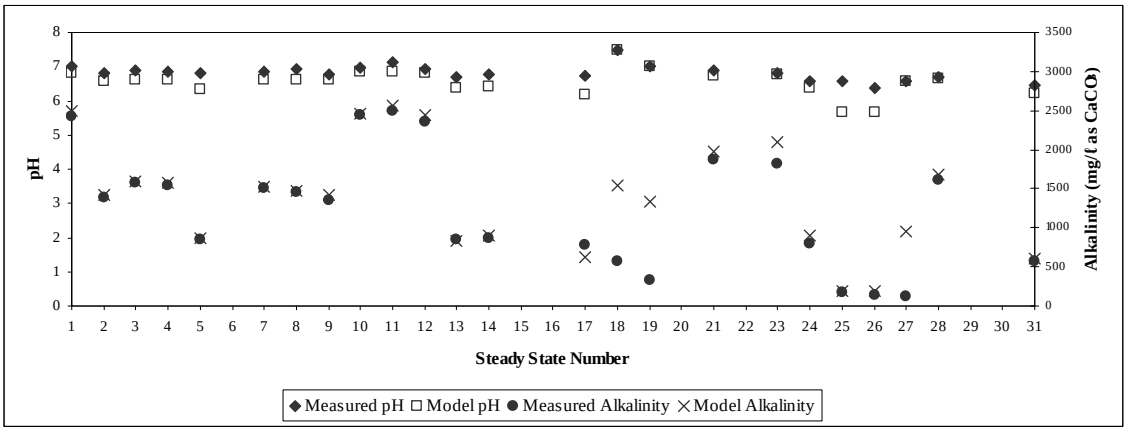

Figure 6.8: Measured and predicted operating pH and effluent alkalinity concentrations for respective steady state methanogenic systems

6.3.2.7 VFA

Figure 6.9 shows a comparison between the model predicted effluent VFA concentrations with the measured values for each of the steady state systems. According to Ristow *et al.* (2005a), the requirement for a stable methanogenic system is a VFA concentration of about 50 mg HAc/ℓ or less (see Chapter 2). For most steady states, from Figure 6.9 the model predicts the almost complete utilisation of substrate VFA by organisms. Although in most cases the predicted values are much lower than measured values, the differences are small in terms of the total COD input (Table 6.3) and the predicted effluent VFA are < 50 mg HAc/ℓ, and hence the requirement for stable methanogenic operation is met. Under prediction of the effluent VFA may be due to uncertainty in the low VFA concentration measurements due to the titration procedure used, or the significant increase in acetoclastic methanogen maximum specific growth rate (from 0.3-0.5 /d to 4.39/d) by Sötemann *et al.* (2005a,b, see Chapter 4) to match the Izzett *et al.* (1992) experimental data. As noted in Chapter 4, this requires further investigation.

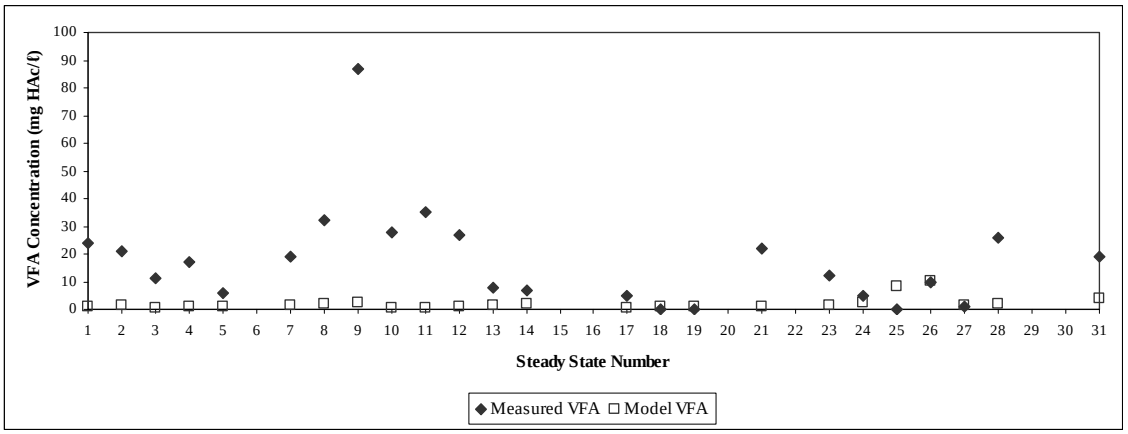

Figure 6.9: Measured and predicted effluent VFA concentrations for respective steady state methanogenic systems

6.3.2.8 Methane Production and Gas Composition

The end product of the anaerobic digestion process is methane and its production is a good indication of the stability of the system. Comparisons between the model predicted and experimentally measured methane production as well as the methane gas composition are shown in Figure 6.10. It is evident that the model predicted values compare relatively well to the measured values for both methane production and methane composition, although for most steady states a slightly higher methane production is predicted than observed. The gas produced consists of methane and carbon dioxide only, and therefore by difference, the carbon dioxide composition can be determined.

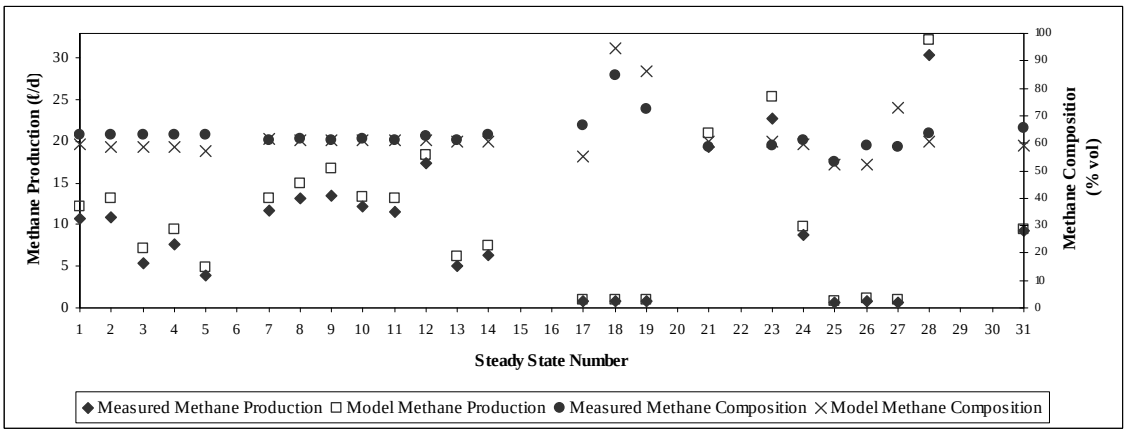

Figure 6.10: Measured and predicted methane production and methane composition for respective steady state methanogenic systems

6.3.2.9 FSA and TKN

Figures 6.11 and 6.12 illustrate the comparison of predicted to measured effluent TKN and FSA concentrations respectively for each steady state system. Model predictions of effluent

FSA compare fairly well with the measured data, with the exception of a few steady states where a greater effluent value is predicted than measured.

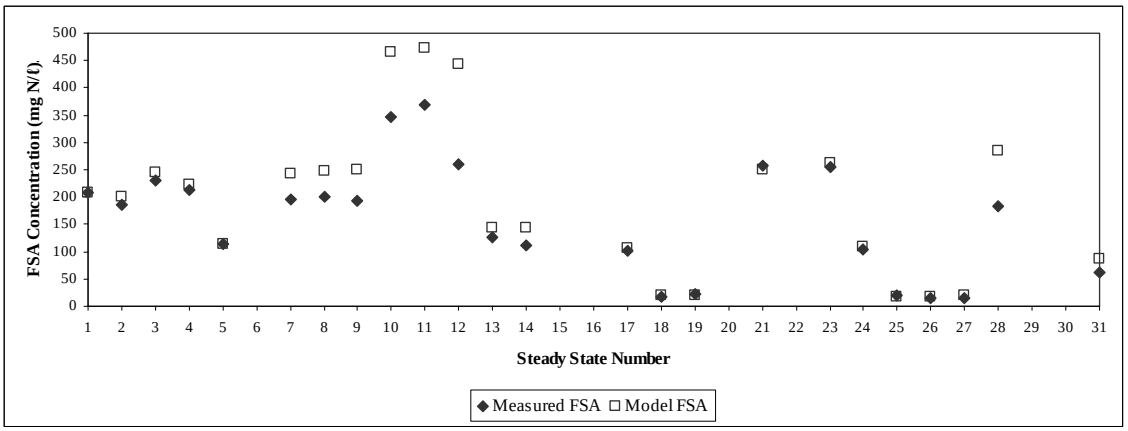

Figure 6.11: Measured and predicted effluent FSA concentrations for respective steady state methanogenic systems

As with the case of FSA concentrations, the predicted effluent TKN values (Figure 6.12) compare reasonably well to the measured effluent values, with the exception of a few steady states in which predicted values are higher than those measured.

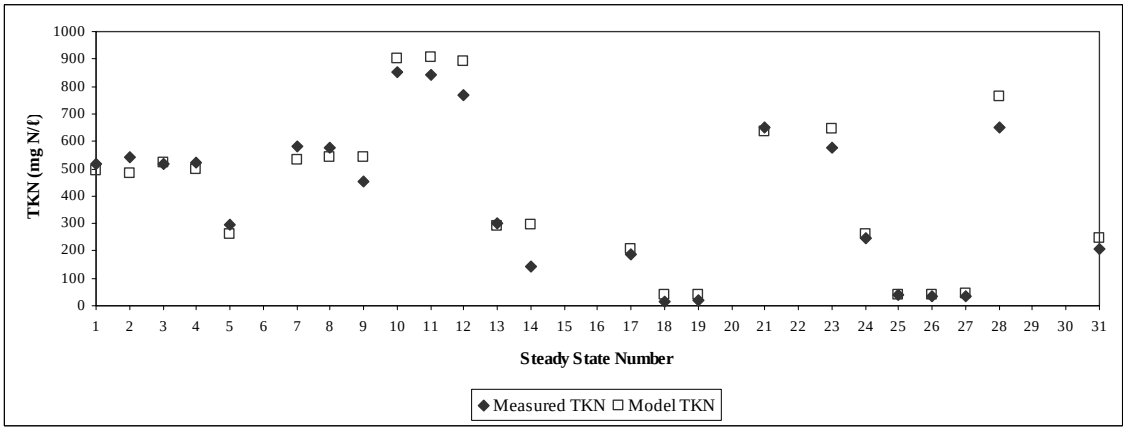

Figure 6.12: Measured and predicted effluent TKN for respective steady state methanogenic systems

6.3.3 Summary

Application of the WEST implementation of the UCTADM1 model to the experimental methanogenic anaerobic digestion systems described in Chapter 2 gave reasonably close correlations between predicted and measured data for a single set of stoichiometric and kinetic constants, with the exception of the hydrolysis rate constants, see Section 6.5. This model now needed to be extended to incorporate sulphate reduction.

6.4 APPLICATION OF THE SULPHIDOGENIC ANAEROBIC DIGESTION MODEL IMPLEMENTED IN WEST TO THE UCT LABORATORY EXPERIMENTS

6.4.1 Systems simulated

The methanogenic anaerobic digestion model was extended to include sulphate reduction, by incorporating the processes and compounds described in Chapter 5. The resultant model was applied to the laboratory-scale steady state sulphate reducing systems described in Chapter 2, Table 2.3. These steady state sulphidogenic systems were operated in completely mixed flow-through anaerobic digesters with excess sulphate, except for steady state number 6 which had excess COD. Comparison of sulphate reducing systems to other sulphate reducing systems and to the corresponding methanogenic system was made possible with a single parameter changed (the influent sulphate) between the steady states in a single experiment. All steady states with the exception of steady state number 16 listed in Table 2.3, Chapter 2, were modelled and simulated in WEST; according to Ristow *et al.* (2005a) no steady state was observed in operation of this particular experiment. All steady states with the exception of steady state number 6 had acidogenic, acetogenic and sulphidogenic biological groups present; in steady state number 6 additionally methanogenic organisms were present. In the experiments, a Methane production of 8.88 ℓ/d and a methane composition of 64.53% volume were observed for steady state number 6 only, due to the presence of methanogenic bacteria in this steady state only; the remaining sulphidogenic steady states showed negligible methane production and therefore zero methane composition and methanogenic bacteria presence. In the simulations it was not possible to induce unstable methanogenic operation and washing out of methanogens by progressively reducing retention times in the digester during simulation. Therefore the absence of methanogenic organisms for the relevant steady states was achieved by setting the initial methanogenic organism masses to zero in the digester. This indicates that under excess sulphate conditions, competition between sulphidogens and methanogens for substrate with the observed consequent exclusion of the methanogens could not be correctly predicted; this clearly requires further investigation.

6.4.2 Influent characterisation

The influent was characterised according to the procedures outlined for the methanogenic systems in Section 6.3.2.3. Additionally, the influent sulphate concentrations were available from measurement and were accepted to be in the form SO_4^{2-} due to the influent pH values.

6.4.3 Values for constants

In all simulations the “default” set of kinetic and stoichiometric constant values were used (Section 6.3.2.1), except for the hydrolysis rate constants which were determined for each steady state via the optimiser function in WEST (see Section 6.5), as had been done for the methanogenic systems above.

6.4.4 Results

The summary of results for the steady state simulation of sulphidogenic systems are presented in Table 6.4. Available experimental measurements include effluent total and

soluble COD concentrations, pH, VFA, alkalinity, FSA, TKN and sulphate concentrations (Chapter 2).

Table 6.4: Summary of results from the simulation of each steady state sulphidogenic system; steady state number refers to Table 2.3

			INFLUENT			EFFLUENT							
Steady State Number	**Reactor Volume (ℓ)**	**Retention Time (d)**	**Total COD (S_{ti}) (mg COD/ℓ)**	**Soluble COD (S_{si}) (mg COD/ℓ)**	**Sulphate (mg SO_4/ℓ)**	**Total COD (S_t) (mg COD/ℓ)**	**Soluble COD (S_s) (mg COD/ℓ)**	**Sulphate (mg SO_4/ℓ)**	**pH**	**VFA (mg HAc/ℓ)**	**Alkalinity (mg/ℓ as $CaCO_3$)**	**FSA (mg N/ℓ)**	**TKN (mg N/ℓ)**
6	16	10	28876	5254	1000	11066.06	217.70	1.23	6.99	0.80	3507.14	207.17	490.12
15	16	8	13269	1524	9600	7769.77	2030.16	4.89	6.87	6.21	3472.22	145.54	292.10
20	16	8	1949	283	2000	1664.02	789.09	380.53	7.50	7.20	2661.95	17.12	38.97
22	16	8	1949	283	2000	1213.26	338.29	379.60	6.99	6.80	2046.79	19.14	40.99
36	16	8	1949	283	2000	1063.30	188.30	378.43	6.46	6.32	1206.15	22.13	43.98
41	20	16	2012	212	2000	1097.20	262.90	103.96	6.96	5.13	2148.11	19.46	41.39
42	20	13.3	2017	224	2000	1112.57	261.37	136.51	6.94	4.91	2115.80	22.39	44.47
46	20	10	989	102	1000	567.42	160.02	123.29	6.47	7.23	1038.38	12.91	23.63
47	16	8	1900	203	2000	2293.89	1476.42	300.41	8.30	6.16	3390.66	14.48	35.43

6.4.4.1 Total and Soluble COD

As illustrated in Figure 6.13, for each steady state sulphidogenic system the model was able to accurately predict the effluent total COD concentration when compared to the experimental data, with the exception of steady state number 15. For steady state 15, the feed was supplemented with Fe to precipitate FeS and thereby eliminate sulphide toxicity (see Chapter 2). The resultant FeS reflects in the COD test as COD, contributing to the measured value. The model does not include the Fe component in the COD and hence the difference. The model predicted effluent total COD concentrations are a result of the optimised hydrolysis kinetic parameters, see Section 6.5. Influent total and soluble COD concentrations for steady state number 6 have been adjusted to include the additional predicted fraction of S_{VFAi}.

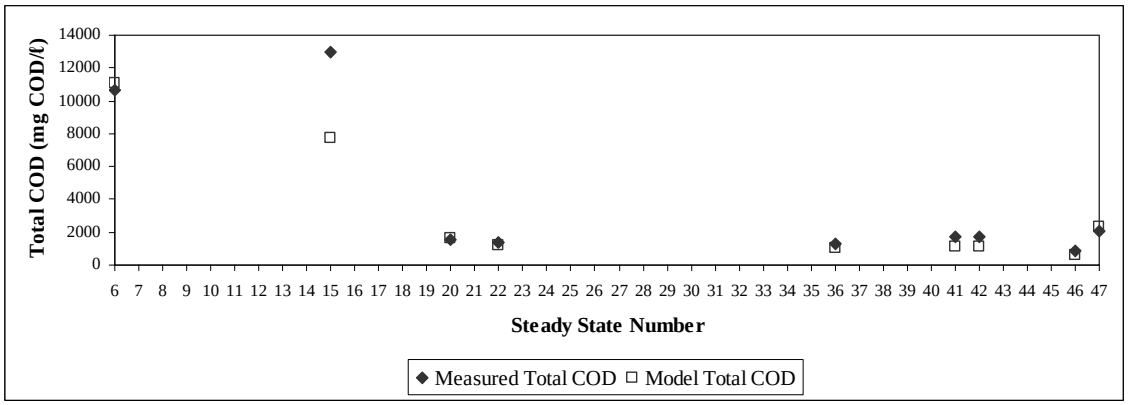

Figure 6.13: Measured and predicted effluent total COD concentrations for respective steady state sulphidogenic systems

Comparing the predicted effluent soluble COD to the measured data for each steady state in Figure 6.14, it can be seen that accurate predictions are only observed for steady states 6 and 20. As a consequence of reasons described above, the greatest deviation is evident for steady state 15. According to simulation effluent data, the factor that influences the soluble COD concentration most is the contribution to the COD value due to total dissolved sulphides. As a result of the aqueous sulphide concentration not being available for experiments, it is therefore not possible to validate this comparison.

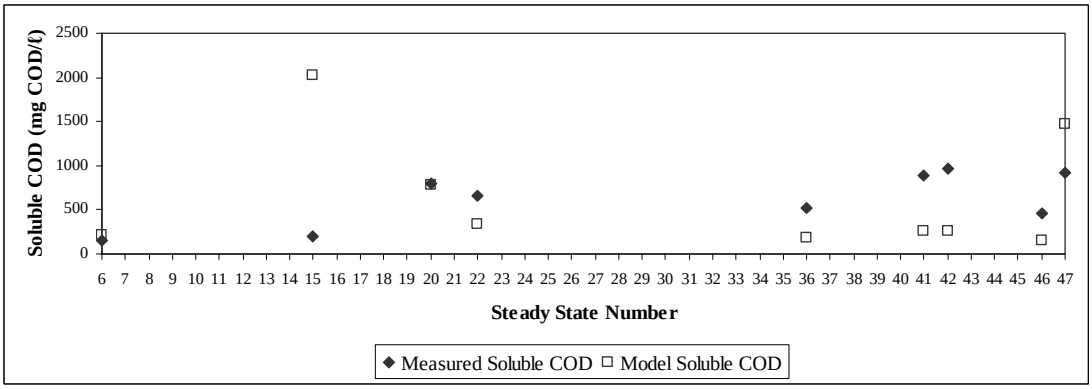

Figure 6.14: Measured and predicted effluent soluble COD concentrations for respective steady state sulphidogenic systems

6.4.4.2 pH and Alkalinity

The model predicted steady state operating pH and effluent alkalinity values for each sulphidogenic system are compared with the measured values in Figure 6.15. The pH for all steady states, except for steady state numbers 41, 42 and 46, were controlled experimentally to set values (see Chapter 2) and in the simulations by manually adding either hydrogen or hydroxyl ion to the influent to maintain a given pH. The model predicts a lower pH for systems where pH was not controlled experimentally (or in the simulations), but observed from steady state operation. For all steady state sulphidogenic systems higher alkalinity values were predicted than measured experimentally, and this requires further investigation.

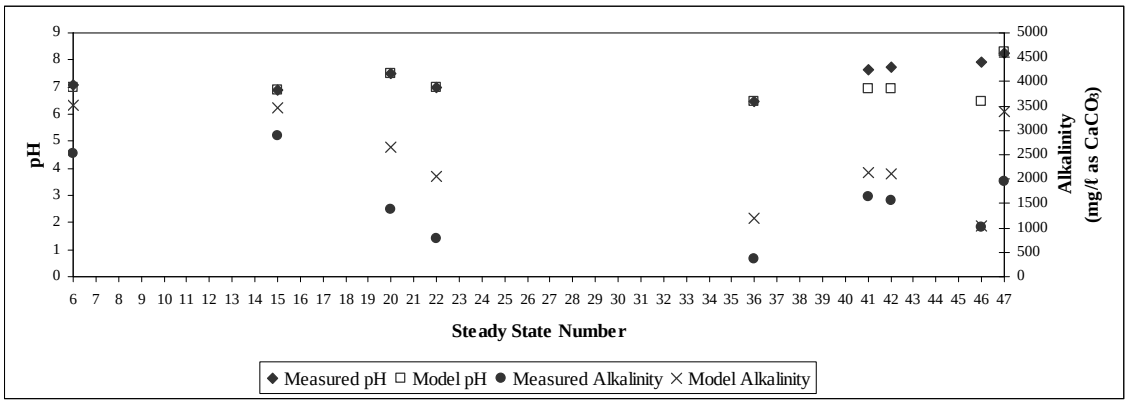

Figure 6.15: Measured and predicted operating pH and effluent alkalinity concentrations for respective steady state sulphidogenic systems

6.4.4.3 VFA

Figure 6.16 shows the comparison between model predicted and experimentally measured values for effluent VFA concentrations. The model is only able to accurately predict the effluent VFA concentration for steady state number 15. Largest deviations of the model predictions from measured data are for steady state numbers 6, 22, 42 and 47. As for methanogenic systems, stable sulphate reducing conditions were accepted to require a low VFA concentration i.e. less than about 50 mg HAc/ℓ (Ristow *et al.*, 2005a). Predicted VFA concentrations range from 0.80 mg HAc/ℓ to 7.23 mg HAc/ℓ for steady state numbers 6 and 46 respectively, hence maintaining stable sulphate reducing conditions.

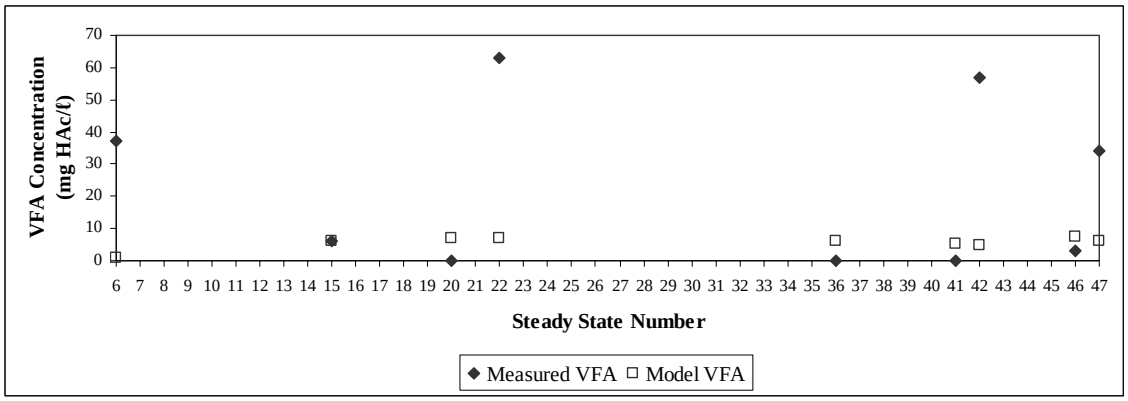

Figure 6.16: Measured and predicted effluent VFA concentrations for respective steady state sulphidogenic systems

6.4.4.4 Sulphate

For steady state number 6 sulphate conversion of 99.88% was predicted and according to Ristow *et al.* (2005a), complete sulphate reduction was probable for this steady state. This is due to the utilisation of a very high influent COD:SO_4 ratio, which can result in the complete reduction of sulphate. For the other steady states, the model predicted effluent sulphate concentrations are compared to the experimental values in Figure 6.17. It can be seen that, when compared to the measured values, the model predicts reasonable sulphate reduction for steady states 6 and 42, where in agreement with observations greater than 90% sulphate reduction is predicted. For steady states 15, 20, 22 and 36 predicted effluent sulphate concentrations are less than the measured values, while for steady states 46 and 47 these are greater; no experimental measurement was made for steady state number 41. However, except for steady states 22 and 47 the differences are not large considering the influent sulphate concentration of 1 300 mg/ℓ. Undissociated aqueous sulphide concentrations range from a minimum of 0.96 mg/ℓ to a maximum of 42.34 mg/ℓ for steady states 6 and 20 respectively, therefore maintaining sulphide inhibition to a minimum.

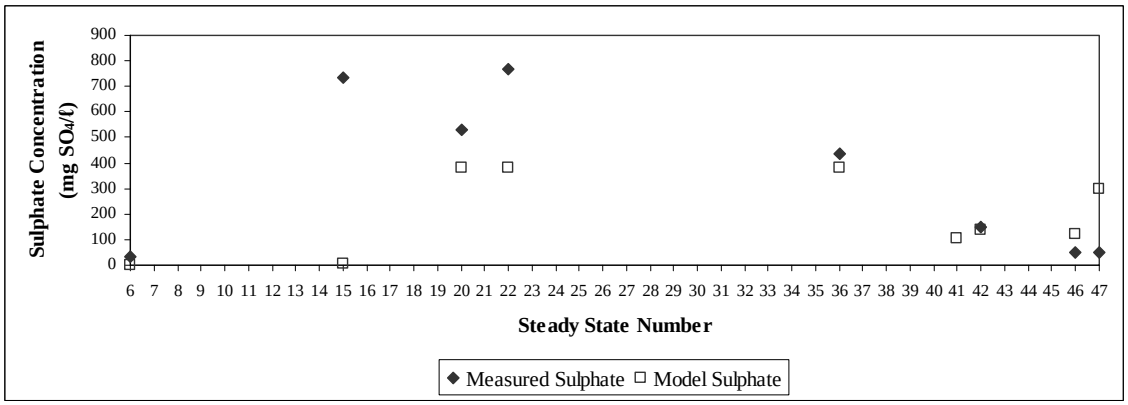

Figure 6.17: Measured and predicted effluent sulphate concentrations for respective steady states

6.4.4.5 FSA and TKN

For the sulphidogenic systems, other than for steady state number 15, in Figure 6.18 the predicted effluent FSA compare reasonably well to measured data. It must be noted that effluent FSA measurements were not recorded for steady state numbers 46 and 47.

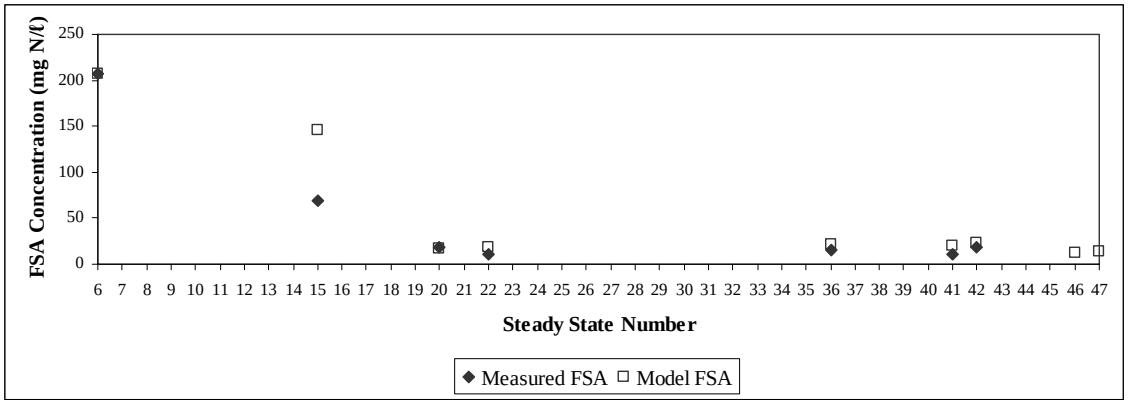

Figure 6.18: Measured and predicted effluent FSA concentrations for respective steady state sulphidogenic systems

As illustrated in Figure 6.19, the model is able to accurately predict the effluent TKN for steady state numbers 20, 22, 36 and 41. Effluent TKN values for steady state numbers 6 and 15 compare relatively well, whereas a larger deviation is apparent for steady state number 42. When comparing the model predicted and measured effluent TKN and FSA values for steady state number 15, it is evident that the model over-predicts the effluent FSA, but only has a 7.57% deviation from the experimental data for effluent TKN. This shows that the effluent nitrogen content of organisms and biodegradable particulate COD for TKN is inaccurate or under-predicted, and therefore implies that effluent organism concentration and biodegradable particulate COD is low. Once again, no measurements were recorded for steady states 46 and 47.

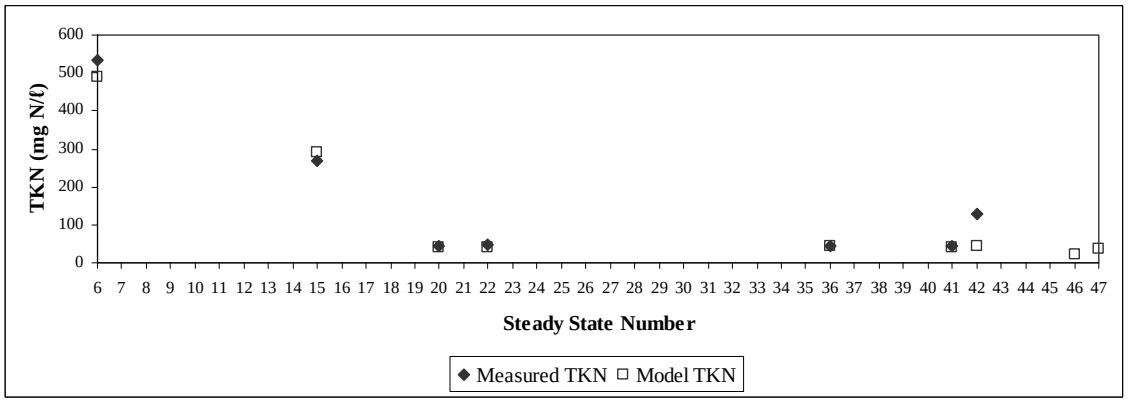

Figure 6.19: Measured and predicted effluent TKN for respective steady state sulphidogenic systems

6.5 SENSITIVITY ANALYSIS AND OPTIMISATION

6.5.1 Sensitivity analysis

Sensitivity of a given variable due to a perturbation of a given parameter will indicate which parameters need to be calibrated, in order to get accurate simulation outputs. For each steady state simulation in WEST, sensitivity analysis was performed on the model to identify and determine the model parameters that influence simulated outputs. The absolute and relative sensitivity of a given variable due to a change in the given parameter was calculated by using the sensitivity function in WEST. Upon analysing all the steady state sensitivity output data, it was clearly evident that the model outputs were most sensitive to the hydrolysis maximum specific rate constant ($k_{max,HYD}$) and half saturation constant ($K_{SS,HYD}$). This result is in agreement with Chapter 2, where it is noted that PSS hydrolysis is the rate-limiting step in the anaerobic digestion process with PSS as substrate.

6.5.2 Optimisation

In the simulations the value of the volumetric hydrolysis rate would vary from one simulation to another depending on the operating conditions and the amount of particulate organic matter fed into a given system. For the hydrolysis rate constants above, initial values of 650 g COD S_{bp}/mol Z_{AD}.d (4.95 mol S_{bp}/mol Z_{AD}.d) and 630 g COD S_{bp}/mol Z_{AD} (4.798 mol S_{bp}/mol Z_{AD}) for $k_{max,HYD}$ and $K_{SS,HYD}$ respectively were obtained from the UCT Group, who determined these values from initial simulations of the Izzett *et al.* (1992) data set. The next step involved determining for each system simulated the values for these kinetics parameters that would best describe the effluent effectively. This was achieved by using the optimiser function in WEST whereby model parameters are adjusted to fit the model output to the experimental data set. The "end-value optimisation" in WEST is best suited to steady state simulations and was performed for each steady state system discussed above. The "cost" variable selected for optimisation of hydrolysis kinetic parameters was effluent total COD. This cost variable was minimised by minimising the sum of squared errors between the model output and measured values of effluent total COD, by optimising the hydrolysis kinetic constants. No optimisation was performed on the pilot-plant (see below) since the effluent total COD was not measured. Table 6.5 lists the hydrolysis kinetic parameters for all steady state systems (methanogenic and sulphidogenic) derived from the model optimisation, and these are plotted in Figures 6.20 and 6.21 for the maximum specific hydrolysis rate and half saturation coefficient respectively.

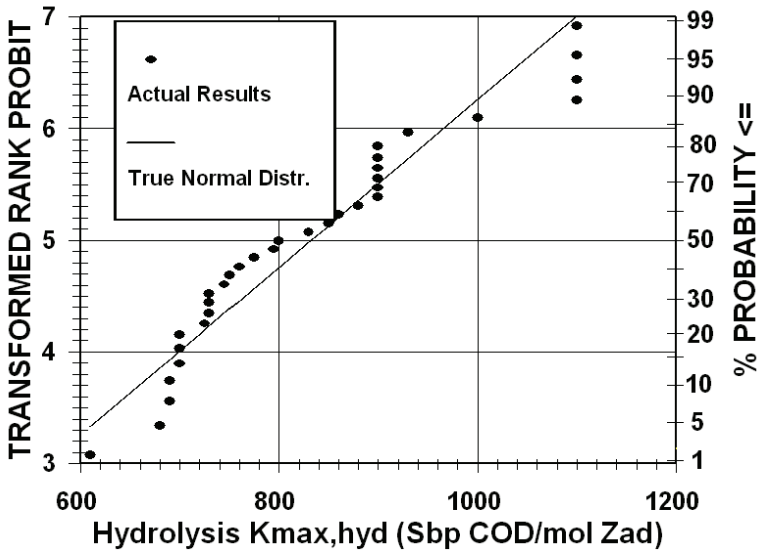

Figure 6.20: Statistical plot of hydrolysis maximum specific rate constant ($K_{max,HYD}$) for all steady states simulated (methanogenic and sulphidogenic), determined from optimisation

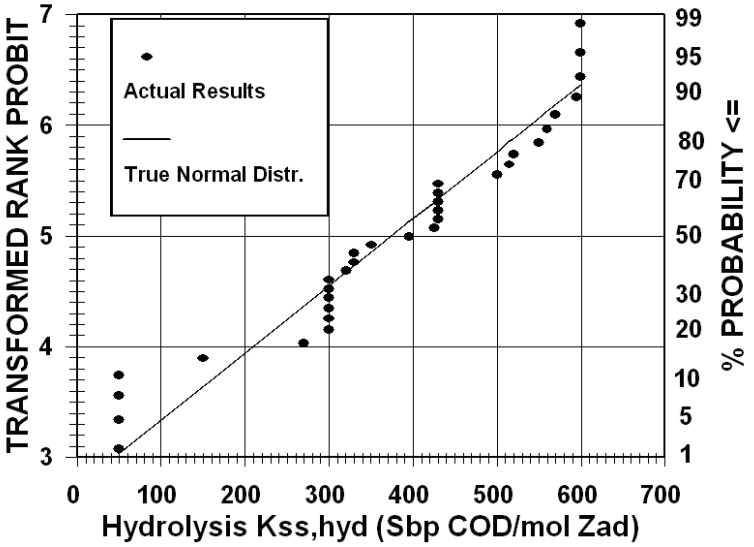

Figure 6.21: Statistical plot of hydrolysis half saturation coefficient ($K_{SS,HYD}$) for all steady states simulated (methanogenic and sulphidogenic), determined from optimisation

Table 6.5: Results of optimisation performed on hydrolysis kinetic parameters from the model for each steady state system; maximum specific rate ($K_{Max,HYD}$) and half saturation coefficient ($K_{SS,HYD}$)

Steady state number	$k_{max,HYD}$ (g COD S_{bp}/mol Z_{ai}.d)	$K_{SS,HYD}$ (g COD S_{bp}/mol Z_{ai})
1	900	300
2	900	300
3	900	300
4	1100	50
5	900	300
6	900	300
7	700	570
8	745	550
9	795	520
10	725	560
11	690	600
12	610	600
13	700	595
14	690	600
15	830	330
17	1100	50
18	1100	50
19	1100	50
20	730	430
21	800	395
22	730	430
23	860	320
24	850	350
25	700	500
26	930	270
27	880	330
28	775	425
31	680	515
36	730	430
41	760	430
42	750	430
46	1000	150
47	900	300

Referring to Figures 6.20 and 6.21 and Table 6.5, it is apparent that (i) there is considerable consistency in the optimised hydrolysis kinetic constants across virtually all steady states, (ii) for both constants no difference is apparent between the values for the methanogenic and sulphidogenic systems as concluded in Chapter 2, (iii) there does appear to be some grouping of constants according to feed batch number, but this is not sufficiently significant to be confirmed statistically; this grouping may be due to using a single influent unbiodegradable particulate COD fraction for all feed batches (and hence changing the hydrolysis constants), whereas it would be expected that the unbiodegradable particulate fraction would vary slightly for different feed batches. For the maximum specific hydrolysis rate ($K_{max,HYD}$) and half saturation coefficient ($K_{SS,HYD}$), mean values were 832 g COD S_{bp}/mol Z_{AD}.d and 374 g COD S_{bp}/mol Z_{AD} respectively, with standard deviations of 134 and 165 respectively. Converting units gives means of 5.2 g COD S_{bp}/g COD Z_{AD}.d and 2.4 g COD S_{bp}/g COD Z_{AD} respectively, which are very close to the values of 3.5 and 1.7 derived in Chapter 4 for the methanogenic steady states by "eye fit", providing substantive support for the approach used to describe the hydrolysis process.

6.6 MODIFICATIONS TO THE REACTION KINETICS

In merging the sulphate reduction processes (Chapter 5) with the methanogenic anaerobic digestion model (Chapter 4) one issue of importance identified was pH and H_2S inhibition. The UCTADM1 methanogenic reactions did not consider H_2S inhibition, since H_2S is not present in the absence of sulphate reduction. The Kalyuzhnyi *et al.* (1998) model from which the bioprocesses for sulphate reduction were extracted (Chapter 5) included pH inhibition in the form of a bell-shaped pH function. However, the model version of Kalyuzhnyi and Fedorovich (1998) did not explicitly consider pH inhibition because it is difficult to distinguish between the effects of pH and H_2S inhibition experimentally: H_2S is present in solution as H_2S and HS^-, and only the H_2S form appears to be toxic to the micro-organisms. As the pH drops, HS^- is progressively converted to H_2S, and this occurs chiefly in the pH range where pH inhibition becomes significant. Hence the H_2S inhibition coefficients in the Kalyuzhnyi and Fedorovich model implicitly contain the pH inhibition effect also. For H_2S inhibition of the methanogenic digestion processes it was decided to adopted the reaction scheme used by both Kalyuzhnyi *et al.* and Kalyuzhnyi and Fedorovich for both sulphidogenic and methanogenic organism groups, because it would provide a proper balance between the two sets of biological reactions, in particular with a consistent set of inhibition terms applied to all the reactions.

However, when this was implemented, as noted in Chapter 5 a problem was found with the form of the H_2S inhibition terms used by Kalyuzhnyi *et al.* and Kalyuzhnyi and Fedorovich, which is $1-\frac{[H_2S]}{K_I}$ where K_I is the inhibition coefficient. Where the H_2S concentration becomes higher than K_I, the inhibition term becomes negative, which causes the reaction to reverse.

To overcome this problem, the form of the inhibition term was changed to:

$$\exp\left(-\left(\frac{[H_2S]}{0.6063K_I}\right)^2\right) \qquad (6.9)$$

The factor 0.6063 was chosen to get the two inhibition functions to match at the 50% inhibition point using the same value of K_I, as illustrated in Figure 6.22. The pH inhibition terms for the non-sulphidogenic reactions in UCTADM1 (Chapters 4 and 5) were deactivated by setting the coefficients to very high values. In simulating the steady state laboratory-scale systems above, neither pH not H_2S inhibition was experienced, due to the pH values obtained and the low influent

sulphate concentrations fed in operation. However, for application to the Erwat Ancor pilot-plant (see below) these effects may be important and accordingly were included.

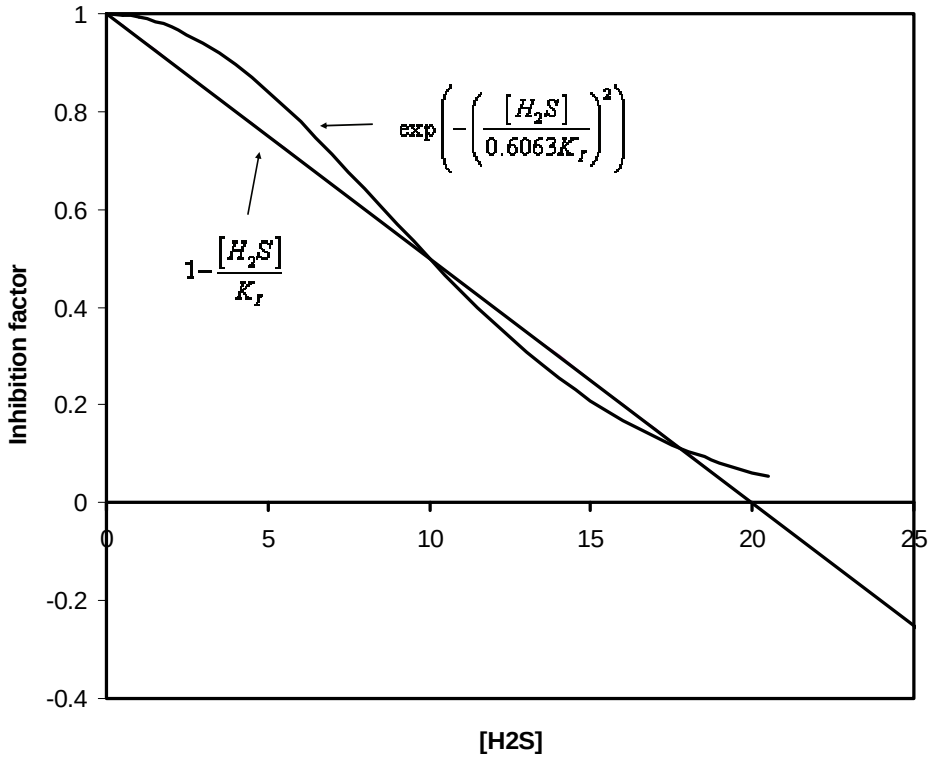

Figure 6.22: Comparison of inhibition factor forms.

A further difficulty in including pH inhibition is that it is not clear whether the inhibition is due to pH itself, or due to the action of specific weak acid/base species (e.g. undissociated acetic acid, HAc) the concentration of which changes as the pH changes. Elucidation and separation of the various pH inhibition effects requires further investigation.

6.7 MODELLING THE ERWAT ANCOR PILOT PLANT

Having successfully applied the WEST implementation of the combined methanogenic and sulphidogenic anaerobic digestion model to the laboratory-scale digesters described in Chapter 2, the model was applied to the pilot-scale BioSURE® system at Erwat's Ancor treatment plant (Springs, South Africa). The pilot plant had only been in operation for a short time due to a change in the biological sulphate reduction reactor from the recycling sludge bed reactor (RSBR) to the upflow anaerobic sludge bed (UASB) configuration, and various equipment failures, and hence the available data was minimal. Figure 6.23 contains all the information that has been supplied by Dr. Ristow, including estimated values and qualitative statements. It is also not known how representative or reliable the values are. Consequently the model application presented here must be considered as very much a preliminary one, and any specific conclusions can only be regarded as tentative.

6.7.1 Reactor configuration

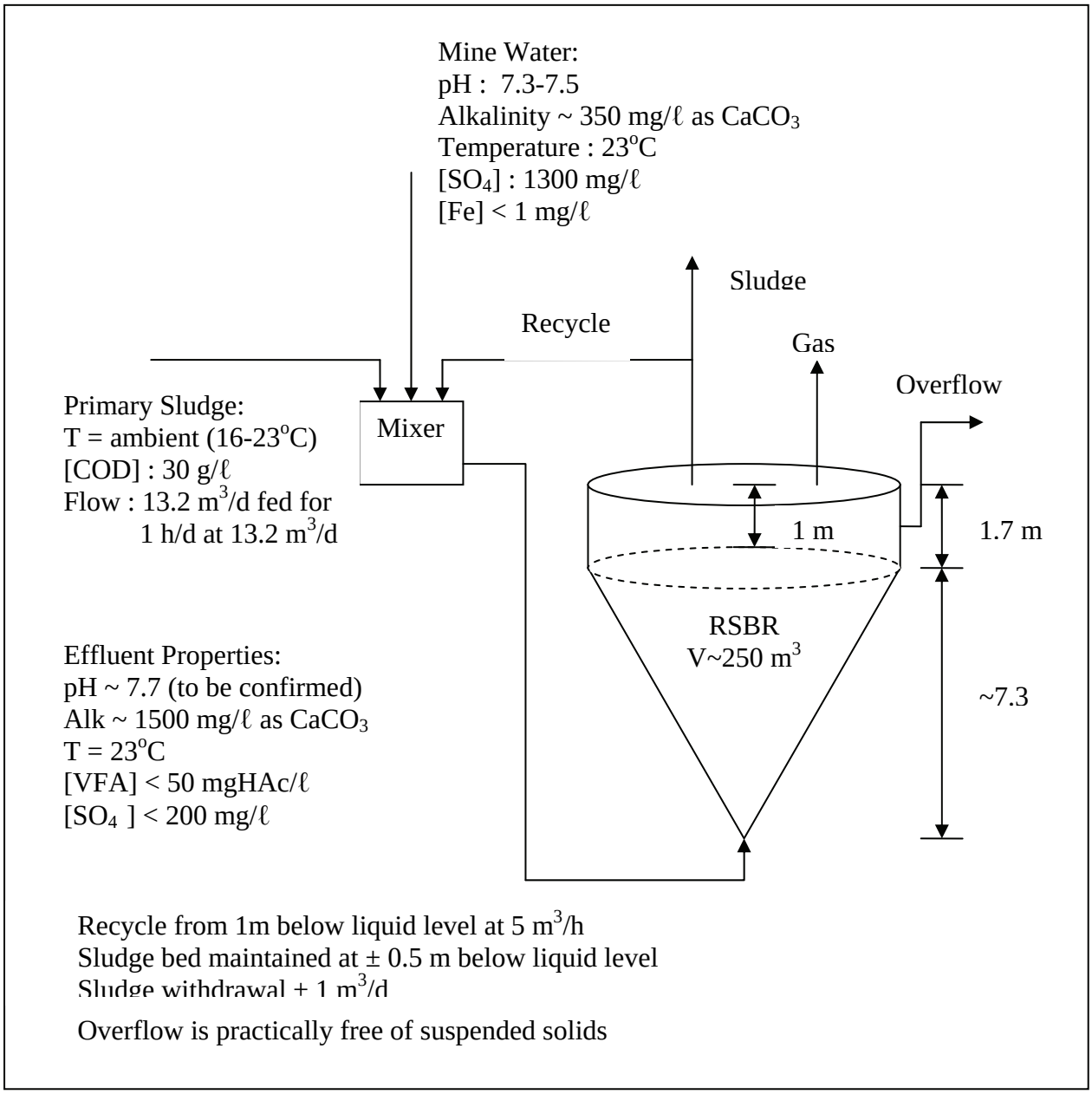

Figure 6.23: Configuration and operating data for the Erwat Ancor pilot-plant reactor.

The reactor has an UASB (upflow anaerobic sludge blanket) configuration with recycle of sludge from a point 1m below the level of the clarified liquid (i.e. from the top of the sludge blanket) to the influent, following the recommendations from the feasibility study in Chapter 3. Sludge wasting to maintain the sludge bed volume and prevent sludge overflow to the effluent was from the recycle line. The most significant characteristic of the UASB configuration is the separation of particulates from the overflow effluent and their retention in the reactor. This was simply modelled by providing the reactor with three outlets (overflow, recycle and gas), and creating two additional parameters, fraction of feed that is recycled and ratio of particulate concentration in overflow to particulate concentration in reactor. The latter concentration ratio was set to a very low value (0.0001) to represent the statement that the "overflow is practically free of solids".

The representation of the reactor configuration in WEST is shown in Figure 6.24.

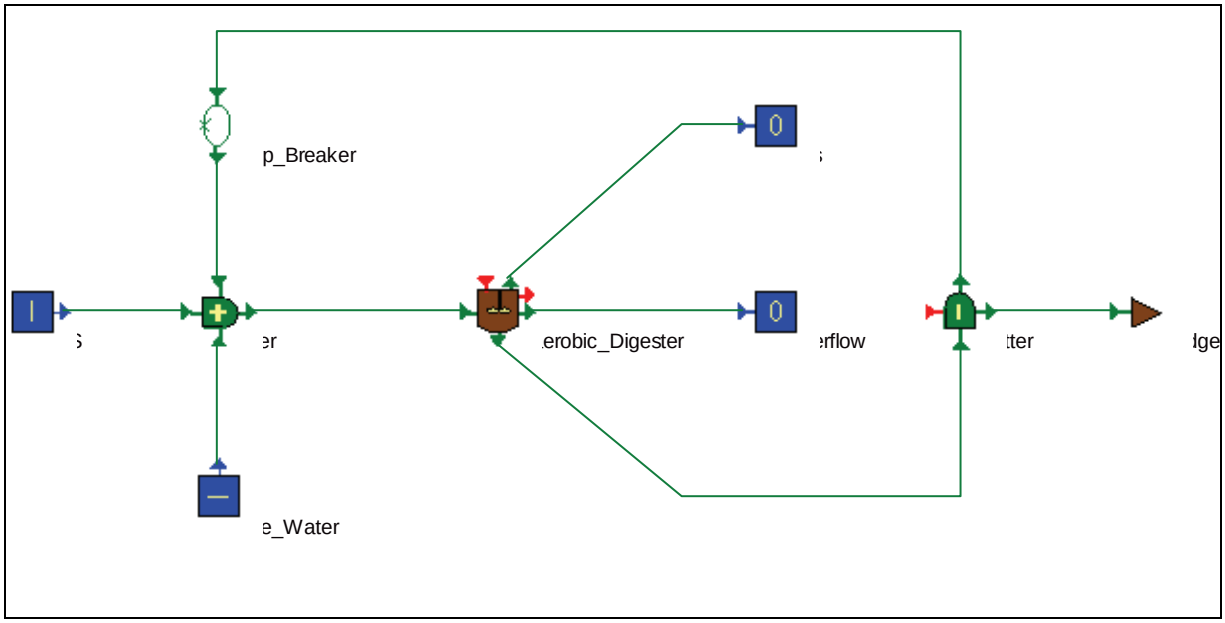

Figure 6.24: Configuration of the Erwat Ancor pilot-plant reactor model in WEST.

6.7.2 Model kinetic parameters

As discussed in Section 6.6, it was decided to use the modified H_2S inhibition term in this model implementation. For the kinetic and stoichiometric parameters, the parameters in Tables 6.2 and 6.3 describe the values at 35 °C instead of at 23°C which is the operating temperature for the pilot-scale plant, and which means that the kinetic rates will be substantially too high. Lacking a complete set of temperature dependence data for the processes, it was decided to reduce all the kinetic rate coefficients by the same factor, which would maintain the relative relationships between them.

To establish the temperature dependency factor, it was noted that the ADM1 task team (Batstone *et al.*, 2002) concluded that the temperature changes in the rates of hydrolysis could be described by an equation of the form:

$$\frac{K_2}{K_1} = e^{\tau(T_2 - T_1)} \qquad (6.2)$$

A value of 0.0667 for τ was calculated from data at 35 ºC and 25 ºC provided by Gujer and Zehnder (1983).

6.7.3 Feed characterisation

As can been seen in Figure 6.21, only the total COD concentration is known for the primary sewage sludge (PSS) feed, and only the sulphate concentration and alkalinity for the mine water feed. The remainder of the feed characteristics had to be constructed from assumptions. This section explains the basis of these constructions: the feed characterisation results are summarised in Appendix B, and detailed by Rajkumar (2006).

6.7.3.1 COD Fractionation

Measured and calculated values of the various components of the feed and effluent COD measurements (in mg cod/ℓ) were obtained from Chapter 2 and Ristow *et al.* (2005a).

From Section 6.3.2.3 Equation 6.1, the total COD balance on the influent is:

$$S_{ti} = S_{upi} + S_{bpi} + S_{usi} + S_{bsfi} + S_{VFAi} \quad (6.10)$$

From Chapter 2, assumptions accepted were:

(1) $$S_{upi} = 0.3345 \times S_{ti} \quad (6.11)$$

This accepts that the unbiodegradable particulate COD (S_{upi}) fraction for the Erwat Ancor PSS is the same as that derived in Chapter 2 and accepted in simulation of the UCT laboratory experiments (Section 6.3.2.3) for the Athlone PSS. This is not unreasonable, since the independent data of O'Rouke (1968) gave a very similar value (Chapter 2), and both agree with the values expected from a mass balance around a primary settling tank (Chapter 4).

(2) $$S_{bsfi} = S_{VFAi} \quad (6.12)$$

This seems reasonable from the experimental observations of Lilley *et al.* (1993) and Ristow *et al.* (2005a).

(3) COD/Glucose fraction = 1.0656835 (6.13)

This is the theoretical COD of glucose.

From Chapter 2 and Section 6.3.2.3, the equations utilised to obtain unknown influent COD fractions were:

$$S_{upi} = 0.3345 \times S_{ti} \quad (6.14)$$

$$S_{usi} = S_{us}(Effluent) \quad (6.15)$$

$$S_{bsi} = S_{si} - S_{usi} \quad (6.16)$$

where $$S_{bsfi} = S_{VFAi} = \frac{S_{bsi}}{2} \quad (6.17)$$

$$S_{bpi} = S_{ti} - S_{upi} - S_{si} \quad (6.18)$$

By utilising the influent flowrate to the reactor, all COD fractions were converted from concentration units of mg cod/ℓ to flux units of g cod/d, except that of S_{bsfi} which was converted to flux units of g/d by additionally dividing by the COD/Glucose fraction.

6.7.3.2 H^+ and OH^-

Since the PSS was obtained directly from the Erwat Ancor primary settling tanks without being stored prior to feeding, a pH value of 7 was accepted for the PSS. For the AMD, the measured pH was accepted. The calculation of the hydrogen and hydroxyl ion influx was based on the blended influent pH, via Equations 6.2 and 6.3 respectively with equilibrium constants at 25°C. The molar concentrations were converted to flux units (g/d) by multiplying with the reactor flowrate and their respective molecular weights.

6.7.3.3 Volatile Fatty Acids (VFA)

The species which form the VFA component are HPr (propionic acid), Pr^- (propionate), HAc (acetic acid) and Ac^- (acetate). These species were fractioned from the VFA component of COD as described in Section 6.3.2.3, with equilibrium constants at 25°C. The molar concentrations of the species that make up the VFA component were converted to flux units (g/d) by multiplying with the reactor flowrate and their respective molecular weights.

6.7.3.4 Free and Saline Ammonia (FSA)

The PSS influent FSA value of 39 mg N/ℓ was accepted from the measured data for steady state number 6 above, since this steady state closely matched the COD of the PSS fed to the pilot-plant. The calculation of ammonia and the ammonium ion influx was based on the influent FSA (mg N/ℓ) together with the ammonium ion equilibrium constant at 25°C, Equations 6.4 and 6.5. The molar concentrations of NH_3 and NH_4^+ were converted to flux units (g/d) by multiplying with the reactor flowrate and their respective molecular weights.

6.7.3.5 Alkalinity

For the PSS, the influent alkalinity was assumed to be 300 mg/ℓ as $CaCO_3$ to correspond with typical measurements on sewages influents and the pH of 7. For the AMD, the measured alkalinity was available. The carbonate system CO_3^{2-}, HCO_3^- and H_2CO_3 influxes were determined from the influent alkalinity (mg/ℓ as $CaCO_3$) together with the equilibrium constants for the carbonate system at 25°C, Equations 6.6 to 6.8. The molar concentrations of CO_3^{2-}, $HCO3^-$ and H_2CO_3 were converted to flux units (g/d) by multiplying with the influent flowrate and their respective molecular weights.

6.7.3.6 Sulphate

The AMD influent sulphate concentration was available from measurement (1 300 mg/ℓ) and due to the high pH was accepted to be all in the SO_4^{2-} form. The PSS was accepted to have no influent sulphate, due to sulphate reduction in the sewer system.

6.7.4 Model application

The initial model, applied as described above seemed to exhibit too great a biological reduction of SO_4 compared to the data given in Figure 6.23. Although the effluent SO_4 concentration is not given specifically (only specified as < 200 mg/ℓ), the alkalinity of the effluent also provides some guidance, because generated sulphides contribute to alkalinity, and the simulated alkalinity at 1800 mg/ℓ was higher than the measured value of 1500 mg/ℓ. Experience with anaerobic digestion at temperatures around 23°C in WRC project K5/1248 and the experiments described in

Chapter 2 indicate that hydrolysis is the rate limiting process, so the hydrolysis rate constant in the model ($K_{max,HYD}$) was adjusted from the initial value of 4.1 g cod S_{bp}/g COD Z_{AD} at 35 ^{o}C to 1.83 at 23^{o}C and then to 0.34, to match the overall SO_4 conversion as evidenced by the measured effluent SO_4 and alkalinity concentrations. Table 6.5 summarises the comparison between the model outputs and the available data; the correspondence is reasonably close.

Table 6.6: Comparison between pilot plant measurements at simulated values.

Determinand	**Pilot Plant**	**Model**
Effluent pH	~ 7.7 (not confirmed)	7.4
Effluent SO_4 (mg/ℓ)	< 200	189
Effluent alkalinity (mg/ℓ as $CaCO_3$)	1500	1655
Effluent VFA (mg/ℓ as Acetic acid)	< 20	3

An issue which is not possible to resolve at present is the *state of the micro-organism groups in the reactor*. The external reaction mass balance is dependent on the concentrations of the various populations of micro-organisms that have built up in the reactor. This in turn depends on the seeding of the reactor at start-up, and its operational history thereafter. It is not possible to infer this from the snapshot of reactor data that is currently available. The model results were generated by allowing the populations to reach steady state, by running the model for a simulated period of 200 days, starting from very low concentrations of all the organism groups. The simulations therefore represent an equilibrium population, which is not likely to have been achieved in reality in the pilot-plant due to the relatively short period of operation; however there is no information on how the real population might deviate from equilibrium.

6.7.5 Conclusion

Clearly, the model application to the pilot-plant is preliminary and relies on a number of assumptions; however it is the best that could be achieved with the information available. Nevertheless, it establishes the model at a similar stage of development to that of the pilot plant itself, which provides an opportunity for the modelling and experimental programmes with the pilot-plant to evolve together and mutually reinforce each other.

6.8 INVESTIGATION OF OPERATING SCENARIOS USING THE MODEL

Since the pilot-plant is still in the stage of ironing out equipment teething problems, not much is known about process related issues. The model provides an extremely useful tool to explore various scenarios, to select the more promising for experimental evaluation. Accordingly, the model was used to explore the effects of changing the ratio between PSS and AMD fed to the reactor.

The preliminary nature of the model calibration, as reported in Section 6.7, means that the reliability of results of this section of the investigation is unknown, and these results should only

be taken as indicating qualitative trends. Nevertheless, discussions with Dr. Ristow have confirmed that certain important features of the model that have emerged while simulating various scenarios correctly reflect qualitative observations on the pilot plant:

1. The process seems to be quite resilient in the face of upsets. In particular, it does not seem to suffer from the pH related instabilities typical of methanogenic anaerobic digestion.
2. Production of methane is negligible under the current operating conditions.
3. H_2S inhibition is not an important factor under the current operating conditions.

6.8.1 Qualitative characteristics of the model

A simplified conceptual view of the model is useful for qualitative understanding of its behaviour. The rate limiting process is the first step of hydrolysing the particulate biodegradable COD (the PSS), and thus the dominant factor determining the model's characteristics. Once the substrate has been solubilised, the methanogenic and sulphate reducing populations of micro-organisms compete for it, and the outcome of this competition determines the second level of characteristics, i.e. how much COD goes into sulphate reduction, and how much into methane production. Issues such as H_2S inhibition fall into a third level, and do not seem to be significant under the conditions experienced by the pilot plant.

6.8.2 Investigation of the COD/SO4 feed ratio

It is assumed here that the sulphate rich acid mine drainage water is in excess, so that obtaining the maximum sulphate reduction for the COD used is desirable. Under this assumption there is still a compromise to be made between the effluent quality of the treated water and the load of sulphate removed. If the treated water is to be discharged to a receiving body, the load is the important criterion, whereas if it is to be reused, the quality is relevant. In considering the latter option, it is assumed that there is a follow up process to remove the sulphide generated, so that the water quality can be expressed in terms of the residual sulphate concentration. The model was run with a mine water flowrate of 230 m^3/d (the same as the nominal feed rate to the pilot plant), and a range of sludge flow rates from 5.28 to 26.4 m^3/d (the current nominal feed rate to the pilot plant is 13.2 m^3/d).

The results are summarised in Figure 6.25 which plots ratios representing the effluent quality and the COD utilisation against the ratio of COD to SO_4 fed.

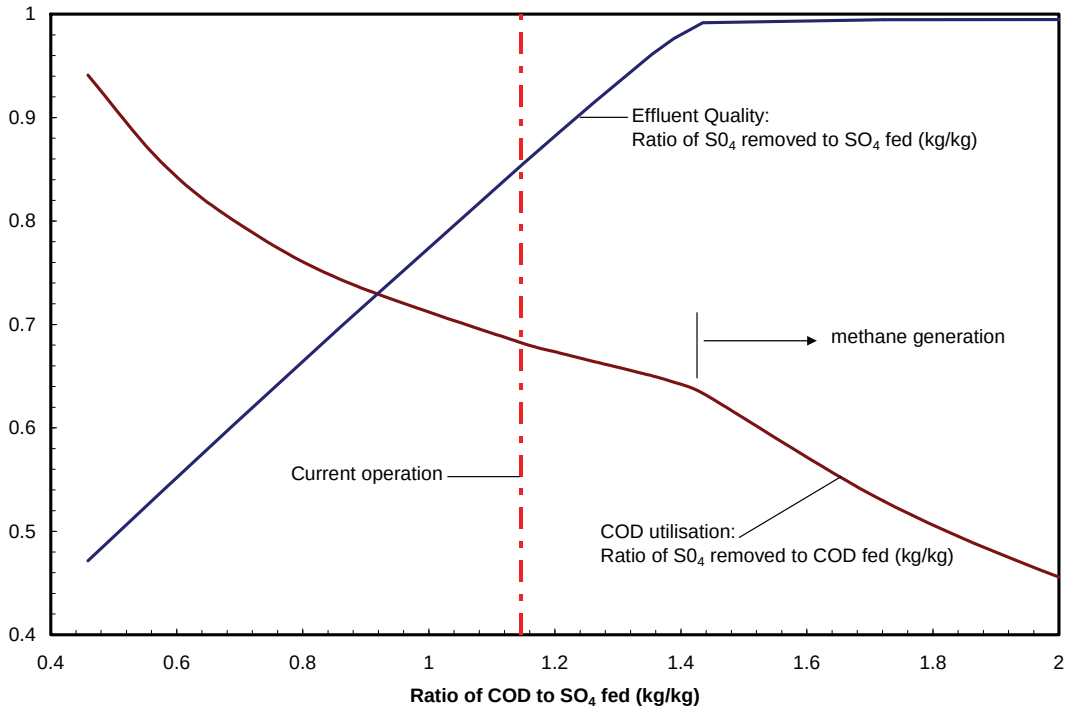

Figure 6.25: Simulated SO_4 removal and COD utilisation ratios for varying sludge feed rate

The lower the ratio of COD to SO_4 of the feed, the more SO_4 is reduced by a given amount of COD. The model predicts that this trend continues with stable operation down to much lower COD / SO_4 ratios than current operation; this may or may not be realistic. The SO_4 removal ratio increases almost linearly up to almost complete removal. This is a consequence of the reactions being limited by the PSS hydrolysis rate. The model predicts practically no methane generation until the residual SO_4 runs out.

In the series of simulations reflected in Figure 6.25 the AMD feed rate was held constant while the PSS feed rate was varied in order to vary the feed COD / SO_4 ratio. The ratio could also be altered by holding the PSS feed rate constant and varying the AMD feed rate. This gives a different system response, as shown in Figure 6.26.

In this case the effluent quality responds much as before, but the SO_4 removed/COD utilisation ratio remains effective constant until the residual SO_4 runs out. This is again a consequence of the limiting PSS hydrolysis rate; since the sludge residence time is held constant, the reaction rate remains constant.

Figures 6.25 and 6.26 tend to obscure the effect of the limitation of reactor volume, although it is implied in the results, and is part of the explanation as to why the two plots differ. When designing a system, the reactor size would be a variable, which adds a degree of freedom to the system response. The above diagrams should be seen as examples of how the model could be used, rather than as definitive characteristics of the process, particularly in view of the uncertainties in the kinetic parameter values.

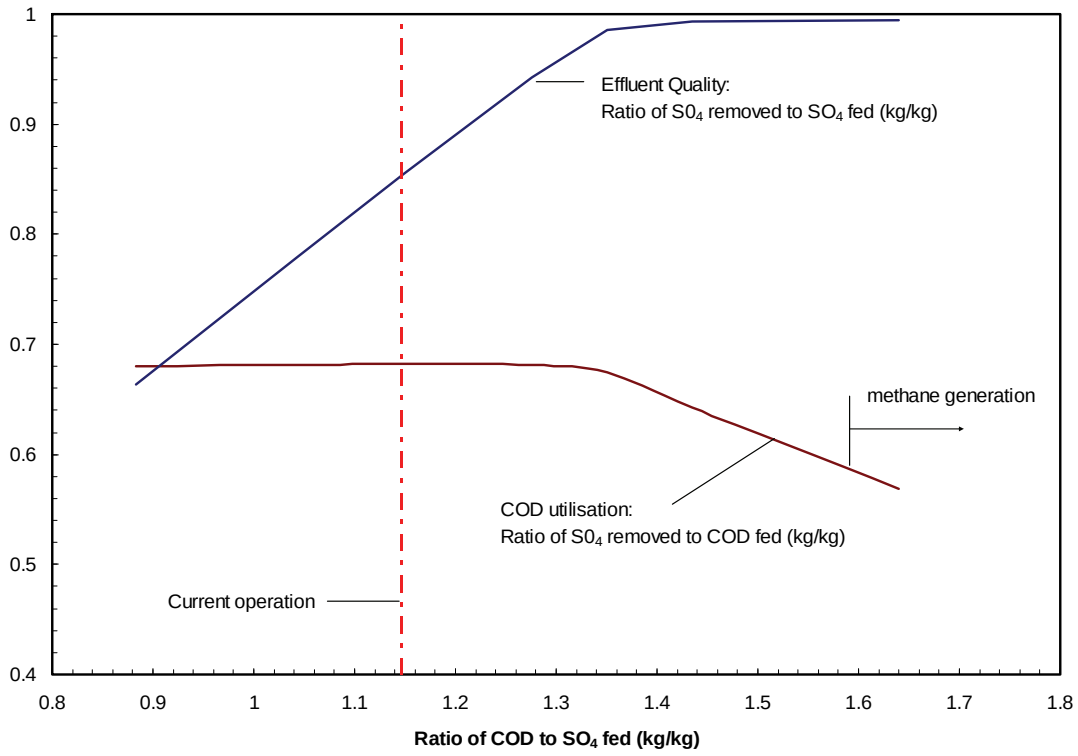

Figure 6.26: Simulated SO_4 removal and COD utilisation ratios for varying mine water feed rate

6.9 AREAS FOR FURTHER RESEARCH

The most obvious needs for further research are to reduce the uncertainties in the kinetic parameters values that are appropriate for the operating conditions of the pilot plant, and to obtain information on the hydraulic separation process that retains sludge in the reactor.

6.9.1 Reaction kinetics

The most important aspects of the operating conditions seem to be:

- Operating temperatures around 20°C rather than 35°C.

  Temperature dependences are available for the normal anaerobic digestion reaction rates, but not for the sulphidogenic reactions. However, the approximate and interactive nature of the model makes it probable that the entire set of reaction parameters needs to be determined together, rather than attributing an independent reality to any subset.

- Feed concentrations for sludge (as COD) and minewater (as SO_4) around 1.5 g/ℓ.

  The issue here appears to be the inhibitory effects of H_2S (and possibly pH). At these feed concentrations the H_2S levels are much lower than those that were encountered in the some of the laboratory studies, but are the same as in most of the lab studies.

- Separate regulation of the sludge residence time and the hydraulic residence time in the reactor.

This would provide the clearest confirmation of the extent to which hydrolysis is the dominant limiting process in the reaction scheme.

The conventional way of addressing this need would be to embark on a comprehensive programme of laboratory experiments similar to that in Chapter 2 and described in detail by Ristow *et al.* (2005a). Although the ultimately efficacy of this approach is proven, the requirements in terms of time, expense and experimental effort are known to be high.

The exercise of applying the model to the pilot plant operation has demonstrated that that it is not necessary to know all the parameters to the same degree of accuracy, and that it may well be that only a small number of them are critically important. Clearly the experience of the actual pilot plant operation is the best source of information for determining which the critical parameters are.

With the variability and contingencies of pilot plant operating conditions, it may not always be possible to determine kinetic parameters accurately, and laboratory tests might be needed to complement the pilot plant data. Here the *serum bottle tests* which have been extensively developed as part of WRC Project K5/1075 could be useful. They are relatively rapid and inexpensive, and, while not able to provide comprehensive data about a process, can be tailored to investigate specific questions by spiking the test mixture with specific components.

6.9.2 Hydraulic separation

The pilot plant reactor uses settling of the sludge to retain sludge in the reactor and produce a clarified effluent. Lacking any information on the settling characteristics of the sludge, this is represented in the current model as a single parameter which sets the ratio between the sludge concentration in the effluent and the reactor, which was set to an arbitrarily low value (0.0001) based entirely on qualitative observation of the clarity of the effluent under current operating conditions.

In reality the retention ratio must be a function of the settling characteristics of the sludge and the flow regime in the reactor, and it sets important operating conditions and physical constraints for the reactor operation which are not currently represented in the model. These relate to the biomass concentration in the reactor and the sludge retention time. In operating the pilot plant sludge withdrawal rate is set so as to maintain the sludge level in the reactor and prevent it overflowing into the effluent. In the model simulations presented here, the sludge withdrawal flow rate was set at 1 m^3/d, the value estimated by the operators for current operation. It is quite likely that this rate would need to be adjusted to maintain the sludge separation when varying the feed rates to the reactor.

6.10 CONCLUSIONS AND RECOMMENDATIONS

The situation of having a model and a pilot plant investigation at a similar stage of development provides an opportunity for the modelling and experimental programmes to evolve together and mutually reinforce each other. Thus the model could be used to explore gaps in the understanding of the process and suggest experiments to be tried on the pilot plant. The data from the pilot plant can then be fed back to improve the model. This is the basic strategy of *optimal experimental design* as outlined by Dochain and Vanrolleghem (2001). What is novel here is the opportunity to apply the technique to such a large scale reactor, and it may represent a significant advance in the practice of piloting biological treatment processes, which frequently only confirm the operability of a process and add little to the scientific knowledge of the process.

Thus it is strongly recommended that the pilot plant investigation be supported by a simultaneous modelling investigation. To be fully effective, this should have a strong interaction with the experimental work. Theoretically this would be best achieved if the modelling and experimentation were carried out by the same team, but it could also be carried out by separate teams as long there is sufficient communication between them.

7 DISCUSSION AND FUTURE WORK

7.1 DISCUSSION

In this research project the main objective has been to develop a kinetic model for the core unit process in BioSURE® and similar systems, of biological sulphate reduction (BSR) with primary sewage sludge (PSS) as substrate. This model was to serve as an aid to the design, operation and control of sulphidogenic anaerobic digestion systems. More fundamentally, it was to serve as a research tool to improve understanding of the underlying processes and their interactions.

Development of the BSR kinetic model required initial extensive experimental investigations, to gather data on the biological, chemical and physical processes involved in methanogenic and sulphidogenic anaerobic digestion of PSS. The experimental data also would serve as a basis for calibration and validation of the kinetic models developed. The experimental investigation quantified and compared the rate of PSS hydrolysis (the rate limiting step) under methanogenic, acidogenic and sulphidogenic conditions. The rates under methanogenic and sulphidogenic conditions have been found to be similar, but the rate under acidogenic conditions was significantly reduced. This implies that the end products of acidogenesis inhibit the PSS hydrolysis step, but if these are removed through either methanogenesis or sulphidogenesis this inhibition is alleviated. Importantly from this comparison, since the rates under methanogenic and sulphidogenic conditions are closely similar, the model structure and kinetics developed for PSS hydrolysis can be applied under both sets of conditions, i.e. can be common.

The experimental investigation also encompassed a feasibility study to evaluate the UASB reactor configuration for BSR with PSS. By passing the entire feed through the sludge bed in the UASB system, contact between the PSS and sulphate is enhanced so that PSS hydrolysis and sulphate reduction processes occur concomitantly in the sludge bed, with no short-circuiting of the sulphate as may happen in recycling sludge bed type reactors. Furthermore, the UASB configuration should facilitate solids removal, allowing improved uncoupling of the solids and hydraulic retention times, leading to higher sulphate loading rates and reduced reactor volumes. The feasibility study demonstrated that the USAB reactor configuration is a worthwhile option for the treatment of sulphate-rich waters, but that this system requires more intensive investigation to delineate the principle design and operational parameters.

Simultaneously to the experimental investigation, model development was initiated. This development was in stages, with the underlying approach of developing a more general model structure that has wider potential application to anaerobic digestion systems. First, a two phase (aqueous/gas) integrated chemical, physical and biological processes model describing the kinetics of methanogenic anaerobic digestion of sewage sludges was developed. In this model, by incorporating the kinetics of weak acid/base chemistry, pH is included (via H^+) as a predictive parameter. This facilitated including the effect of the biological processes on the pH, and *visa versa*.

The model follows a novel approach to characterising the influent PSS, principally in terms of parameters usually or readily measured on sewage sludges (e.g. COD, TKN) and of the sewage sludge CHON composition, which can be readily determined from the measurements and model application to experimental data or elemental analysis. This approach allows COD, C and N mass balances to be set up over the digester. In the model, various formulations for the PSS hydrolysis rate were evaluated and, based on its widespread application in activated sludge systems treating

the same particulate organics, surface reaction (Contois) kinetics selected for this rate limiting process. The model has been successfully calibrated principally with values for constants extracted from the literature, but also through application to experimental data sets from the literature and gathered in this research project. The methanogenic kinetic model development demonstrated that the integration in a kinetic manner of the two phase mixed weak acid/base chemistry, physical and biological processes provides a sound basis for further model development, in particular the integration of BSR and related processes.

Having completed the methanogenic anaerobic digestion model, the focus shifted to development of the BSR kinetic model by the UCT Research Group, and its implementation in the WEST platform by the UKZN Research Group. For this model, the methanogenic anaerobic digestion model served as the basis, to be extended to include BSR. This required identification of the kinetics and stoichiometry for the biological, chemical and physical processes associated with BSR in two phases (aqueous/gas). The biological processes were extracted from the literature, and the associated chemical and physical BSR biological processes delineated. Values for the required constants also were obtained from the literature.

The developed methanogenic and BSR kinetic models were implemented in WEST by the UKZN Research Group. It was envisaged that, if developed early enough, the models could be used to inform the experimental programmes at UCT and on the ERWAT Ancor pilot scale plant. However, the scope of the UCT experimental programme expanded considerably, and the methanogenic digestion model proved more complex than originally thought, and these delayed the UKZN Research Group acquiring the required information for model implementation timeously. The methanogenic anaerobic digestion model has been implemented in WEST and the implementation verified through correspondence between AQUASIM and WEST predicted results (which also provide a cross-check on the AQUASIM version). The WEST versions of the two models have been applied with success to the laboratory scale data collected at UCT on methanogenic and sulphidogenic anaerobic digestion respectively. The BSR kinetic model then was applied to the ERWAT Anchor pilot plant. Unfortunately, only limited data were available for this pilot plant, due to the change in reactor configuration to the UASB, following from the feasibility studies above. Considering the limited data available, the WEST model was able to simulate the pilot plant performance reasonably well. The model was used to evaluate operating scenarios for the pilot plant, and this demonstrates the usefulness of such a model. The model and experiments on the pilot plant can evolve mutually to provide a cross flow of information between the modelling exercise and pilot plant operation.

From the discussions above, it is evident that the principle objective of this research project, namely development of a kinetic model for BSR with PSS has been achieved. The model has been implemented in WEST (and is currently being implemented in AQUASIM), and successfully applied to the laboratory scale systems and the ERWAT Ancor pilot plant. Furthermore, the model has been applied to investigate preliminary operational scenarios for the pilot plant. However, the model has not yet reached a state of finality which would allow it to be used for design. This requires model refinement, in collaboration with the pilot plant operation.

7.2 FUTURE WORK

From these investigations, the following recommendations can be made:

- The experimental investigation on the feasibility of the UASB system for BSR with PSS has indicated that this system holds considerable promise. However, a more detailed

investigation is required to identify the principle design and operational parameters. In this investigation, the effects of sludge bed recycling need to be examined.

- The methanogenic anaerobic digestion model developed at UCT has been applied to steady state anaerobic digesters, with good correspondence between predicted and measured data. However, application to dynamic situations was limited to hypothetical exploration of the effects of digester failure. The predicted responses appear to correspond to anecdotal information from experience, but rigorous evaluation of the model under dynamic conditions has not been undertaken. Such an evaluation will be hindered by the lack of suitable experimental information.
- The BSR kinetic model developed at UCT requires implementation in AQUASIM. This will provide a cross-check of the WEST implementation, and will be undertaken at UCT in future research. The AQUASIM implementation will be evaluated by simulation of the data collected from sulphidogenic digesters in this research project.
- In the BSR kinetic model and its integration with the methanogenic digestion model, the effect of H_2S inhibition on the biological processes was included. However, in the application of the model implemented in WEST, the H_2S inhibition effects could not be evaluated since in the experiments simulated the H_2S concentrations were low. Limited experimental data on H_2S inhibition of the biological processes will hinder this evaluation.
- In application of the WEST model to the laboratory scale sulphidogenic systems, the methanogenic process were artificially restricted by making the initial methanogenic organism groups concentrations zero. This essentially removed competition between sulphidogens and methanogens in model application, clearly an undesirable result, since the model is structured to include such competition. This requires further investigation.
- In application to the pilot scale plant, the model in WEST and pilot plant implementation of the BioSURE system were recognised to be at similar stages of early development. It has been recommended that the model and experiments on the pilot plant evolve simultaneously to provide a mutually beneficial cross flow of information between the modelling exercise and pilot plant operation.
- The focus of this research project has been on BSR with PSS and the development of kinetic models for this system. The BSR has the main advantages of removing sulphate to low residual concentrations and generating alkalinity. However, the sulphate is reduced to sulphide which requires further treatment for sulphur recovery. One treatment train option for sulphur recovery is sulphide stripping with carrier gas, chemical oxidation of sulphide to sulphur by ferric iron, with the recovery of the ferric by biological oxidation. This sulphur recovery treatment proposal requires investigation, to evaluate its feasibility.

REFERENCES

ANDREASEN, K., PETERSEN, G., THOMSEN, H. AND STRUBE, R. (1997). Reduction of nutrient emission by sludge hydrolysis. *Wat. Sci. Tech.* **35**(10) 79-85.

BANERJEE, A., ELEFSINIOTIS, P. AND TUHTAR, D. (1998). Effect of HRT and temperature on the acidogenesis of municipal primary sludge and industrial wastewater. *Wat. Sci. Tech.* **38**(8-9) 417-423.

BANISTER, S.S. AND PRETORIUS, W.A. (1998). Optimisation of primary sludge acidogenic fermentation for biological nutrient removal. *Water SA* **24**(1) 35-41.

BARNARD (1984) Activated primary tanks for phosphate removal. *Water SA*, **10**(3), 121-126.

BATSTONE DJ, KELLER J, ANGELIDAKI I, KALYUZHNYI SV, PAVLOSTATHIS SG, ROZZI A, SANDERS WTN, SIEGRIST H AND VAVILIN VA (2002) *Anaerobic digestion model No 1*, Scientific and Technical Report (STR) No 13, International Water Association, London.

BRINCH, P.P., RINDEL, K. AND KALB, K. (1994). Upgrading to nutrient removal by means of internal carbon from sludge hydrolysis. *Wat. Sci. Tech.* **29**(12) 31-40.

BRYERS JD (1985) Structural modelling of anaerobic digestion of biomass particulates. *Biotech. & Bioeng.* **27** 638-649.

CAPRI M AND MARAIS GVR (1975) pH adjustment in anaerobic digestion. *Water Research* **9**(3) 307-314.

COUT D, GENNON G, RANZINI M AND ROMANO P (1994). Anaerobic co-digestion of municipal sludges and industrial organic wastes. In: Proceedings of the 7th International Symposium on Anaerobic Digestion. Johannesburg, South Africa.

CHRISTENSEN, B., LAAKE, M. AND LIENE, T. (1996). Treatment of acid mine drainage by sulfate-reducing bacteria: results from a bench scale experiment. *Wat.Res.* **30**(7) 1617-1624.

CORBETT, C.J., WHITTINGTON-JONES, K., HART, O.O. AND ROSE, P.D. (2000). Biological treatment of acid mine drainage wastewaters using a sewage sludge carbon source. Proceeding of the *WISA Biennial Conference*, Sun City, South Africa.

DEVAI, I. AND DELAUNE, R.D. (1999). Emission of reduced malodorous sulfur gases from wastewater treatment plants. *Wat. Environ. Res.* **71**(2) 203-208.

DOLD PL, EKAMA GA AND MARAIS GVR (1980) A general model for the activated sludge process. *Prog. Wat. Tech*. **12**(6): Tor 47-77.

EASTMAN JA AND FERGUSON JF (1981) Solubilization of particulate organic compounds during the acid phase of anaerobic digestion. *Journal WPCF* **53**(3) 352-366.

ELEFSINIOTIS, P AND OLDHAM, W.K. (1994). Anaerobic acidogenesis of primary sludge: The role of solids retention time. *Biotech. Bioeng.* **44** 7-13.

ELIOSOV B AND ARGAMAN Y (1995) Hydrolysis of particulate organics in activated sludge systems *Water Research* **29**(1) 155-163.

ENONGENE, G.N. (2003). The enzymology of enhanced hydrolysis within the biosulphidogenic Recycling Sludge Bed Reactor (RSBR). *PhD Thesis*, Rhodes University, Grahamstown, South Africa.

GUJER W AND ZEHNDER AJB (1983). Conversion processes in anaerobic digestion. *Wat. Sci. Tech*. **15**(8/9): 127-167.

HATZICONSTANTINOU, G.J., YANNAKOPOLOUS, P. AND ANDREADAKIS, A. (1996). Primary sludge hydrolysis for biological nutrient removal. *Wat. Sci. Tech.* **34**(1-2) 417-423.

HENZE M AND HARREMÖES P (1983) Anaerobic treatment of wastewater in fixed film reactor – A literature review *Water Sci. Technol.* **15** 1-101.

HENZE M, GRADY C P L, GUJER W, MARAIS GVR AND MATSUO T (1987). *Activated sludge model No.1.* IAWPRC Scientific and Technical Reports No 1, International Association on Water Pollution Research and Control, IAWPRC, London, ISSN 1010-707X. 33pp.

HENZE M, GUJER W, MINO T, MATSUO T, WENTZEL M C AND MARAIS GVR (1995) *Activated sludge model No.2*, IAWQ Scientific and Technical Report No. 3, IAWQ, London, ISBN 1 900222 00 0.

HILL DT AND BARTH CL (1977). A dynamic model for simulation of animal waste digestion. Technical Contribution No. 1318. *Journal WPCF* Oct 2129-2143.

IZZETT HB, WENTZEL MC AND EKAMA GA (1992). The effect of thermophilic heat treatment on the anaerobic digestibility of primary sludge. Research Report W76, Univ. of Cape Town, Dept. of Civil Eng. Rondebosch 7701, Cape, South Africa.

KATEHIS D, DIYAMANDOGLU V AND FILLOS J (1998) Stripping and recovery of ammonia from centrate of anaerobically digested biosolids at elevated temperatures *Water Environ. Research* **70**(2) 231-240.

KAUFMAN, E.N., LITTLE, M.H. AND SELVARAJ, P.T. (1996). Recycling of FGD gypsum to calcium carbonate and elemental sulfur using mixed sulfate-reducing bacteria with sewage digest as a carbon source. *J. Chem. Tech. Biotechnol.* **66** 365-374.

KAYHANIAN M AND TCHOBANOGLOUS G (1992). Pilot investigation of an innovative two-stage anaerobic digestion and aerobic composting process for the recovery of energy from the organic fraction of MSW. In: Proceedings of the 5th International Symposium on Anaerobic Digestion. Venice, Italy.

KIELY G, TAYFUR G, DOLAN C AND TANJI K (1997). Physical and mathematical modelling of anaerobic digestion of organic wastes. *Water Research* **31**(3) 534-540.

KNAPP, J.S. AND HOWELL, J.A. (1978). Treatment of primary sewage sludge with enzymes. *Biotech. Bioeng.* **20** 1221-1234.

KALYUZHNYI S AND FEDOROVICH V (1998). Mathematical modelling of competition between sulphate reduction and methanogenesis in anaerobic reactors. *Bioresource Technology* **65** 227-242.

KALYUZHNYI S, FEDOROVICH V, LENS P, POL LH AND LETTINGA G (1998). Mathematical modelling as a tool to study population dynamics between sulfate reducing and methanogenic bacteria. *Biodegration* ***9***(3-4) pps. 187-199).

LAHAV O AND LOEWENTHAL RE (2000). Measurement of VFA in anaerobic digestion: The five-point titration method revisited. *Water SA*, **26**(3), 389-392.

LEHNINGER AL (1977) *Biochemistry*. 2nd Ed, Worth Publishers, New York, ISBN 0-87901-047-9.

LEVENSPIEL O (1972) *Chemical reaction engineering*. 2nd Ed. John Wiley, New York, 465-469.

LILLEY I D, WENTZEL M C, LOEWENTHAL R E, EKAMA G A AND MARAIS GVR (1991). Acid fermentation of primary sludge at 20EC. *Research Report W64*, Dept. Civil Eng., Univ. of Cape Town, Rondebosch 7701, South Africa.

LOEWENTHAL RE, WIECHERS HNS AND MARAIS GVR (1986). *Softening and stabilization of municipal waters*. Water Research Commission, P/Bag X03, Gezina 0031, South Africa, ISBN 0 908356 54 4.

LOEWENTHAL RE, EKAMA GA AND MARAIS GVR (1989). Mixed weak acid/base systems: Part I – Mixture characterisation. *Water SA* **15**(1): 3-24.

LOEWENTHAL RE, WENTZEL MC, EKAMA GA AND MARAIS GVR (1991). Mixed weak acid/base systems: Part II – Dosing estimation, aqueous phase. *Water SA* **17**(2): 107-122.

LOEWENTHAL RE, SÖTEMANN SW, WENTZEL MC AND EKAMA GA (2004) Three phase mixed weak acid base chemistry kinetic modelling of multiple mineral precipitation problems. IWA conference on *Struvite: Its role in phosphorus recovery and re-use*, Cranfield University, UK, 18-18 June.

MCCARTY PL (1964). Thermodynamics of biological synthesis and growth. *2nd Int. Conf. on Wat. Pollut. Research*, Pergamon Press, New York, 169-199.

MCCARTY PL (1974) Anaerobic processes. Presented at International Association of Water Pollution Research (IAWPR, now IWA) short course on Design Aspects of Biological treatment, Birmingham, UK, 18 Sept. 1974.

MOOSBRUGGER R E, WENTZEL M C, EKAMA G A AND MARAIS GVR (1992). *Simple titration procedures to determine H_2CO_3*alkalinity and short chain fatty acids in aqueous solutions containing known concentrations of ammonium, phosphate and sulphide weak acid/bases*. Water Research Commission, P/Bag X03, Gezina 0031, South Africa, ISBN 1 874858 54 3. WRC Report No. TT 57/92. (70 pp)

MOOSBRUGGER RE, WENTZEL MC, EKAMA GA AND MARAIS GVR (1993) Grape wine distillery waste in UASB systems – Feasibility, alkalinity and pH control. *Water SA* **19**(1) 53-68.
Musvoto EV, Wentzel MC, Loewenthal RE and Ekama (1997). Kinetic-based model for weak acid/base systems. *Water SA* **23**(4) 311-322.

MUSVOTO EV, EKAMA GA, WENTZEL MC AND LOEWENTHAL RE (2000a). Extension and application of the three – phase weak acid/base kinetic model to the aeration treatment of anaerobic digester liquors. *Water SA* **26**(4): 417-438.

MUSVOTO EV, WENTZEL MC, LOEWENTHAL RE AND EKAMA GA (2000b). Integrated chemical – physical processes modelling – I. Development of a kinetic based model for mixed weak acid/base systems. *Water Research* **34**(6): 1857-1867.

MUSVOTO EV, WENTZEL MC, LOEWENTHAL RE AND EKAMA GA (2000c). Integrated chemical – physical processes modelling – II. Simulation aeration treatment of anaerobic digester supernatants. *Water Research* **34**(6): 1868-1880.

O'ROURKE JT (1968). Kinetics of anaerobic treatment at reduced temperatures. PhD dissertation, Department of Civil Engineering, Stanford University.
Oude Elferink, S.J.W.H., Visser, A., Hulshoff Pol, L.W. and Stams, A.J.M. (1994). Sulfate reduction in methanogenic bioreactors. *FEMS Microbiol. Reviews* **15** 119-136.

PAVLOSTATHIS SG AND GIRALDO-GOMEZ E (1991) Kinetics of anaerobic treatment. *Wat. Sci. Tech.* **24**(8) 35-59.

PIPES, W.O. (1961). Sludge digestion by sulfate reducing bacteria. In Proceedings of the *15th Industrial Waste Conference* Purdue University, Lafayette, Indiana.
Rajkumar S (2006) Implementation of a sulphate reduction kinetic model in WEST. MSc thesis, University of KwaZulu-Natal (in preparation).

REICHERT P (1998) *Concepts underlying a computer programme for the identification and simulation of aquatic systems (Aquasim 2.0).* Swiss Federal Institute of Environmental Science and Technology (EAWAG), CH-8600, Switzerland.

RISTOW NE, SÖTEMANN SW, LOEWENTHAL RE, WENTZEL MC AND EKAMA GA (2005a). Hydrolysis of primary sewage sludge under methanogenic, acidogenic and sulphate reducing conditions. *WRC Report 1216/1/05*, Water Research Commission, P/Bag X03, Gezina 0031, South Africa.

RISTOW NE, SÖTEMANN SW, WENTZEL MC, LOEWENTHAL RE AND EKAMA GA (2005b). Sulphate measurement in organic-rich solutions: Carbonate fusion pre-treatment to remove organic interferences. *Water SA* **31**(2) 267-270.

ROSE, P.D., CORBETT, C.J., WHITTINGTON-JONES, K. AND HART, O.O. (2002). The Rhodes BioSURE Process® Part 1: Biodesalination of mine drainage wastewaters. Report TT 195/02, Water Research Commission, P/Bag X03, Gezina 0031, South Africa.

SAM-SOON PALNS, WENTZEL MC, DOLD PL, LOEWENTHAL RE AND MARAIS, GVR (1991). Mathematical modelling of upflow anaerobic sludge bed (UASB) systems treating carbohydrate waste waters. *Water SA* **17**(2) 91-106.

SKALSKY, D.S. AND DAIGGER, G.T. (1995). Wastewater solids fermentation for volatile acid production and enhanced biological phosphorous removal. *Wat. Environ. Res.* **67** 230-237.
Sötemann SW, Musvoto EV, Wentzel MC and Ekama GA (2005a) Materials mass balances and modelling of wastewater treatment plants. *WRC Report 1338/1/05*, Water Research Commission, P/Bag X03, Gezina 0031, South Africa.

SÖTEMANN SW, VAN RENSBERG P, RISTOW NE, WENTZEL MC, LOEWENTHAL RE AND EKAMA GA (2005b). Integrated chemical/physical and biological processes modelling Part2 – Anaerobic digestion of sewage sludges. *Water SA* **31**(4) 545-568.

SÖTEMANN SW, RISTOW NE, WENTZEL MC AND EKAMA GA (2005c) A steady state model for anaerobic digestion of sewage sludges *Water SA* **31**(4) 511-528.

Standard methods for the Examination of Water and Wastewater. (1985). 19th Edn, American Public Health Association/American Water Works Association/Water Environment Federation, Washington DC, USA.

VANHOOREN H, MEIRLAEN J, AMERLINCK Y, CLAEYS F, VANGHELUWE H AND VANROLLEGHEM PA (2005). WEST: Modelling biological wastewater treatment. *J Hydroinformatics* **5**(1) 27-50.

VAN RENSBURG P, MUSVOTO EV, WENTZEL MC AND EKAMA GA (2003) Modelling multiple mineral precipitation in anaerobic digester liquor. *Water Research* **37** (13) 3087-3097.

VAN WAGENINGEN S, SÖTEMANN SW, WENTZEL MC AND EKAMA GA (2006). The development of a kinetic model for biological sulphate reduction with primary sewage sludge as substrate (in preparation).

VAVILIN VA, LOKSHINA LYA (1996). Modelling of volatile fatty acids degradation kinetics and evaluation of microorganism activity. *Biores. Tech*. **57**(1) 69-80.

VENTER, S.L.V., HALLIDAY, J. AND PITMAN, A.R. (1977). Optimization of the Johannesburg Olifantsvlei extended aeration plant for phosphorous removal. *Prog. Wat. Tech.* **10** 279-292.

WHITTINGTON-JONES, K. (2000). Sulfide-enhanced hydrolysis of primary sewage sludge: implications for the bioremediation of acid mine drainage. *Ph.D. Thesis*, Rhodes University, Grahamstown, South Africa.

WRC (1984). *Theory, design and operation of nutrient removal activated sludge processes* (7 Chapters). Ed. Wiechers HNS, Water Research Commission, P/Bag X03, Gezina 0031, South Africa, ISBN 0 908356 13 7.

ZEHNDER AJB AND WUHRMANN K (1977) Physiology of a methanobacterium strain AZ. *Arch Mikrobiol*. **III** 199-205.

ZEHNDER AJB, HUSER BA, BROCK TD AND WUHRMANN K (1980) Characterizing an acetate decarboxylating non-hydrogen oxidizing methane bacteria. *Arch. Microbiol*. **124** 1-11.

APPENDIX A

THEORETICAL ANALYSIS OF SOME ISSUES RELATING TO THE IMPLEMENTATION OF THE UCT ANAEROBIC DIGESTION MODEL IN WEST

A.1 Stoichiometry of Hydrolysis Reaction

$$C_xH_yO_zN_a \Rightarrow \left(\frac{2z-y+3a}{4}\right)H_2CO_3 + aNH_3 + \left(\frac{4x+y-2z-3a}{24}\right)C_6H_{12}O_6 + \left(\frac{y-2x-3a}{2}\right)H_2O$$

$$C_xH_yO_zN_a \Rightarrow \left(x-\frac{e}{4}\right)H_2CO_3 + aNH_3 + \frac{e}{24}C_6H_{12}O_6 + \left(z-3x+\frac{e}{2}\right)H_2O$$

where: $e = 4x + y - 2z - 3a$ (the electron demand of $C_xH_yO_zN_a$ per mole)

The chemical oxygen demand of $C_xH_yO_zN_a$ is $\frac{e}{2}$ moles of O , or $8e$ grams of O.

In the model $C_xH_yO_zN_a$ is represented as kg.m^{-3} COD, and all the other species (except H_2O) as kmol.m^{-3}, so the stoichiometric coefficients are:

$C_xH_yO_zN_a$: -1	H_2CO_3 :	$\frac{x}{8e}-\frac{1}{32}$	
NH_3 :	$\frac{a}{8e}$	$C_6H_{12}O_6$:	$\frac{1}{192}$

(The stoichiometric coefficient for water would not be experimentally observable)

If we transform the stoichiometric coefficients *x*, *y*, *z* and *a* to ratios as follows:

$$\lambda = \frac{y}{4x} \qquad \theta = \frac{2z}{4x} \qquad \alpha = \frac{3a}{4x}$$

Then $e = (1+\lambda-\theta-\alpha)\cdot 4x$ and the stoichiometric coefficients become

$C_xH_yO_zN_a$: -1	H_2CO_3 :	$\frac{1}{32}\left(\frac{\lambda+\alpha-\theta}{1+\lambda-\theta-\alpha}\right)$	
NH_3 :	$\frac{1}{3}\left(\frac{\alpha}{1+\lambda-\theta-\alpha}\right)$	$C_6H_{12}O_6$:	$\frac{1}{192}$

This can be further simplified, because λ and θ always occur in the combination $(\lambda - \theta)$.

Let $(\lambda - \theta) = \beta$, which makes the stoichiometric coefficients:

$C_xH_yO_zN_a$	: -1	H_2CO_3	: $\frac{1}{32}\left(\frac{\beta+\alpha}{1+\beta-\alpha}\right)$
NH_3	: $\frac{1}{3}\left(\frac{\alpha}{1+\beta-\alpha}\right)$	$C_6H_{12}O_6$	: $\frac{1}{192}$

This result means that the 4 parameters (*x, y, z* and *a*) can be reduced to just 2 (α and β).

A.2 Basis components

In the implementation of a model (particularly in WEST) it would be desirable to keep reaction scheme parameters separate from stream characterisation, and therefore characterise the stream composition entirely in terms of the concentrations of components. This requires finding a set of basis components which can represent the same overall stoichiometry as the *x, y, z* and *a* parameters (or α and β).

Thus stated, the problem has far too many degrees of freedom; one needs to find some further justification for choosing a particular set. It is proposed to choose a set which is similar to the ADM1 model, which considers biodegradable particulate matter as a composite of proteins, lipids and carbohydrates. However, these are still broad categories of components, with considerable variation possible. ADM1 suggests representing the stoichiometries of carbohydrates and lipids as glucose ($C_6H_{12}O_6$) and palmitic triglyceride ($C_{51}H_{98}O_6$). The treatment of proteins is more complex, based on the proportions of 18 amino acids which make up the protein. Two examples of amino acid content of proteins are presented in the ADM1 document, beef flesh and casein, from which the elemental formulae can be calculated as $C_{4.91}H_{9.708}O_{2.591}N_{1.284}$ and $C_{5.208}H_{9.91}O_{2.676}N_{1.199}$

For the present exercise, the three groups will be represented as carbohydrate: $C_6H_{12}O_6$, lipid: $C_{51}H_{98}O_6$ and protein: $C_{5.059}H_{9.809}O_{2.6335}N_{1.2415}$ (averaging beef flesh and casein).

The range of compositions that can be spanned by these basis components is limited by their range of atomic ratios. The range of H/C ratios is particularly narrow, and causes a problem in representing empirical formulae provided by UCT as shown in Table A1.1.

Table A1.1: Elemental ratios in the basis components and empirical formulae

Component	H/C	O/C	H/O	N/C
$C_6H_{12}O_6$	2.000	1.000	2.000	0.000
$C_{51}H_{98}O_6$	1.922	0.118	16.33	0.000
$C_{5.208}H_{9.91}O_{2.676}N_{1.199}$	1.903	0.513	3.703	0.230
$C_{3.5}H_7O_2N_{0.196}$	2.000	0.571	3.500	0.056
$C_4H_7O_{2.295}N_{0.72}P_{0.05}$	1.750	0.574	3.050	0.180
$C_{3.91}H_7O_{2.82}N_{0.54}P_{0.09}$	1.790	0.721	2.482	0.138
$C_{4.32}H_7O_{3.44}N_{0.65}P_{0.07}$	1.620	0.796	2.035	0.150
$C_{4.31}H_7O_{3.39}N_{0.61}P_{0.11}$	1.624	0.787	2.065	0.142
$C_{3.91}H_7O_{2.04}N_{0.16}P_{0.01}$	1.790	0.522	3.431	0.041
$C_{3.92}H_7O_{2.64}N_{0.35}P_{0.1}$	1.786	0.673	2.652	0.089
$C_{3.38}H_7O_{1.9}N_{0.21}P_{0.01}$	2.071	0.562	3.684	0.062
$C_{4.08}H_7O_{3.63}N_{0.22}P_{0.04}$	1.716	0.890	1.928	0.054

Table A1.2 then shows how the empirical formulae can be expressed of the expanded set of basis components.

Table A1.2: Empirical formula expressed as combinations of the basis components (% mass)

Formula	% lipid	% protein	% carbohydrate	% H_2O	% CO_2
$C_{3.5}H_7O_2N_{0.196}$	25.0	24.5	49.7	1.4	-0.6
$C_4H_7O_{2.295}N_{0.72}P_{0.05}$	0.3	74.1	29.0	-6.1	2.7
$C_{3.91}H_7O_{2.82}N_{0.54}P_{0.09}$	0.0	53.1	43.8	-3.2	6.4
$C_{4.32}H_7O_{3.44}N_{0.65}P_{0.07}$	0.0	55.4	27.0	-2.6	20.2
$C_{4.31}H_7O_{3.39}N_{0.61}P_{0.11}$	0.0	52.6	32.6	-3.4	18.2
$C_{3.91}H_7O_{2.04}N_{0.16}P_{0.01}$	26.8	18.9	57.5	-5.7	2.5
$C_{3.92}H_7O_{2.64}N_{0.35}P_{0.1}$	6.1	36.2	60.6	-5.4	2.4
$C_{3.38}H_7O_{1.9}N_{0.21}P_{0.01}$	26.7	27.2	44.0	3.8	-1.7
$C_{4.08}H_7O_{3.63}N_{0.22}P_{0.04}$	0.0	19.7	74.7	-4.4	10.0

This formulation has extra degrees of freedom; these were taken up by minimising the masses of H_2O and CO_2 used to correct the ratios.

Except for 2 or possibly 3 cases, the H_2O and CO_2 corrections are quite small, and might well be within the range of experimental error associated with the chemical analyses.

However the line of thinking prompts consideration of the possibility that they may represent some real physical effects. In particular, part of the analytic methodology involves drying the organic material at 100°C. This could cause some denaturing of the material, driving off H_2O bound in molecular structures. The fate of inorganic carbon also deserves consideration. Carbonates and bicarbonates would be precipitated, but some might be driven off as CO_2, e.g.

$$2NaHCO_3 \Rightarrow Na_2CO_3 \downarrow + CO_2 \uparrow + H_2O \uparrow$$

The precipitated carbonate would be reflected in the elemental analysis of the dried material, but the CO_2 would be lost.

These considerations suggest a modification to the experimental procedure. The inorganic carbon can be determined in the normal way as alkalinity, and the material should be freeze dried instead of oven dried to minimise any changes that might occur before the elemental analysis.

APPENDIX B

INFLUENT CHARACTERISATION

Table B-1: Feed batch data for steady state experiments (Ristow *et al.*, 2005a)

Feed batch number	**pH**	**Alkalinity (mg/ℓ as $CaCO_3$)**
F12	4.91	47.3
F13	5.73	151.6
F14	5.38	90.28
F15	5.38	90.28

Table B-2: Influent characterisation for steady state numbers 1-11

Steady state number	**1**	**2**	**3**	**4**	**5**	**6**	**7**	**8**	**9**	**10**	**11**
Feed batch number	F12	F12	F12	F12	F12	F12	F13	F13	F13	F13	F13
Reactor volume (ℓ)	16	16	20	20	20	16	16	16	16	20	20
Retention time (d)	10	8	20	15	15	10	6.67	5.71	5	15	15
Flowrate (ℓ/d)	1.6	2	1	1.33	1.33	1.6	2.40	2.80	3.2	1.33	1.33
H_20 (g/d)	1600	2000	1000	1333.33	1333.33	1600	2398.80	2802.10	3200	1333.33	1333.33
pH	4.91	4.91	4.91	4.91	4.91	4.91	5.73	5.73	5.73	5.73	5.73
H^+ (g/d)	1.98E-05	2.48E-05	1.24E-05	1.65E-05	1.65E-05	1.98E-05	4.50E-06	5.26E-06	6.01E-06	2.50E-06	2.50E-06
OH^- (g/d)	2.21E-08	2.76E-08	1.38E-08	1.84E-08	1.84E-08	2.21E-08	2.19E-07	2.56E-07	2.92E-07	1.22E-07	1.22E-07
S_{VFAi} (mgCOD/ℓ)	4000	1740	1775	1900	1060	4000	1260	1250	1196	1830	2020
Ac^- (g/d)	3.53E+00	1.92E+00	9.78E-01	1.40E+00	7.79E-01	3.53E+00	2.56E+00	2.97E+00	3.25E+00	2.07E+00	2.28E+00
HAc (g/d)	2.52E+00	1.37E+00	6.99E-01	9.98E-01	5.57E-01	2.52E+00	2.77E-01	3.21E-01	3.51E-01	2.24E-01	2.47E-01
Pr^- (g/d)	0	0	0	0	0	0	0	0	0	0	0
HPr (g/d)	0	0	0	0	0	0	0	0	0	0	0
FSA (mgN/ℓ)	39	39	39	39	20	39	106	124	131	180	198
NH_3 (g/d)	3.45E-06	4.32E-06	2.16E-06	2.88E-06	1.48E-06	3.45E-06	9.29E-05	1.27E-04	1.53E-04	8.77E-05	9.65E-05
NH_4^+ (g/d)	8.04E-02	1.00E-01	5.02E-02	6.70E-02	3.43E-02	8.04E-02	3.27E-01	4.47E-01	5.40E-01	3.09E-01	3.40E-01
Alkalinity (mg/ℓ as $CaCO_3$)	47.3	47.3	47.3	47.3	47.3	47.3	151.6	151.6	151.6	151.6	151.6
CO_3^{2-} (g/d)	3.50E-07	4.38E-07	2.19E-07	2.92E-07	2.92E-07	3.50E-07	1.10E-05	1.28E-05	1.47E-05	6.11E-06	6.11E-06
HCO_3^- (g/d)	9.35E-02	1.17E-01	5.84E-02	7.79E-02	7.79E-02	9.35E-02	4.44E-01	5.18E-01	5.92E-01	2.47E-01	2.47E-01
H_2CO_3 (g/d)	2.69	3.36	1.68	2.24	2.24	2.69	1.93	2.26	2.58	1.07	1.07
Sulphate (mg/ℓ)	0	0	0	0	0	1000	0	0	0	0	0
SO_4^{2+} (g/d)	0	0	0	0	0	1.6	0	0	0	0	0
COD Fractionation											
S_{bp} (mgCOD/ℓ)	14940.72	14596.72	14945.72	14624.72	7630.78	14624.72	14531.31	14107.88	13864.31	22959.25	22490.25
S_{bp} (gCOD/d)	23.91	29.19	14.95	19.50	10.17	23.40	34.86	39.53	44.37	30.61	29.99
S_{up} (mgCOD/ℓ)	8681.28	8681.28	8681.28	8681.28	4555.22	8681.28	8322.69	8349.12	8322.69	13309.76	13309.76
S_{up} (gCOD/d)	13.89	17.36	8.68	11.58	6.07	13.89	19.96	23.40	26.63	17.75	17.75
S_{bs} (mgCOD/ℓ)	1076	1253	1073	1245	668	1076	914	1149	1196	1635	1846
S_{bs} (g/d)	1.62	2.35	1.01	1.56	0.84	1.62	2.06	3.02	3.59	2.05	2.31
S_{us} (mgCOD/ℓ)	178	168	179	157	97	178	200	205	301	250	299
S_{us} (gCOD/d)	2.85E-01	3.36E-01	1.79E-01	2.09E-01	1.29E-01	2.85E-01	4.80E-01	5.74E-01	9.63E-01	3.33E-01	3.99E-01

Table B-3: Influent characterisation for steady state numbers 12-23

Steady state number	**12**	**13**	**14**	**15**	**17**	**18**	**19**	**20**	**21**	**22**	**23**
Feed batch number	F13	F13	F13	F13	F12	F14	F14	F14	F14	F14	F14
Reactor volume (ℓ)	20	20	20	16	20	16	16	16	20	16	20
Retention time (d)	10	10	8	8	60	8	8	8	8	8	6.67
Flowrate (ℓ/d)	2	2	2.5	2	0.33	2	2	2	2.5	2	3.00
H_20 (g/d)	2000	2000	2500	2000	333.33	2000	2000	2000	2500	2000	2998.50
pH	5.73	5.73	5.73	5.73	4.91	5.38	5.38	5.38	5.38	5.38	5.38
H^+ (g/d)	3.75E-06	3.75E-06	4.69E-06	3.75E-06	4.13E-06	8.40E-06	8.40E-06	8.40E-06	1.05E-05	8.40E-06	1.26E-05
OH^- (g/d)	1.83E-07	1.83E-07	2.28E-07	1.83E-07	4.61E-09	8.16E-08	8.16E-08	8.16E-08	1.02E-07	8.16E-08	1.22E-07
S_{VFAi} (mgCOD/ℓ)	2090	533	710	710	558	116	116	116	1812	116	2096
Ac^- (g/d)	3.54E+00	9.04E-01	1.51E+00	1.20E+00	1.02E-01	1.76E-01	1.76E-01	1.76E-01	3.43E+00	1.76E-01	4.76E+00
HAc (g/d)	3.84E-01	9.78E-02	1.63E-01	1.30E-01	7.33E-02	4.26E-02	4.26E-02	4.26E-02	8.31E-01	4.26E-02	1.15E+00
Pr^- (g/d)	0	0	0	0	0	0	0	0	0	0	0
HPr (g/d)	0	0	0	0	0	0	0	0	0	0	0
FSA (mgN/ℓ)	214	59	73	72	15	7	8	8	44	10	70
NH_3 (g/d)	1.56E-04	4.31E-05	6.67E-05	5.26E-05	2.77E-07	2.29E-06	2.61E-06	2.61E-06	1.80E-05	3.27E-06	3.43E-05
NH_4^+ (g/d)	5.51E-01	1.52E-01	2.35E-01	1.85E-01	6.44E-03	1.80E-02	2.06E-02	2.06E-02	1.42E-01	2.58E-02	2.70E-01
Alkalinity (mg/ℓ as $CaCO_3$)	151.6	151.6	151.6	151.6	47.3	90.28	90.28	90.28	90.28	90.28	90.28
CO_3^{2-} (g/d)	9.16E-06	9.16E-06	1.15E-05	9.16E-06	7.30E-08	2.44E-06	2.44E-06	2.44E-06	3.05E-06	2.44E-06	3.66E-06
HCO_3^- (g/d)	3.70E-01	3.70E-01	4.62E-01	3.70E-01	1.95E-02	2.21E-01	2.21E-01	2.21E-01	2.76E-01	2.21E-01	3.31E-01
H_2CO_3 (g/d)	1.61	1.61	2.01	1.61	0.56	2.15	2.15	2.15	2.69	2.15	3.22
Sulphate (mg/ℓ)	0	0	0	9600	0	0	0	2000	0	2000	0
SO_4^{2+} (g/d)	0	0	0	19.2	0	0	0	4	0	4	0
COD Fractionation											
S_{bp} (mgCOD/ℓ)	22057.56	7657.19	7306.19	7306.19	5324.56	1013.73	1013.73	1013.73	19343.38	1013.73	18773.38
S_{bp} (gCOD/d)	44.12	15.31	18.27	14.61	1.77	2.03	2.03	2.03	48.36	2.03	56.29
S_{up} (mgCOD/ℓ)	13316.45	4438.82	4438.82	4438.82	3281.45	652.28	652.28	652.28	11646.62	652.28	11646.62
S_{up} (gCOD/d)	26.63	8.88	11.10	8.88	1.09	1.30	1.30	1.30	29.12	1.30	34.92
S_{bs} (mgCOD/ℓ)	2090	533	710	710	558	116	116	116	1812	116	2096
S_{bs} (g/d)	3.92	1.00	1.67	1.33	0.17	0.22	0.22	0.22	4.25	0.22	5.90
S_{us} (mgCOD/ℓ)	256	108	104	104	88	51	51	51	205	51	207
S_{us} (gCOD/d)	5.12E-01	2.16E-01	2.60E-01	2.08E-01	2.93E-02	1.02E-01	1.02E-01	1.02E-01	5.13E-01	1.02E-01	6.21E-01

Table B-4: Influent characterisation for steady state numbers 24-28, 31, 36, 41, 42, 46 and 47

Steady state number	**24**	**25**	**26**	**27**	**28**	**31**	**36**	**41**	**42**	**46**	**47**
Feed batch number	F14	F14	F14	F15	F15	F15	F15	F15	F15	F15	F15
Reactor volume (ℓ)	20	20	20	16	20	20	16	20	20	20	16
Retention time (d)	6.67	10	8	8	5.71	5.71	8	16	13.3	10	8
Flowrate (ℓ/d)	3.00	2	2.5	2	3.50	3.50	2	1.25	1.50	2	2
H_20 (g/d)	2998.50	2000	2500	2000	3502.63	3502.63	2000	1250	1503.76	2000	2000
pH	5.38	5.38	5.38	5.38	5.38	5.38	5.38	5.38	5.38	5.38	5.38
H^+ (g/d)	1.26E-05	8.40E-06	1.05E-05	8.40E-06	1.47E-05	1.47E-05	8.40E-06	5.25E-06	6.32E-06	8.40E-06	8.40E-06
OH^- (g/d)	1.22E-07	8.16E-08	1.02E-07	8.16E-08	1.43E-07	1.43E-07	8.16E-08	5.10E-08	6.13E-08	8.16E-08	8.16E-08
S_{VFAi} (mgCOD/ℓ)	875	111	116	104	1144	418	116	98	104	47	94
Ac^- (g/d)	1.99E+00	1.68E-01	2.20E-01	1.58E-01	3.04E+00	1.11E+00	1.76E-01	9.28E-02	1.19E-01	7.12E-02	1.42E-01
HAc (g/d)	4.82E-01	4.07E-02	5.32E-02	3.82E-02	7.35E-01	2.69E-01	4.26E-02	2.25E-02	2.87E-02	1.73E-02	3.45E-02
Pr^- (g/d)	0	0	0	0	0	0	0	0	0	0	0
HPr (g/d)	0	0	0	0	0	0	0	0	0	0	0
FSA (mgN/ℓ)	37	5	7	8	40	18	13	6	10	7	4
NH_3 (g/d)	1.81E-05	1.63E-06	2.86E-06	2.61E-06	2.29E-05	1.03E-05	4.25E-06	1.22E-06	2.46E-06	2.29E-06	1.31E-06
NH_4^+ (g/d)	1.43E-01	1.29E-02	2.25E-02	2.06E-02	1.80E-01	8.12E-02	3.35E-02	9.66E-03	1.94E-02	1.80E-02	1.03E-02
Alkalinity (mg/ℓ as $CaCO_3$)	90.28	90.28	90.28	90.28	90.28	90.28	90.28	90.28	90.28	90.28	90.28
CO_3^{2-} (g/d)	3.66E-06	2.44E-06	3.05E-06	2.44E-06	4.28E-06	4.28E-06	2.44E-06	1.53E-06	1.84E-06	2.44E-06	2.44E-06
HCO_3^- (g/d)	3.31E-01	2.21E-01	2.76E-01	2.21E-01	3.86E-01	3.86E-01	2.21E-01	1.38E-01	1.66E-01	2.21E-01	2.21E-01
H_2CO_3 (g/d)	3.22	2.15	2.69	2.15	3.76	3.76	2.15	1.34	1.62	2.15	2.15
Sulphate (mg/ℓ)	0	0	0	0	0	0	2000	2000	2000	2000	2000
SO_4^{2+} (g/d)	0	0	0	0	0	0	4	2.5	3.01	4	4
COD Fractionation											
S_{bp} (mgCOD/ℓ)	7191.82	1043.73	1013.73	1118.31	24996.99	7819.28	1013.73	1127.32	1118.31	556.18	1061.45
S_{bp} (gCOD/d)	21.56	2.09	2.53	2.24	87.56	27.39	2.03	1.41	1.68	1.11	2.12
S_{up} (mgCOD/ℓ)	4542.18	652.28	652.28	674.69	13862.01	4410.72	652.28	672.68	674.69	330.82	635.55
S_{up} (gCOD/d)	13.62	1.30	1.63	1.35	48.55	15.45	1.30	0.84	1.01	0.66	1.27
S_{bs} (mgCOD/ℓ)	875	111	116	104	1144	418	116	98	104	47	94
S_{bs} (g/d)	2.46	0.21	0.27	0.20	3.76	1.37	0.22	0.11	0.15	0.09	0.18
S_{us} (mgCOD/ℓ)	96	32	51	16	295	120	51	16	16	8	15
S_{us} (gCOD/d)	2.88E-01	6.40E-02	1.28E-01	3.20E-02	1.03E+00	4.20E-01	1.02E-01	2.00E-02	2.41E-02	1.60E-02	3.00E-02

Table B-5: Influent characterisation of the PSS and mine water feed streams to the pilot plant

Feed Stream	**PSS**	**Mine water**
Reactor volume (ℓ)	250000	250000
Retention time (d)	18.94	1.09
Flowrate (ℓ/d)	13200	230000
H_20 (g/d)	13200000	230000000
pH	7*	7.5
H^+ (g/d)	1.33E-03	7.33E-03
OH^- (g/d)	2.24E-02	1.24
S_{VFAi} (mgCOD/ℓ)	1245	0
Ac^- (g/d)	15332.51	0
HAc (g/d)	89.08	0
Pr^- (g/d)	0	0
HPr (g/d)	0	0
FSA (mgN/ℓ)	39*	0
NH_3 (g/d)	3.49	0
NH_4^+ (g/d)	659.28	0
Alkalinity (mg/ℓ as $CaCO_3$)	300*	350
CO_3^{2-} (g/d)	2.22	142.74
HCO_3^- (g/d)	4823.78	97856.93
H_2CO_3 (g/d)	1127.23	7231.32
Sulphate (mg/ℓ)	0	1300
SO_4^{2+} (g/d)	0	299000
COD Fractionation		
S_{bp} (mgCOD/ℓ)	17271.00	0
S_{bp} (gCOD/d)	227977.20	0
S_{up} (mgCOD/ℓ)	10035.00	0
S_{up} (gCOD/d)	132462.00	0
S_{bs} (mgCOD/ℓ)	1245	0
S_{bs} (g/d)	15421.09	0
S_{us} (mgCOD/ℓ)	204	0
S_{us} (gCOD/d)	2692.80	0

* Guesstimate Value

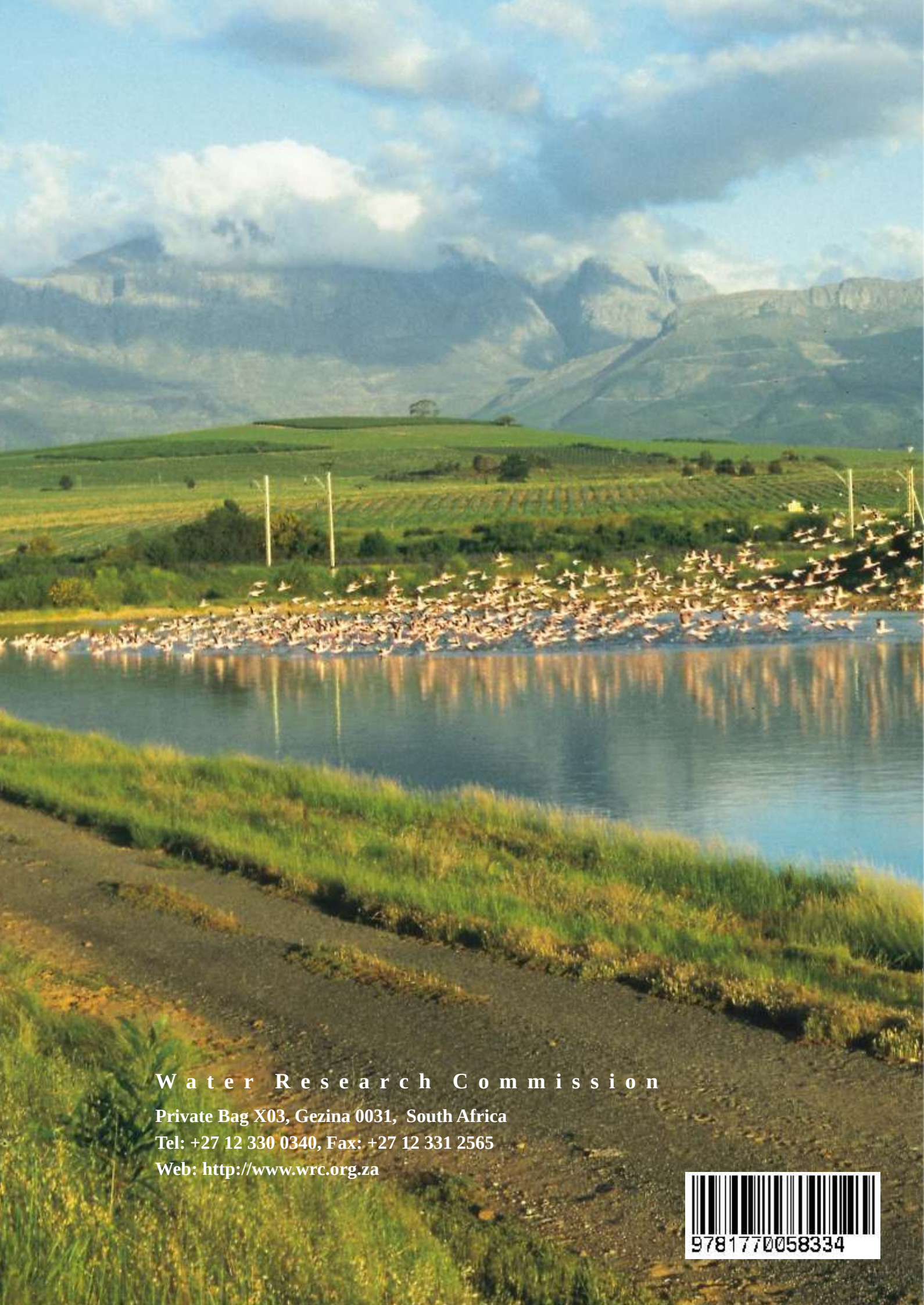

Water Research Commission

Private Bag X03, Gezina 0031, South Africa
Tel: +27 12 330 0340, Fax: +27 12 331 2565
Web: http://www.wrc.org.za

9781770058334